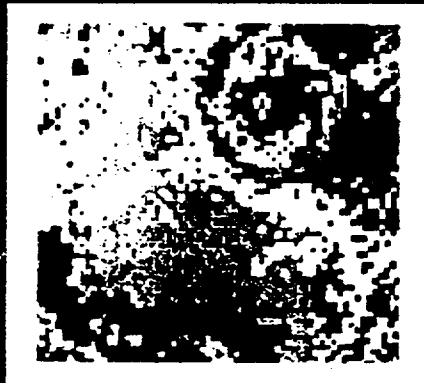


1987
ANNUAL
TROPICAL
CYCLONE
REPORT



JOINT TYPHOON WARNING CENTER
GUAM, MARIANA ISLANDS

FRONT COVER: The digitized image (center of lower square) of surface wind speed shows Typhoon Kelly (19W) (circular pattern at the top right) and the Philippine Islands (black shapes at bottom left). The technique to develop these surface wind speed fields is currently under development. The surface wind speed field algorithm uses the polarized 19 (horizontal), 22 (vertical) and 37 (vertical and horizontal) gigahertz (GHz) channels of the Defense Meteorological Satellite Program's new special sensor, the microwave imager (SSM/I), which is a four-channel passive microwave radiometer.

U.S. NAVAL OCEANOGRAPHY COMMAND CENTER
JOINT TYPHOON WARNING CENTER
COMNAV Marianas Box 17
FPO San Francisco, CA 96630

CARL W. HOFFMAN

CAPTAIN, UNITED STATES NAVY
COMMANDING OFFICER

* **VERNON G. PATTERSON**

COLONEL, UNITED STATES AIR FORCE
DIRECTOR, JOINT TYPHOON WARNING CENTER
COMMANDER, DETACHMENT 1, 1ST WEATHER WING

DANIEL J. McMORROW

LIEUTENANT COLONEL, UNITED STATES AIR FORCE
DIRECTOR, JOINT TYPHOON WARNING CENTER
COMMANDER, DETACHMENT 1, 1ST WEATHER WING



* TRANSFERRED DURING 1987

STAFF

	LCDR	GEORGE M. DUNNAVAN,	USN
*	LT	JOHN L. SHOEMAKE,	USN
*	CAPT	SUSAN V. BERRY,	USAF
	LT	JOHN L. HEISHMAN,	USN
	LT	BRIAN J. WILLIAMS,	USN
	LT	DOUGLAS H. SCOVIL, JR.,	USN
	CAPT	STEVEN B. DREKSLER,	USAF
	CAPT	ROBERT F. CROSBY,	USAF
*	LT	HARRY S. GATANIS,	USN
	1LT	JOHN D. PICKLE,	USAF
**	LT(JG)	STACY R. STEWART,	USNR-R
*	TSGT	MARGURITTA H. SMITH,	USAF
	SSGT	JACK L. WILSON,	USAF
*	AG2	DEBRA L. MAHONEY,	USN
	SSGT	DONALD L. NOVAK, JR.,	USAF
	AG3	SHIRLEY A. MURDOCK,	USN
	SGT	MICHAEL STEELE,	USAF
	AG3	DEANNA L. HAMMACK,	USN
	SGT	ANGELIA C. BLAISDELL,	USAF
*	AG3	SUSAN M. HICKEY,	USN
	SGT	JAMES B. WIEMANN,	USAF
	AG3	SEAN L. KLOPE,	USN
	SRA	JAMES B. BUNKER,	USAF
	A1C	DONALD L. MILLER,	USAF
	AGAN	JEFFERY L. CHAPIN,	USN
EDITORS:	LT	STEVE J. FATJO,	USN
	MR	FRANK H. WELLS,	CIV

CONTRIBUTORS:

DET 1, 1WW SATELLITE OPERATIONS

*	CAPT	FREDERICK J. SVETZ,	USAF
	CAPT	JOHN M. ROGERS,	USAF
	CAPT	DAN B. MUNDELL,	USAF
	CAPT	KENNETH W. REESE,	USAF
	TSGT	JEFFERY L. FLEMING,	USAF
*	TSGT	FABRICE F. CLARK,	USAF
	TSGT	CHARLES J. BONINI,	USAF
	TSGT	TONI D. HUMPHREY,	USAF
	TSGT	ALAN W. ROBB,	USAF
	SSGT	ROBERT C. GRAY,	USAF

* TRANSFERRED DURING 1987

** ON ACTIVE DUTY TRAINING WITH JTWC



DEPARTMENT OF THE NAVY
U.S. NAVAL OCEANOGRAPHY COMMAND CENTER/
JOINT TYPHOON WARNING CENTER
COMNAVMARIANAS BOX 12
FPO SAN FRANCISCO 96630-2926

3140
Ser 012
19 January 1988

From: Commanding Officer, U.S. Naval Oceanography Command
Center/Joint Typhoon Warning Center, Guam
To: Distribution

Subj: PROMULGATION OF 1987 ANNUAL TROPICAL CYCLONE REPORT

Ref: (a) USCINCPACINST 3140.1S (NOTAL)

1. The Annual Tropical Cyclone Report for 1987 is promulgated in accordance with the provisions of reference (a).
2. The 1987 tropical cyclone season marked the beginning of a new era in tropical cyclone forecasting. Despite an unusually active season, forecasters made a mid-season transition from an aircraft based reconnaissance system to one based mostly on satellites, while recording the lowest track errors in the center's history.
3. The initial release of the Joint Typhoon Warning Center Automation Program hardware and software package also arrived on Guam in 1987. This program has already proved very successful and promises to be one of the most significant advances in the operational forecasting of tropical cyclones.
4. Despite the tremendous added pressures of the 1987 season, the staff has pulled together and done an outstanding job in publishing this document six months ahead of last year. I hope you find this report a valuable contribution to your library.


C. W. HOFFMAN

DISTRIBUTION LIST

1 COPY

BRUNEI SHELL PETROLEUM CO
CATHOLIC UNIVERSITY OF AMERICA
CENTRAL MET OBSERVATORY, BEIJING
CENTRAL METEOROLOGICAL OFFICE, SEOUL
CHULALONGKORN UNIVERSITY, BANGKOK
CHUNG CHENG INSTITUTE, TAIWAN
CITIES SERVICES OIL GAS CORP
CIUDAD UNIVERSITARIA, MEXICO
CIVIL DEFENSE, SAIPAN
CINCPACFLT
CNO (OP-096)
CNO (OP-096T)
CNO (OP-981D)
CNO (OP-943G)
COLORADO STATE UNIVERSITY LIBRARY
COMNAVOCEANCOM
COMNAV SURFGRU WESTPAC
COMNAV SURFPAC
COMPHIBGRU ONE
COMSC
COMSEVENTHFLT
COMSUBGRU SEVEN
COMTHIRDFLT
CONGRESSIONAL INFORMATION SERVICE, MD
DCA GUAM
DET 2, 20 WS
DET 4, 20 WS
DET 5, 20 WS
DET 8, 20 WS
DET 10, 30 WS
DET 13, 20 WS/CC
DET 15, 30 WS
DET 17, 20 WS
DISASTER CONTROL OFFICE, SAIPAN
ECMWF, BERKSHIRE, UK
FAIRECONRON ONE
FOREST DIVISION, JMA
GEOLOGICAL FLUID DYNAMICS LAB, PRINCETON, NJ
GEOLOGICAL SURVEY, GUAM
GODDARD SPACE FLIGHT CENTER
GUAM PUBLIC LIBRARY
HQ AWS/DN
HQ MAC/DOOS
HQ USAF/XOORZ
HUGHES AIRCRAFT CO
INSTITUTO DE GEOFISICA, MEXICO
JCS ENV SERVICES DIV (J3(OES))
LOS ANGELES PUBLIC LIBRARY
MASS INST OF TECH
MCAS KANEOHE BAY HI
METEOROLOGY DEPT, BANGKOK
MOBIL OIL GUAM INC
MOUNTAIN STATES WEATHER SERVICES
NATIONAL TAIWAN UNIVERSITY
NAVAL CIVIL ENG LAB, PORT HUENEME, CA
NAVDEP NOAA
NAVEASTOCEANCEN
NAVHISTCEN
NAVOCEANCOMCEN ROTA
NAVOCEANCOMDET AGANA
NAVOCEANCOMDET ALAMEDA
NAVOCEANCOMDET ASHEVILLE
NAVOCEANCOMDET ATSUGI
NAVOCEANCOMDET BARBERS POINT
NAVOCEANCOMDET KADENA
NAVOCEANCOMDET MONTEREY
NAVOCEANCOMFAC JACKSONVILLE
NAVOCEANCOMFAC YOKOSUKA
NAVPGSCOL LIBRARY
NAV POLAROCEANCEN SUTT LAND
NOAA/ACQUISITION SECTION, ROCKVILLE, MD
NOAA/AOML, HRD, MIAMI, FL
NOAA/HYDROMETEOROLOGY BR, SILVER SPRINGS, MD
NOAA/NESDIS, REDWOOD CITY, CA
NOAA/PMEL, SEATTLE, WA
NOAA LIBRARY, MIAMI, FL
NOBEL DENTON
OCEAN ROUTES INC, CA
OCEANO SERVICES INC. LIBRARY
PACIFIC STARS & STRIPES
PACNAVFACENGCOM
PENNSYLVANIA STATE UNIVERSITY
SRI LIBRARY
TEXAS A & M UNIVERSITY
UNIVERSITY OF CHICAGO
UNIVERSITY OF GUAM, BIOLOGY DEPT
UNIVERSITY OF HAWAII (LIBRARY)
UNIVERSITY OF WASHINGTON
USCINCPAC
USCINCPAC REP GUAM
USCINCPAC REP PHILIPPINES
USNA (OCEANOGRAPHY DEPT/LIBRARY)
USS BELLEAU WOOD (LHA 3)
USS CARL VINSON (CVN 70)
USS CONSTELLATION (CV 64)
USS CORAL SEA (CV 43)
USS ENTERPRISE (CVN 65)
USS KITTY HAWK (CV 63)
USS LONG BEACH (CGN 9)
USS MIDWAY (CV 41)
USS NEW ORLEANS (LPH 11)
USS NIMITZ (CVN 68)
USS OKINAWA (LPH 3)
USS RANGER (CV 61)
USS TARAWA (LHA 1)
USS TRIPOLI (LPH 10)
WORLD DATA CENTER B1, MOSCOW
WORLD WEATHER BUILDING, MD

3AD/DO
3WW/CC
3WW/DN
7WW/OL-A
20 WS/DO
34 AWF, 920 WRG
43 SW/DO
3350 TCHTG/TTMV-S

2 COPIES

AFGWC/WFMP
BUREAU OF METEOROLOGY, BRISBANE
BUREAU OF METEOROLOGY, DARWIN
BUREAU OF METEOROLOGY, PERTH
BUREAU OF PLANNING, GUAM
DEPARTMENT OF COMMERCE
ESCAP LIBRARY, BANGKOK
FLENUMOCEANCEN
FLORIDA STATE UNIVERSITY
HQ AWS/DOR
HQ AWS GP, JAPAN
INSTITUTE OF PHYSICS, TAIWAN
MARATHON OIL CO, TX
MARINERS WEATHER LOG
MCAS FUTENMA
MET RESEARCH INST LIBRARY, TOKYO
METEOROLOGY SOCIETY OF NEW SOUTH WALES, AUST
MICRONESIAN RESEARCH CENTER UOG, GUAM
NATIONAL METEOROLOGICAL LIBRARY, BRACKNELL, UK
NATIONAL WEATHER OFFICE, PAGASA
NATIONAL WEATHER SERVICE, HONOLULU
NAVOCEANCOMDET DIEGO GARCIA
NAVOCEANCOMDET MISAWA
NAVOCEANCOMFAC CUBI PT
NAVWESTOCEANCEN
NOAA CORAL GABLES LIBRARY
NOAA GUAM
OKINAWA METEOROLOGY OBSERVATORY
PACAF/DOW

SAT APPL LAB, NOAA/NESDIS, REDWOOD CITY, CA
TYPHOON COM SECR, MANILA
UNIVERSITY OF PHILIPPINES
US ARMY, FORT SHAFTER
WORLD DATA CENTER A, NOAA
17 WS/DON
23 AF/HQ
73 WEATHER GROUP, ROK AF

3 COPIES

AWS TECH LIBRARY
CENTRAL WEATHER BUREAU, TAIWAN
HQ AWS/DN
INOSHAC, DDGM (WF)
JAPAN METEOROLOGY AGENCY
MCAS IWAKUNI
NATIONAL HURRICANE CENTER, MIAMI
NAVPGSCOL DEPT OF METEOROLOGY
UNIVERSITY OF HAWAII, METEOROLOGY DEPT
1WW/DN
1WW/DON

4 COPIES

BUREAU OF METEOROLOGY, MELBOURNE
COLORADO STATE UNIVERSITY
METEOROLOGY DEPT, BANGKOK
5WW/CC

5 COPIES

CIVIL DEFENSE, GUAM
PAGASA WEATHER BUREAU, RP
R & D UNIT, NHC, MIAMI
ROYAL OBSERVATORY HONG KONG

6 COPIES

NEPRF

12 COPIES

DEFENSE DOCUMENTATION CENTER

FOREWORD

The Annual Tropical Cyclone Report is prepared by the staff of the Joint Typhoon Warning Center (JTWC), a combined USAF/USN organization operating under the command of the Commanding Officer, U.S. Naval Oceanography Command Center/Joint Typhoon Warning Center, Guam. JTWC was established in April 1959 when USCINCPAC directed USCINCPACFLT to provide a single tropical cyclone warning center for the western North Pacific region. The operations of JTWC are guided by CINCPACINST 3140.1 (series).

The mission of the Joint Typhoon Warning Center is multi-faceted and includes:

1. Continuous monitoring of all tropical weather activity in the northern and southern hemispheres, from 180 degrees longitude westward to the east coast of Africa, and the prompt issuance of appropriate advisories and alerts when tropical cyclone development is anticipated.
2. Issuing warnings on all significant tropical cyclones in the above area of responsibility.
3. Determination of reconnaissance requirements for tropical cyclone surveillance and assignment of appropriate priorities.
4. Post-storm analysis of all significant tropical cyclones occurring within the western North Pacific and North Indian Oceans, which includes an in-depth analysis of tropical cyclones of note and all typhoons.
5. Cooperation with the Naval Environmental Prediction Research Facility (NEPRF), Monterey, California, on the operational evaluation of tropical cyclone models and forecast aids, and the development of new techniques to support operational forecast scenarios.

Satellite imagery used throughout this report represents data obtained by the tropical cyclone satellite surveillance network. The personnel of Detachment 1, 1WW, collocated with JTWC at Nimitz Hill, Guam, coordinate the satellite acquisitions and tropical cyclone surveillance with the following units:

Det 4, 20WS, Hickam AFB, Hawaii

Det 5, 20WS, Clark AB, RP

Det 8, 20WS, Kadena AB, Japan

Det 15, 30WS, Osan AB, Korea

Air Force Global Weather Central,
Offutt AFB, Nebraska

In addition, the Naval Oceanography Command Detachment, Diego Garcia, and Defense Meteorological Satellite Program (DMSP) equipped U.S. Navy aircraft carriers have been instrumental in providing vital satellite position fixes of tropical cyclones in the Indian Ocean.

Should JTWC become incapacitated, the Alternate Joint Typhoon Warning Center (AJTWC) located at the U.S. Naval Western Oceanography Center, Pearl Harbor, Hawaii, assumes warning responsibilities. Assistance in determining satellite reconnaissance requirements, and in obtaining the resultant data, is provided by Det 4, 20WS Hickam AFB, Hawaii.

Changes to this year's publication include: statistical verification for individual warnings for the North Indian Ocean and the southern hemisphere are provided. Again, as last year, raw fix data files previously printed in Annex A, plus the raw warning, forecast and best track data, will be available, upon request (the requested data will be copied onto 5.25 inch "floppy" diskettes provided by the requestor); and, with reference to best track philosophy, a conscious effort has been made to extend the post-warning best tracks to provide better verification for the 48- and 72-hour forecasts.

A special thanks is extended to the men and women of: 27th Information Systems Squadron, Operating Location C and the Operations section of the Naval Oceanography Command Center, Guam for their continuing support by providing high quality real-time satellite imagery; Marine Corps Air Station, Futenma, Japan for their satellite fix support; the Pacific Fleet Audio-Visual Center, Guam for their assistance in the reproduction of satellite data for this report; to the Navy Publications and Printing Service Branch Office, Guam; the Royal Observatory Hong Kong for supporting synoptic data on Super Typhoon Lynn (20W); the Central Weather Bureau, Taiwan for radar scope photographs of Typhoons Vernon (06W), Alex (08W) and Gerald (14W); Dr. Bob Abbey of the Office of Naval Research for his technical support to this publication; Mr. Michael Fiorino at NEPRF for his software conversion for the statistical programs; Mr. S.D. Rice, manager of Mobil Oil Micronesia, Inc. for his damage photos of Ulithi Atoll after Typhoon Orchid (01W); Dr. Greg Holland for sharing the ship's log account of Typhoon Lynn (20W); and Captain K. W. Reese (USAF) for the reconnaissance photograph of Typhoon Wynne (07W)

Note: Appendix IV contains information on how to obtain past issues of the Annual Tropical Cyclone Report (titled Annual Typhoon Report prior to 1980).

TABLE OF CONTENTS

CHAPTER I	OPERATIONAL PROCEDURES	PAGE			
	1. General	1			
	2. Data Sources	1			
	3. Communications	2			
	4. Analyses	3			
	5. Forecast Aids	3			
	6. Forecasting Procedures	3			
	7. Warnings	4			
	8. Prognostic Reasoning Messages	5			
	9. Tropical Cyclone Formation Alert	5			
	10. Significant Tropical Weather Advisory	5			
CHAPTER II	RECONNAISSANCE AND FIXES				
	1. General	7			
	2. Reconnaissance Availability	7			
	3. Aircraft Reconnaissance Summary	8			
	4. Satellite Reconnaissance Summary	9			
	5. Radar Reconnaissance Summary	10			
	6. Tropical Cyclone Fix Data	13			
CHAPTER III	SUMMARY OF WESTERN NORTH PACIFIC AND NORTH INDIAN OCEAN TROPICAL CYCLONES				
	1. General	17			
	2. Western North Pacific Tropical Cyclones	17			
INDIVIDUAL TROPICAL CYCLONES					
<u>TROPICAL CYCLONE</u>	<u>AUTHOR</u>	<u>PAGE</u>	<u>TROPICAL CYCLONE</u>	<u>AUTHOR</u>	<u>PAGE</u>
(01W) TY	ORCHID	GATANIS 24	(14W) TY	GERALD	MUNDELL 86
(02W) TS	PERCY	CROSBY 30	(15W) STY	HOLLY	CROSBY 92
(03W) TS	RUTH	FATJO 34	(16W) TY	IAN	FATJO 98
(04W) TY	SPERRY	HEISHMAN 36	(17W) TD	17W	HEISHMAN 104
(05W) STY	THELMA	DREKSLER 40	(02C) TY	PEKE	DREKSLER 106
(06W) TY	VERNON	WILLIAMS 44	(18W) TS	JUNE	HEISHMAN 110
(07W) TY	WYNNE	CROSBY 50	(19W) TY	KELLY	MUNDELL 112
(08W) TY	ALEX	FATJO 54	(20W) STY	LYNN	SCOVIL 116
(09W) STY	BETTY	HEISHMAN 62	(21W) TS	MAURY	DREKSLER 122
(10W) TY	CARY	DREKSLER 66	(02W) STY	NINA	PICKLE 124
(11W) STY	DINAH	STEWART 70	(23W) TS	OGDEN	HEISHMAN 132
(12W) TS	ED	SCOVIL 76	(24W) TY	PHYLLIS	FATJO 134
(13W) TY	FREDA	PICKLE 80			

3. North Indian Ocean Tropical Cyclones	138
---	-----

INDIVIDUAL TROPICAL CYCLONES

<u>TROPICAL CYCLONE</u>	<u>AUTHOR</u>	<u>PAGE</u>	<u>TROPICAL CYCLONE</u>	<u>AUTHOR</u>	<u>PAGE</u>
TC 01B	DREKSLER	140	TC 05B	STEWART	148
TC 02B	SCOVIL	142	TC 06B	CROSBY	150
TC 03A	PICKLE	144	TC 07A	MUNDELL	152
TC 04B	FATJO	146	TC 08B	FATJO	154
CHAPTER IV	SUMMARY OF SOUTH PACIFIC AND SOUTH INDIAN OCEAN TROPICAL CYCLONES				
	1. General	157			
	2. South Pacific and South Indian Ocean Tropical Cyclones	160			
CHAPTER V	SUMMARY OF FORECAST VERIFICATION				
	1. Annual Forecast Verification	163			
	2. Comparison of Objective Techniques	173			
CHAPTER VI	TROPICAL CYCLONE SUPPORT SUMMARY				
	1. Naval Environmental Research Prediction Facility	179			
	2. Joint Typhoon Warning Center	181			
ANNEX A	TROPICAL CYCLONE TRACK AND FIX DATA				
	1. General	183			
	2. Warning Verification Statistics	183			
APPENDICES	I. Definitions				
		209			
	II. Names of Tropical Cyclones				
		210			
	III. References				
		211			
	IV. Past Annual Tropical Cyclone Reports				
		213			

CONTRACTIONS

ABIO	Significant Tropical Weather Advisory for the Indian Ocean	CM	Centimeter	INJAH	North Indian Ocean Component of TYAN
ABPW	Significant Tropical Weather Advisory for the Western Pacific Ocean	COSMOS	Cyclops Objective Steering Model Output Statistics	INST	Instruction
ABS MAG	Absolute Magnitude	CPA	Closest Point of Approach	IR	Infrared
ACCRY	Accuracy	CSC	Cloud System Center	JTWC	Joint Typhoon Warning Center
ACFT	Aircraft	CSUM	Colorado State University (CSU84) Model	KM	Kilometer(s)
ADP	Automated Data Processing	CYCLOPS	Tropical Cyclone Steering Program (HATTRACK and MOHATT)	KT	Knot(s)
AFGWC	Air Force Global Weather Central	DEG	Degree	LLCC	Low-Level Circulation Center
AIREP	Aircraft Weather Report(s) (Commercial and Military)	DIR	Direction	LVL	Level
AOR	Area of Responsibility	DMSF	Defense Meteorological Satellite Program	M	Meter(s)
APT	Automatic Picture Transmission	DTG	Date Time Group	M/SEC	Meter(s) per Second
ARWO	Aerial Reconnaissance Weather Officer	FI	Forecast Intensity (Dvorak)	MAX	Maximum
AVG	Average	FLT	Flight	MB	Millibar(s)
AWN	Automated Weather Network	FNOC	Fleet Numerical Oceanography Center	MIN	Minimum
BPAC	Blended Persistence and Climatology	FT	Feet	MOHATT	Modified HATTRACK
BT LAT	Best Track Latitude	GMT	Greenwich Mean Time	MOVG	Moving
BT LON	Best Track Longitude	GOES	Geostationary Operational Environmental Satellite	MSLP	Minimum Sea-level Pressure
BT WN	Best Track Wind	HATTRACK	Hurricane and Typhoon Tracking and Steering Program	MSN	Mission
CDO	Central Dense Overcast	HGT	Height	NEDN	Naval Environmental Data Network
CI	Cirriform Cloud or Cirrus (or) Current Intensity (Dvorak)	HPAC	Mean of XTRP and CLIM Techniques (Half Persistence and Climatology)	NEDS	Naval Environmental Display Station
CINCPAC	Commander-in-Chief Pacific AF - Air Force, FLT - Navy	HR(S)	Hour(s)	NEPRF	Naval Environmental Prediction Research Facility
CLD	Cloud	ICAO	International Civil Aviation Organization	NESDIS	National Environmental Satellite, Data, and Information Service
CLIM	Climatology	INT	Initial		

NET	Near-Equatorial Trough	SLP	Sea-Level Pressure	TUTT	Tropical Upper-Tropospheric Trough
NM	Nautical Mile(s)	SRP	Selective Reconnaissance Program	ULAC	Upper-Level Anticyclone
NOAA	National Oceanic and Atmospheric Administration	STNRY	Stationary	ULCC	Upper-Level Circulation Center
NOCC	Naval Oceanography Command Center	SST	Sea Surface Temperature	VEL	Velocity
NOGAPS	Navy Operational Global Atmospheric Prediction System	ST	Subtropical	VIS	Visual
NORAPS	Navy Operational Regional Atmospheric Prediction System	STR	Subtropical Ridge	WESTPAC	Western (North) Pacific
NORAPS	Navy Operational Regional Atmospheric Prediction System	STY	Super Typhoon	WMO	World Meteorology Organization
NTCM	Nested Tropical Cyclone Model	TAPT	Typhoon Acceleration Prediction Technique	WND	Wind
NWOC	Naval Western Oceanography Center	TC	Tropical Cyclone	WRNG(S)	Warning(s)
NR	Number	TCARC	Tropical Cyclone Aircraft Reconnaissance Coordinator	WRS	Weather Reconnaissance Squadron
NRL	Naval Research Laboratory	TCFA	Tropical Cyclone Formation Alert	WW ER	Wind Warning Error
OBS	Observations	TCM	Tropical Cyclone Model	W#	Warning Number
OTCM	One Way (Interactive) Tropical Cyclone Model	TD	Tropical Depression	XTRP	Extrapolation
PACOM	Pacific Command	TDO	Typhoon Duty Officer	Z	Zulu Time (Greenwich Mean Time)
PCN	Position Code Number	TIROS	Television Infrared Observational Satellite	24 ER	24-Hour (Position) Error
POS ER	(Initial) Position Error	TPAC	Extrapolation and Climatology Blend	48 ER	48-Hour (Position) Error
RADOB	Radar Observation	TS	Tropical Storm	72 ER	72-Hour (Position) Error
RECON	Reconnaissance	TY	Typhoon	24 WE	24-Hour Wind (Warning) Error
RT	Right	TYAN	Typhoon Analog Program	48 WE	48-Hour Wind (Warning) Error
SAT	Satellite	TYFN	Western North Pacific Component (Revised) of TYAN	72 WE	72-Hour Wind (Warning) Error
SFC	Surface				

CHAPTER I - OPERATIONAL PROCEDURES

1. GENERAL

The Joint Typhoon Warning Center (JTWC) provides a variety of routine services to the organizations within its area of responsibility, including:

a. Significant Tropical Weather Advisories: issued daily, these products describe all tropical disturbances and assess their potential for further development during the advisory period;

b. Tropical Cyclone Formation Alerts: issued when synoptic, satellite and/or aircraft reconnaissance data indicate development of a significant tropical cyclone in a specified area is likely;

c. Tropical Cyclone Warnings: issued periodically throughout each day for significant tropical cyclones, giving forecasts of position and intensity of the system; and

d. Prognostic Reasoning Messages: issued twice daily for tropical storms and typhoons in the western North Pacific; these messages discuss the rationale behind the most recent JTWC warnings.

The recipients of the services of JTWC essentially determine the content of JTWC's products according to their ever changing requirements. Therefore, the spectrum of routine services is subject to change from year to year. Such changes are usually the result of deliberations held at the Annual Tropical Cyclone Conference.

2. DATA SOURCES

a. COMPUTER PRODUCTS:

A standard array of synoptic-scale computer analyses and prognostic charts are available from the Fleet Numerical Oceanography Center (FLENUMOCEANCEN) at Monterey, California. These products are provided to JTWC via the Naval Environmental Data Network (NEDN).

b. CONVENTIONAL DATA:

This data set is comprised of land-based and shipboard surface and upper-air observations taken at, or near, synoptic times, cloud-motion winds derived twice daily from satellite data, and enroute meteorological observations from commercial and military aircraft (AIREPS) within six hours of synoptic times. Conventional data charts are prepared daily at 0000Z and 1200Z using computer- and hand-plotted data for the surface/gradient and 200 mb (upper-tropospheric) levels. In addition to these analyses, charts at the 925, 850, 700, 500 and 400 mb levels are computer-plotted from rawinsonde/pibal observations at the 12-hour synoptic times.

c. AIRCRAFT RECONNAISSANCE:

Data provided by aircraft weather reconnaissance are invaluable for locating the position of the center of developing systems and essential for the accurate determination of:

- maximum surface and flight-level wind
- minimum sea-level pressure
- horizontal surface and flight-level wind distribution
- eye/center temperature and dew point

In addition, wind and pressure-height data at the 500 and/or 400 mb levels, provided by the aircraft while enroute to, or from fix missions, or during dedicated synoptic-scale flights, provide a valuable supplement to the all too sparse data fields of JTWC's area of responsibility. A more detailed discussion of aircraft weather reconnaissance is presented in Chapter II.

d. SATELLITE RECONNAISSANCE:

Meteorological satellite data obtained from the Defense Meteorological Satellite Program (DMSP) and National Oceanic and Atmospheric Administration (NOAA) spacecraft played a major role in the early

detection and tracking of tropical cyclones in 1987. A discussion of the role of these programs is presented in Chapter II.

e. RADAR RECONNAISSANCE:

During 1987, as in previous years, land-based radar coverage was utilized extensively when available. Once a tropical cyclone moved within the range of land-based radar sites, their reports were essential for determination of small-scale movement. Use of radar reports during 1987 is discussed in Chapter II.

f. DRIFTING METEOROLOGICAL BUOYS:

JTWC received wind speed, sea-level pressure, sea surface temperature and air temperature reports from six drifting meteorological buoys deployed by the U. S. Navy beginning in the middle of June 1987. One line of three buoys was deployed along 7 degrees North Latitude from south of Guam eastward toward the Marshall Islands. Another set of three was deployed along 11 degrees North Latitude from southwest of Guam eastward through the Caroline Islands. The buoys performed flawlessly throughout most of the western North Pacific tropical cyclone season. At the end of the year, four buoys continued to operate, one no longer transmitted data and another was apparently taken to Tandag City, Mindanao, R.P., where it continued to transmit. The three northernmost buoys tracked basically westward and covered 25 to 35 degrees of longitude. The southern buoys drifted more slowly and erratically. One buoy either snagged its drouge on a submerged reef east of Woleai Atoll or became trapped in an eddy within the island/reef chain.

JTWC received at least one position update from each buoy per day and up to eight meteorological data updates per buoy per day. Buoy data were consistent with the data from other conventional sources to the extent that they was considered to be, in most cases, more reliable and more accurate than ship reports and some island reporting stations. As a backup and position check, JTWC also received buoy data, on a delay basis, over the AWN (Manop header SSVX6 LFPW).

An expanded buoy network for the 1988 tropical cyclone season is being planned.

a. JTWC currently has access to three primary communications circuits.

3. COMMUNICATIONS

(1) The Automated Digital Network (AUTODIN) is used for dissemination of warnings, alerts and other related bulletins to Department of Defense installations. These messages are relayed for further transmission over U.S. Navy Fleet Broadcasts, and U.S. Coast Guard CW (continuous wave Morse Code) and voice broadcasts. Inbound message traffic for JTWC is received via AUTODIN addressed to NAVOCEANCOMCEN GQ or DET 1, 1WW NIMITZ HILL GQ.

(2) The Air Force Automated Weather Network (AWN) provides weather data to JTWC through a dedicated circuit from the Automated Digital Weather Switch (ADWS) at Hickam AFB, Hawaii. The ADWS selects and routes the large volume meteorological reports necessary to satisfy JTWC requirements for the right data at the right time. Weather bulletins prepared by JTWC are inserted into the AWN circuit via the Naval Environmental Display Station (NEDS) through the Nimitz Hill Naval Telecommunications Center (NTCC) of the Naval Communications Area Master Station Western Pacific.

(3) The Naval Environmental Data Network (NEDN) is the communications link with the computers at FLENUMOCEANCEN. JTWC is able to receive environmental data from FLENUMOCEANCEN and provide data directly to the computers to execute numerical techniques.

b. NEDS has been the backbone of the JTWC communications system for several years. Currently, JTWC is undergoing an upgrade that will make use of microcomputer technology and automate much of the work that goes into message preparation and transmission. This will decrease the work load on the NEDS and allow JTWC to interface directly with NTCC for AWN and AUTODIN messages.

4. ANALYSES

A composite surface/gradient-level (3000 ft (914 m)) manual analysis of the JTWC area of responsibility is accomplished daily on the 0000Z and 1200Z conventional data. Analysis of the wind field using streamlines is stressed for tropical and subtropical regions. Analysis of the pressure field outside the tropics is accomplished routinely by the Naval Oceanography Command Center Operations watch team and is used by JTWC in conjunction with their analysis of the tropical wind fields.

A composite upper-tropospheric manual streamline analysis is accomplished daily utilizing rawinsonde data from 300 mb through 100 mb, winds obtained from satellite-derived cloud motion analysis, and AIREPS (taken plus or minus three hours of chart valid time) at or above 31,000 feet (9,449m). Wind and height data are used to generate a representative analysis of tropical cyclone outflow patterns, mid-latitude steering currents, and features that may influence tropical cyclone intensity. All charts are hand-plotted in the tropics to provide all available data as soon as possible to the Typhoon Duty Officer (TDO). These charts are augmented by computer-plotted charts for the final analysis.

Computer-plotted charts for the 925, 850, 700, 500 and 400 mb levels are available for streamline and/or height-change analysis from the 0000Z and 1200Z data base. Additional sectional charts at intermediate synoptic times and auxiliary charts, such as station-time plot diagrams and pressure-change charts, are also analyzed during periods of significant tropical cyclone activity.

5. FORECAST AIDS

The following objective techniques were employed in tropical cyclone forecasting during 1987 (a description of these techniques is presented in Chapter V):

a. MOVEMENT

- (1) 12-HOUR EXTRAPOLATION
- (2) CLIMATOLOGY
- (3) COSMOS (Model Output Statistics)
- (4) CSUM (Colorado State University Model)
- (5) OTCM (Dynamic Model)
- (6) TAPT (Empirical)
- (7) HPAC (Half Persistence - Half Climatology Blend)
- (8) TYAN78 (Analog)

b. INTENSITY

- (1) CLIMATOLOGY
- (2) DVORAK (Empirical)
- (3) THETA -E (Empirical)

c. WIND RADIUS (Analytical)

6. FORECAST PROCEDURES

a. INITIAL POSITIONING

The warning position is the best estimate of the center of the surface circulation at synoptic time. It is estimated from an analysis of all fix information received up to one and one-half hours after synoptic time. This analysis is based on a semi-objective weighting of fix information based on the historical accuracy of the fix platform and the meteorological features used for the fix. The interpolated warning position reduces the weighting of any single fix and results in a more consistent movement and a warning position that is more representative of the larger-scale circulation. If the fix data are not available due to reconnaissance platform malfunction or communication problems, synoptic data or extrapolation from previous fixes are used.

b. TRACK FORECASTING

A preliminary forecast track is developed based on an evaluation of the rationale behind the previous warning and the guidance given by the most recent set of objective techniques and numerical prognoses. This preliminary track is then subjectively modified based on the following considerations:

(1) The prospects for recurvature or erratic movement are evaluated. This determination is based primarily on the present and forecast positions and amplitudes of the middle-tropospheric, mid-latitude troughs and ridges as depicted on the latest upper-air analysis and numerical forecasts.

(2) Determination of the best steering level is partly influenced by the maturity and vertical extent of the tropical cyclone. For mature tropical cyclones located south of the subtropical ridge axis, forecast changes in speed of movement are closely correlated with anticipated changes in the intensity or relative position of the ridge. When steering currents are relatively weak, the tendency for tropical cyclones to move northward due to internal forces is an important consideration.

(3) Over the 12- to 72-hour (12- to 48-hour in the southern hemisphere) forecast period, speed of movement during the early forecast period is usually biased towards persistence, while the later forecast periods are biased towards objective techniques. When a tropical cyclone moves poleward, and toward the mid-latitude steering currents, speed of movement becomes increasingly more biased toward a selective group of objective techniques capable of estimating acceleration.

(4) The proximity of the tropical cyclone to other tropical cyclones is closely evaluated to determine if there is a possibility of binary interaction.

A final check is made against climatology to determine whether the forecast track is reasonable. If the forecast deviates greatly from one of the climatological tracks, the forecast rationale may be reappraised.

c. INTENSITY FORECASTING

For this parameter, heavy reliance is placed on intensity trends from aircraft reconnaissance reports when available, wind and pressure data from ships and land stations in the vicinity of the tropical cyclone, the Dvorak satellite empirical model and climatology. An evaluation of the entire synoptic situation is made, including the location of major troughs and ridges, the position and intensity of any nearby tropical upper-tropospheric troughs (TUTTs), the vertical and horizontal extent of the tropical cyclone's circulation and the extent of the associated upper-level outflow pattern. An essential element affecting each intensity forecast is the accompanying forecast track and the environmental influences along that track, such as terrain, vertical wind shear, and the existence of an extratropical environment.

d. WIND RADII FORECASTING

Once the forecast intensities have been derived, the horizontal distribution of surface winds (winds greater than 30-, 50-, and 100-kt) is determined. The most recent wind radii and associated asymmetrics are deduced from all available surface wind observations and reconnaissance aircraft reports. Based on the current surface wind distribution, preliminary estimates of future wind radii are provided by an empirically derived objective technique (Holland, 1980). These estimates may be subjectively modified based upon the anticipated interaction of the tropical cyclone's circulation with forecast locations of large-scale wind regimes and significant land masses. Other factors including the tropical cyclone's speed of movement and possible extratropical transition are also considered.

7. WARNINGS

Tropical cyclone warnings are issued when a closed circulation is evident and maximum sustained winds are forecast to increase to 34 kt (18 m/sec) within 48-hours, or if the tropical cyclone is in such a position that life or property may be endangered within 72-hours. Warnings may also be issued in other situations if it is determined that there is a need

to alert military or civil interests to threatening tropical weather conditions.

Each tropical cyclone warning is numbered sequentially and includes the following information: the position of the surface center; estimate of the position accuracy and the supporting reconnaissance (fix) platforms; the direction and speed of movement during the past six hours (past 12-hours in the southern hemisphere); the intensity and radial extent of over 30-, 50-, and 100-knot surface winds, when applicable. At forecast intervals of 12-, 24-, 48-, and 72-hours (12-, 24-, and 48-hours in the southern hemisphere), information on the tropical cyclone's anticipated position, intensity and wind radii are also provided. Vectors indicating the mean direction and mean speed between forecast positions are also included in all warnings.

Warnings in the western North Pacific and North Indian Oceans are issued every six hours valid at standard times; 0000Z, 0600Z, 1200Z and 1800Z (every 12-hours; 0000Z, 1200Z or 0600Z, 1800Z in the southern hemisphere). All warnings are released to the communications network no earlier than synoptic time and no later than synoptic time plus two and one-half hours so that recipients will have a reasonable expectation of having all warnings "in hand" by synoptic time plus three hours (0300Z, 0900Z, 1500Z and 2100Z).

Warning forecast positions are later verified against the corresponding "best track" positions (obtained during detailed post-storm analysis to determine the actual path and intensity of the cyclone). A summary of the verification results for 1987 is present in Chapter V.

8. PROGNOSTIC REASONING MESSAGES

For tropical storms and typhoons in the western North Pacific Ocean, prognostic reasoning messages are transmitted following the 0000Z and 1200Z warnings, or whenever the previous forecast reasoning is no longer valid. This plain language message is intended to provide meteorologists with the reasoning behind the latest forecast.

In addition to this message, prognostic reasoning information applicable to all customers is provided in the remarks section of warnings when significant forecast changes are made or when deemed appropriate by the TDO.

9. TROPICAL CYCLONE FORMATION ALERTS

Tropical Cyclone Formation Alerts (TCFAs) are issued whenever interpretation of satellite imagery and other meteorological data indicate that the formation of a significant tropical cyclone is likely. These formation alerts will specify a valid period not to exceed twenty-four hours and must either be cancelled, reissued, or superseded by a tropical cyclone warning prior to the expiration of the valid time.

10. SIGNIFICANT TROPICAL WEATHER ADVISORIES

This product contains a general, non-technical description of all tropical disturbances in JTWC's area of responsibility (AOR) and an assessment of their potential for further (tropical cyclone) development. In addition, all tropical cyclones in warning status are briefly discussed. Two separate messages are issued daily and are valid for a 24-hour period. The Significant Tropical Weather Advisory for the western Pacific Ocean (ABPW PGTW) covers the area east of 100 degrees East Longitude to the dateline and is issued by 0600Z. The Significant Tropical Weather Advisory for the Indian Ocean (ABIO PGTW) covers the area west of 100 degrees East Longitude to the coast of Africa and is issued by 1800Z. It is reissued whenever the situation warrants. For each suspect area, the words "poor", "fair", and "good" are used to describe the potential for development. "Poor" will be used to describe a tropical disturbance in which meteorological conditions are currently unfavorable for development; "fair" will be used to describe a tropical disturbance in which the meteorological conditions are favorable for development but significant development has not commenced; and "good" will be used to describe the potential for development of a tropical disturbance covered by a TCFA.

CHAPTER II - RECONNAISSANCE AND FIXES

1. GENERAL

The Joint Typhoon Warning Center depends on reconnaissance to provide necessary, accurate, and timely meteorological information in support of each warning. JTWC relies primarily on three reconnaissance platforms: aircraft, satellite, and radar. In data rich areas, synoptic data are also used to supplement the above. Optimum utilization of all available reconnaissance resources is obtained through the Selective Reconnaissance Program (SRP); various factors are considered in selecting a specific reconnaissance platform including capabilities and limitations, and the tropical cyclone's threat to life and property both afloat and ashore. A summary of reconnaissance fixes received during 1987 is included in Section 6 of this chapter.

2. RECONNAISSANCE AVAILABILITY

a. Aircraft

Aircraft weather reconnaissance for JTWC was performed by the 54th Weather Reconnaissance Squadron (54th WRS) located at Andersen Air Force Base, Guam. Due to budgetary decisions, 1987 was the final year for dedicated weather reconnaissance in the western North Pacific. The 54th WRS was deactivated effective 1 October 1987. The phaseout of aircraft and personnel began well before the actual deactivation of the squadron and effected aircraft availability from the very beginning of the tropical cyclone season. Only four aircraft were on station at the start of the year, three of which were storm-capable. One storm-capable aircraft was transferred to Keesler Air Force Base, Mississippi on 15 July leaving just two capable airframes to fly reconnaissance missions up to the date of deactivation. The shortage of both aircraft and personnel significantly limited the number of reconnaissance missions that the 54th WRS was able to fly throughout the season until closure. The JTWC aircraft reconnaissance requirements were provided daily to the Tropical Cyclone Aircraft Reconnaissance Coordinator (TCARC). The TCARC then married the tasking from

JTWC with the available airframes from the 54th WRS.

As in the previous years, aircraft reconnaissance provided direct measurements of standard pressure-level heights, temperatures, flight-level winds, sea-level pressures, estimated surface winds and numerous additional parameters. The meteorological data were gathered by the Aerial Reconnaissance Weather Officer and dropsonde operators from Detachment 3, 1st Weather Wing who flew with the 54th WRS. These data provided the Typhoon Duty Officer with indications of changing tropical cyclone characteristics, radii of associated winds and current tropical cyclone position and intensity. Another important aspect was the availability of the data for research on tropical cyclone analysis and forecasting.

b. Satellite

Satellite fixes from USAF/USN ground sites and USN ships provide day and night coverage in JTWC's area of responsibility. Interpretation of this satellite imagery provides tropical cyclone positions and estimates of current and forecast intensities through the Dvorak technique.

c. Radar

Land-based radar provides positioning data on well-developed tropical cyclones when in the proximity (usually within 175 nm (324 km)) of the radar sites in the Philippines, Taiwan, Hong Kong, Japan, South Korea, Kwajalein, and Guam.

d. Synoptic

JTWC also determines tropical cyclone positions based on the analysis of the surface/gradient-level synoptic data. These positions were helpful in situations where the vertical structure of the tropical cyclone was weak or accurate surface positions from aircraft or satellite were not available.

TABLE 2-1. AIRCRAFT RECONNAISSANCE EFFECTIVENESS

MISSIONS	TASKED	COMPLETED	MISSED	PERCENT
FIXES	68	57	11	82.9%
INVESTS	20	16	4	76.6%
SYNOPTIC TRACKS	8	7	1	87.5%

MISSION EFFECTIVENESS GRADING

	TOTAL	PERCENT
FIX MISSIONS TASKED	68	-----
SATISFACTORY	55	81.0%
DEGRADED (BUT SATISFACTORY)	6	8.8%
UNSATISFACTORY	13	19.0%

LEVIED VS. MISSED FIXES

	LEVIED	MISSED	PERCENT
AVERAGE 1965-1970	507	10	2
1971	802	61	2
1972	624	126	20.2
1973	227	13	5.7
1974	358	30	8.4
1975	217	7	3.2
1976	317	11	3.5
1977	203	3	1.5
1978	290	2	0.7
1979	289	14	3
1980	213	4	1.9
1981	201	3	1.5
1982	276	17	6.2
1983	157	3	1.9
1984	210	2	1
* 1985	210	14	6.7
1986	250	10	4.0
1987	68	11	17.1

* CORRECTED DATA FOR 1985

3. AIRCRAFT RECONNAISSANCE SUMMARY

During 1987, JTWC levied requirements for 68 vortex fixes and 20 investigative missions of which only 1 was flown into a disturbance which did not develop. In addition to the levied fixes, 54 intermediate fixes were obtained. Two airborne radar fixes were provided from C-141 aircraft of opportunity missions which are not included in the statistics below. Eight synoptic track missions were requested, seven of which were completed. The synoptic tracks provide mid-level steering flow information. The average position error for the combined fixes during the 1987 season was 12 nm (22 km).

Aircraft reconnaissance effectiveness for the 1987 season is summarized in Table 2-1. The grading criteria is based on the Mission Effectiveness Grading (MEG) system which was developed and employed for the first time in 1986. This system grades the performance of each mission as satisfactory, degraded but satisfactory, unsatisfactory or missed. A mission could be degraded if certain critical weather parameters were not obtained such as temperature, dew point, minimum sea-level pressure, flight-level height in meters, etc. If the required time constraints between the primary and intermediate fixes were not met, the mission could still be deemed satisfactory but degraded.

4. SATELLITE RECONNAISSANCE SUMMARY

The Air Force provides satellite reconnaissance support to JTWC through a tropical cyclone satellite surveillance network consisting of both tactical and centralized facilities. Tactical DMSP sites monitoring DMSP, NOAA and geostationary satellite data are located at Nimitz Hill, Guam; Clark AB, Republic of the Philippines; Kadena AB, Okinawa, Japan; Osan AB, Republic of Korea; and Hickam AFB, Hawaii. These sites provide a combined coverage that includes most of JTWC's area of responsibility in the western North Pacific from near the dateline westward to the Malay Peninsula. For the remainder of its AOR, JTWC relies on the Air Force Global Weather Central (AFGWC) to provide coverage using stored satellite data. The Naval Oceanography Command Detachment, Diego Garcia, provides NOAA polar orbiting coverage in the central Indian Ocean as a supplement to this support. U.S. Navy ships equipped for direct readout also provide supplementary support.

AFGWC, located at Offutt AFB, Nebraska, is the centralized member of the tropical cyclone satellite surveillance network. In support of JTWC, AFGWC processes stored imagery from DMSP and NOAA spacecraft. Imagery recorded onboard the spacecraft as they pass over the earth is later down-linked to AFGWC via a network of command readout sites and communication satellites. This enables AFGWC to obtain the coverage necessary to fix all tropical systems of interest to JTWC. AFGWC has the primary responsibility to provide tropical cyclone surveillance over the entire Indian Ocean, southwest Pacific, and the area near the dateline. Additionally, AFGWC can be tasked to provide tropical cyclone positions in the entire western North Pacific as backup to coverage routinely available in that region.

The hub of the network is Detachment 1, First Weather Wing (Det 1, 1WW), colocated with JTWC on Nimitz Hill, Guam. Based on available satellite coverage, Det 1, 1WW is responsible for coordinating satellite reconnaissance requirements with JTWC and tasking

the individual network sites for the necessary tropical cyclone fixes, intensity estimates and forecast intensities. When a particular fix is important to the development of JTWC's next tropical cyclone warning, two sites are tasked to fix the tropical cyclone from the same satellite pass. This "dual-site" concept provides the necessary redundancy to virtually guarantee JTWC an accurate satellite fix on the tropical cyclone.

The network provides JTWC with several products and services. The main service is one of monitoring its AOR for indications of tropical cyclone development. If an area exhibits the potential for development, JTWC is notified. Once JTWC issues either a Tropical Cyclone Formation Alert or warning, the network is tasked to provide three products: tropical cyclone positions, intensity estimates and forecast intensities. Each satellite tropical cyclone position is assigned a Position Code Number (PCN) to indicate the accuracy of the fix position. This is determined by the availability of visible landmarks in the image for precise gridding, and the degree of organization of the tropical cyclone's cloud system (Table 2-2).

TABLE 2-2. POSITION CODE NUMBERS (PCN)

PCN METHOD OF CENTER DETERMINATION/GRIDDING

1	EYE/GEOGRAPHY
2	EYE/EPHEMERIS
3	WELL-DEFINED CIRCULATION CENTER/GEOGRAPHY
4	WELL-DEFINED CIRCULATION CENTER/EPHEMERIS
5	POORLY DEFINED CIRCULATION CENTER/GEOGRAPHY
6	POORLY DEFINED CIRCULATION CENTER/EPHEMERIS

During 1987, Detachment 1, First Weather Wing increased the number of estimates of the tropical cyclone's current intensity from two to four per day once a Tropical Cyclone Formation Alert or tropical cyclone warning was issued. Intensity estimates and 24-hour intensity forecasts were made using the Dvorak technique (NOAA Technical Report

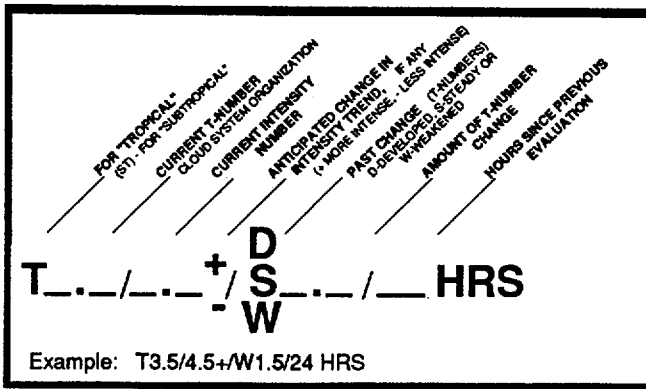
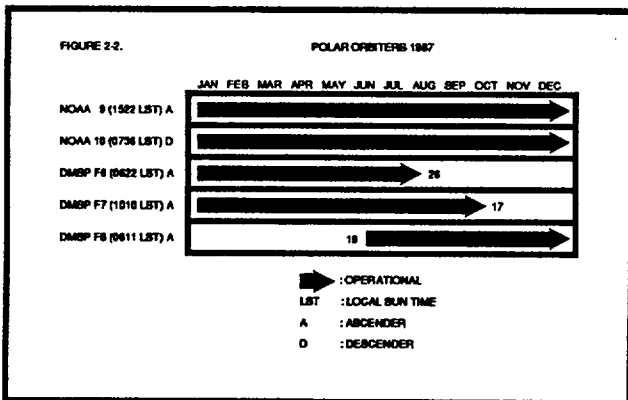


Figure 2-1. Dvorak code for communicating estimates of current and forecast intensity derived from satellite data. In the example, the current 'T-number' is 3.5, but the current intensity is 4.5 (equivalent to 77 kt (40 m/sec)). The cloud system has weakened by 1.5 'T-numbers' since the previous evaluation conducted 24-hours earlier. The plus (+) symbol indicates an expected reversal of the weakening trend or very little further weakening of the tropical cyclone during the next 24-hour period.

NESDIS 11) for both visual and enhanced infrared imagery (Figure 2-1).

Figure 2-2 shows the status of operational polar orbiting spacecraft. Three Defense Meteorological Satellite Program (DMSP) spacecraft were operational in 1987. The 19543 (F8) satellite was launched in June as a replacement for the aging 17540 (F6) spacecraft. The imaging instrument on the 18541 (F7) spacecraft failed on 17 October, which left only one DMSP spacecraft for support during the remainder of the tropical cyclone season. The special passive sensor, microwave imager (SSM/I) on the F8 spacecraft performed well until overheating forced the sensor to be temporarily shut down on 3



December. The NOAA 9 and NOAA 10 spacecraft performed well throughout the year.

On 16 August with the loss of dedicated aircraft reconnaissance, data from the satellite reconnaissance network became the primary input to warnings and best tracks in the western North Pacific. This heightened emphasis on satellite data resulted in an increase from 60 percent (in 1986) to 88 percent of warnings based on satellite.

During 1987, the satellite reconnaissance network provided JTWC with a record total of 2,835 satellite fixes on 25 tropical cyclones in the western North Pacific Ocean. In addition, 311 fixes were made on tropical cyclones in the North Indian Ocean, more than eight times the total for 1986. For the southern hemisphere, 1,192 satellite fixes were provided. A comparison of those fixes in the JTWC area of responsibility and their corresponding JTWC best track is shown in Tables 2-3A and 2-3B. (Note: Those fixes which were out-of-limits when compared with the best track are not included.)

The relationship between tropical cyclone "T-number", maximum surface wind speed and minimum sea-level pressure is outlined in Table 2-4. Table 2-5A, B and C address the verification of satellite-derived intensity estimates for developing, weakening and all cases of tropical cyclones, respectively. In each table the first column states the "T-number" in parentheses and expected current and forecast intensity. The verifying average intensities from the current and 24-hour best tracks are included to the right in the second and third columns, respectively.

5. RADAR RECONNAISSANCE SUMMARY

Fifteen of the twenty-five significant tropical cyclones in the western North Pacific during 1987 passed within range of land-based radar with sufficient cloud pattern organization to be fixed. The land-based radar fixes that were obtained and transmitted to JTWC totaled 806. Only one radar fix was obtained by reconnaissance aircraft.

TABLE 2-3A. MEAN DEVIATION (NM) OF ALL SATELLITE DERIVED TROPICAL CYCLONE POSITIONS FROM THE JTWC BEST TRACK POSITIONS IN THE WESTERN NORTH PACIFIC AND NORTH INDIAN OCEANS. NUMBER OF CASES (IN PARENTHESES).

PCN	WESTERN NORTH PACIFIC OCEAN		NORTH INDIAN OCEAN	
	1977-1986 AVERAGE	1987	1980-1986 AVERAGE	1987
	(ALL SITES)	(ALL SITES)	(ALL SITES)	(ALL SITES)
1	14.2 (1689)	14.9 (182)	16.7 (40)	20.6 (2)
2	16.3 (2118)	13.0 (511)	18.9 (7)	10.0 (2)
3	21.3 (2410)	21.4 (219)	24.1 (22)	26.0 (12)
4	23.9 (1546)	18.7 (576)	58.3 (10)	33.1 (11)
5	37.8 (4456)	32.6 (195)	36.3 (232)	44.1 (81)
6	39.5 (4222)	34.6 (1048)	44.2 (225)	36.1 (192)
1&2	15.4 (3807)	13.5 (693)	17.2 (47)	15.3 (4)
3&4	22.3 (3956)	19.5 (795)	34.8 (32)	29.4 (23)
5&6	38.6 (8678)	34.6 (1243)	40.2 (457)	38.5 (273)
TOTAL	29.3 (16441)	24.2 (2731)	37.9 (536)	37.5 (300)

TABLE 2-3B
MEAN DEVIATION (NM) OF ALL SATELLITE-DERIVED TROPICAL CYCLONE POSITIONS IN THE SOUTH PACIFIC AND SOUTH INDIAN OCEANS. NUMBER OF CASES ARE IN PARENTHESES.

PCN	1985 - 1986 AVERAGE		1987	
		(ALL SITES)		(ALL SITES)
1	17.6 (68)	14.5 (14)		
2	15.5 (312)	17.4 (130)		
3	33.7 (97)	40.4 (15)		
4	27.2 (301)	26.5 (107)		
5	46.8 (399)	28.8 (75)		
6	38.1 (2152)	32.9 (786)		
1 & 2	15.9 (380)	17.3 (144)		
3 & 4	28.8 (398)	28.2 (122)		
5 & 6	39.5 (2551)	32.6 (861)		
TOTALS	35.5 (3329)	30.1 (1127)		

TABLE 2-4. MAXIMUM SUSTAINED WIND SPEED (KT) AS A FUNCTION OF DVORAK CI & FI (CURRENT AND FORECAST INTENSITY) NUMBER AND MINIMUM SEA-LEVEL PRESSURE (MSLP)

TROPICAL CYCLONE INTENSITY NUMBER	WIND SPEED	MSLP (NW PACIFIC)
0.0	<25	----
0.5	25	----
1.0	25	----
1.5	25	----
2.0	30	1000
2.5	35	997
3.0	45	991
3.5	55	984
4.0	65	976
4.5	77	966
5.0	90	954
5.5	102	941
6.0	115	927
6.5	127	914
7.0	140	898
7.5	155	879
8.0	170	858

TABLE 2-5A. DEVELOPING STAGE				TABLE 2-5B. WEAKENING STAGE			
CURRENT OR FORECAST INTENSITY*		VERIFYING AVERAGE BT INTENSITY	VERIFYING AVE 24HR BT INTENSITY	CURRENT OR FORECAST INTENSITY*		VERIFYING AVERAGE BT INTENSITY	VERIFYING AVE 24HR BT INTENSITY
(T #)	KT	KT	KT	(T #)	KT	KT	KT
(0.0)	<25	---	---	(0.0)	<25	---	---
(1.0)	25	22	28	(1.0)	25	19	14
(1.5)	25	25	31	(1.5)	25	27	22
(2.0)	30	30	37	(2.0)	30	30	24
(2.5)	35	35	47	(2.5)	35	38	30
(3.0)	45	47	65	(3.0)	45	43	31
(3.5)	55	57	75	(3.5)	55	57	40
(4.0)	65	65	80	(4.0)	65	65	50
(4.5)	77	75	92	(4.5)	77	77	53
(5.0)	90	88	110	(5.0)	90	88	70
(5.5)	102	102	110	(5.5)	102	98	75
(6.0)	115	115	122	(6.0)	115	113	90
(6.5)	127	127	123	(6.5)	127	123	108
(7.0)	140	138	115	(7.0)	140	133	114
(7.5)	155	---	---	(7.5)	155	---	---
(8.0)	170	---	---	(8.0)	170	---	---

* DVORAK, 1984

TABLE 2-5C.

ALL CASES

CURRENT OR FORECAST INTENSITY*		VERIFYING AVERAGE BT INTENSITY	VERIFYING AVE 24HR BT INTENSITY
(T #)	KT	KT	KT
(0.0)	<25	---	---
(1.0)	25	22	26
(1.5)	25	25	29
(2.0)	30	29	33
(2.5)	35	36	41
(3.0)	45	46	55
(3.5)	55	57	59
(4.0)	65	65	65
(4.5)	77	76	76
(5.0)	90	88	88
(5.5)	102	99	88
(6.0)	115	114	101
(6.5)	127	125	114
(7.0)	140	135	114
(7.5)	155	---	---
(8.0)	170	---	---

* DVORAK, 1984

The WMO radar code defines three categories of accuracy: good (within 10 km (5 nm)), fair (within 10-30 km (5-16 nm)), and poor (within 30-50 km (16-27 nm)). Of the 807 radar fixes coded in this manner; 309 were good, 190 were fair, and 308 were poor. Compared to JTWC's best track, the mean vector deviation for land-based radar sites was 19 nm (35 km). Excellent support through timely and accurate radar fix positioning allowed JTWC to track and forecast tropical cyclone movement through even the most difficult erratic tracks.

6. TROPICAL CYCLONE FIX DATA

As in previous years, no radar reports were received on North Indian Ocean tropical cyclones.

A total of 3,754 fixes on twenty-five western North Pacific tropical cyclones and 311 fixes on eight North Indian Ocean tropical cyclones were received at JTWC. Table 2-6A, Fix Platform Summary, delineates the number of fixes per platform for each individual tropical cyclone. Season totals and percentages are also indicated. (Table 2-6B provides the same information for the South Pacific and South Indian Oceans.)

TABLE 2-6A.

FIX PLATFORM SUMMARY FOR 1987

WESTERN NORTH PACIFIC	AIRCRAFT	SATELLITE	RADAR	SYNOPTIC	TOTAL
TY ORCHID (01W)	17	100	0	0	117
TS PERCY (02W)	4	60	0	0	64
TS RUTH (03W)	0	41	20	0	61
TS SPERRY (04W)	12	82	8	0	102
STY THELMA (05W)	24	141	72	0	237
TS VERNON (06W)	11	97	27	0	135
TY WYNNE (07W)	21	198	41	0	260
TY ALEX (08W)	1	100	77	0	178
STY BETTY (09W)	13	144	71	0	228
TY CARY (10W)	9	181	72	0	262
STY DINAH (11W)	0	159	106	0	265
TS ED (12W)	0	68	0	0	68
TY FREDA (13W)	0	176	29	0	205
TY GERALD (14W)	0	119	81	0	200
STY HOLLY (15W)	0	151	0	0	151
TY IAN (16W)	0	138	5	0	143
TD 17W (17W)	0	30	0	0	30
TY PEKE (02C)	0	131	0	0	131
TS JUNE (18W)	0	43	0	0	43
TY KELLY (19W)	0	111	63	0	174
STY LYNN (20W)	0	159	56	0	215
TS MAURY (21W)	0	95	0	0	95
STY NINA (22W)	0	176	79	0	255
TS OGDEN (23W)	0	17	0	0	17
TY PHYLLIS (24W)	0	118	0	0	118
TOTALS	112	2835	807	0	3754
% OF TOTAL NR OF FIXES	3.0%	75.5%	21.5%	0.0%	100.0%

NORTH INDIAN OCEAN	SATELLITE	SYNOPTIC	TOTALS
TC 01B	59	0	59
TC 02B	59	0	59
TC 03A	38	0	38
TC 04B	15	0	15
TC 05B	43	0	43
TC 06B	32	0	32
TC 07A	16	0	16
TC 08B	49	0	49
TOTALS	311	0	311
% OF TOTAL NR OF FIXES	100.0%	0.0%	100.0%

TABLE 2-6B. FIX PLATFORM SUMMARY FOR 1987

THE SOUTH PACIFIC AND SOUTH INDIAN OCEANS	SATELLITE	RADAR	SYNOPTIC	TOTAL
TC 01S -----	21	0	0	21
TC 02P OSEA	59	0	0	59
TC 03P PATSY	69	0	0	69
TC 04P RAJA	113	0	0	113
TC 05P SALLY	32	0	0	32
TC 06S -----	26	0	0	26
TC 07S -----	45	0	0	45
TC 08P TUSI	21	0	0	21
TC 09S ALININA	39	0	0	39
TC 10S CONNIE	55	0	0	55
TC 11P IRMA	32	0	0	32
TC 12S DAMIEN	59	0	0	59
TC 13P -----	8	0	0	8*
TC 14P UMA	34	0	0	34
TC 15P JASON	67	0	0	67
TC 16P VELI	10	0	0	10
TC 17S CLOTILDA	21	0	0	21
TC 18S ELSIE	53	0	1	54
TC 19P -----	1	0	0	1*
TC 20P WINI	21	0	0	21
TC 21S DAODO	71	0	0	71
TC 22P YALI	58	0	0	58
TC 23P KAY	118	0	0	118
TC 24S -----	29	0	0	29
TC 25P ZUMAN	15	0	0	15
TC 26S -----	20	0	0	20
TC 27P BLANCHE	70	0	0	70
TC 28S -----	25	0	0	25
TOTAL	1192	0	1	1193
# OF TOTAL NR OF FIXES	99.9%	0.0%	0.1%	100.0%

* Incomplete data set

CHAPTER III - SUMMARY OF WESTERN NORTH PACIFIC AND NORTH INDIAN OCEAN TROPICAL CYCLONES

1. GENERAL

During the calendar year 1987, JTWC issued warnings on 25 different significant tropical cyclones in the western North Pacific -- six super typhoons, 12 typhoons, six tropical storms and one tropical depression. This includes one typhoon, Peke (02C), which initially developed in the central North Pacific (Table 3-1). The total number of western North Pacific tropical cyclones is lower than the climatological mean of 30.7, and two tropical cyclones below the 1986 total (Table 3-2). A record-setting eight significant tropical cyclones (all were of tropical storm intensity) developed in the North Indian Ocean. This is twice the climatological mean of four. Therefore, during 1987, JTWC issued warnings on a total of 33 northern hemisphere tropical cyclones.

During 1987 in the western North Pacific there were 139 "warning days". (A warning day is defined as a day during which JTWC was issuing warnings on at least one tropical cyclone. A "two-cyclone day" refers to a day when there were warnings issued on two different tropical cyclones simultaneously, a "three-cyclone day" -- three tropical cyclones at one time, and so on...). Considering only the western North Pacific, there were 30 two-cyclone days, 10 three-cyclone days and no four or five-cyclone days (Table 3-3). When North Indian Ocean tropical cyclones are included, there were 156 warning days, 38 two-cyclone days, 11 three-cyclone days and no four- or five-cyclone days. Thus, JTWC was in warning status 42.7 percent of the year; it was in a multiple-cyclone situation (that is, warning on two or more tropical cyclones) for 38 days or about 10.4 percent of the year.

JTWC issued 668 warnings on the 25 western North Pacific tropical cyclones (two warnings from January 1st on Typhoon Norris (26W) of 1986 are included in the total) and 83 warnings on the eight North Indian Ocean tropical cyclones, for a grand total of 751 warnings. There were thirty-one initial Tropical Cyclone Formation Alerts (TCFAs) issued for western North Pacific and eleven for the North

Indian Ocean. Twenty-four western North Pacific and seven North Indian Ocean tropical cyclones developed subsequent to the issuance of a TCFA. Three of the western North Pacific tropical cyclones regenerated during their lifetime and each was covered by a TCFA. Typhoon Peke (02C) was passed to JTWC while in warning status and thus no TCFA was required (Table 3-4). For the western North Pacific, the false alarm rate was 24 percent and the mean lead time (to issuance of the first warning) was 13.5 hours. For the North Indian Ocean, the false alarm rate was 18 percent, with a mean lead time of 10.1 hours. One system (Tropical Cyclone 03A) was warned on without the benefit of a preceding TCFA.

2. WESTERN NORTH PACIFIC TROPICAL CYCLONES

The distinguishing features of 1987 in the western North Pacific were the low number of total tropical cyclones (25), the large number of super typhoons (6) and the number of "midgets" (4).

JANUARY THROUGH JUNE

The activity began in early in January with Typhoon Orchid (01W). Orchid (01W) was an unusually small system which transited the wintertime western North Pacific before being sheared apart by the northeast monsoon east of the Philippine Islands. The island of Ulithi experienced 100 kt (51 m/sec) winds and extensive damage when Orchid (01W) passed directly overhead. Tropical Storm Percy (02W) was the only significant tropical cyclone in April. It struggled to get started, but tenaciously resisted dissipation until it passed over the island of Luzon. Tropical Storm Ruth (03W) was a short-lived system which developed southeast of Hong Kong and eventually dissipated over southern China. Typhoon Sperry (04W) was the second tropical cyclone to reach typhoon intensity and also the second "midget" typhoon (Orchid (01W) was the first) of 1987. It was also the first to enter

TABLE 3-1.

WESTERN NORTH PACIFIC
1987 SIGNIFICANT TROPICAL CYCLONES

TROPICAL CYCLONE	PERIOD OF WARNING	CALENDAR DAYS OF WARNING	NUMBER OF WARNINGS ISSUED	MAXIMUM SURFACE WINDS-KT (M/SEC)	ESTIMATED MSLP - MB	
01W	TY ORCHID	08 JAN - 14 JAN	7	23	95 (49)	956
02W	TS PERCY	11 APR - 13 APR	3	9	40 (21)	1000
03W	TS RUTH	18 JUN - 19 JUN	2	6	35 (18)	997
04W	TY SPERRY	27 JUN - 01 JUL	5	18	75 (38)	981
05W	STY THELMA	07 JUL - 16 JUL	10	34	130 (67)	911
06W	TY VERNON	16 JUL - 21 JUL	6	21	65 (33)	983
07W	TY WYNNE	22 JUL - 01 AUG	11	40	125 (63)	921
08W	TY ALEX	23 JUL - 28 JUL	6	22	65 (33)	976
09W	STY BETTY	09 AUG - 16 AUG	8	32	140 (72)	891
10W	TY CARY	13 AUG - 22 AUG	10	39	85 (44)	968
11W	STY DINAH	21 AUG - 31 AUG	11	42	130 (67)	910
12W	TS ED	22 AUG - 23 AUG	2	6	30 (15)	1001
12W	TS ED*	26 AUG - 28 AUG	3	6	35 (18)	998
13W	TY FREDA	04 SEP - 17 SEP	14	50	125 (63)	916
14W	TY GERALD	04 SEP - 10 SEP	7	24	105 (53)	937
15W	STY HOLLY	05 SEP - 15 SEP	11	43	140 (72)	898
16W	TY IAN	23 SEP - 01 OCT	9	33	110 (56)	933
17W	TD 17W	24 SEP - 26 SEP	3	7	30 (15)	1000
02C	TY PEKE	28 SEP - 03 OCT	6	23	100 (51)	941
18W	TS JUNE	29 SEP - 01 OCT	3	9	35 (18)	997
19W	TY KELLY	10 OCT - 16 OCT	7	28	95 (49)	950
20W	STY LYNN	16 OCT - 27 OCT	12	44	140 (72)	898
21W	TS MAURY	11 NOV - 12 NOV	2	4	30 (15)	1000
21W	TS MAURY*	13 NOV - 19 NOV	7	25	45 (23)	991
22W	STY NINA	19 NOV - 29 NOV	11	40	145 (75)	891
23W	TS OGDEN	24 NOV - 25 NOV	2	4	35 (18)	997
24W	TY PHYLLIS	10 DEC - 14 DEC	5	14	35 (18)	997
24W	TY PHYLLIS*	14 DEC - 19 DEC	5	20	100 (51)	941
1987 TOTALS:			139**	668***		

* REGENERATED

** OVERLAPPING DAYS INCLUDED ONLY ONCE IN SUM.

*** YEAR-END TOTAL INCLUDES TWO WARNINGS ON TY NORRIS (26W) ON 01 JAN 87.

the mid-latitude westerlies and recurve toward the northeast.

JULY

Super Typhoon Thelma (05W) was the first of four significant tropical cyclones to develop in July and the first super typhoon of 1987. Forecasting the timing and location of recurvature presented a problem for JTWC. Dynamic forecast aids did indicate recurvature, but much sooner than was ultimately observed. After damaging northern Luzon and causing the

evacuation of aircraft from Okinawa, Japan, Thelma (05W) slammed into Korea causing \$124 million in damages and the loss of several hundred lives. Typhoon Vernon (06W) followed closely on the heels of Super Typhoon Thelma (05W). It was weak and disorganized throughout most of its life. As a result, initial positioning problems arose in the Philippine Sea due to differences between real-time fix information from radar, satellite and aircraft. Typhoon Wynne (07W) was the third "midget" typhoon of the season. It tracked along a constant bearing of 294 degrees for four days

and maintained a visible eye for six days. Meteorologists on Kwajalein Atoll provided radar fix information which was instrumental in relocating Wynne (07W) early on. Wynne (07W) caused extensive damage as it passed through the northern Mariana Islands¹. Typhoon Alex (08W) was the final tropical cyclone in July. Together with Wynne (07W) it formed the first multiple tropical cyclone situation during 1987. Alex (08W) brushed the eastern coast of Taiwan before making landfall on the coast of mainland China. Although damage to Taiwan and mainland China was relatively light, the remnants of Alex (08W) enhanced a band of precipitation that stalled over Korea, and as a consequence, 12 inches (308 mm) of rain fell in 24-hours causing major flooding and loss of life.

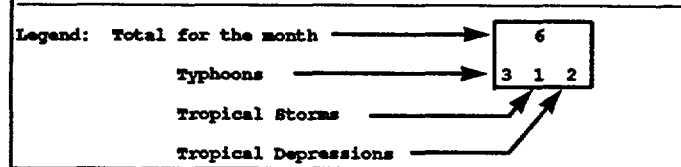
AUGUST

Super Typhoon Betty (09W) was the second super typhoon of the season and had the lowest reported minimum sea-level pressure (891 mb) up to that time. It explosively deepened just prior to making landfall in the Philippine Islands, where 20 people were killed and 60,000 left homeless. Typhoon Cary (10W), together with Betty (09W) and Dinah (11W) formed the first three-storm situation for 1987. The last scheduled western North Pacific aircraft reconnaissance mission was flown on Cary (10W) on the 15th of August. Cary (10W) eventually made landfall on the coast of northern Vietnam and ultimately dissipated over Burma. Super Typhoon Dinah (11W) was the most destructive typhoon to strike Okinawa and the southern islands of Japan in the past 20 years. Throughout its life, JTWC consistently forecast recurvature and accelerations towards the northeast through the Sea of Japan, as a result, Dinah's (11W) forecast track errors were smaller than average. Tropical Storm Ed (12W) was a very difficult tropical cyclone to locate and forecast due to fluctuations in its intensity, speed and track direction and its poorly defined

¹Personal communication with Mr. Paul M. Hattori of the U.S. Geological Survey (Department of Interior) revealed the following event of interest. Prior to 251145Z July there was no increase in microseismic activity on the World Wide Standardized Seismograph Network (WWSSN) long- and short-period records from the Mount Santa Rosa station (13° 32' 18" N, 144° 54' 42" E), Guam. From 251145Z to 251800Z, the short-period microseisms increased noticeably and were irregular in comparison to microseisms caused by higher surf levels or squall-like weather. After 251800Z, the background returned to approximately pre-251145Z levels. Also, the long-period microseisms approximately doubled in amplitude from 251000Z to 251700Z. The maximum being in the east-west component. Hence, the possibility exists that this unique microseismic activity may be coincident with, or causally related to, Typhoon Wynne's (07W) transit of the Mariana Trench. Similar activity has been observed with other tropical cyclones, but with less clarity. With an absence of other organized weather systems in the area, the typhoon's compact size and distance from the WWSSN station on Guam resulted in an unusually clear recording of Wynne's approach to the northern Marianas.

TABLE 3-2. WESTERN NORTH PACIFIC TROPICAL CYCLONE DISTRIBUTION

Year	JAN	FEB	MAR	APR	MAY	JUN	JUL	AUG	SEP	OCT	NOV	DEC	TOTALS	
1959	0	1	1	1	0	0	1	3	8	9	3	2	31	
1960	1	0	1	1	1	3	3	9	5	4	1	1	30	
1961	1	1	1	1	1	6	5	7	6	7	2	1	42	
1962	0	1	0	1	3	0	8	8	7	5	4	2	39	
1963	0	0	1	1	0	4	5	4	4	6	0	3	28	
1964	0	0	0	0	3	2	8	8	8	7	6	2	44	
1965	2	2	1	1	2	4	6	7	9	3	2	1	40	
1966	0	0	0	1	2	1	4	9	10	4	5	2	38	
1967	1	0	2	1	1	1	8	10	8	4	4	1	41	
1968	0	1	0	1	0	4	3	8	4	6	4	0	31	
1969	1	0	1	1	0	0	3	3	6	5	2	1	23	
1970	0	1	0	0	0	2	3	7	4	6	0	0	27	
1971	1	0	1	2	5	2	8	5	7	4	2	0	37	
1972	1	0	1	0	4	5	5	6	5	2	3	2	32	
1973	0	0	0	0	0	0	4	3	3	4	3	0	23	
1974	1	0	1	1	1	4	5	7	5	4	4	2	35	
1975	1	0	0	1	0	0	1	6	5	6	3	2	25	
1976	1	1	0	2	2	2	4	5	0	2	2	2	25	
1977	0	0	1	0	1	1	4	2	5	4	2	1	21	
1978	1	0	0	1	0	3	3	4	7	4	1	0	32	
1979	1	0	1	1	2	0	5	4	6	3	2	3	28	
1980	0	0	1	1	4	1	5	3	7	4	1	1	28	
1981	0	0	1	1	1	2	5	8	4	2	3	2	29	
1982	0	0	3	0	1	3	4	5	6	4	1	1	28	
1983	0	0	0	0	0	1	3	6	11	5	2	2	25	
1984	0	0	0	0	0	2	5	7	4	8	3	1	30	
1985	2	0	0	0	1	3	1	7	5	5	1	2	27	
1986	0	1	0	1	2	2	2	5	2	5	4	3	27	
1987	1	0	0	1	0	2	4	7	2	3	1	1	25	
(1959-1987)	AVG	0.6	0.3	0.6	0.8	1.2	2.1	4.6	6.2	5.7	4.6	2.8	1.4	30.9
CASES	16	9	18	22	36	60	132	179	164	132	81	42	891	



The criteria used in the above table are as follows:

1. If a tropical cyclone was first warned on during the last two days of a particular month and continued into the next month for longer than two days, then that system was attributed to the second month.
2. If a tropical cyclone was warned on prior to the last two days of a month, it was attributed to the first month - no matter how long the system lasted.
3. If a tropical cyclone began on the last day of the month and ended on the first day of the next month, that tropical cyclone was attributed to the first month. However, if a tropical cyclone began on the last day of the month and continued into the next month for two days only, then it was attributed to the second month.

cloud signature. Drifting buoy reports of 30 kt (15 m/sec) were key to the decision to issue the first warning on Ed (12W).

SEPTEMBER

Typhoon Freda (13W) was the first of seven tropical cyclones to develop during September and was the middle (geographically) of a three-storm situation (the other tropical cyclones being Gerald (14W) and Holly (15W)). This was the second three-storm situation of the year. Freda (13W) was unusual because it traversed less than 10 degrees of longitude, but 25 degrees of latitude. Freda's (13W) thirteen day life span and 50 warnings were records for 1987. Typhoon Gerald (14W) was unique in that it matured within the monsoon trough, but did not detach from it. The most distinctive feature was its unusually large eye. Super Typhoon Holly (15W) was the third tropical cyclone to develop from the active monsoon trough which also spawned Freda (13W) and Gerald (14W). Although very intense, it had a very uneventful life as it recurved far to the east of Japan. After a six day respite in tropical cyclone activity, Typhoon Ian (16W) developed about 330 nm (611 km) to the east-northeast of Guam. Andersen Air Force Base Weather was able to provide several radar fixes of Ian (16W) as it passed to the north of Guam. It eventually recurved and transitioned to a sub-tropical system north of 25 degrees North Latitude. Tropical Depression 17W developed north of the Marshall Islands at about the same time as Ian. Tropical Depression 17W did not reach tropical storm strength because it was suppressed by the combined effects of the outflow from Ian (16W) and a mid-level short-wave trough to the north. Typhoon Peke (02C) was the first hurricane to form in the central North Pacific and cross to the western North Pacific in the past twenty years. It meandered basically north-northwestward and eventually dissipated just west of the dateline. Tropical Storm June (18W) was the third tropical cyclone of the final three-storm situation during 1987. Throughout its life, June's (18W) upper-level outflow was restricted by the strong outflow from Ian.

TABLE 3-3.		WESTERN NORTH PACIFIC SUMMARY											
TYPHOONS (1945-1958)													
	JAN	FEB	MAR	APR	MAY	JUN	JUL	AUG	SEP	OCT	NOV	DEC	TOTALS
AVG	0.4	0.1	0.3	0.4	0.7	1.1	2.0	2.9	3.2	2.4	2.0	0.9	16.3
CASES	5	1	4	5	10	15	28	41	45	34	28	12	228
(1959-1987)													
	JAN	FEB	MAR	APR	MAY	JUN	JUL	AUG	SEP	OCT	NOV	DEC	TOTALS
AVG	0.2	0.1	0.2	0.5	0.7	1.0	2.8	3.2	3.3	3.0	1.7	0.7	17.4
CASES	7	2	6	15	19	30	80	94	96	87	48	20	504
TROPICAL STORMS AND TYPHOONS (1945-1958)													
	JAN	FEB	MAR	APR	MAY	JUN	JUL	AUG	SEP	OCT	NOV	DEC	TOTALS
AVG	0.4	0.1	0.4	0.5	0.8	1.6	3.0	3.9	4.1	3.3	2.8	1.1	22.0
CASES	6	1	6	7	11	22	42	54	58	46	39	16	308
(1959-1987)													
	JAN	FEB	MAR	APR	MAY	JUN	JUL	AUG	SEP	OCT	NOV	DEC	TOTALS
AVG	0.5	0.3	0.5	0.7	1.0	1.8	4.1	5.2	4.9	4.1	2.6	1.3	27.0
CASES	15	8	14	21	30	51	120	151	142	118	76	37	783
FORMATION ALERTS: 24 of 34 Initial Formation Alerts developed into significant tropical cyclones (not including three on systems that regenerated). Tropical Cyclone Formation Alerts were issued for all of the significant tropical cyclones that developed in 1987.													
WARNINGS:													
Number of calendar warning days: 139													
Number of calendar warning days with two tropical cyclones: 30													
Number of calendar warning days with three tropical cyclones: 10													

OCTOBER

Typhoon Kelly (19W) was the first of only two significant tropical cyclones to occur during October. Kelly (19W) developed when the monsoon trough re-established itself in low-latitudes after it had been displaced to a position about 25 degrees North Latitude the previous week due to Ian (16W), June (18W) and Peke (02C). Super Typhoon Lynn (20W) was the fifth super typhoon of the year and the third to produce winds of at least 140 kt (72 m/sec). It attained a minimum sea-level pressure of 898 mb. At one point, Lynn (20W) appeared to be headed straight for Guam. Fortunately, a last minute jog toward the north spared the island from a direct hit. Saipan, which is north of Guam, received gusts to 65 kt (33 m/sec), however. Lynn (20W) eventually passed south Taiwan, enhanced convection and increased

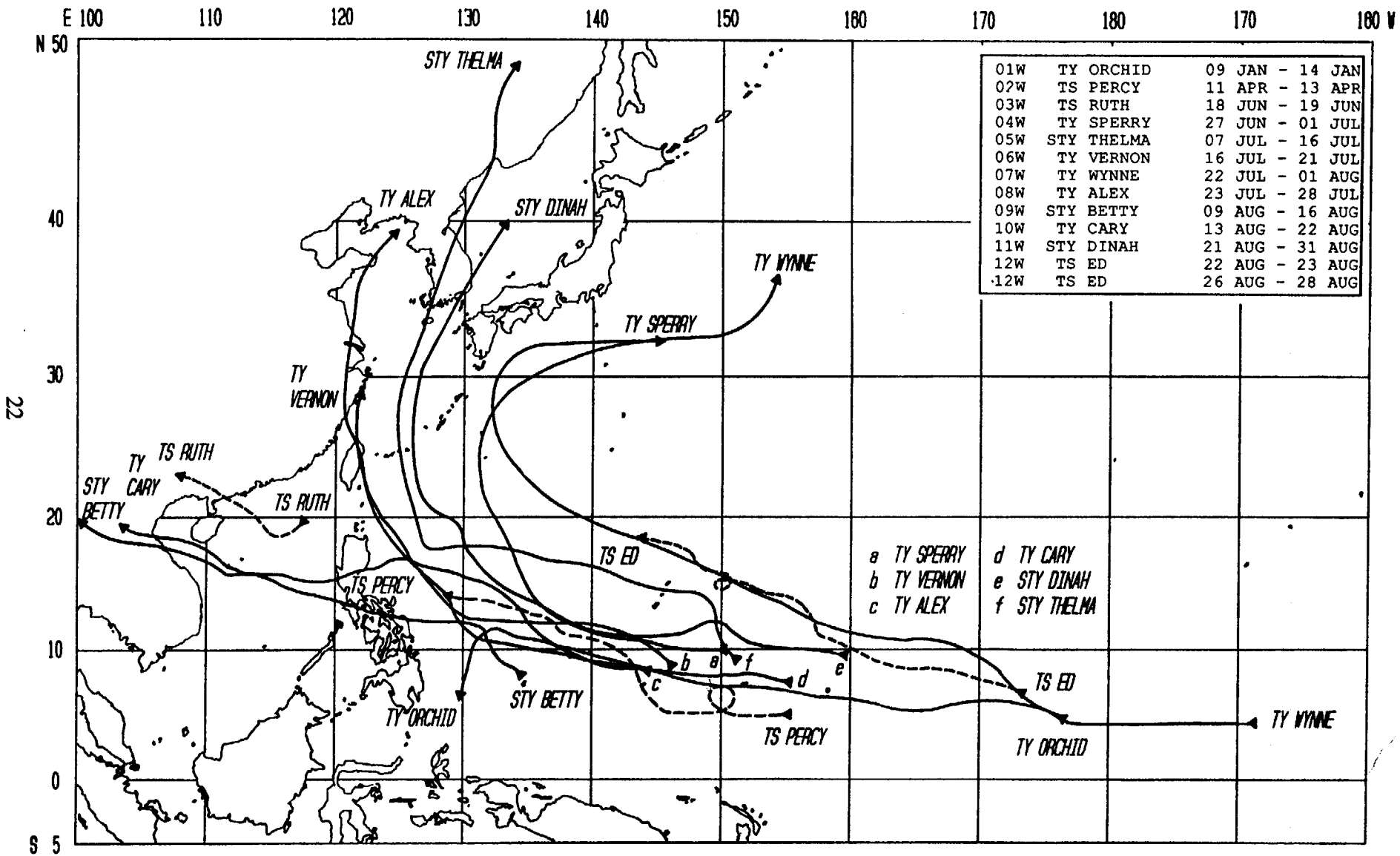
**TABLE 3-4. FORMATION ALERT SUMMARY
WESTERN NORTH PACIFIC**

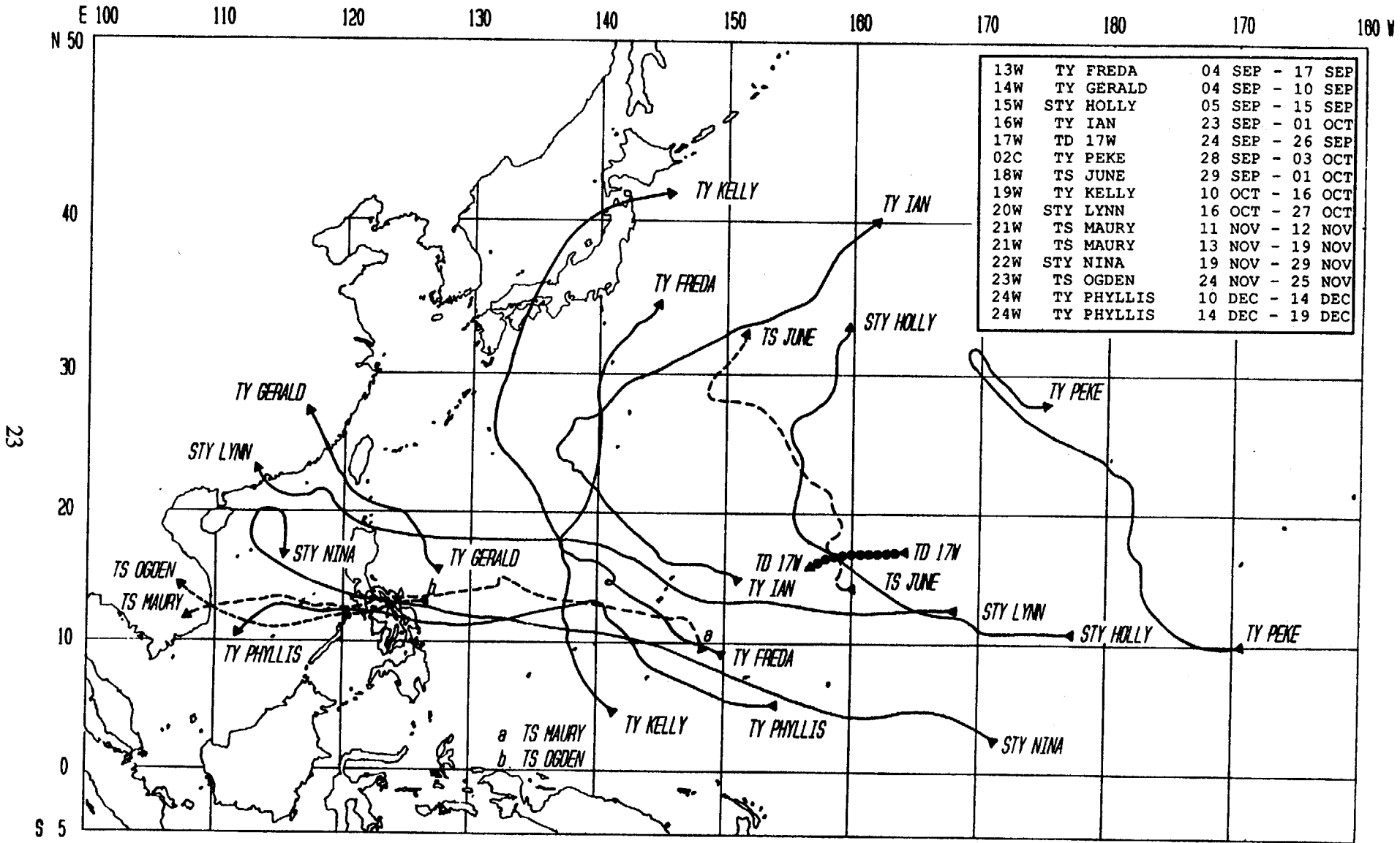
YEAR	NUMBER OF TCFAs	NUMBER OF SYSTEMS WARNED ON	TOTAL NUMBER OF SYSTEMS	FALSE ALARM RATE
1975	34	25	25	26%
1976	34	25	25	26%
1977	26	20	21	23%
1978	32	27	32	16%
1979	27	23	28	15%
1980	37	28	28	24%
1981	29	28	29	3%
1982	36	26	28	28%
1983	31	25	25	19%
1984	37	30	30	19%
1985	39	26	27	33%
1986	38	27	27	29%
1987	31	24	25	23%
(1975-1987) AVERAGE	33.1	25.7	26.9	21.8%
CASES	431	334	350	

wind speeds to the north that caused the deaths of 42 people. Over 68 inches (1744 mm) of rain fell on Taipei over a two day period due to Lynn (20W). Tropical Storm Maury (21W) was a relatively weak, but persistent, tropical cyclone which formed southeast of Guam and tracked basically westward across the Philippine Sea, through the Philippine Islands and into the South China Sea.

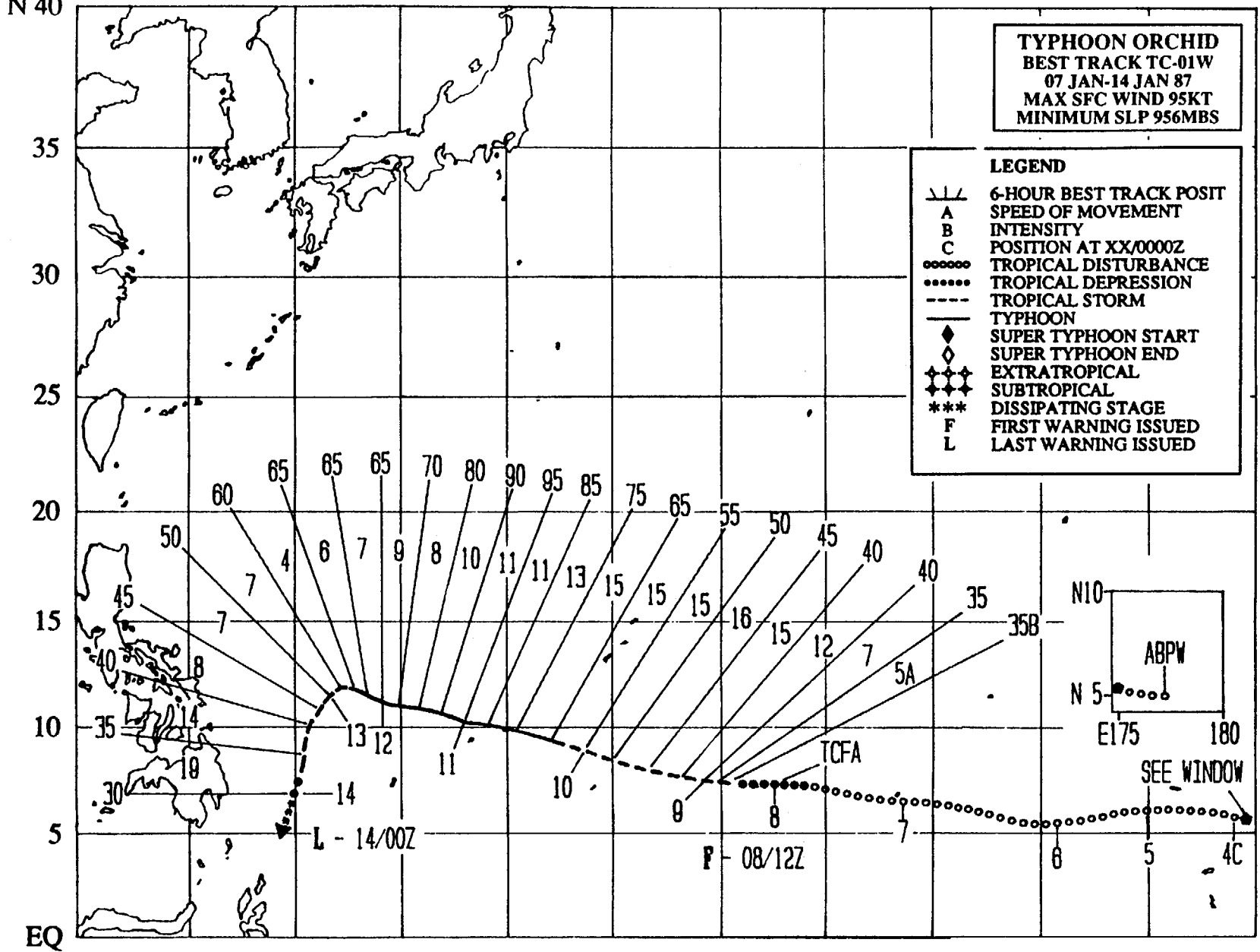
NOVEMBER THROUGH DECEMBER

Super Typhoon Nina (22W) was the sixth, and last, super typhoon. It also proved to be the most intense and destructive tropical cyclone of the year. Nina was interesting from a meteorological point of view because it unexpectedly intensified while still accelerating toward the west. It devastated Truk, killing five and injuring 38, before moving on to the Philippine Sea. Once there Nina (22W) explosively intensified, to 145 kt (75 m/sec), prior to making landfall. An estimated 658 people were killed on southern Luzon, making it the most destructive typhoon to hit the Philippine Islands in 20 years. Tropical Storm Ogden (23W) was another minimal tropical storm which developed in the South China Sea and moved westward before making landfall on the Vietnam coast, north of Cam Rahn Bay. Typhoon Phyllis (24W), the fourth "midget" of 1987, was the last tropical cyclone of the 1987 season. Phyllis (24W) formed southeast of Guam and initially followed what appeared to be a broad recurvature track, passing to the southwest of Guam. Unfortunately, it weakened, moved toward the west-southwest and then explosively intensified (to 100 kt (51 m/sec)) before striking the island of Samar in the central Philippine Islands and moving into the South China Sea.





E 120 125 130 135 140 145 150 155 160 165 170 175 E



TYPHOON ORCHID (01W)

Typhoon Orchid (01W), the first tropical cyclone of 1987, was an unusually small system. It transited across the wintertime western North Pacific before being sheared apart by the northeast monsoon east of the Philippines.

The disturbance that eventually developed into Typhoon Orchid was first detected at 0000Z on January 3rd as a small area of persistent convection in the near-equatorial trough near the dateline. It was first mentioned on the Significant Tropical Weather

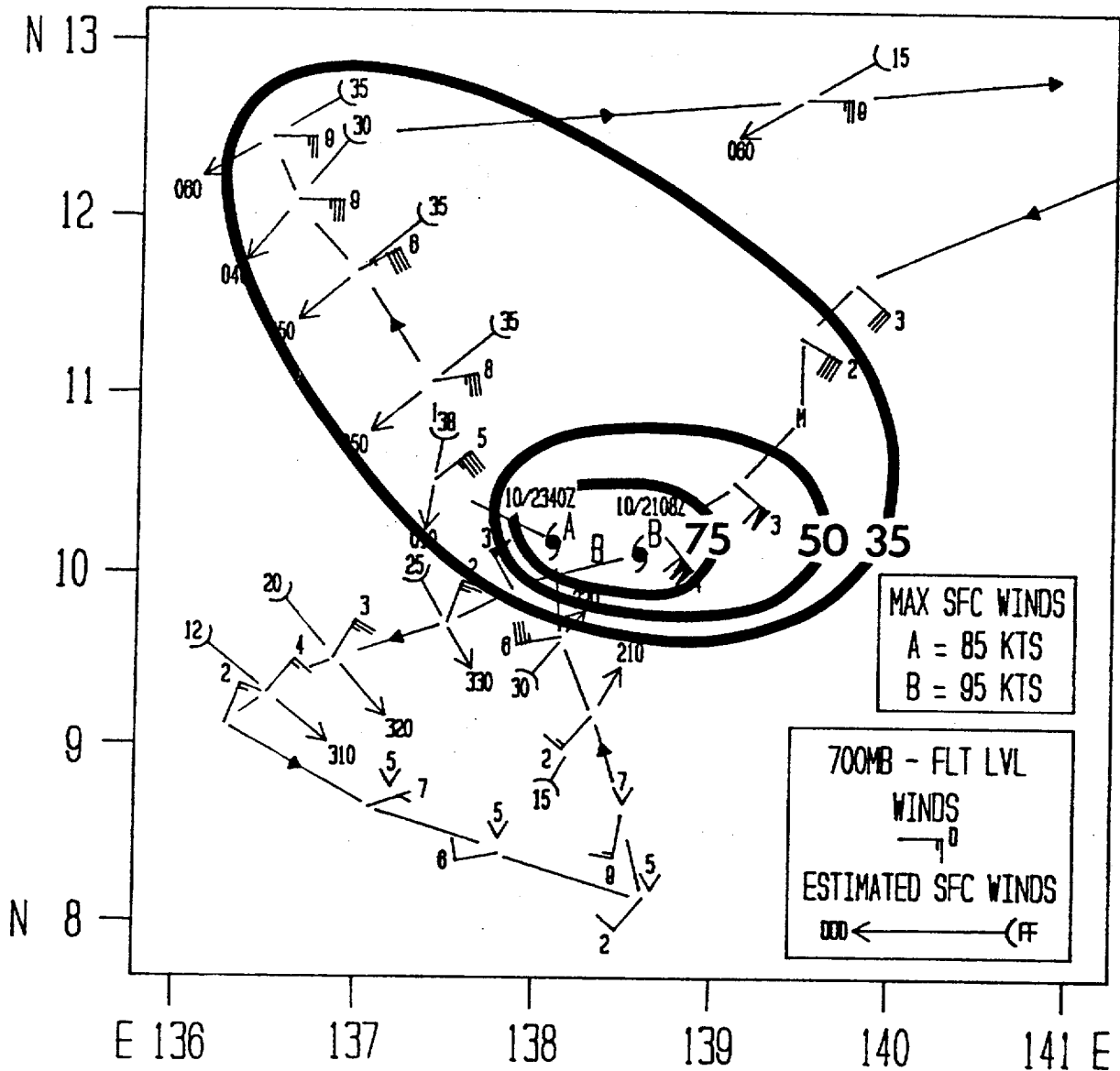


Figure 3-01-1. The 110000Z January aircraft reconnaissance fix mission of Typhoon Orchid (01W) near maximum intensity. Note the tight gradient of surface winds to the south of the vortex center.



Figure 3-01-2. Damage to the Outer-Island School located on the north side of Falalop Island on the Ulithi Atoll. All these buildings sustained some damage while others (dormitories and classrooms) were totally destroyed (Photo courtesy of Mobil Oil Micronesia, Inc.).

Advisory (ABPW PGTW) at 030600Z. Over the next four to five days, this area drifted toward the west and slowly increased in organization and convection until a small ragged central dense overcast (CDO) formed and upper-level outflow improved. A Tropical Cyclone Formation Alert followed at 072130Z and a daylight hours aircraft reconnaissance investigative mission was tasked for the next day. No surface data was available near the system; however, at 080419Z Dvorak satellite

intensity analysis of the disturbance estimated maximum sustained surface winds of 25 to 30 kt (13 to 15 m/sec). This prompted JTWC to issue the first warning on Tropical Depression 01W at 081200Z. The next morning, the aircraft investigative mission reported maximum sustained surface winds of 45 kt (23 m/sec). This prompted the upgrade of the system on the third warning (at 090000Z) to Tropical Storm Orchid (01W).



Figure 3-01-3. Corrugated sheet roofing embedded in a coconut log on Falalop Island on Ulithi Atoll. This building material becomes a deadly object to life and property when airborne (Photo courtesy of Mobil Oil Micronesia, Inc.).

There were two unusual aspects of Typhoon Orchid (01W). The first was its small radius of maximum winds. For example, at its peak intensity of 95 kt (49 m/sec) at 110000Z, the radii of 30 kt (15 m/sec) winds were only 45 nm (83 km) in the south semicircle and 140 nm (259 km) in the northwest semicircle (see Figure 3-01-1). The larger wind radius in the northwest semicircle was due partly to interaction with high pressure ridging to the north and the motion vector addition to the

winds in the west-northwest, or right front, quadrant. Typhoon Orchid (01W), near maximum intensity, passed directly over the island of Ulithi (WMO 91203). As a result, Ulithi reported surface winds near 100 kt (51 m/sec) and sustained extensive damage (Figures 3-01-2 and 3-01-3). A few hours later, however, Typhoon Orchid passed about 45 nm (83 km) north of the island of Yap (WMO 91413), where surface winds of only 20 to 25 kt (10 to 13 m/sec) and fair skies were reported.

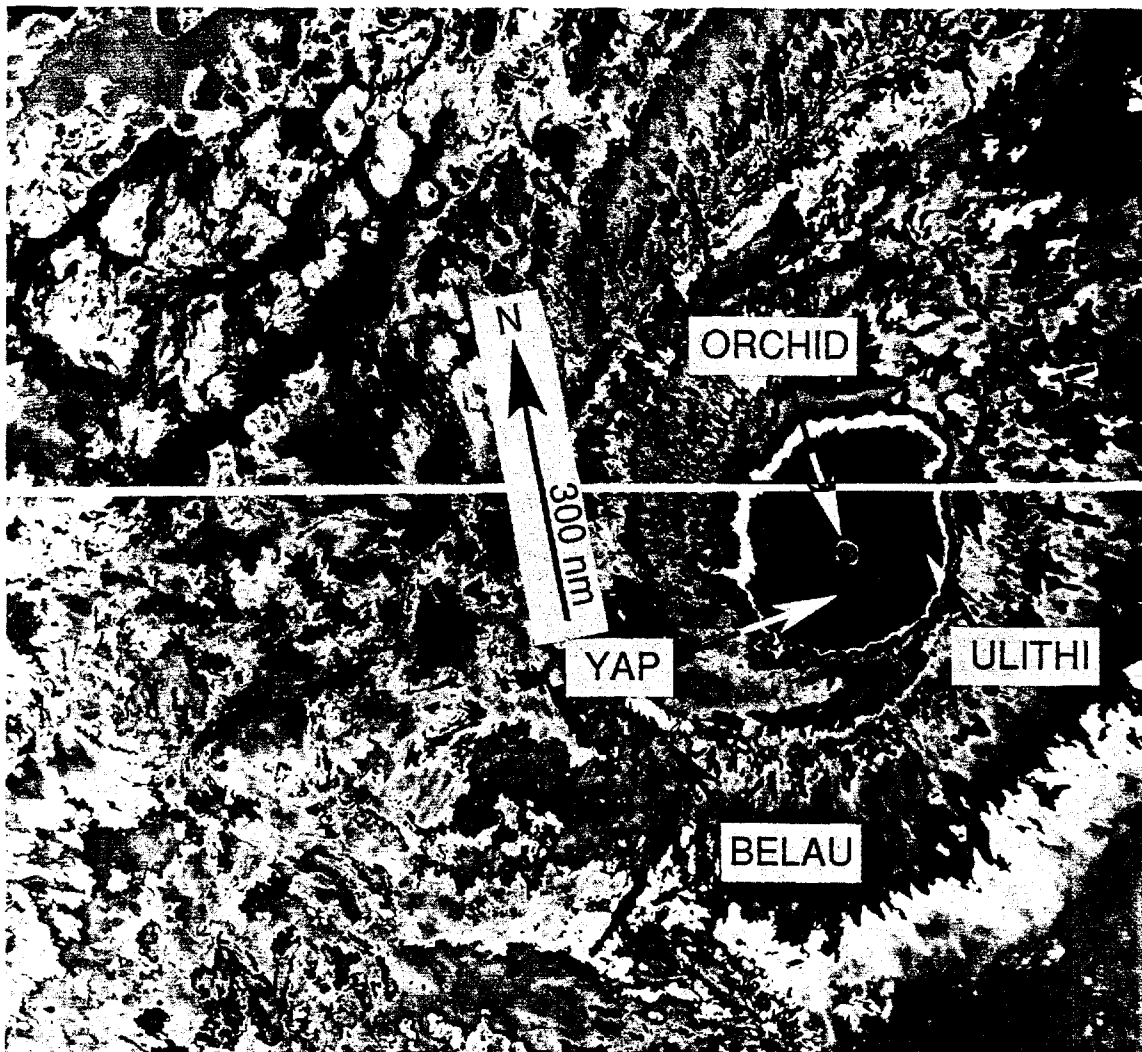


Figure 3-01-4. Enhanced infrared (EIR) imagery of Typhoon Orchid (01W) near maximum intensity. Note the small well-defined eye (102259Z January NOAA infrared imagery).

The second unusual aspect of Typhoon Orchid was the fact that during the two days from 101200Z to 121200Z when Orchid was the most intense (Figure 3-01-4), the Dvorak intensity estimates were 10 to 20 kt (5 to 10 m/sec) higher than the intensity reported by aircraft reconnaissance (Figure 3-01-5).

After reaching maximum intensity, Orchid continued moving northwestward. Between 110000Z and 140000Z (when the last warning was issued), Orchid came under the influence of the strong wintertime low-level

northeast monsoonal flow. This, coupled with 200 mb westerly flow aloft, set up a strong vertical shearing environment in which the upper portion of Orchid was displaced toward the east. Once the central convection stripped away, the remaining surface circulation was then steered by the low-level northeast monsoonal flow toward the southwest before dissipating over water. This wintertime shearing situation was a common factor in the end of the last five significant tropical cyclones in November and December of 1986.

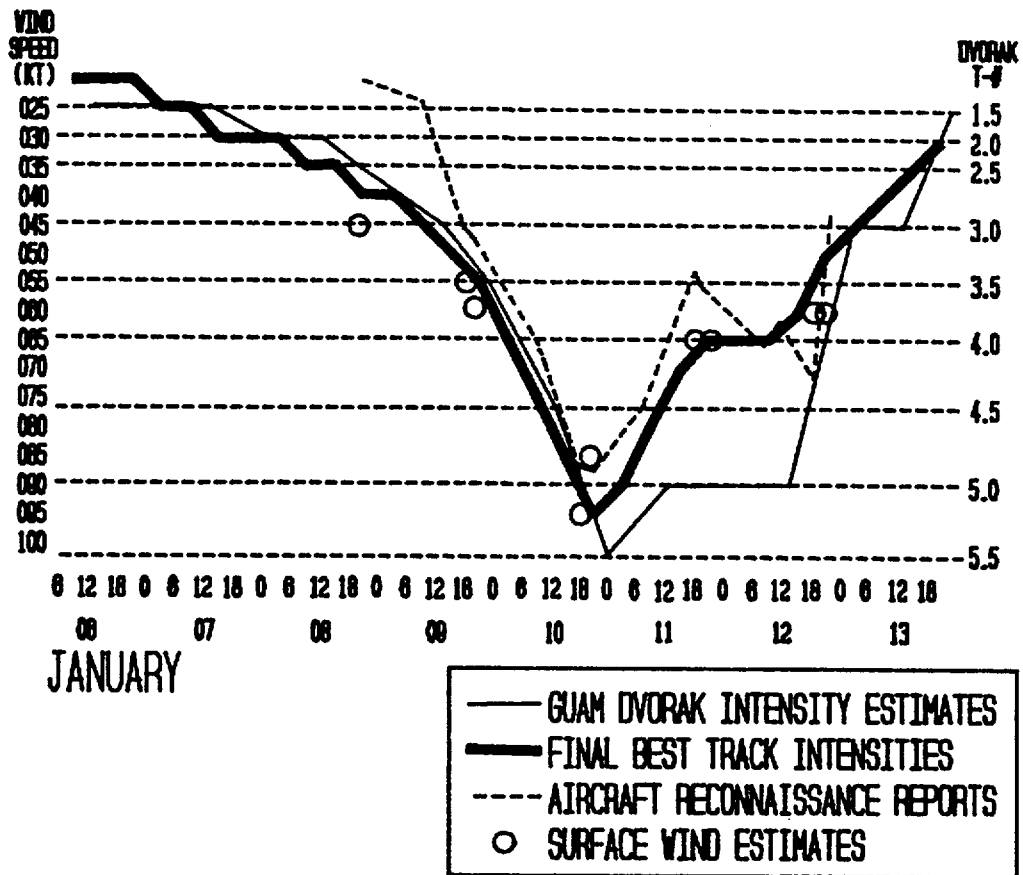


Figure 3-01-5. Plot of intensities obtained for Typhoon Orchid (01W) by aircraft reconnaissance vortex fixes and Dvorak analysis of satellite imagery. Also plotted are the Final Best Track intensities for comparison. Note the higher satellite intensities especially around the time of maximum intensity.

TROPICAL STORM PERCY (O2W)

Percy was the only significant western North Pacific tropical disturbance during April. The vortex struggled to get started, only achieved minimal tropical storm intensity and tenaciously resisted dissipation.

During the first week of April, brisk 30 kt (15 m/sec) northeasterly trades clashed with a low-latitude westerly surge associated with a tropical disturbance in the southern hemisphere. This created an area of cyclonic rotation in the low-level wind field and slightly lower pressures in the eastern Caroline Islands. The resulting

convection was first noted on the Significant Tropical Weather Advisory (ABPW PGTW) for 030600Z April. The slow formation of a cloud system led to the issuance of a Tropical Cyclone Formation Alert (TCFA) at 061800Z. Maximum sustained surface winds, at that time, were estimated to be 25 to 30 kt (13 to 15 m/sec). The TCFA was reissued at 071800Z because the area had increased in organization, although the overall convection decreased. By 081800Z, the mid- to upper-level winds over the system increased and the second TCFA was cancelled.

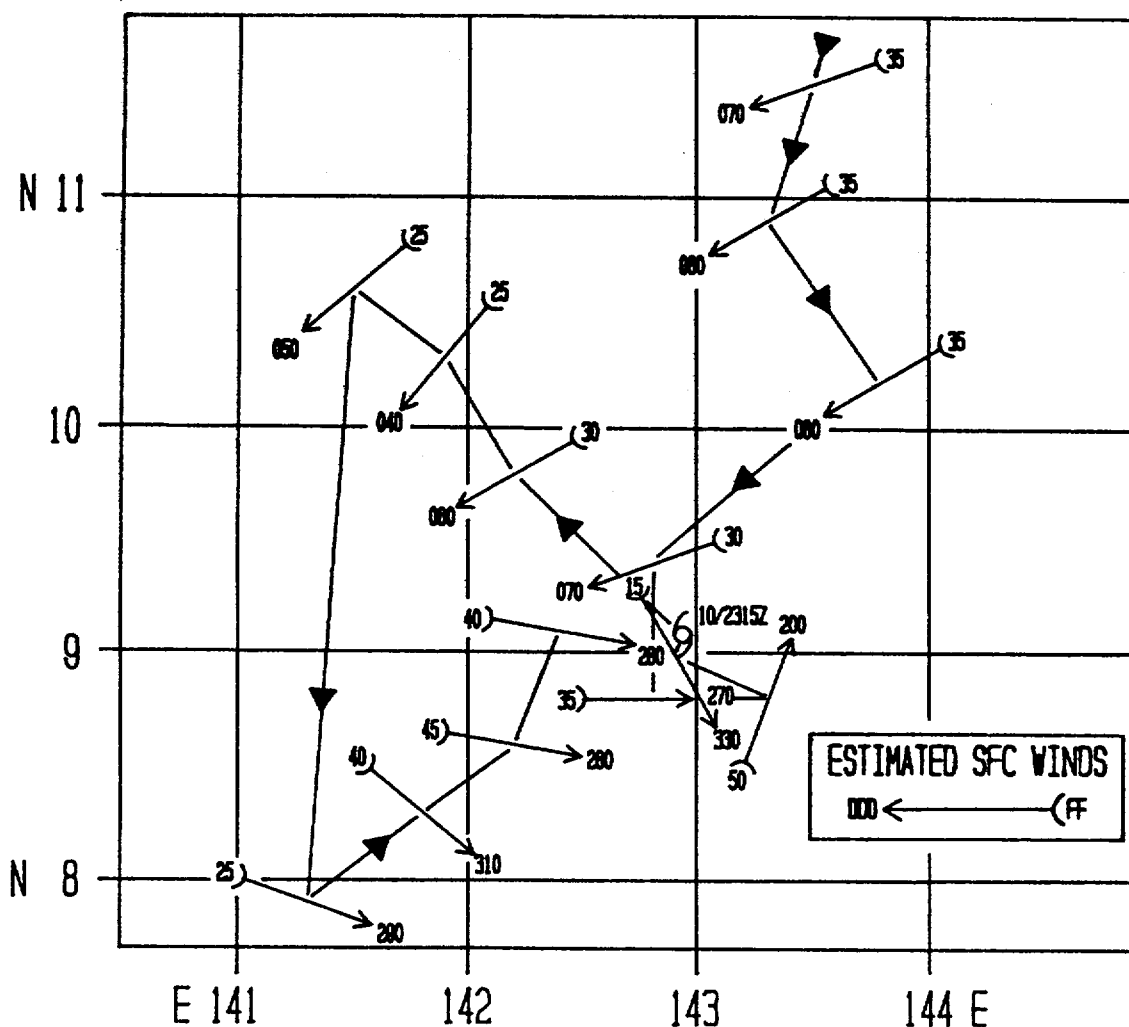


Figure 3-02-1. Plot of aircraft reconnaissance data from the third mission into Tropical Storm Percy (02W) shows increasing surface winds near the center.

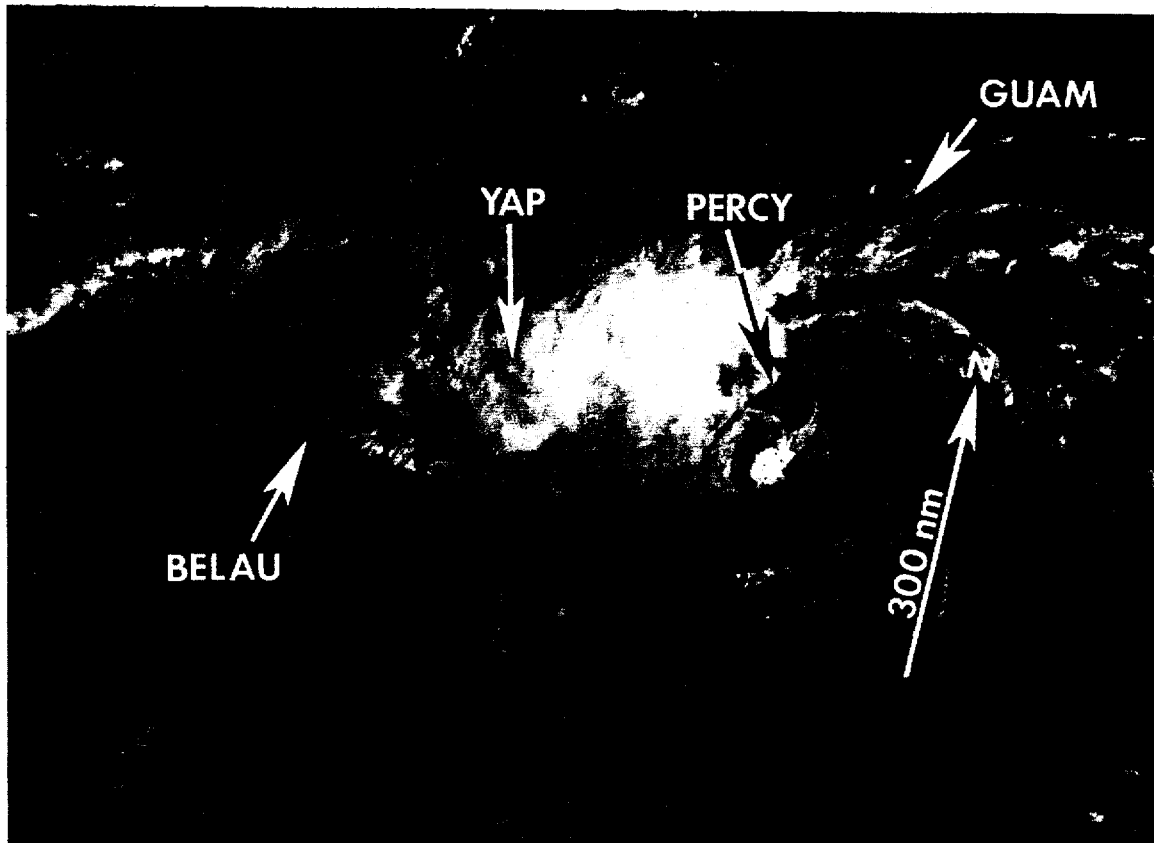


Figure 3-02-2. Tropical Storm Percy (02W), while southwest of Guam, showing an exposed low-level circulation center (110022Z April DMSP visual imagery).

However, the weakened disturbance continued to drift slowly westward for the next three days and possessed fair potential for significant development. By 101407Z the convection and organization had again improved, and the vertical wind shear on the system decreased sufficiently to justify the issuance of a third TCFA. Satellite intensity analysis (Dvorak, 1984) estimated maximum surface winds of 25 kt (13 m/sec) at that time, however, an aircraft daylight investigative mission flown on the morning of the 10th produced unexpected results.

Enroute to the circulation, the aircraft reported gradually increasing flight-level winds (1500 ft (457 m)) and observed surface winds from 30 kt (15 m/sec) near Guam to 40 kt (21 m/sec). Upon reaching the expected location of the low-level cyclonic circulation, the Aerial Reconnaissance Weather Officer (ARWO) reported flight-level winds of 56 kt (29 m/sec) and surface winds of 50 kt (26 m/sec) at 102325Z. The center location was consistent with the increasing surface winds encountered enroute (Figure 3-02-1); however, the magnitude of the winds were inconsistent with

the minimum sea-level pressures (MSLPs) enroute (1010 mb to 1003 mb) and at the circulation center (1001 mb). Dvorak satellite intensity analysis at 110022Z estimated 25 kt (13 m/sec) surface winds (Figure 3-02-2). This was more consistent with the extrapolated MSLPs. According to Atkinson and Holliday (1977), an environmental MSLP of near 1012 mb, together with maximum sustained surface winds of 50 kt (26 m/sec) usually implies a central MSLP of about 987 mb. After the aircraft reconnaissance flight-level wind observations, were double-checked, Tropical Depression 02W was upgraded to a tropical storm.

Aircraft reconnaissance was available again at 112100Z. Flight-level and surface winds were much lighter than observed 24-hours earlier. Values ranged from 20 to 32 kt (10 to 16 m/sec) at flight level enroute to the early fix at 112120Z, and 15 to 20 kt (8 to 10 m/sec) prior to the primary fix at 112354Z. The Dvorak satellite intensity analysis at 122304Z estimated 25 kt (13 m/sec) maximum sustained surface winds. As a result, the final warning on Tropical Storm Percy (02W) followed at 130000Z. Percy's circulation persisted as an exposed low-level center through the 15th, with the remaining convection located well to the northeast and southwest (Figure 3-02-3). The residual low-level eddy, that remained, finally dissipated near northern Luzon on the 19th of April.

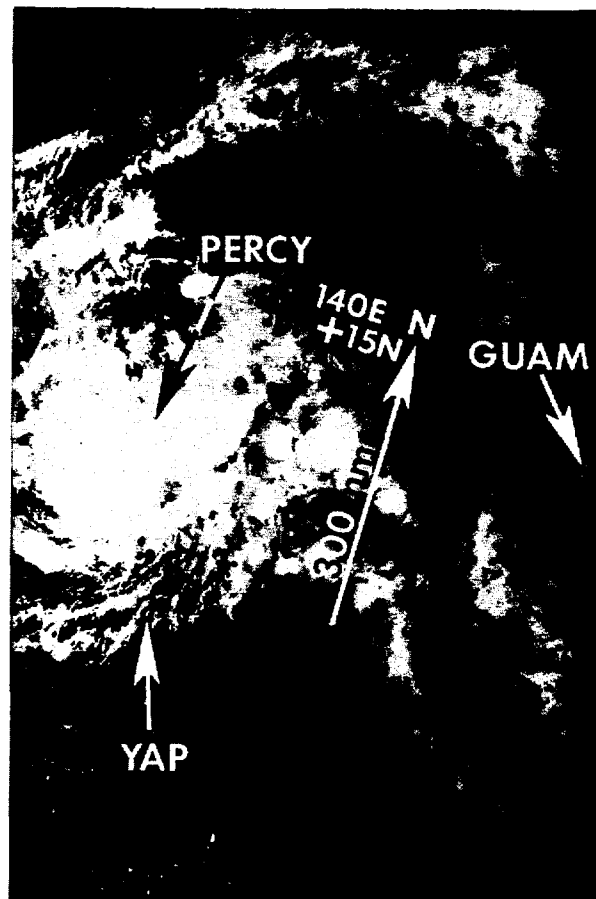
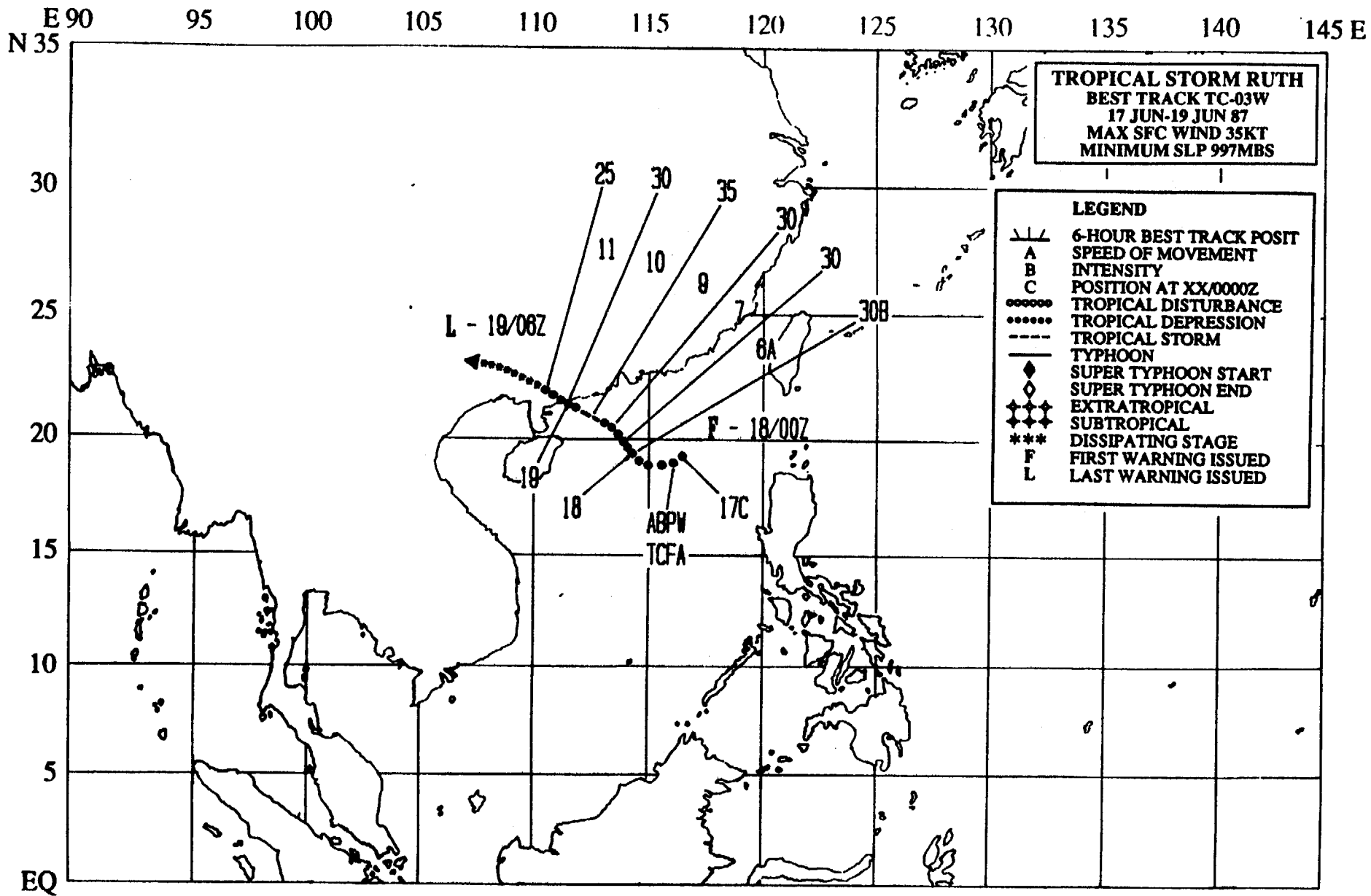


Figure 3-02-3. Tropical Storm Percy (02W) in the Philippine Sea just before the final warning was issued (122341Z April DMSP visual imagery).



34

TROPICAL STORM RUTH (03W)

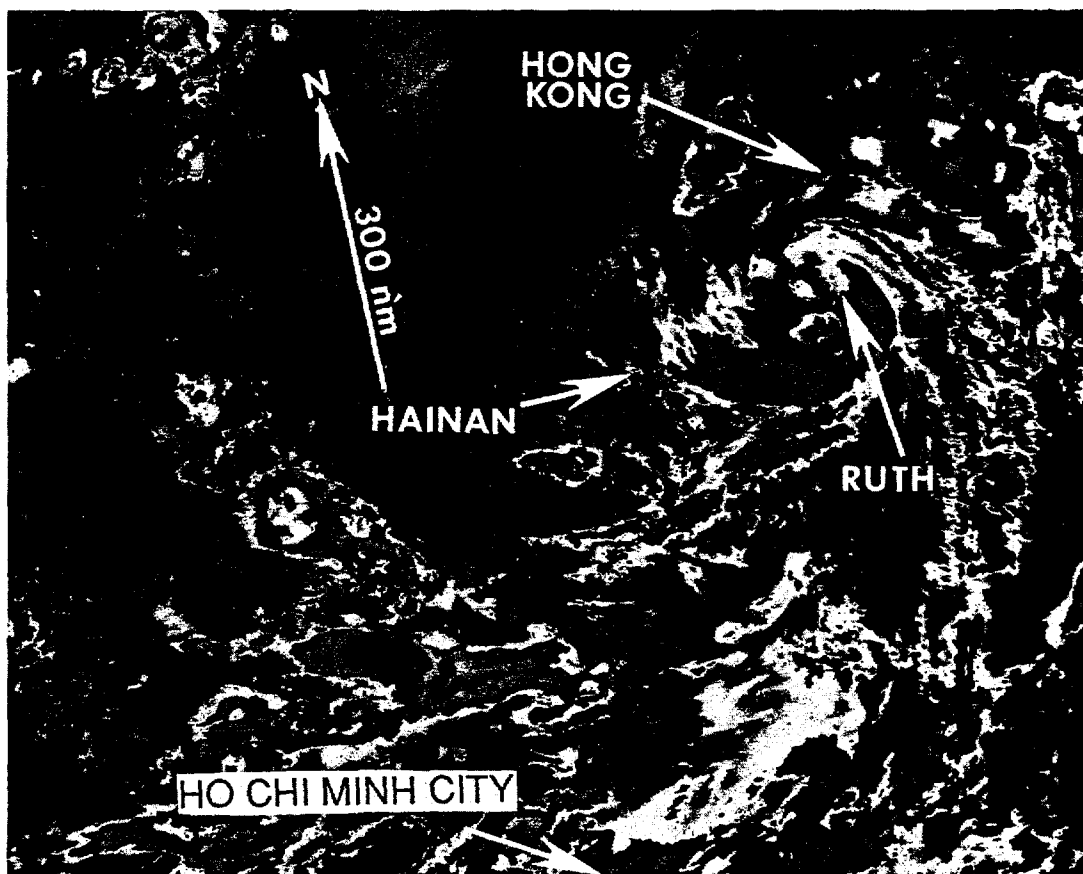


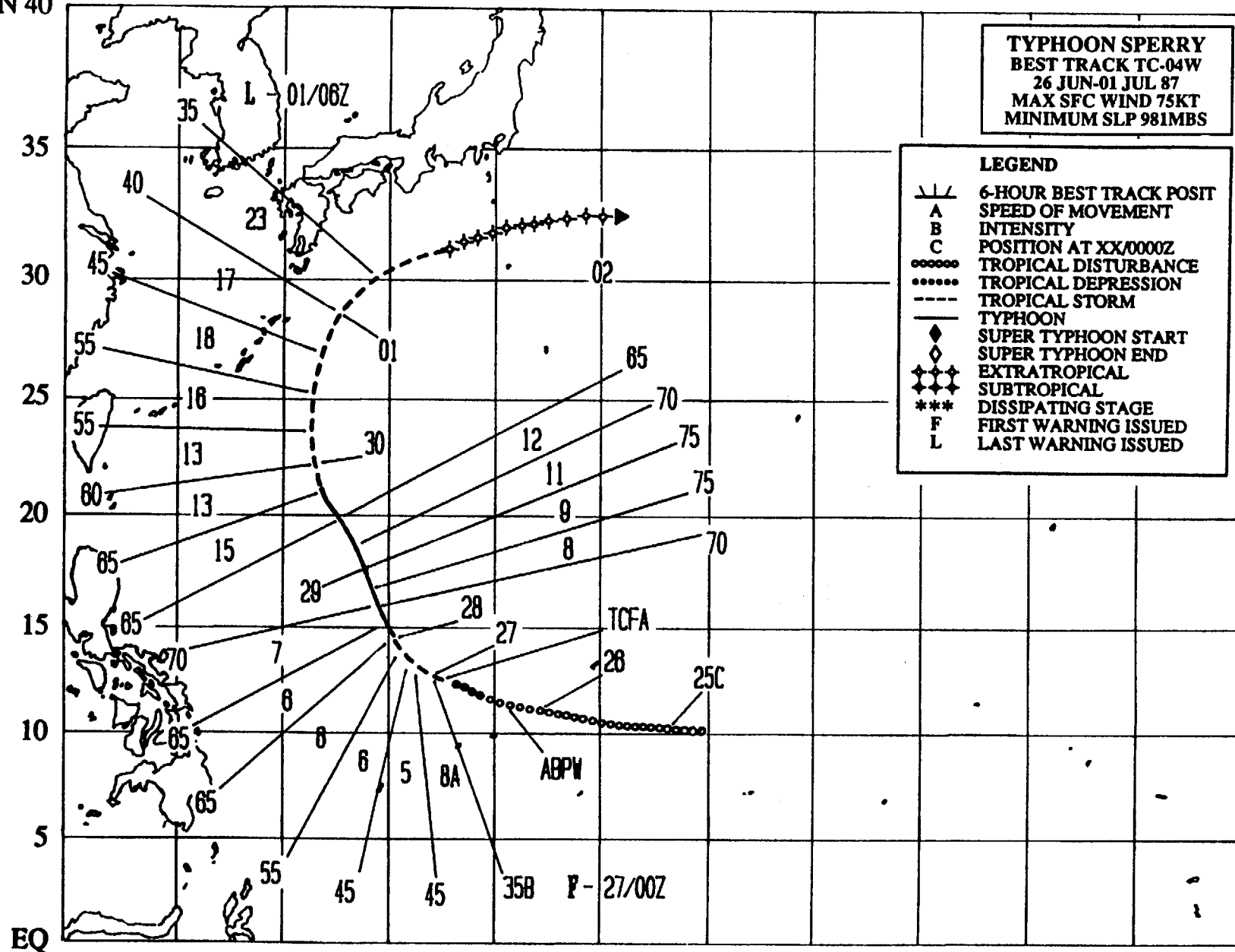
Figure 3-03-1. Tropical Storm Ruth was a short-lived tropical cyclone. Only six warnings were issued on the system before it moved inland and dissipated over southern China. It began as a monsoon depression 240 nm (444 km) southeast of Hong Kong over the South China Sea. Early on 17 June, convection consolidated into convective bands prompting its mention on the Significant Tropical Weather Advisory (ABPW PGTW) at 0600Z as having good potential for development. As a result, JTWC issued a Tropical Cyclone Formation Alert, valid at the same time, because satellite imagery indicated upper-level anticyclonic outflow was becoming established. JTWC issued the first warning on Tropical Depression 03W at 180000Z, after synoptic reports indicated surface pressures in the area had dropped significantly overnight from 1001 mb to 995 mb. The initial forecast tracks indicated the system would move northwestward, but subsequent forecasts gradually shifted the track further west as the subtropical ridge east of Ruth began ridging slowly westward across southern China. The system was upgraded to tropical storm intensity at 181800Z based upon a Dvorak intensity estimate of 35 kt (18 m/sec) maximum sustained surface winds associated with convective bands which were wrapped halfway around the center (see image above). Ruth was downgraded to a tropical depression on the fifth warning as it interacted with the southern coast of China. Hong Kong (WMO 45005) radar reports were excellent and proved instrumental in accurately tracking this tropical cyclone for a day before it made landfall. Ruth dissipated within eighteen hours of moving inland, causing little damage and no known deaths (181138Z June DMSP infrared imagery).

E 120 125 130 135 140 145 150 155 160 165 170 175 E
 N 40

TYPHOON SPERRY
BEST TRACK TC-04W
26 JUN-01 JUL 87
MAX SFC WIND 75KT
MINIMUM SLP 981MBS

LEGEND

- ||| 6-HOUR BEST TRACK POSIT
- A SPEED OF MOVEMENT
- B INTENSITY
- C POSITION AT XX/0000Z
- TROPICAL DISTURBANCE
- TROPICAL DEPRESSION
- - - - TROPICAL STORM
- TYPHOON
- ◆ SUPER TYPHOON START
- ◇ SUPER TYPHOON END
- ◆◆◆◆ EXTRATROPICAL
- ◆◆◆◆ SUBTROPICAL
- *** DISSIPATING STAGE
- F FIRST WARNING ISSUED
- L LAST WARNING ISSUED



36

TYPHOON SPERRY (04W)

Typhoon Sperry was the second tropical cyclone to reach typhoon intensity and also the second "midget" typhoon in 1987. It was also the season's first to enter the mid-latitude westerlies and recurve toward the northeast.

The tropical disturbance that eventually developed into Typhoon Sperry was first detected by synoptic data on 24 June as a broad, weak surface circulation in the western extension of the monsoon trough 200 nm (370 km) to the northwest of the island of Truk in the eastern Caroline Islands. The convection in this area appeared to be random. At the same

time, a second area of disorganized convection was developing 210 nm (389 km) east of the island of Enewetak in the Marshalls. To the north and east, a Tropical Upper-Tropospheric Trough (TUTT) extended from Wake Island southwestward to just northeast of Guam. The broad subtropical ridge dominated the low-level flow pattern in the northwest Pacific. Although the two convective areas consolidated on 25 June, the resultant disturbance still struggled for two more days before reaching tropical storm intensity. The most probable cause for this slow intensification was the close proximity of a TUTT low (Sadler, 1979) to the northeast. This low aloft, in conjunction with the lower

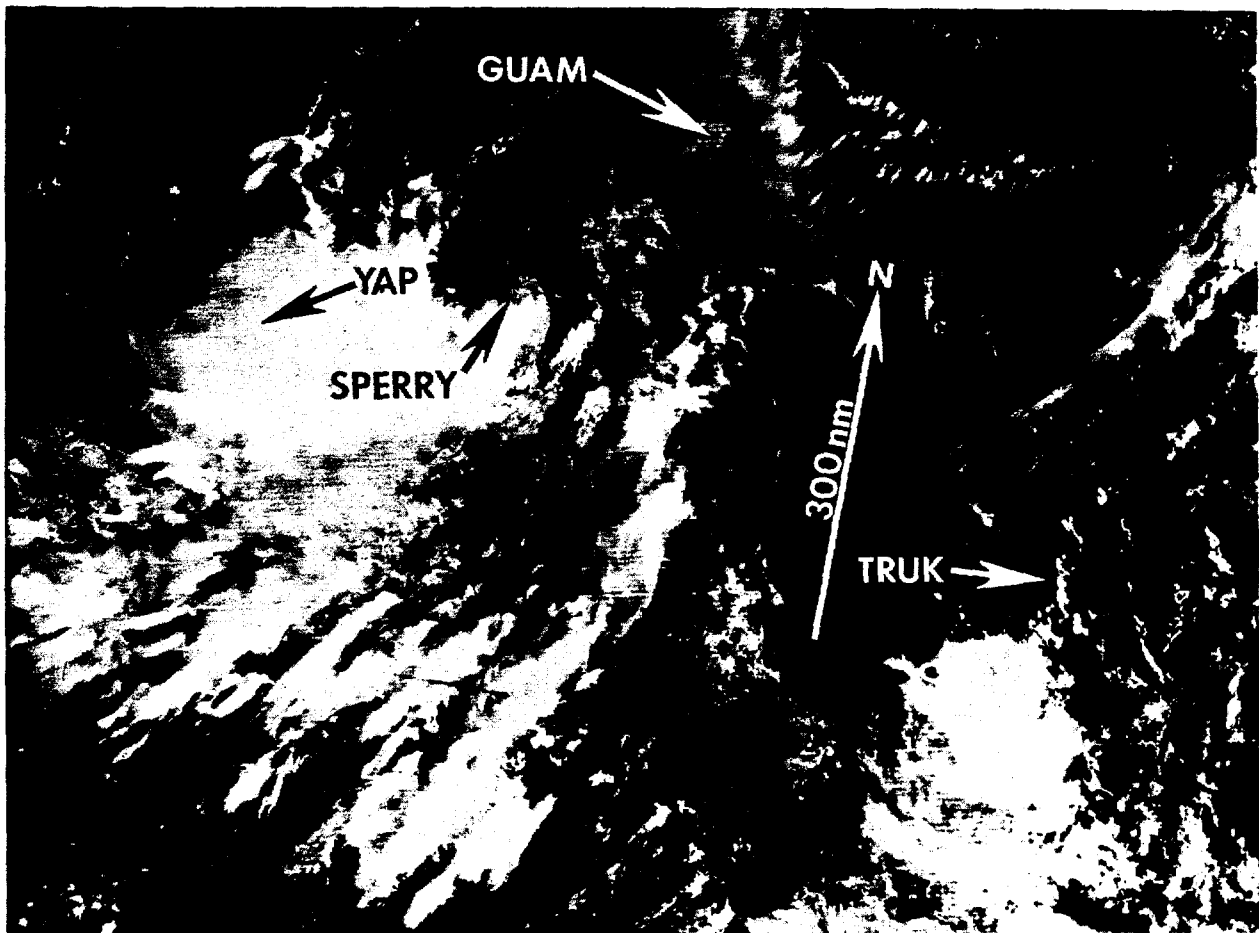


Figure 3-04-1. Visual satellite imagery showing the tropical disturbance that would later develop into Typhoon Sperry. Note the low-level circulation center

displaced to the northeast of the main convection (252347Z June DMSP visual imagery).

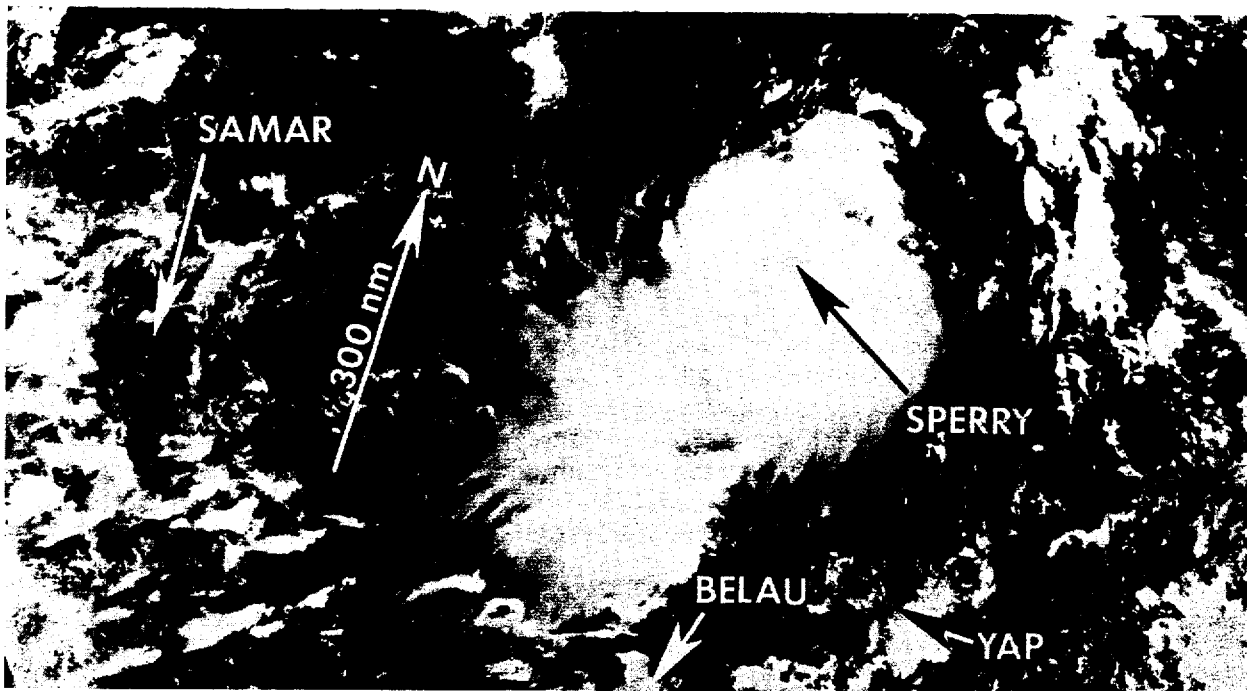


Figure 3-04-2. Typhoon Sperry with an intensity of 65 kt (33 m/sec) just prior to peaking (280047Z June DMSP visual imagery).

tropospheric subtropical ridge, created an area of strong vertical wind shear (Figure 3-04-1).

The low-level disturbance drifted west-northwestward for the next several days. At that point, the separation between the TUTT low, or cell, and the low-level tropical disturbance to the southwest remained static. However, an interesting change occurred aloft. By 251200Z a plume of dense cirrus, associated with a 55 kt (28 m/sec) wind maximum entering the western side of the upper cold low from the north, moved southward. Within eighteen-hours the cirrus plume had plunged into the southwest portion of the TUTT cell. The cell responded. The circulation within the core of the upper low tightened up and became more symmetrical. This, in turn, reduced the vertical wind shear across the system and as a result, the central convection started to increase within the low-level disturbance again. Earlier (at 241200Z), the Navy Operational Global Atmospheric Prediction System upper-air prognoses, had correctly forecast this lessening of vertical shear. The new convection was initially mentioned on the 260600Z Significant

Tropical Weather Advisory (ABPW PGTW).

Based upon satellite intensity analysis (Dvorak, 1984) of satellite imagery between 1500Z and 2100Z on the 26th, analysts of Detachment 1, 1st Weather Wing estimated that the disturbance had 30 kt (15 m/sec) surface winds, based on more organized and intense convection. The satellite reconnaissance inputs prompted the issuance of a Tropical Cyclone Formation Alert (TCFA) at 262230Z. An aircraft reconnaissance investigative mission was requested for the following day. At the time of the TCFA, synoptic data was not available near the center of the disturbance. However, surface data on the periphery of the disturbance implied that at least a 10 kt (5 m/sec) low-level circulation was present. The only reported stronger wind was the gradient-level (3000 ft (914 m)) report at Yap (WMO 91413), which increased from 10 kt (5 m/sec) at 261200Z to 15 kt (8 m/sec) at 270000Z as the disturbance passed northeast of the island on the 26th.

The first warning on Tropical Storm

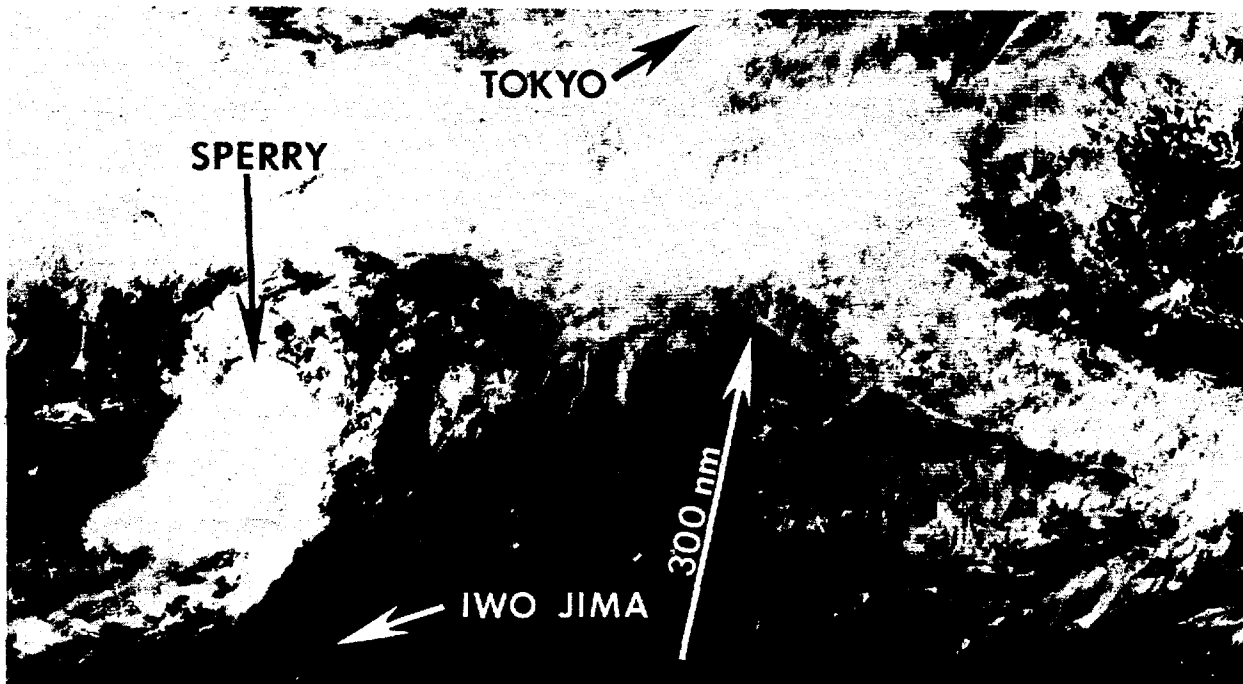


Figure 3-04-3. Sperry interacting with a frontal boundary south of Japan (302345Z June DMSP visual imagery).

Sperry was issued on the 27th, valid at 0000Z, after visual satellite imagery showed that a central dense overcast and 35 kt (18 m/sec) maximum sustained surface winds were present. Aircraft reconnaissance later in the day located a 1001 mb circulation center with 40 kt (21 m/sec) maximum sustained surface winds, extending out to 50 nm (93 km) southeast of the center. Initial forecasts called for Sperry to follow an around-the-ridge scenario and recurve. This forecast philosophy proved to be correct.

Sperry attained typhoon intensity 24-hours later at about 280000Z. The Aerial Reconnaissance Weather Officer reported Sperry as very compact, with 70 kt (36 m/sec) maximum sustained surface winds surrounding a small, circular 15 nm (28 km) diameter eye. The eye was open to the north and had a minimum sea-level pressure of 983 mb. Sperry developed a ragged eye while moving northwestward under the influence of the mid-level steering flow around the western periphery of the subtropical ridge. Its intensity peaked at 75 kt (39 m/sec) between 281200Z and 281800Z (Figure 3-04-2). This set the stage for Typhoon Sperry's final phase.

By 290000Z, with a frontal boundary and associated mid-latitude trough moving eastward across southern Japan, a recurvature scenario appeared most probable. JTWC incorporated this into the warnings and called for recurvature in 48-hours. Sperry came under the influence of the mid-latitude westerlies and recurved passing 175 nm (324 km) to the east of the island of Okinawa in the Ryukyu Island chain.

After recurvature, Sperry started a gradual acceleration toward the northeast. By 1800Z on the 30th, the intense central convection became displaced south-southwest of the low-level circulation center. A steady decrease in cloud organization and intensity followed. Figure 3-04-3 shows the proximity of the frontal boundary and effect of the strong vertical wind shear on the remaining convection. The final warning was issued as Sperry transitioned to extratropical at 010600Z.

After completing extratropical transition, the low-level circulation drifted eastward embedded in the frontal boundary. There were no reports of lives lost or damage to shipping due to Typhoon Sperry.

SUPER TYPHOON THELMA (05W)

Thelma was the first of four significant tropical cyclones to develop in July and the first super typhoon of 1987. Forecasting the timing and location of recurvature presented a problem for JTWC. After recurvature, Thelma slammed into Korea causing extensive damage and the loss of many lives.

As a tropical disturbance, Thelma's initial intensification was slow, but once the system became organized it developed at very near the normal Dvorak rate (Dvorak, 1984) of one "T-number" per day from 25 to 130 kt (13 to 67 m/sec). Thelma originated in the monsoon trough as a broad area of convection with slight curvature. Dvorak analysis estimated an intensity of 25 kt (13 m/sec), while synoptic data indicated a cyclonic surface circulation was present along with upper-level divergence. As a result, the area was mentioned on the Significant Tropical Weather Advisory (ABPW PGTW) at 060600Z. Over the next

eight hours, the amount of convection and its organization increased. In addition, an aircraft reconnaissance investigative mission early on the 7th was able to close off the low-level circulation center and found a minimum sea-level pressure (MSLP) of 1003 mb. They also reported maximum sustained surface winds of 20 kt (10 m/sec). At 070300Z, JTWC issued a Tropical Cyclone Formation Alert.

The first warning on Tropical Depression 05W was issued at 071800Z when the system demonstrated a steady increase in convection and organization, and satellite intensity analysis estimated 30 kt (15 m/sec) sustained surface winds. The forecast philosophy called for movement toward the north for 24-hours through a weakness in the 700 mb ridge. The ridge was then expected to strengthen and drive the system toward the west. This did occur, but at speeds nearly triple those forecast.

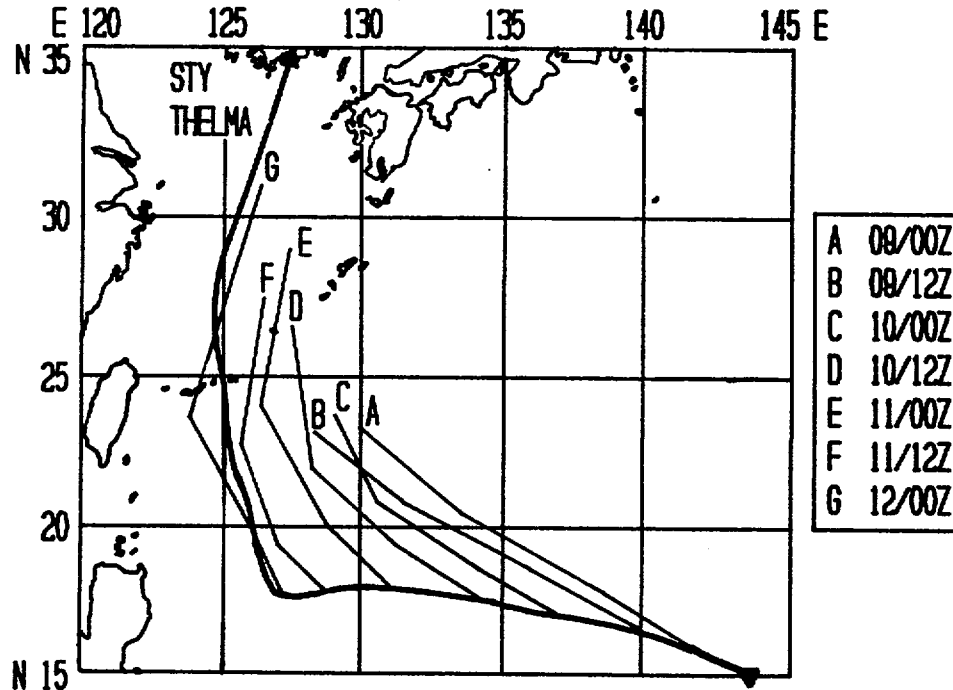


Figure 3-05-1. Plot of OTCM guidance. The OTCM, JTWC's primary dynamic aid, repeatedly indicated recurvature.

Initially, Thelma did not develop as quickly as expected. Once the first warning had been issued on Tropical Depression 05W, the system became broader and less organized. Aircraft reconnaissance scheduled for 080000Z was unable to close off a surface center. Thirteen hours later, the poorly organized system passed about 60 nm (111 km) to the north of Guam. Finally at 090000Z (on warning number six), the system was upgraded to tropical storm intensity. The upgrade was based on aircraft reconnaissance data at 090029Z which reported a MSLP of 996 mb and maximum sustained surface winds of 50 kt (26 m/sec). (Post-analysis indicated that the intensification had most probably occurred 12-hours earlier.)

JTWC's primary aid, the One-Way Interactive Tropical Cyclone Model (OTCM), preferred a northwesterly track or hinted at recurvature in the 48- to 72-hour time frame beginning with the guidance for warning number 3 (080600Z July) (see Figure 3-05-1). Recurvature forecasts started with warning

number 3, valid at 080600Z. Although Thelma continued tracking in a westward direction, JTWC mistakenly continued to forecast recurvature for the next 30-hours (spanning six warnings).

At 091200Z, Thelma began developing a banding eye. Warning number 10, valid at 100000Z, upgraded the system to a typhoon. This action was based on the aircraft reconnaissance data at 092138Z and 100011Z that indicated an extrapolated MSLP of 974 mb and estimated maximum sustained surface winds of 80 kt (41 m/sec). Typhoon Thelma reached its maximum intensity at 111200Z, after a 36-hour pressure fall of 66 mb (and a 12-hour pressure fall of 25 mb) down to 911 mb. During this time, Dvorak intensity estimates kept pace from approximately 77 kt (40 m/sec) to approximately 127 kt (65 m/sec). At 111200Z, Thelma became the season's first super typhoon. Afterward, infrared satellite imagery indicated a warming of the cloud tops which indicated that Thelma had peaked in intensity. Satellite

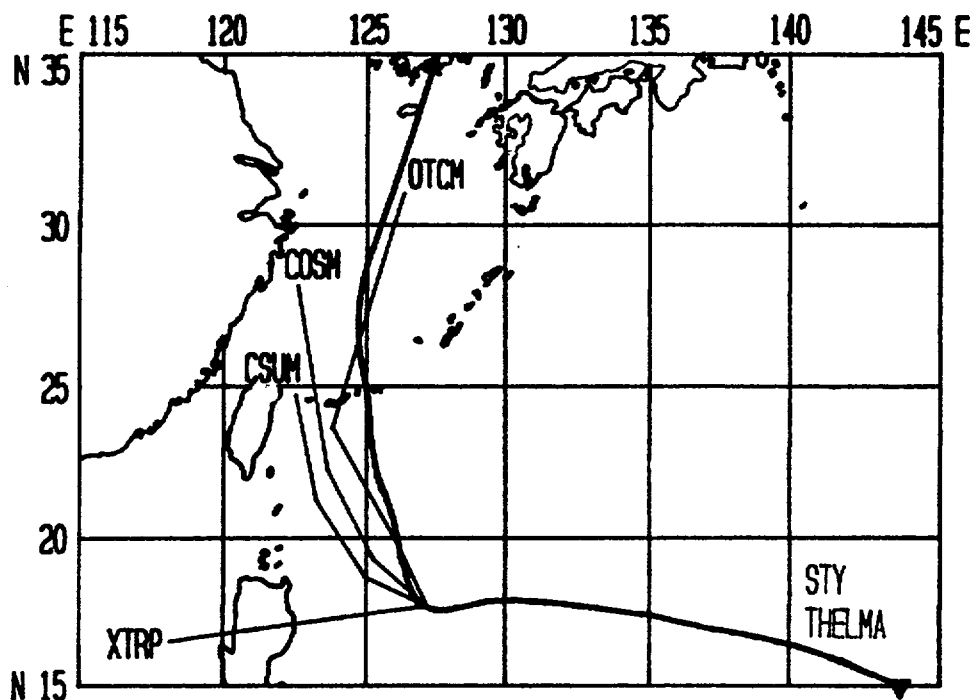


Figure 3-05-2. Plot of statistical aids (CSUM and COSMOS), dynamic numerical aid (OTCM), and persistence (XTRP) along with the final best track at 120000Z, at the point of the abrupt track change toward the north.

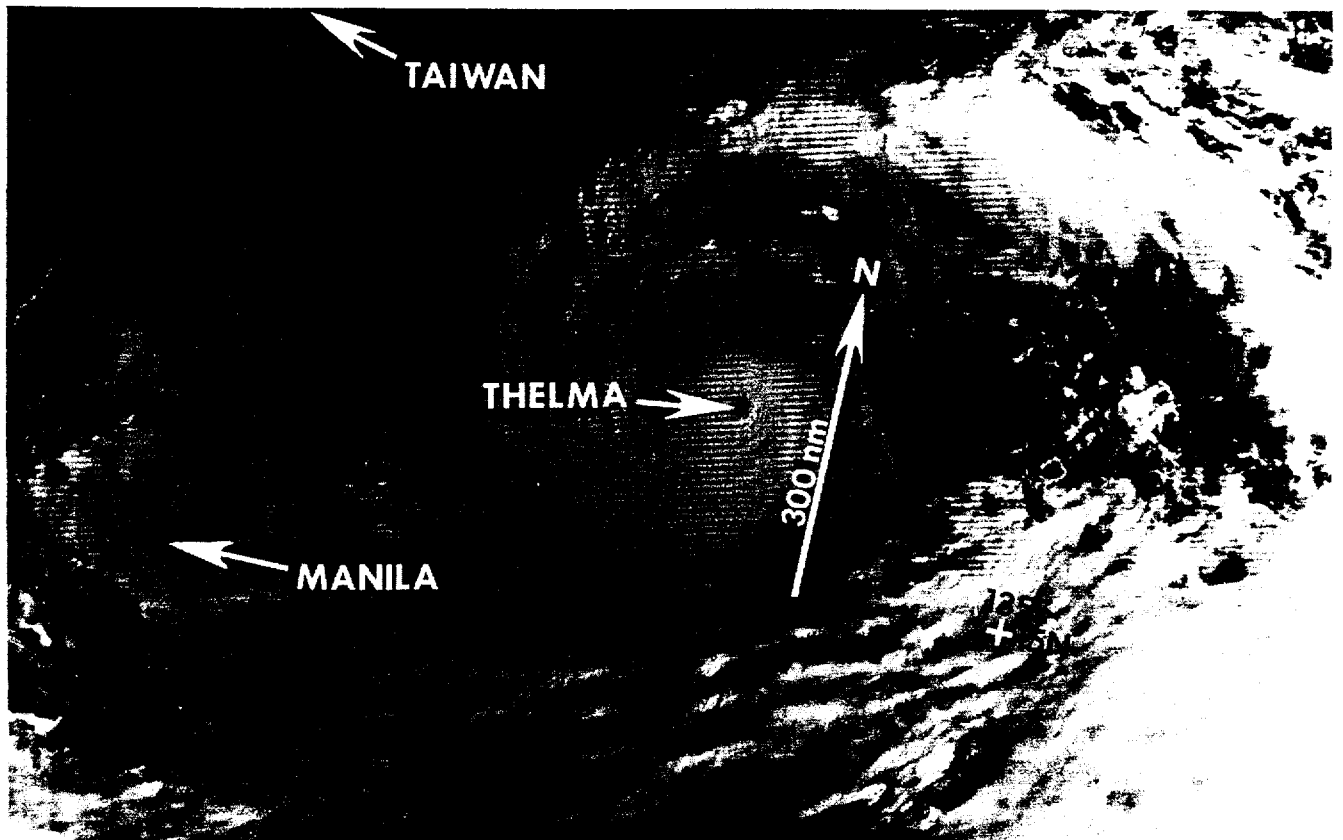


Figure 3-05-3. Visual satellite imagery showing Typhoon Thelma after reaching maximum intensity. Note how the upper-level outflow has become restricted to the north (110632Z July NOAA visual imagery).

imagery also indicated the system's upper-level outflow had become restricted to the north (see Figure 3-05-3). Aircraft reconnaissance at 112353Z found that the eye was open to the north and was becoming elliptical.

Typhoon Thelma began a sharp turn toward the north at 120000Z. Earlier, the dynamic forecast aid OTCM had repeatedly forecast movement toward the north or northwest (see Figure 3-05-2), but the typhoon continued to track westward. By 121200Z, Thelma was heading just west of north and the OTCM guidance was on track.

Even though Thelma's abrupt course change occurred 300 nm (556 km) east of northern Luzon, heavy rains and high seas resulted in at least twelve fatalities in the

Philippine Islands. The northerly track took the typhoon west of the island of Okinawa, Japan, and resulted in the evacuation of military aircraft. Commercial airlines also interrupted service, which stranded thousands of air travelers as Thelma passed by.

Finally Typhoon Thelma slammed into South Korea, where widespread flooding caused death and destruction. Floods from Thelma covered thousands of houses, ruptured reservoirs, and destroyed roads, railroad tracks and embankments. News coverage from Korea reported that Thelma killed at least 123 people with 212 additional people listed as missing. The missing were largely seamen and fisherman, who were caught offshore. Officials estimated losses at more than \$124 million from damaged or destroyed houses, crops, and water craft.

TYPHOON VERNON (06W)

Typhoon Vernon, the second of four significant tropical cyclones to develop in July followed closely on the heels of Super Typhoon Thelma (05W). It was a weak and disorganized system throughout most of its lifetime. As such, initial positioning problems arose in the Philippine Sea due to differences between real-time fix information from radar, satellite and aircraft.

The initial tropical disturbance was first detected in the near-equatorial trough near the island of Truk in the eastern Caroline Islands at 140000Z July and was subsequently listed on the Significant Tropical Weather Advisory (ABPW PGTW) as having poor potential for

development into a significant tropical cyclone. However, six hours later a low-level circulation was apparent on visual satellite imagery. The satellite intensity estimate (Dvorak, 1984) was 25 kt (13 m/sec) and a Tropical Cyclone Formation Alert (TCFA) was issued at 140830Z. Convective activity did not increase appreciably for the next two days, but the TCFA was reissued twice due to its persistence. On 161800Z, the first warning was issued for Tropical Depression 06W, based on an estimate of maximum sustained surface winds of 30 kt (15 m/sec) from satellite imagery. The initial forecasts were based on a persistent westward trend with higher than normal speeds of 17 kt (32 km/hr).

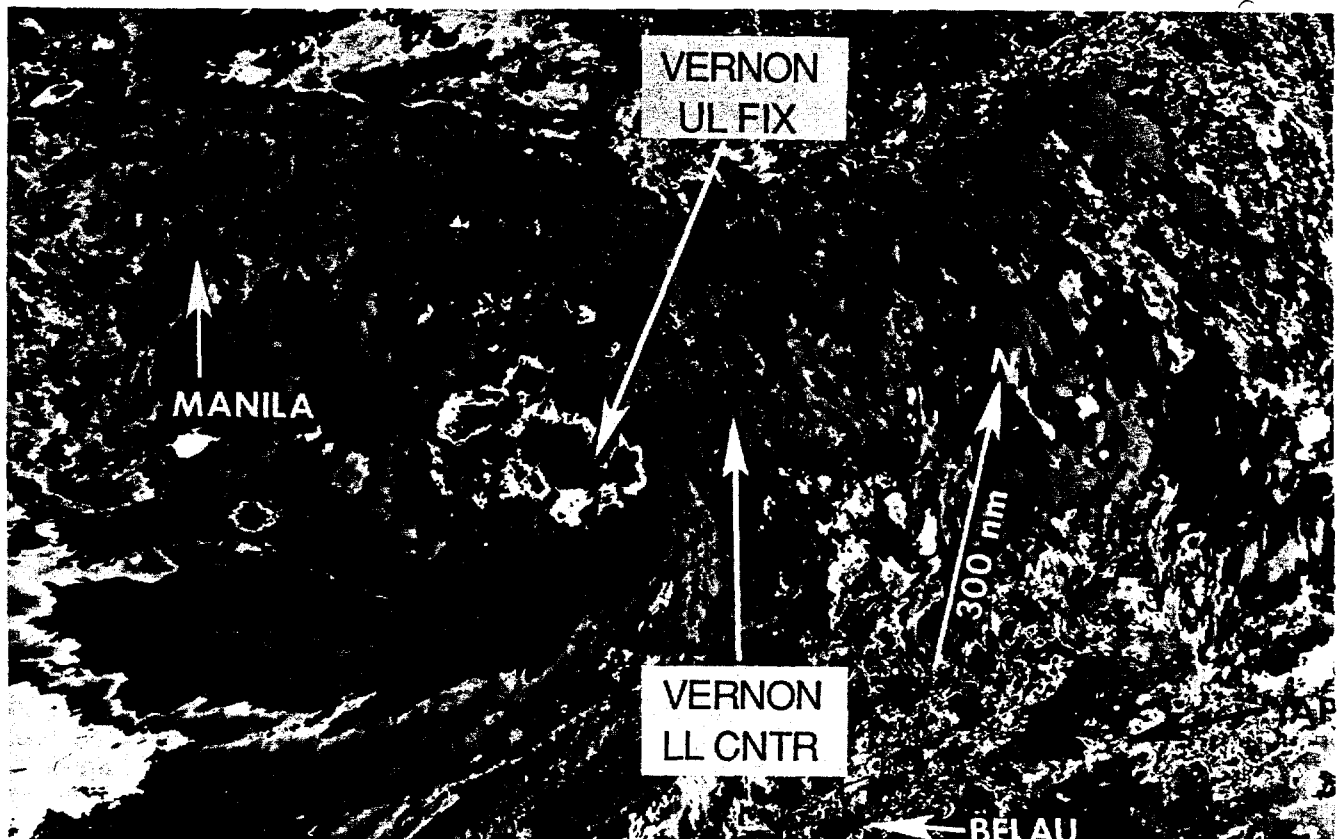


Figure 3-06-1. The area of intense convection as seen on enhanced infrared satellite imagery. This feature was used to fix Vernon during most of the period between 170000Z and the relocation at 181200Z (180042Z July DMSF infrared imagery).

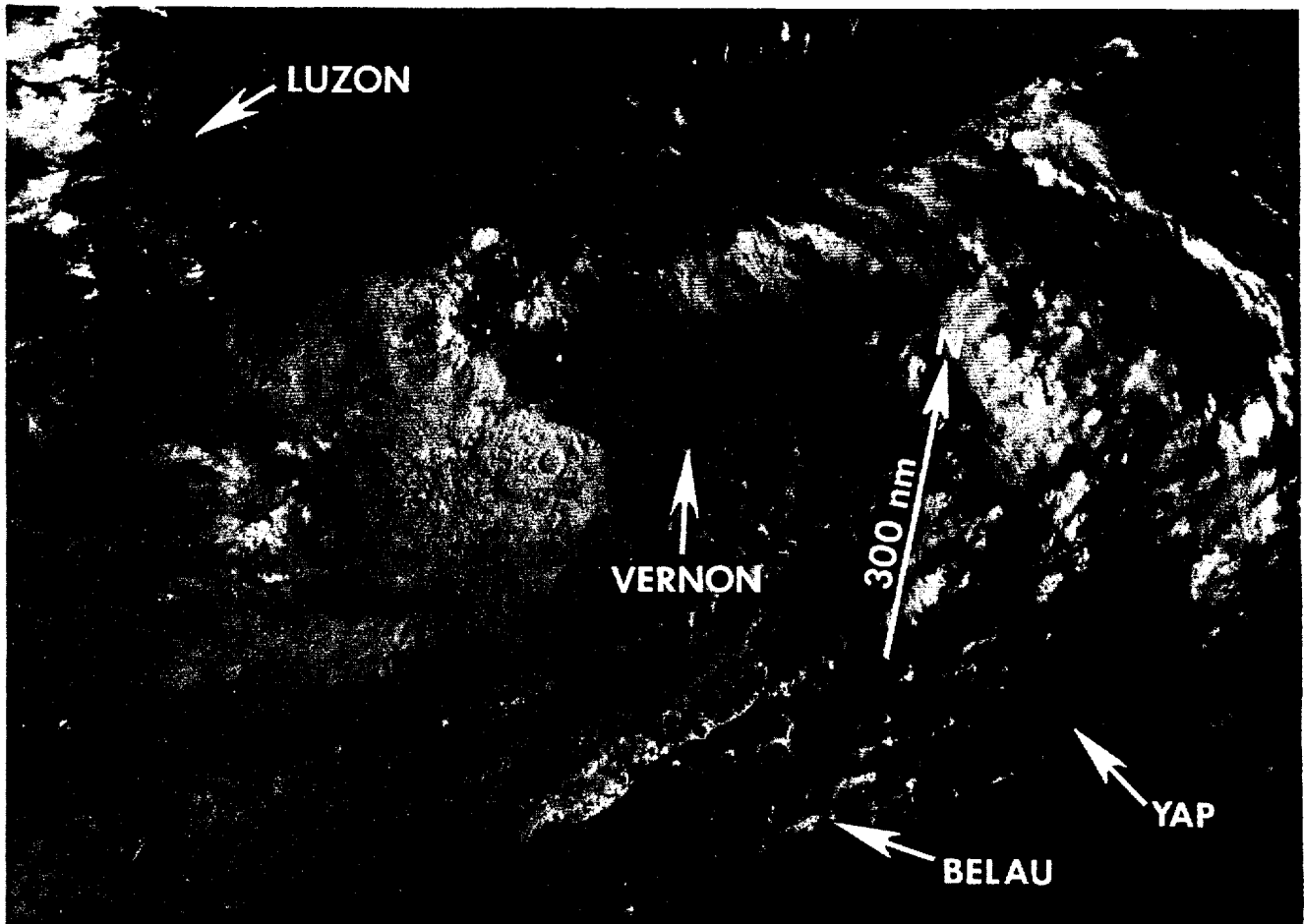


Figure 3-06-2. The exposed low-level circulation center which was mistakenly thought to be a secondary circulation can be seen in the center of the above image. This low-level circulation was not identified as Vernon's main circulation center until 181200Z (180042Z July DMSP visual imagery).

Between 170600Z and 181200Z, satellite fixes and radar reports indicated Vernon had continued to move westward toward the central Philippine Islands. During this time, the most intense area of curved convection remained just east of the Philippines (see Figure 3-06-1) and appeared to be the dominant feature. However, there was also a low-level circulation center northeast of the deep convection which was initially believed to be a secondary circulation center. Figure 3-06-2 shows this exposed low-level circulation center about 180 nm (333 km) northeast of the primary mass of convection at 180042Z.

After the last successful fix at 170224Z July, keeping track of Vernon's weak low-level circulation center became increasingly more difficult. To compound the problem, the radar fixes at two different sites in the Philippine Islands (WMO 98558 and WMO 98447) reinforced the satellite analysis which continued to fix on the main convective mass that was moving towards southern Luzon (see Figure 3-06-3). As a result, Vernon's low-level circulation was not recognized until an exposed low-level circulation was identified by the satellite analyst at 181200Z. Immediately thereafter, Vernon was relocated approximately

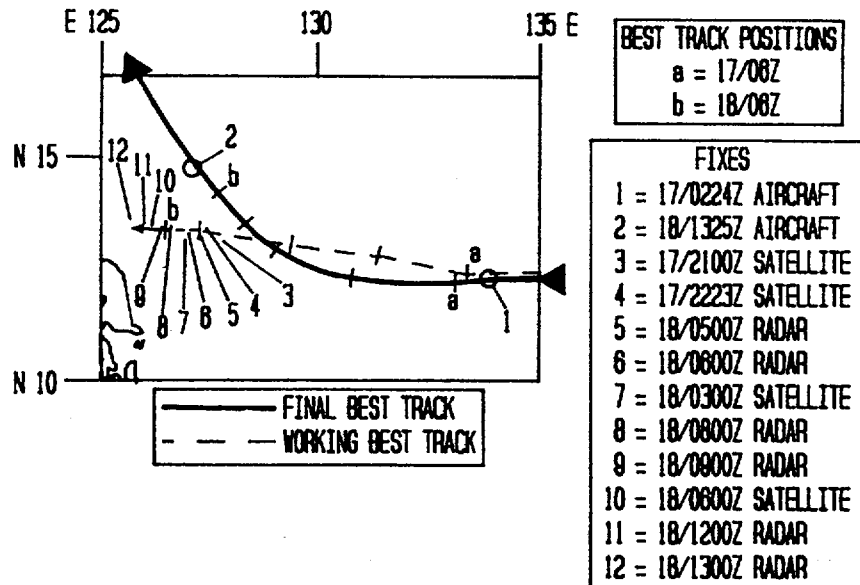


Figure 3-06-3. Typhoon Vernon's best track during the period when the system was relocated. Note that no aircraft fixes were made between 170224Z and 181325Z July. Also note the preponderance of radar fixes and satellite fixes which indicated westward movement when the system was actually moving northwestward (dashed lines). These fixes could not be used in the final best track.

145 nm (269 km) to the north-northeast of the original 180600Z position. This relocation was subsequently verified at 181325Z by the first aerial reconnaissance fix mission in nearly 36-hours.

The Aerial Weather Reconnaissance Officer (ARWO) on the fix mission reported passing a probable vortex center on the inbound leg of the primary fix mission as the aircraft was heading toward the fly-to-point given by the Typhoon Duty Officer. After consulting the

Typhoon Duty Officer, it was decided that the satellite and land radar fix position should be investigated. Once there, the ARWO reported rising heights at the 850 mb level and no low-level vortex. The Typhoon Duty Officer then concluded there was only one circulation center, vice multiple vortices. The aircraft crew was then requested to return to the vortex they had passed earlier and investigate it (see Figure 3-06-4). The ARWO subsequently located the vortex and reported a center height of 1363 m at 850 mb.

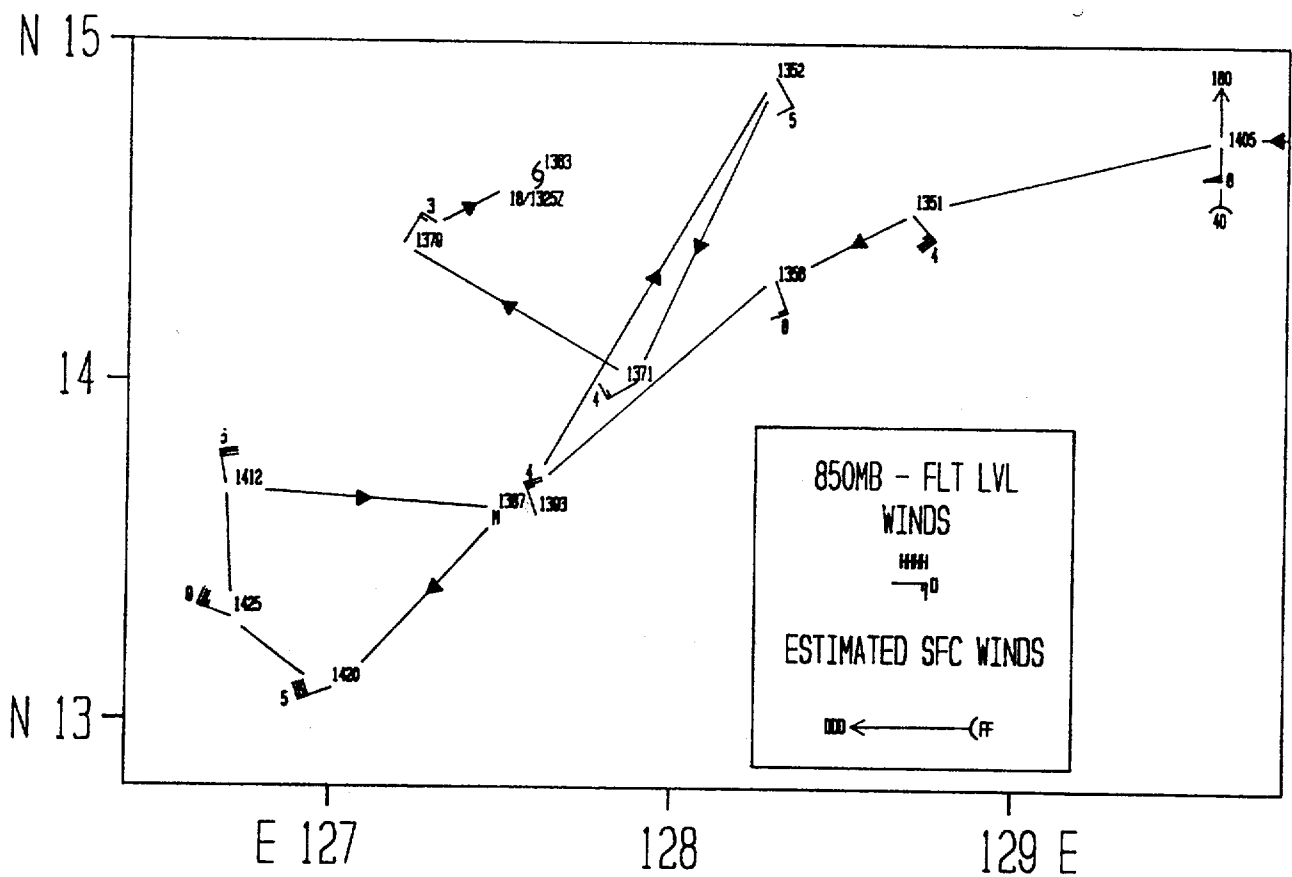


Figure 3-06-4. Plot of the 181325Z July aircraft fix mission which determined the low-level circulation center associated with Vernon.

After the relocation, radar reports from Guiuan Airport (WMO 98558) continued to fix Vernon 170 nm (315 km) south of the aircraft verified position. From synoptic data, there is no evidence that a distinct circulation ever

existed separate from Vernon's exposed low-level center. There is also no evidence that the central Philippine Islands ever experienced any significant winds associated with Vernon.

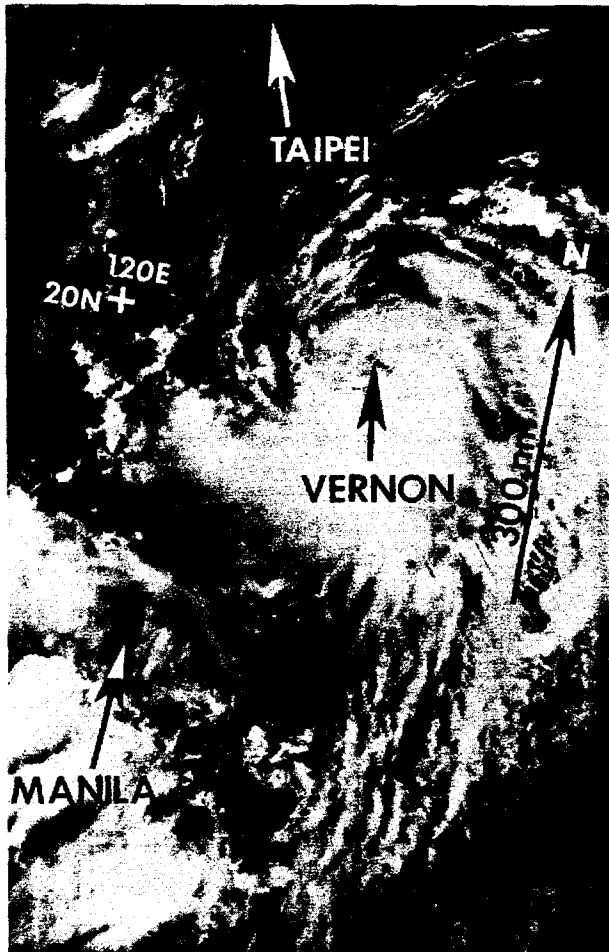


Figure 3-06-5. Typhoon Vernon at its peak intensity of 65 kt (33 m/sec) (200143Z July DMSP visual imagery).

Vernon began to track steadily northeastward toward Taiwan. It reached minimal typhoon intensity at 191200Z (see Figure 3-06-5). At that point positioning by satellite was no longer a problem due to the better defined central features. On 21 July,

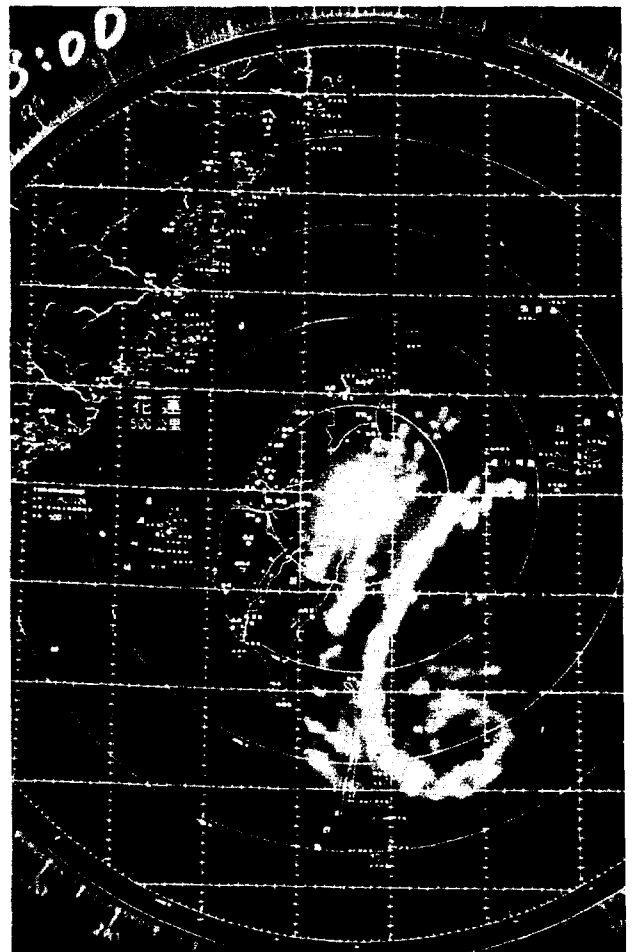
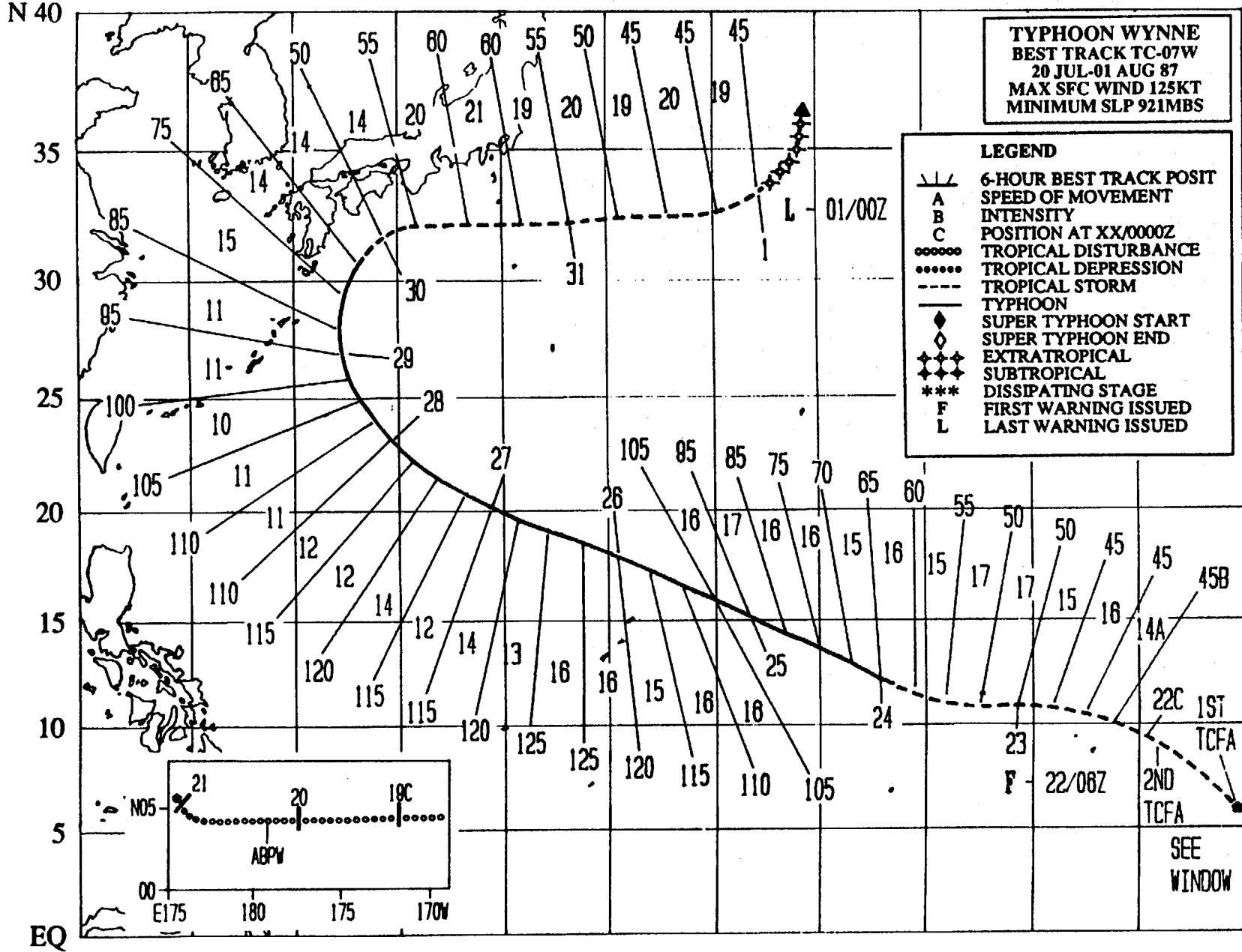


Figure 3-06-6. The spiralling rainband of Vernon as seen by radar from Hualien, Taiwan (WMO 46699) at 201500Z July (Photograph courtesy of Central Weather Bureau, Taipei, Taiwan)..

Typhoon Vernon began to interact with the terrain of Taiwan as it skirted the eastern shore and rapidly weakened to a tropical depression (Figure 3-06-6). Vernon dissipated in the East China Sea on 22 July after passing the northern tip of Taiwan.

E 120 125 130 135 140 145 150 155 160 165 170 175 E



TYPHOON WYNNE (07W)

Typhoon Wynne was the fifth typhoon in the western North Pacific in 1987 and was of interest due to several factors. Early communication with meteorologists from Kwajalein Atoll (WMO 91366) proved instrumental in relocating Wynne, using radar fixes during its formative stages. The system developed into the third "midget" typhoon of the year and maintained a visible eye for six days. Wynne tracked along a constant 294 degree bearing for four consecutive days, during which time, it crossed the northern Mariana Islands, causing extensive damage to the islands of Alamagan and Agrihan.

Wynne appeared as an amorphous, but persistent, mass of cloud in the maximum cloud

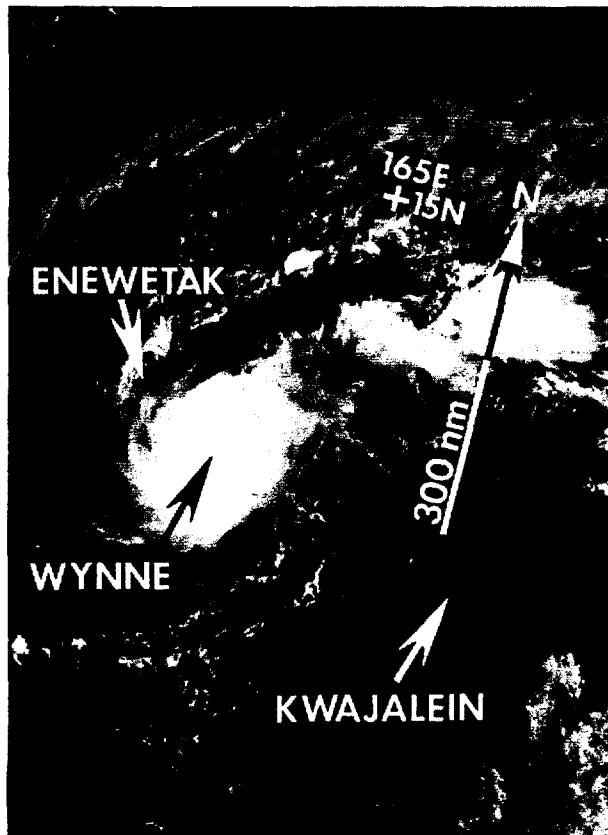


Figure 3-07-1. Wynne at the tropical storm stage of development about 200 nm (370 km) west-northwest of the Kwajalein Atoll. Note the relatively cloud-free ring surrounding the small bright CDO (222300Z July DMSIP visual imagery).

zone east of the dateline and was first mentioned on the 200600Z July Significant Tropical Weather Advisory (ABPW PGTW). Analysis of the sparse synoptic data indicated convergence enhancing cross-equatorial low-level flow into the system in the horizontal with moderate wind shear in the vertical.

Wynne moved westward and continued to improve in convective organization. Satellite intensity analysis (Dvorak, 1984) of the well-defined spiral cloud bands at 210000Z estimated 30 kt (15 m/sec) surface winds and 45 kt (23 m/sec) surface winds were forecast for the next day. Based on this information, a Tropical Cyclone Formation Alert (TCFA) followed at 210430Z. Through the 20th, Wynne's track remained westward in response to the synoptic-scale flow south of the subtropical ridge axis. On 21 July, however, satellite reconnaissance fix positions indicated cloud system center movement towards the northwest. Due to this track change the alert area was redefined at 212030Z and the TCFA was reissued.

Discussions on 22 July between the Typhoon Duty Officer (TDO) and meteorologists on the Kwajalein Atoll, Marshall Islands, provided invaluable positioning information. Kwajalein was receiving light winds and radar showed the main convection associated with the tropical cyclone to be well to the north of their location. The result was a 120 nm (222 km) northward relocation of the 221200Z warning position from its expected location. By the end of the day, Wynne had separated from the maximum cloud zone and drawn down into a small bright central dense overcast (CDO) (Figure 3-07-1).

An eye first became visible on satellite data at 240000Z. From that point onward (a period of six days), the system was characterized by a small eye. The eye diameter changed slightly from 12 nm (22 km) to 18 to 22 nm (33 to 41 km) in diameter. Typical of a smaller than normal system, it had smaller than average 30 kt (15 m/sec) wind radii. Aircraft reconnaissance revealed this anomaly.

Figure 3-07-2. Plot of aircraft reconnaissance data from 252134Z to 260125Z July, showing the surface and 700 mb flight-level wind distribution around Typhoon Wynne. Note the greater extent of the wind radii in the northeastern semicircle.

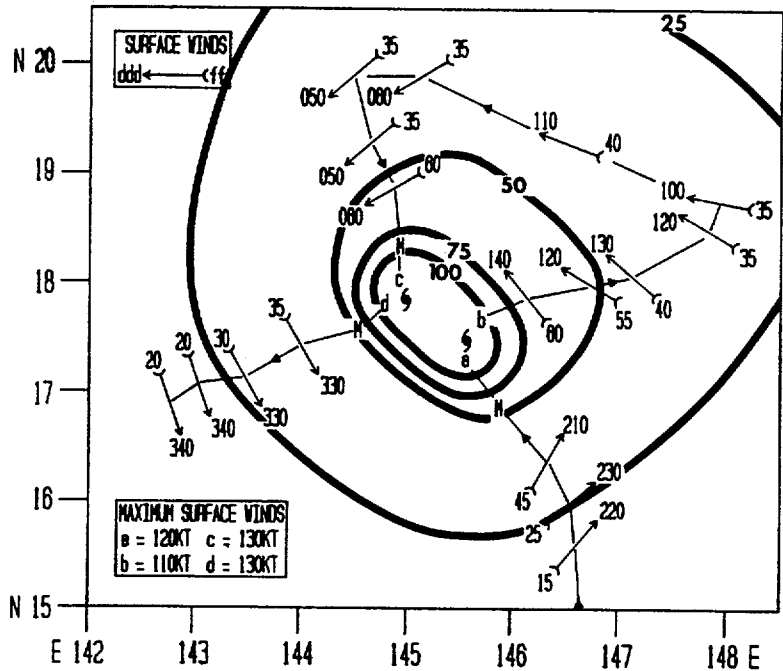


Figure 3-07-3. Typhoon Wynne two hours before crossing the northern Marianas and near its closest point of approach to Guam. With the low morning sun off the right side of the picture, differences in cloud top heights are accentuated by shadowing. In this image an apparent 'stadium' effect can be seen; the larger upper-level inner eye wall boundary slopes downward to the concentric smaller low-level eye (252015Z July DMSP visual imagery).

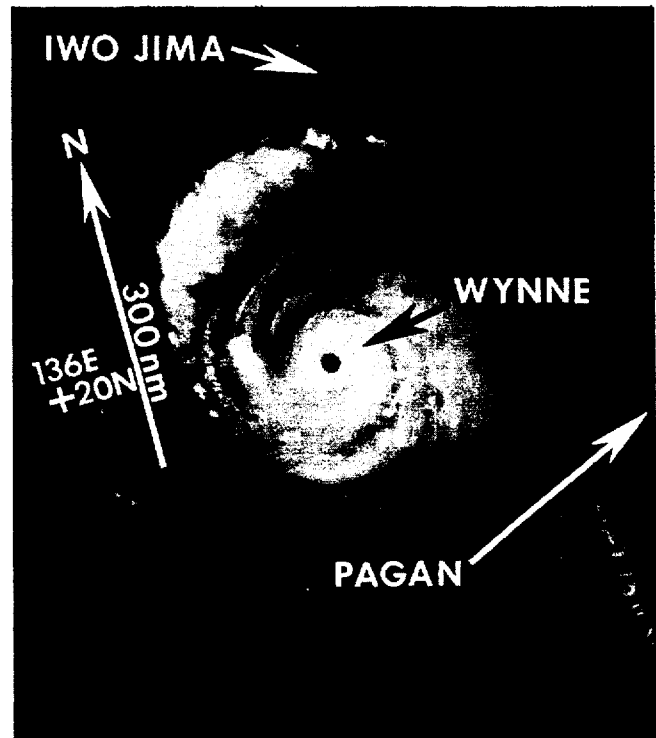
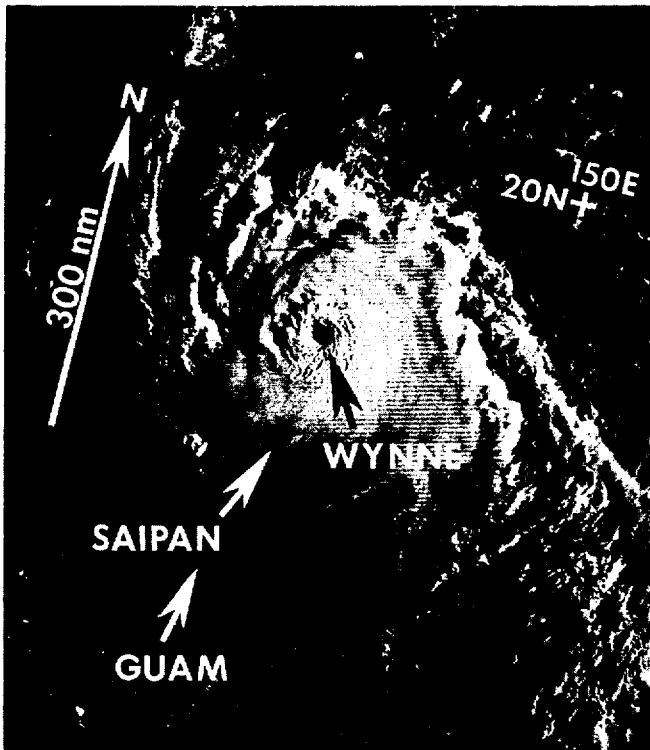


Figure 3-07-4. Midget Typhoon Wynne near maximum intensity. Note the well-defined 15 nm (28 km) eye (261815Z July NOAA infrared imagery).

Wynne's wind radii were nearly twice as large in the northeast semicircle as elsewhere (Figure 3-07-2). This appears to be related to the pressure gradient between Wynne and the subtropical anticyclone to the north. Figure 3-07-3 shows Typhoon Wynne two hours before it passed directly over the northern Marianas island of Alamagan (240 nm (444 km) north-northeast of Guam). At approximately the same time (240000Z through 271200Z) Wynne followed an almost straight track along a mean 294 degree bearing. While on this course and mean speed of 16 kt (30 km/hr), the typhoon attained its maximum intensity of 125 kt (64 m/sec) on the 26th (Figure 3-07-4).

An interesting aspect of Wynne's travel across the western North Pacific was that it maintained a brisk forward speed of movement, even through recurvature, where it slowed only slightly to 10 kt (19 km/hr). Typically, a larger decrease in forward speed is expected as a system passes through the area of weaker steering flow at the break in the subtropical ridge axis.

As Wynne rounded the western end of the mid-level subtropical ridge, it began to experience increasing vertical shear from the north. The exposed low-level cyclonic circulation became visible at 291500Z (Figure 3-07-5). Even with this unfavorable environment in the vertical, there were strong winds associated with the system for the next two days. Aircraft reconnaissance at 291111Z found 700 mb winds of 76 kt (39 m/sec).

Wynne was downgraded from typhoon to tropical storm intensity on the 32nd warning (valid at 300000Z) after a satellite intensity estimate of 50 kt (26 m/sec) was attained. Subsequent aircraft reconnaissance at 292157Z and 300027Z also reported maximum 700 mb flight-level winds of 60 kt (31 m/sec).

Wynne continued slowly weakening as it moved eastward, south and southeast of the main Japanese island of Honshu. Its forward speed increased as a result of stronger mid-level westerly flow. At the same time, Wynne began entraining cooler, drier air from the north. As a consequence, extratropical transition was complete at 010000Z August.

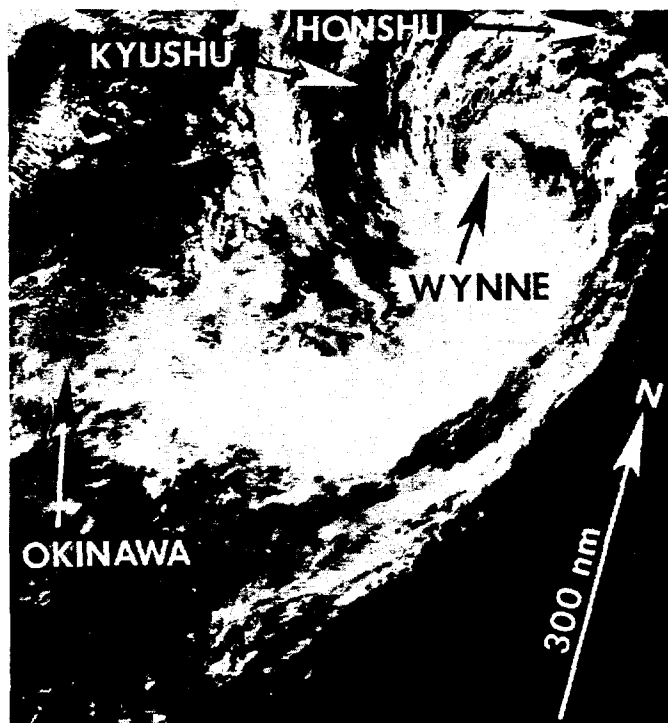


Figure 3-07-5. Wynne, at tropical storm intensity 130 nm (241 km) east of the Japanese island of Kyushu. Low-level cloudiness defines the exposed circulation center. Of interest, the bright and dark patches on the ocean's surface to the east of the system are the result of sun-glint. These patches indicate the areas of relatively smooth ocean surface with less wind waves which are usually the result of lighter surface winds near the axis of the lower-tropospheric subtropical ridge. In this case the ridge axis runs east-to-west near 22 degrees North Latitude. Understanding the location and atmospheric processes associated with this ridge are vitally important to tropical cyclone forecasting (292359Z July DMSP visual imagery).

In retrospect, the islands of Alamagan and Agrihan suffered the only recorded major damage due to Wynne's passage. Their crops were 90 to 100 percent destroyed and all coconut trees were downed. Fortunately no lives were lost. Except for this head-on meeting between Wynne and these islands, no synoptic data revealed the potent punch of this midget typhoon. Only direct aircraft measurement and indirect satellite reconnaissance recorded the wind intensities because of the system's small size.

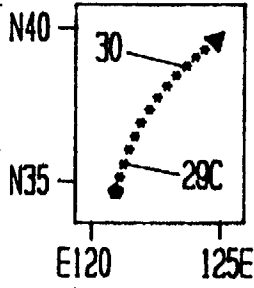
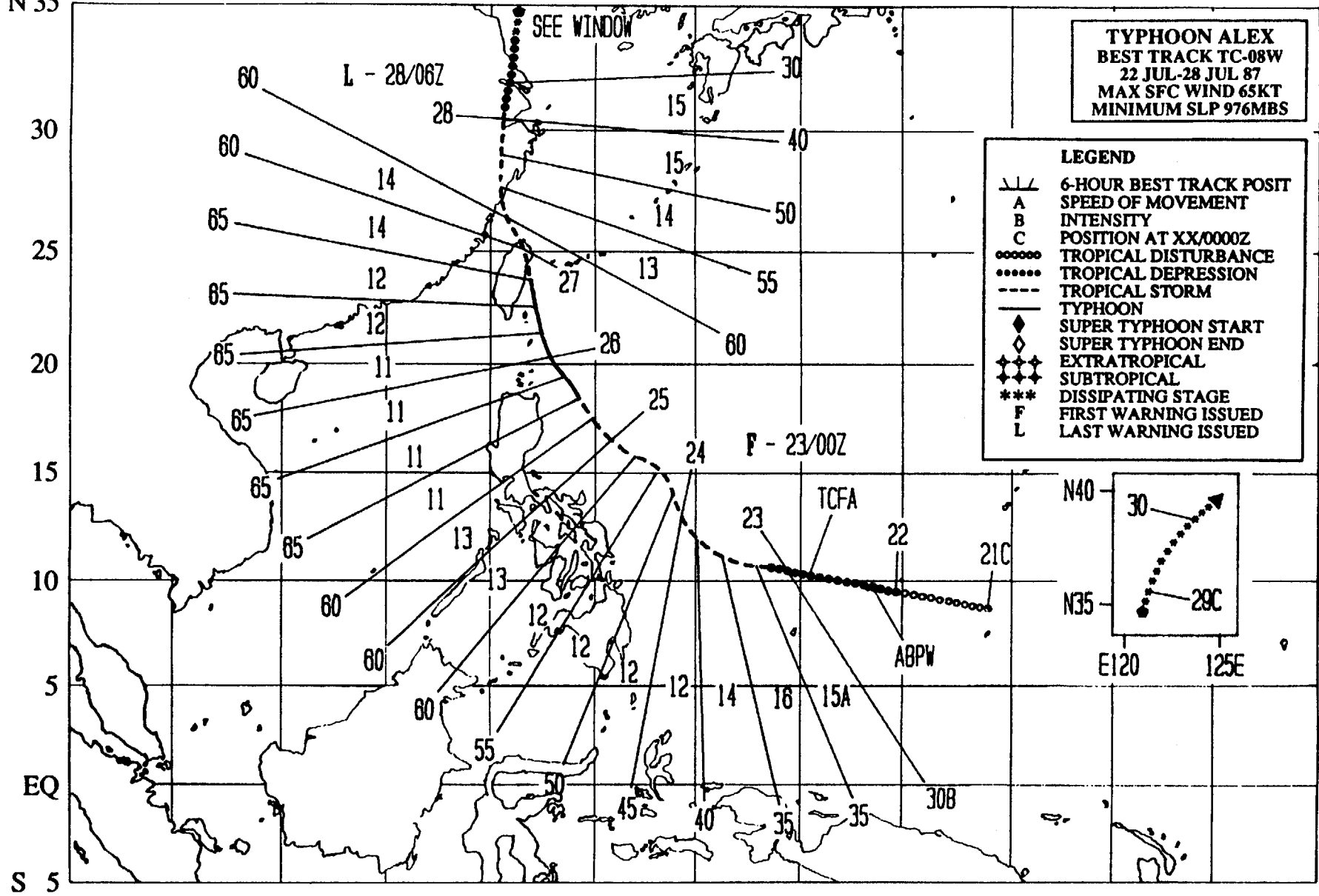
E 100 105 110 115 120 125 130 135 140 145 150 155 160 E

N 35

TYPHOON ALEX
BEST TRACK TC-08W
22 JUL-28 JUL 87
MAX SFC WIND 65KT
MINIMUM SLP 976MBS

LEGEND

- /—/— 6-HOUR BEST TRACK POSIT
- A SPEED OF MOVEMENT
- B INTENSITY
- C POSITION AT XX/0000Z
- TROPICAL DISTURBANCE
- TROPICAL DEPRESSION
- TROPICAL STORM
- TYPHOON
- ◆ SUPER TYPHOON START
- ◇ SUPER TYPHOON END
- ◆◆◆◆ EXTRATROPICAL
- ◆◆◆◆ SUBTROPICAL
- *** DISSIPATING STAGE
- F FIRST WARNING ISSUED
- L LAST WARNING ISSUED



54

S 5

TYPHOON ALEX (08W)

Typhoon Alex was the fourth and final tropical cyclone to develop during the month of July, and combined with Typhoon Wynne (07W) to form the first multiple-storm situation of the 1987 western North Pacific tropical cyclone season. Wynne (07W) passed through the Marshall Islands and intensified to tropical

storm intensity as Alex showed initial signs of development on July 22nd. Six days later, on the 28th, Wynne (07W) began to slowly recurve south of Japan as Alex dissipated over the eastern China coast. The closest the two systems came to one another was 740 nm (1370 km) late on the 28th.

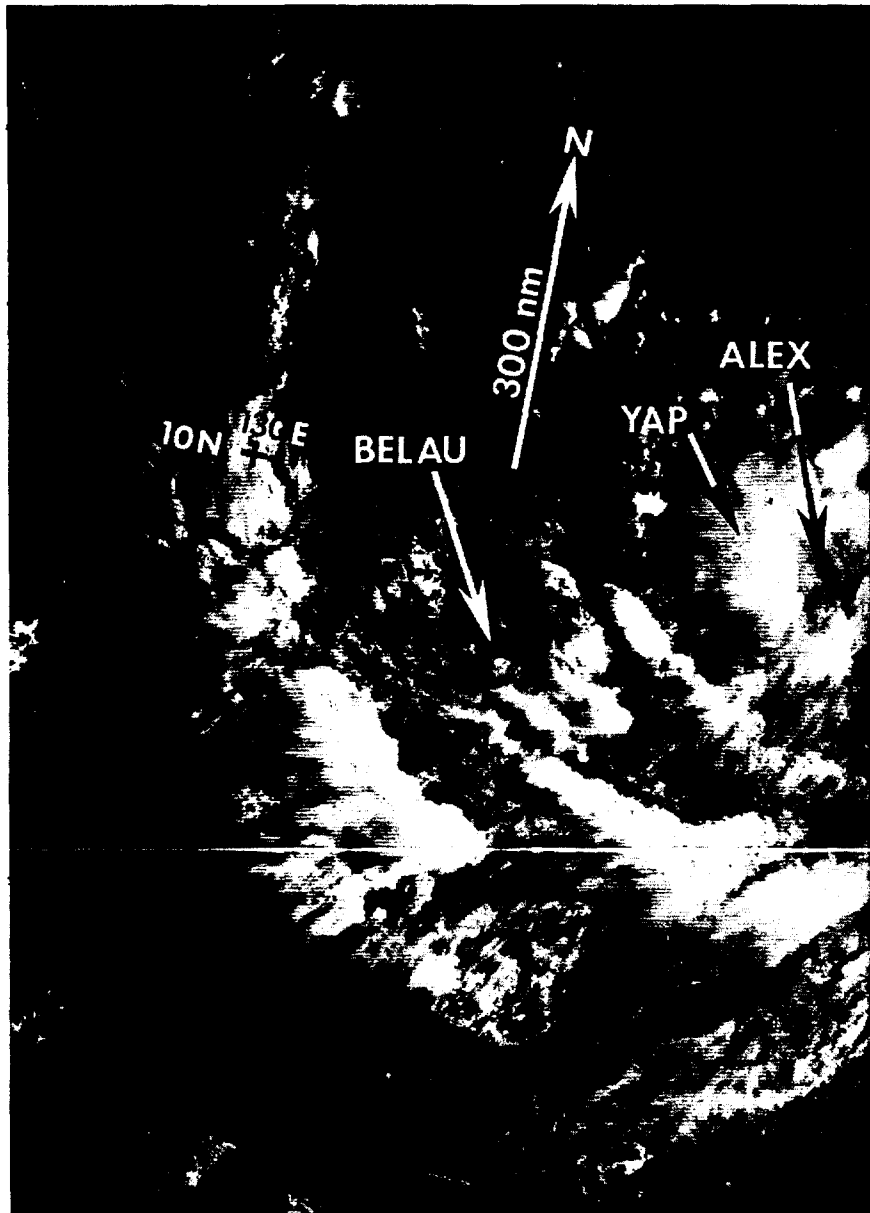


Figure 3-08-1. Morning view of the tropical disturbance in the Philippine Sea which would develop into Typhoon Alex. Convective banding is evident in the low-level cloud lines (220102Z July DMSP visual imagery).

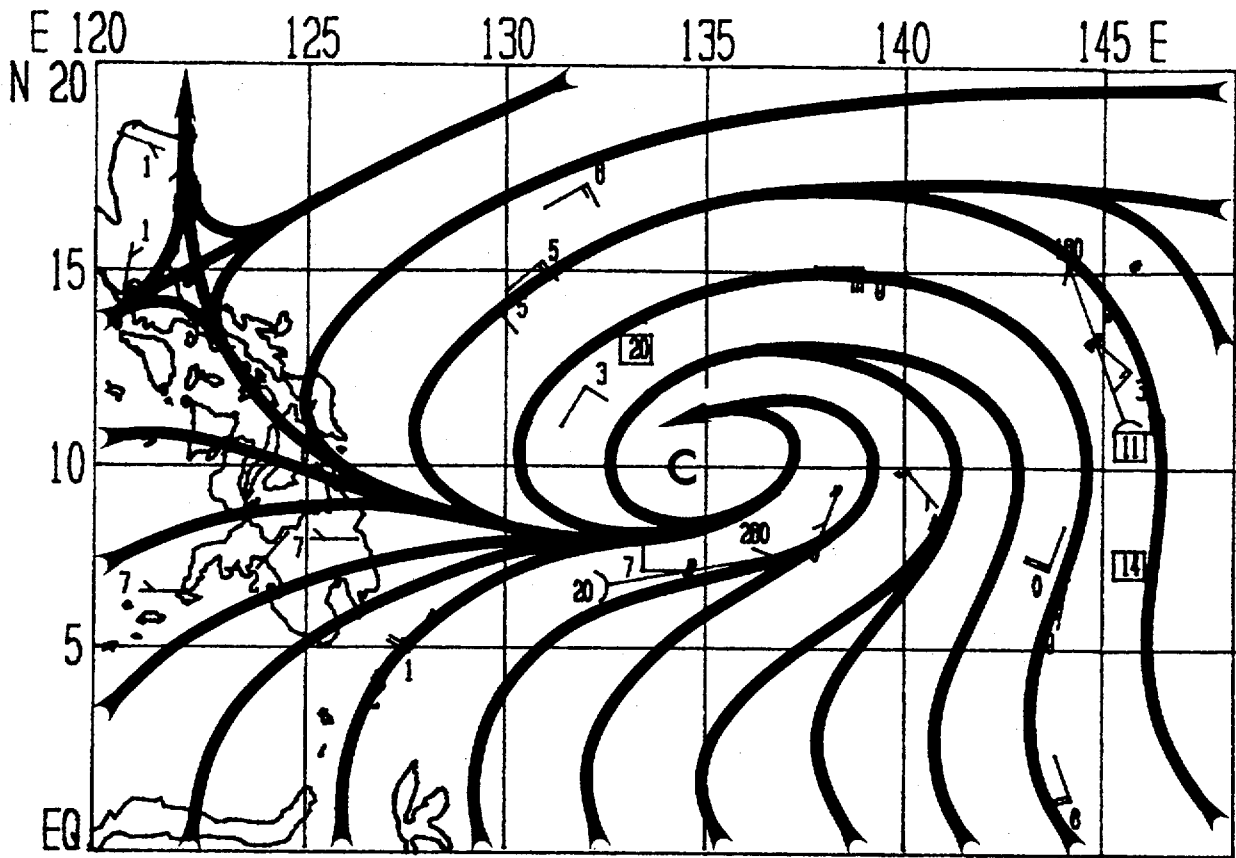


Figure 3-08-2. Synoptic surface/gradient-level streamline analysis of 230000Z July data shows a broad cyclonic circulation in the Philippine Sea with an estimated minimum sea-level pressure of 1000 mb and winds of 30 kt (15 m/sec). (Note: drifting buoy wind speeds (in kt) enclosed in boxes.)

Alex developed in the western end of an active monsoon trough which stretched east-to-west 2400 nm (4445 km) (south of 10 degrees North Latitude) from the dateline across the Marshall and Caroline Islands. Late on the 21st, routine analysis of satellite imagery indicated a tropical disturbance persisting in an area of poorly organized convection 200 nm (370 km) to the southwest of Guam. This area was noted on the Significant Tropical Weather Advisory (ABPW PGTW) at 220600Z due to its persistence and indications of convective banding in the low-level cloud lines visible on visual imagery that morning (Figure 3-08-1).

Over the next twelve hours, the convection increased and upper-level organization improved rapidly. Infrared satellite imagery at 221800Z indicated a central core of heavy convection had developed. Surface winds were estimated at 25 kt (13 m/sec) based on the Enhanced Infrared (EIR) technique (Dvorak, 1984). As a result, JTWC promptly issued a Tropical Cyclone Formation Alert (TCFA) at 221930Z even though synoptic data indicated only a broad surface circulation with an estimated minimum sea-level pressure of 1005 mb.

Satellite intensity analysis at 230000Z estimated surface winds of 35 kt (18 m/sec) associated with this disturbance. A 30 kt (15 m/sec) ship observation north of the disturbance for this same time provided some ground truth to the Dvorak estimate (see Figures 3-08-2 and 3-08-3). Based on these data, JTWC immediately issued the first warning on Tropical

Depression 08W. Six hours later, on the second warning, Alex was upgraded to tropical storm intensity based on increased organization that became evident on satellite imagery at 230600Z. Within 12-hours a well-defined convective band could be seen on satellite imagery wrapping into the center.

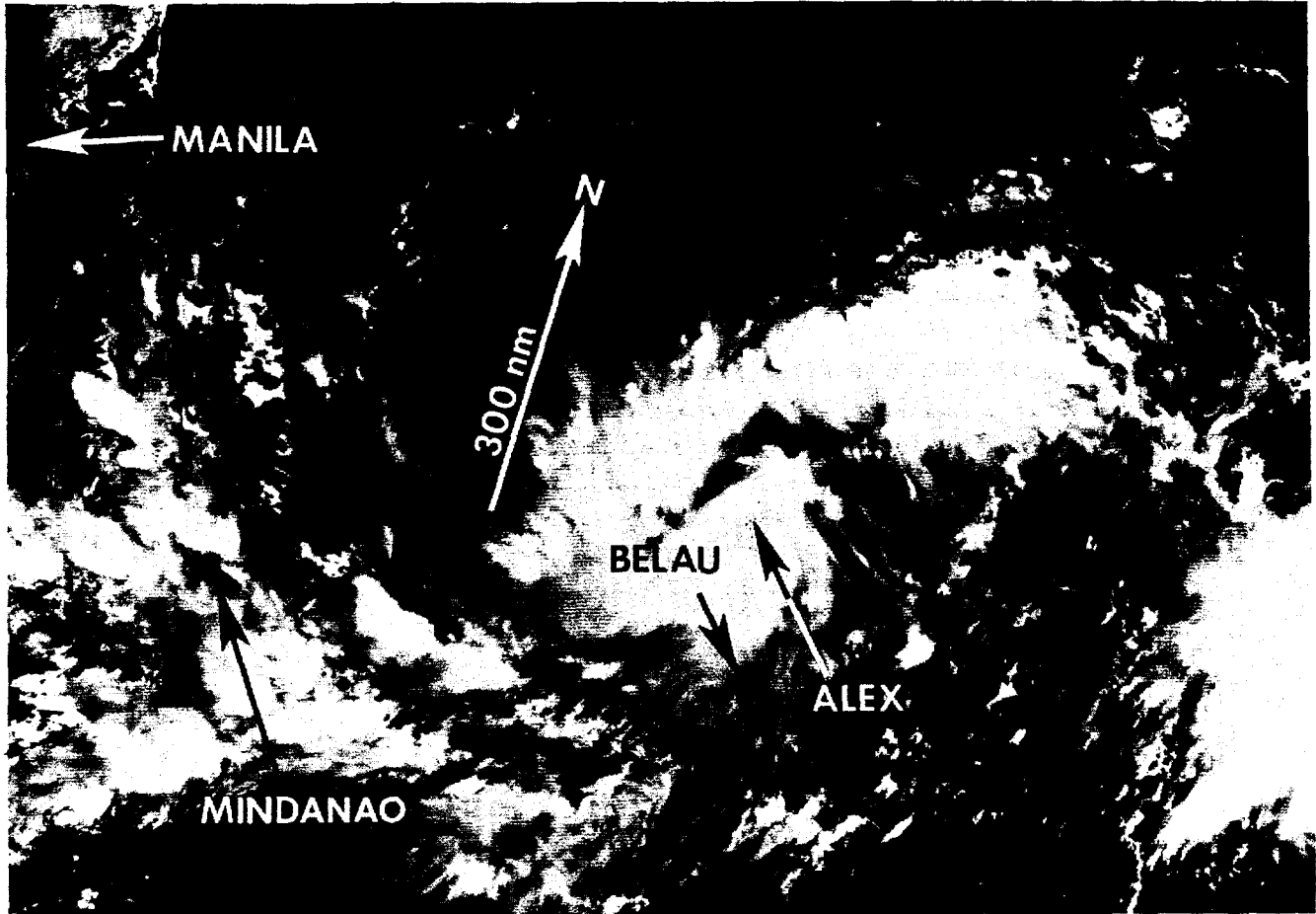


Figure 3-08-3. Visual satellite imagery near the time of the first warning on Tropical Depression 08W. See the 230000Z July synoptic surface/gradient-level streamline analysis in Figure 3-08-2 for comparison (230041Z July DMSP visual imagery).

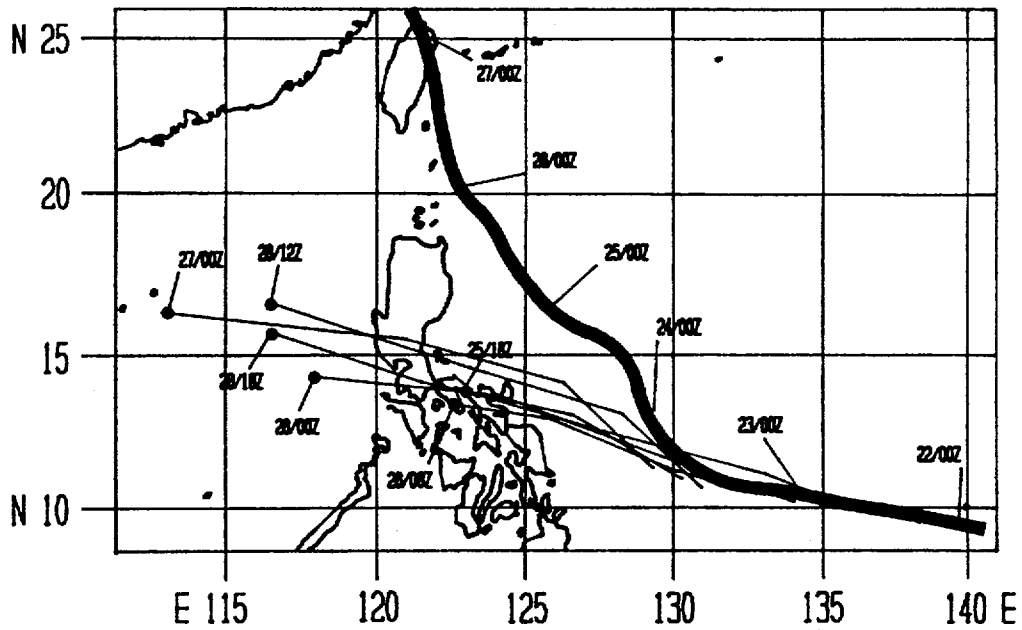


Figure 3-08-4. Initial OTCM 72-hour guidance for Alex indicated the system would remain south of the subtropical ridge and move across the Philippine Islands. Alex's best track is also shown for comparison.

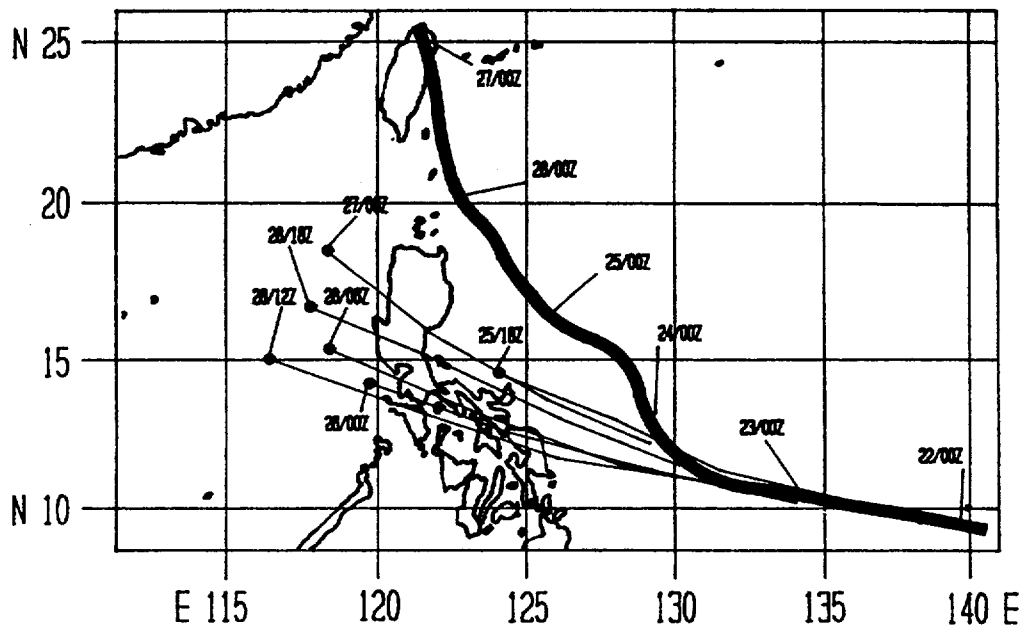


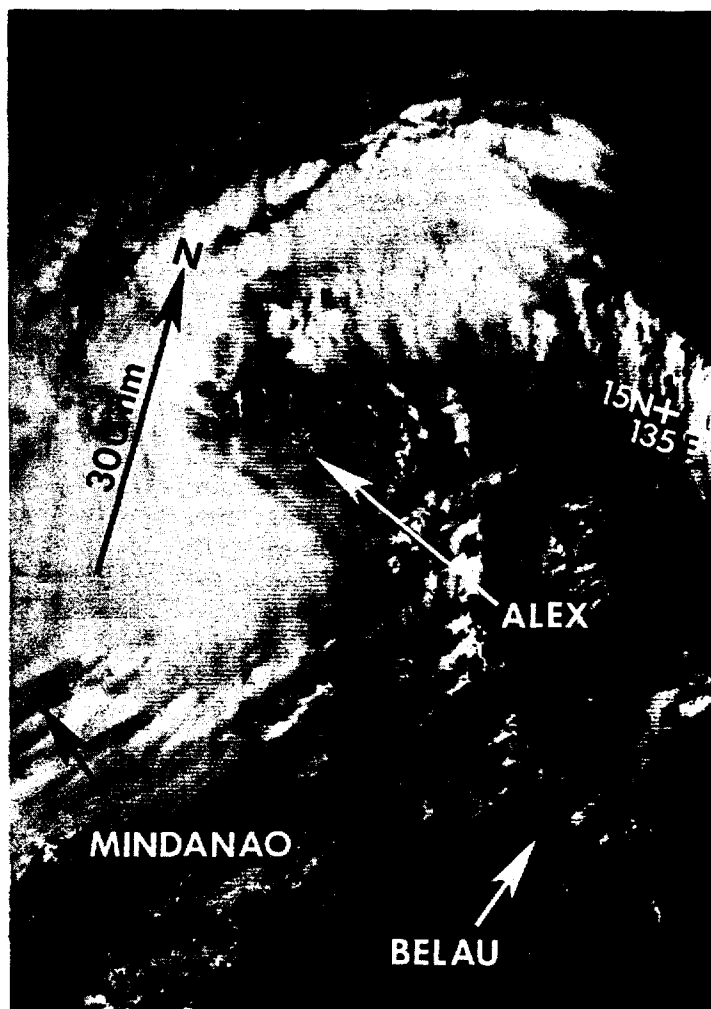
Figure 3-08-5. Initial HPAC 72-hour guidance for Alex agreed with the OTCM in keeping the system south of the subtropical ridge and moving it across the Philippine Islands. Alex's best track is also shown for comparison.

The main forecast problem occurred early, during the first two days of the system's lifetime. Alex was forecast to track across the Philippine Islands on warnings one through five. The primary guidance came from two forecast aids -- the One-Way Interactive Tropical Cyclone Model (OTCM) and the Half Climatology and Persistence Model (HPAC). Figures 3-08-4 and 3-08-5 show the guidance received for the first six warnings from the OTCM and HPAC, respectively. They incorrectly suggested Alex would remain south of the strong subtropical ridge, move across the Philippine Islands and then turn northward towards mainland China. JTWC forecasters determined the OTCM and HPAC guidance was flawed and, on the sixth warning, relocated Alex further north after several satellite fixes indicated it was moving towards the northwest rather than the west-northwest. Unfortunately, beginning at 240900Z, there was increased

scatter in the satellite fixes as a cirrus canopy developed over the center. This left JTWC forecasters with no clear-cut indication of exactly where Alex's low-level center was. A solitary aircraft radar fix was obtained at 240916Z which provided some close in information, however a trained Aerial Weather Reconnaissance Officer was not onboard the flight and the meteorological accuracy of the position was suspect. Figure 3-08-6 shows a satellite image prior to the time of the aircraft fix. Notice the exposed low-level center is displaced slightly northeast of the heaviest convection. The radar site at Guiuan (WMO 98558) in the Philippine Islands fixed this area of heavy convection and added to the uncertainty as to where the actual location of Alex's center was.

Forecast guidance for the next five warnings indicated Alex should track through

Figure 3-08-6. Morning view of Alex. The exposed low-level center is displaced slightly northeast of the heaviest convection (240021Z July NOAA visual imagery).



the Luzon Strait and make landfall over mainland China to the west of Taiwan. JTWC forecasts for this time period (240600Z through 250600Z) reflected this guidance. Also during this period, Alex continued to slowly intensify. Between 241500Z and 241800Z, it developed an eye. This eye was first implied by a warm spot in the central cloud mass on the nighttime infrared imagery (see Figure 3-08-7).

At 1200Z on the 25th, Alex reached its maximum intensity of 65 kt (33 m/sec) and was upgraded to typhoon status. At that time, Alex was 120 nm (222 km) east of the northeast tip of Luzon. Forecast guidance at 251200Z changed significantly, suggesting a more northward movement, which would take Alex east of Taiwan vice through the Luzon Strait. The reason for this change in computer forecast guidance appears to be twofold. First, a surface frontal boundary stalled across the eastern coast of Asia, and second, a large break developed between the upper-level subtropical ridge south of Japan and the Siberian High.

Alex remained at minimal typhoon intensity for another 30-hours and then began to slowly weaken. It was then steered toward the north by the low-level southerly flow east of the stalled front, which caused it to brush the eastern portion of Taiwan (Figure 3-08-8) and pass within 30 nm (56 km) of the capital city of Taipei.

Shortly after passing Taipei, Alex was drawn slightly westward by the lee effect of its interaction with Taiwan's mountainous terrain. This caused Alex to make landfall on the China coast near the city of Wenzhou, 200 nm (370 km) south of Shanghai. The system then moved inland and dissipated as a significant tropical cyclone. Figure 3-08-9 shows Alex with respect to Wynne for this same time period. Near 281800Z, the remnants of Alex, with its residual vorticity and moisture, once again moved over water but did not regenerate into a significant tropical cyclone. It did, however, add to the band of precipitation that had stalled over Korea and, as a consequence, over 12 inches (300 mm) of rain fell within 24-hours. This deluge triggered major flooding, landslides and loss of life. In contrast, the damage to Taiwan and China was minor.

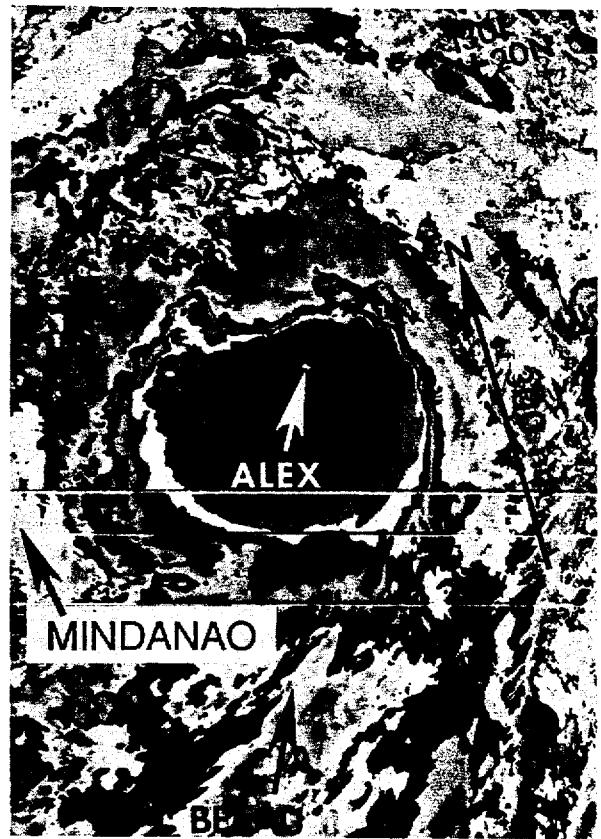


Figure 3-08-7. An implied eye appears as a warm (white) spot in the central cloud mass (dark gray) (241837Z July NOAA enhanced infrared imagery).

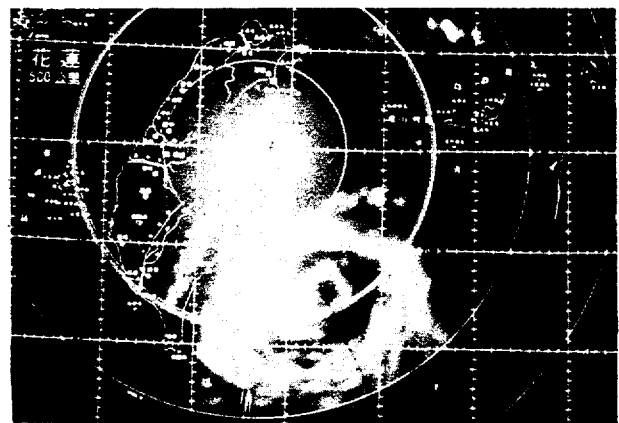


Figure 3-08-8. The tightly curved rainband and eye wall of Typhoon Alex as seen by radar from Hualien, Taiwan (WMO 46699) at 261400Z July (Photograph courtesy of Central Weather Bureau, Taipei).

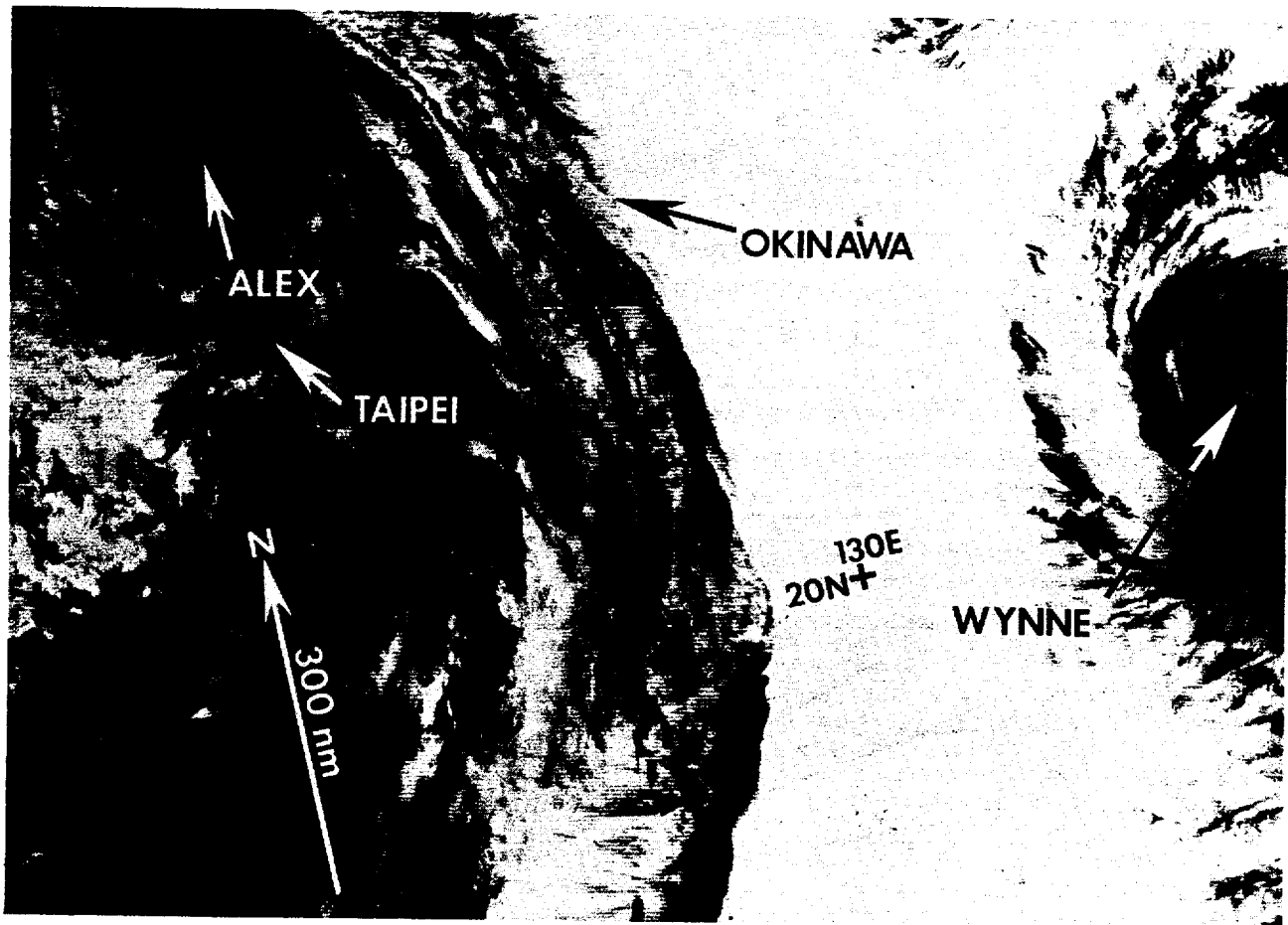


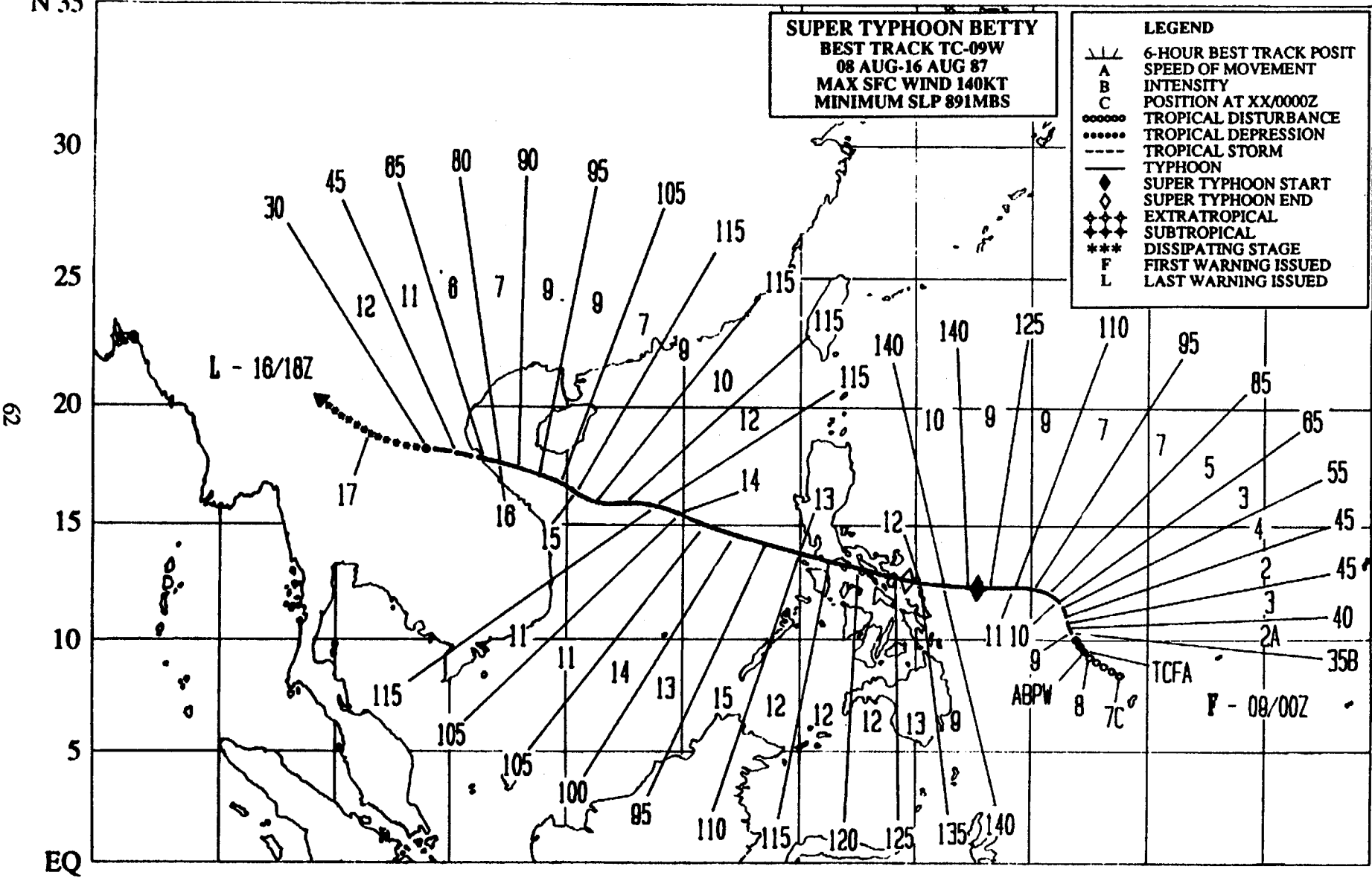
Figure 3-08-9. Typhoons Alex and Wynne (07W) appeared together on this thresholded infrared satellite image (Note: coldest cloud tops appear black). Alex had just moved inland over the eastern coast of China and Wynne was still on a northwestward track, heading toward Okinawa, Japan (271341Z July DMSP inverted infrared imagery).

E 90 95 100 105 110 115 120 125 130 135 140 145 E
 N 35
 30
 25
 20
 15
 10
 5
 EQ

SUPER TYPHOON BETTY
BEST TRACK TC-09W
08 AUG-16 AUG 87
MAX SFC WIND 140KT
MINIMUM SLP 891MBS

LEGEND

- 6-HOUR BEST TRACK POSIT
- A SPEED OF MOVEMENT
- B INTENSITY
- C POSITION AT XX/0000Z
- TROPICAL DISTURBANCE
- TROPICAL DEPRESSION
- TROPICAL STORM
- TYPHOON
- ◆ SUPER TYPHOON START
- ◇ SUPER TYPHOON END
- ◆◆◆ EXTRATROPICAL
- ◆◆◆ SUBTROPICAL
- *** DISSIPATING STAGE
- F FIRST WARNING ISSUED
- L LAST WARNING ISSUED



SUPER TYPHOON BETTY (09W)

Super Typhoon Betty was the first of two tropical cyclones to hit Vietnam during the month of August. Betty was also the second super typhoon (intensity equal to or greater than 130 kt (67 m/sec)) of the 1987 western North Pacific tropical cyclone season and had the lowest reported minimum sea-level pressure (891 mb). It intensified (deepened) explosively (Holliday and Thompson, 1979) prior to making landfall in the Philippine Islands. Other distinguishing characteristics were the large size of the area of intense convection, the small radius of maximum wind and the associated strong low-level southwest monsoonal inflow. Also of note was the large radius of gale force winds in Betty's northwest semicircle, due to the enhancement of surface winds by a strong pressure gradient between the tropical cyclone and the subtropical ridge.

After Typhoon Alex (08W), which had developed in the low-level southwest monsoon

trough, dissipated on the 28th of July, the mid-level subtropical ridge again became well-established over the western North Pacific. Coincident with Alex's (08W) movement toward the north was the replacement of the strong low-level southwest monsoonal flow over the South China Sea by the ridge.

Betty was first detected on the 7th of August as a tropical disturbance embedded in the monsoon trough, which extended from the Marshall Islands westward to the Philippine Islands. Satellite intensity estimates (Dvorak, 1984) showed surface winds of 25 kt (13 m/sec) when the disturbance was 65 nm (120 km) north-northwest of the island of Belau in the western Caroline Islands. The system cloudiness developed rapidly early on the 8th prompting JTWC to issue a Tropical Cyclone Formation Alert at 0300Z. Figure 3-09-1 shows the disturbance on the 8th of August exhibiting

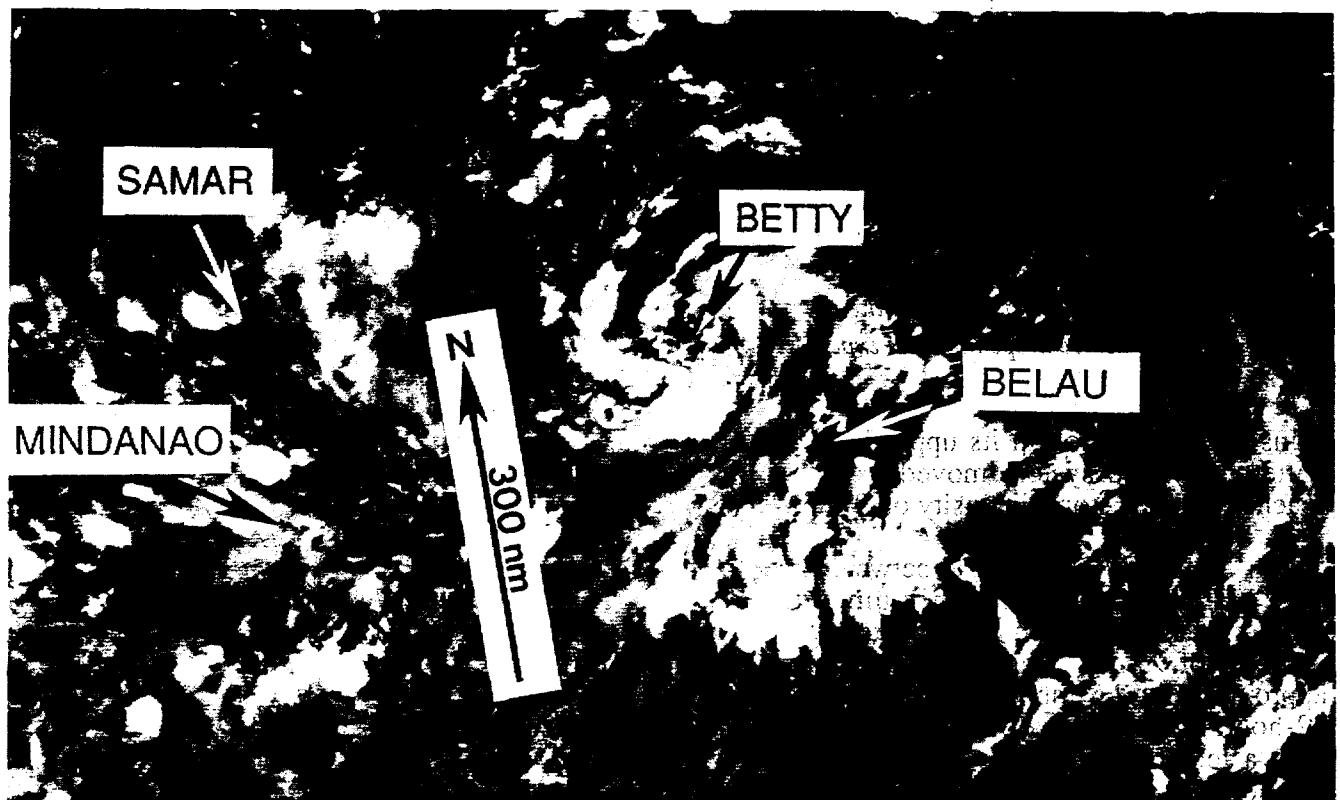


Figure 3-09-1. Super Typhoon Betty as a tropical disturbance in the monsoon trough. Signs of organized upper-level outflow were present (081257Z August DMSP visual imagery).

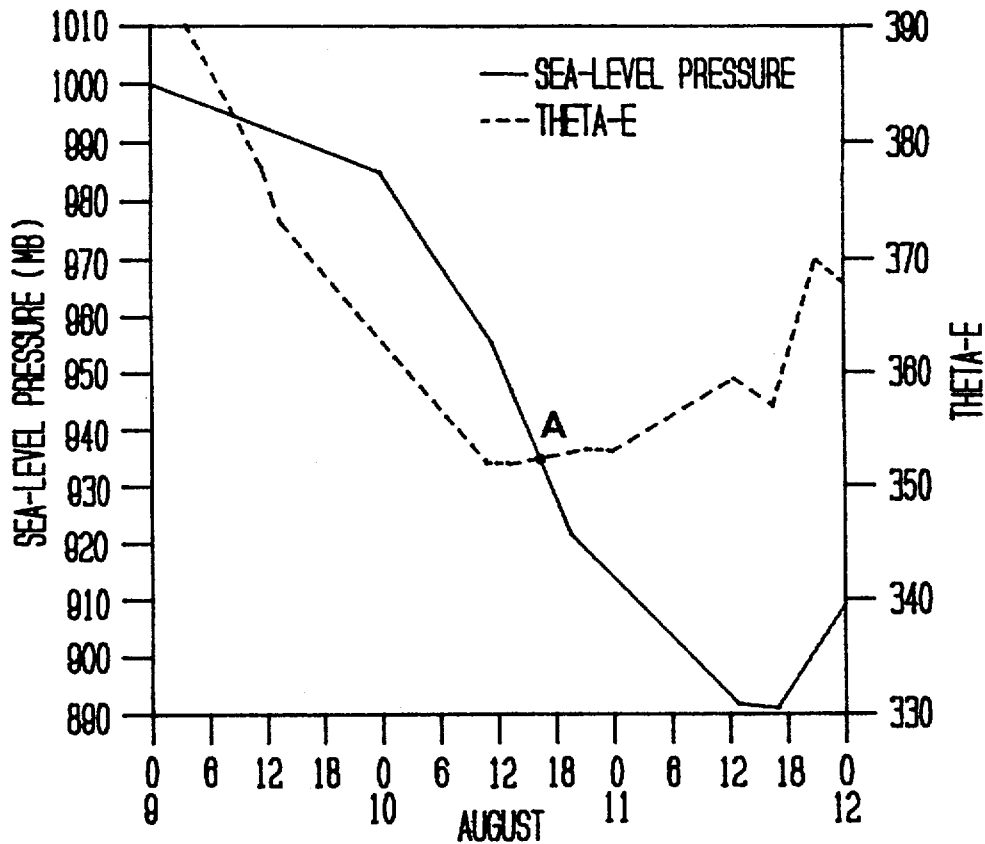


Figure 3-09-2. Plot of Betty's minimum sea-level pressure and central 700 mb equivalent potential temperature during the period 082300Z and 120000Z August. Once the critical crossing of the surface pressure and Theta-E traces occurred (at point A), explosive deepening was expected.

signs of organization in its upper-level outflow pattern. The system moved westward and reached tropical storm intensity on 9 August.

In the 37-hour period between 100000Z and 111300Z, Betty's minimum sea-level pressure dropped from 985 mb to 892 mb, a decrease of 93 mb. This translates to a drop of approximately 2.5 mb/hr (sustained for at least 12-hours) or explosive intensification. JTWC uses a technique (Dunnavan, 1981), in which the 700 mb equivalent potential temperature, Theta-E, (a measure of the tropical cyclone's thermodynamic energy based on the central 700 mb temperature and dew point) and the

minimum sea-level pressure are compared to forecast explosive intensification. This technique forecasts intensification to below 925 mb whenever the plots of minimum sea-level pressure and Theta-E intersect near the critical values of 950 mb and 360 degrees Kelvin, both values being statistical means derived from analysis of past intense tropical cyclones. Figure 3-09-2 is a plot of Betty's minimum sea-level pressure and Theta-E during the period 082300Z to 120000Z. At point A (101730Z) the two lines intersect, as the minimum sea-level pressure at this time is plummeting downward. Based on this information, explosive deepening was forecast.

Figure 3-09-3 shows Super Typhoon Betty near maximum intensity with a well-defined eye and intense convection covering a large area around the system. Aircraft reconnaissance on the 10th and 11th of August consistently located the maximum surface winds 10 to 15 nm (19 to 28 km) from the center and radar eye diameters of 11 to 15 nm (20 to 28 km). Both measurements showed the center to be very small and compact.

The threat posed by Super Typhoon Betty resulted in the evacuation of aircraft from Cubi Point Naval Air Station and Clark Air Base, as well as the movement of several ships from Subic Bay. Later, news services reported at least twenty people were killed, seven missing and more than 60,000 left homeless as a result of Betty's passage over the Philippine Islands. Damage to buildings and crops was estimated in the millions of dollars.

Betty weakened from 140 kt (72 m/sec)

to 110 kt (57 m/sec) as it accelerated across the central Philippine Islands. The subtropical ridge continued to be the dominant synoptic-scale feature, extending westward into the South China Sea.

After entering the South China Sea early on the 13th of August and still maintaining 95 kt (49 m/sec) winds, Super Typhoon Betty began to reintensify over water as it continued on a west-northwesterly track. By 140600Z, Betty's intensity had peaked again, at 115 kt (59 m/sec), 390 nm (722 km) south of Hong Kong. Betty slowly weakened as it began to interact with the mountains of Vietnam and the island of Hainan which prevented further intensification by hampering its low-level inflow. Crossing the Gulf of Tonkin in less than a day, Betty slammed into the coast of Vietnam 190 nm (352 km) south of Hanoi. The final warning on Betty was issued at 161800Z as the system weakened and dissipated over the mountains inland.

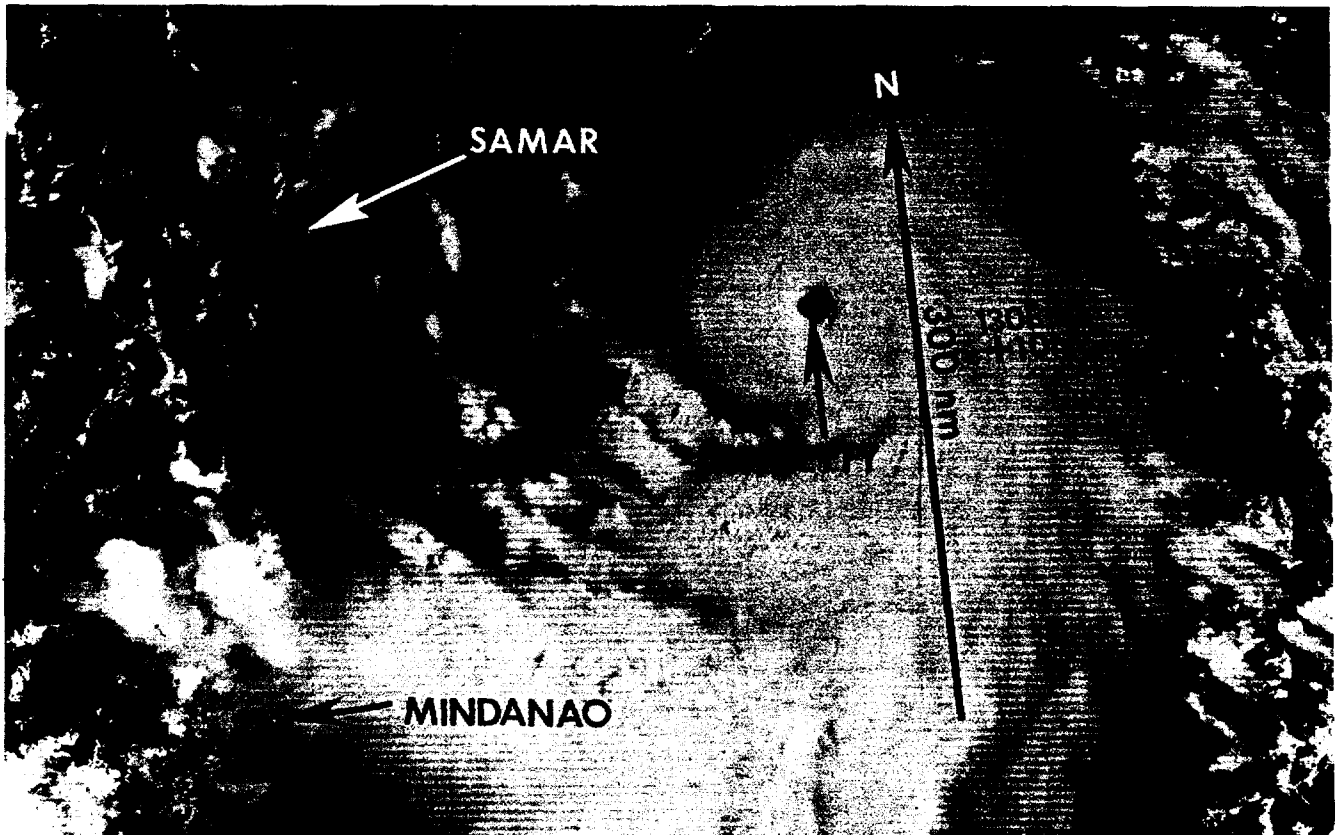
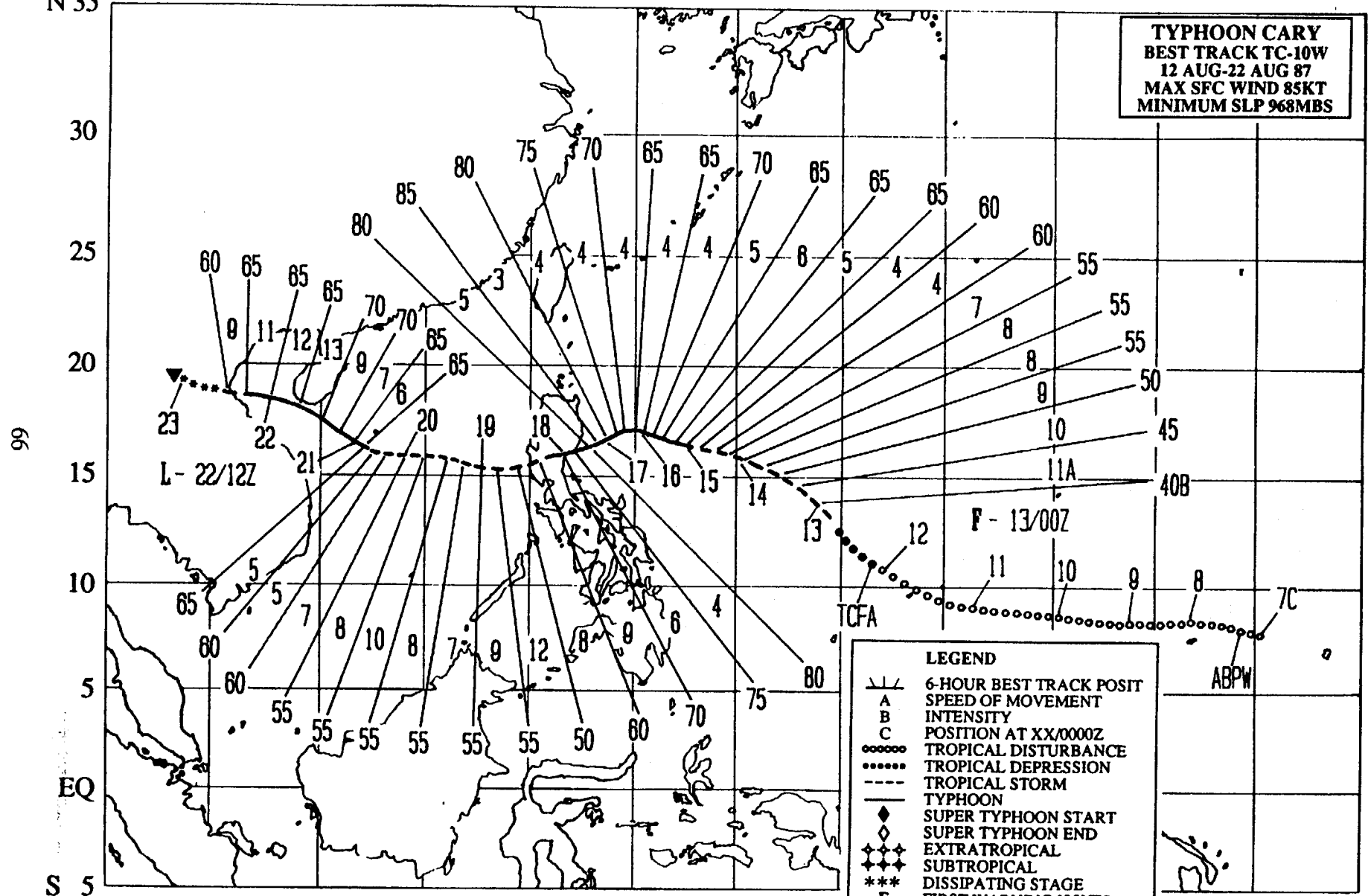


Figure 3-09-3. Super Typhoon Betty near maximum intensity. This expanded image shows the well-defined eye and large symmetrical area of intense convection (110057Z August DMSF visual imagery).

E 100 105 110 115 120 125 130 135 140 145 150 155 160 E
 N 35

TYPHOON CARY
BEST TRACK TC-10W
12 AUG-22 AUG 87
MAX SFC WIND 85KT
MINIMUM SLP 968MBS



LEGEND

- 6-HOUR BEST TRACK POSIT
- A SPEED OF MOVEMENT
- B INTENSITY
- C POSITION AT XX/0000Z
- o o o o o TROPICAL DISTURBANCE
- • • • • TROPICAL DEPRESSION
- - - - - TROPICAL STORM
- TYPHOON
- ◆ SUPER TYPHOON START
- ◇ SUPER TYPHOON END
- ◆◆◆◆ EXTRATROPICAL
- ◆◆◆◆ SUBTROPICAL
- *** DISSIPATING STAGE
- F FIRST WARNING ISSUED
- L LAST WARNING ISSUED

99

EQ

S 5

TYPHOON CARY (10W)

Typhoon Cary was the second significant tropical cyclone to develop in August. It shared the western North Pacific with Super Typhoon Betty (09W) for four days; coexisted with Super Typhoon Dinah (11W) for one and a half days, and then was part of the first three-storm situation of 1987 for 12-hours with Dinah (11W) and Tropical Storm Ed (12W).

Cary was first identified on the 6th of August as an area of convection, that persisted longer than usual in the monsoon trough 200 nm (370 km) to the southwest of the island of

Pohnpei in the eastern Caroline Islands. As a result, the cloud system was placed on the Significant Tropical Weather Advisory (ABPW PGTW) at 070600Z. The system remained broad and poorly organized over the next four days. By the 12th, upper-level outflow had improved and was unrestricted in all quadrants. Additionally, satellite intensity analysis (Dvorak, 1984) showed winds of 25 kt (13 m/sec). A Tropical Cyclone Formation Alert (TCFA) followed at 120300Z.

Aircraft reconnaissance at 122302Z estimated the maximum surface winds at 55 kt

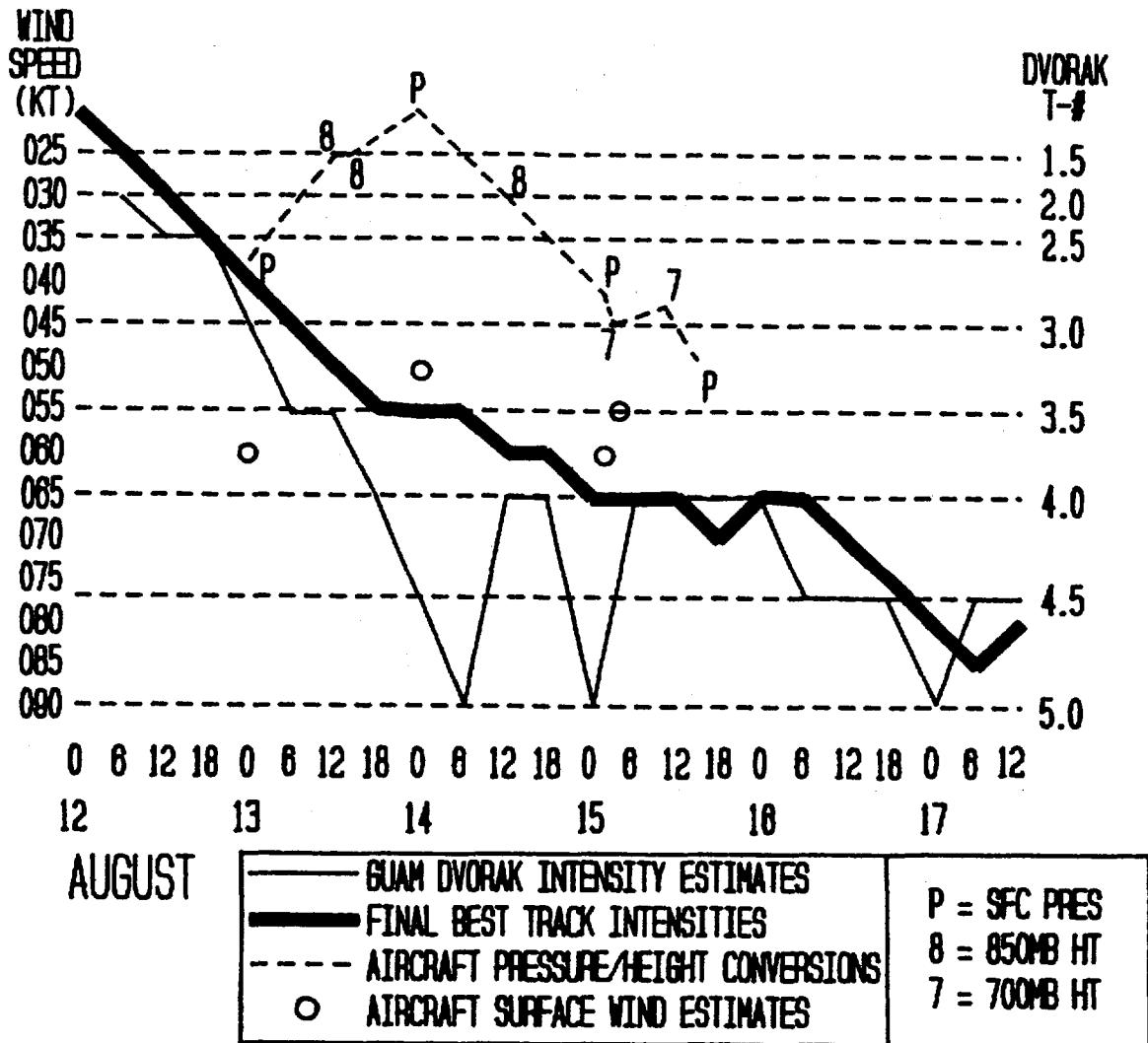


Figure 3-10-1. Time series from 120000Z to 171200Z October showing the natural scatter of raw intensity data and the resulting final best track intensities.

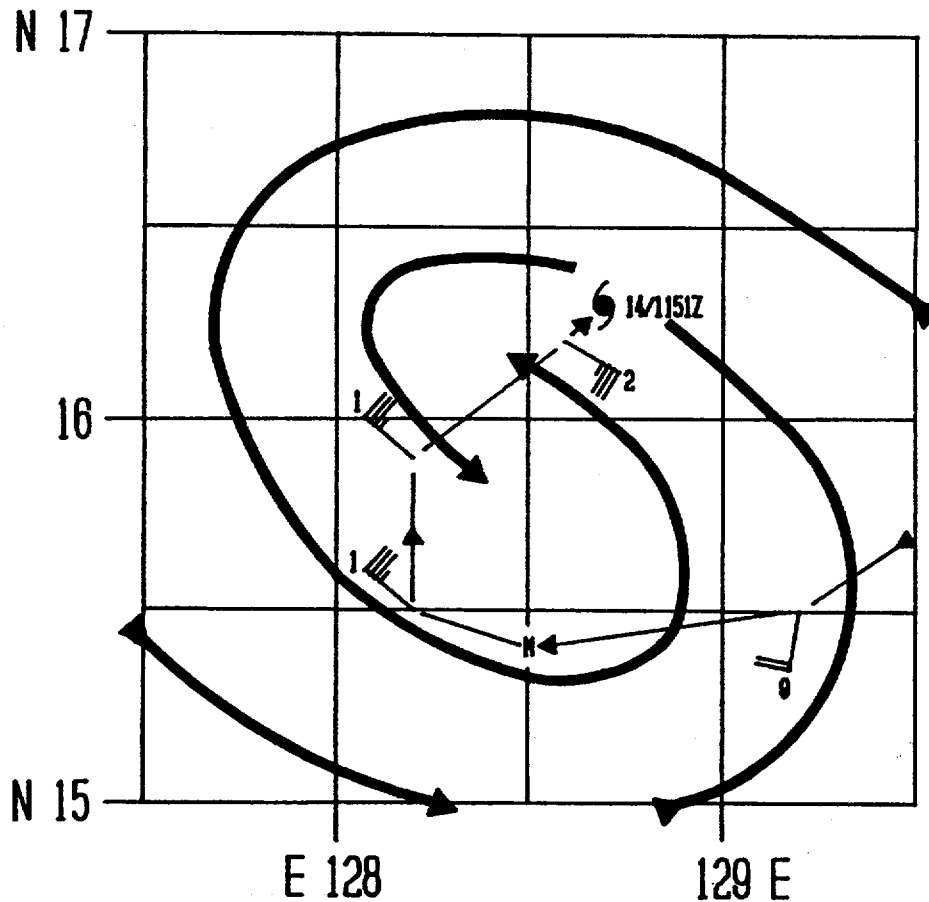


Figure 3-10-2. Plot of data from an aircraft reconnaissance mission at 141151Z August, indicating that the circulation center at flight level (850 mb) was about 18 nm (33 km) to the south of the aircraft fix position.

(25 m/sec), but the minimum surface pressure reported was only 996 mb, which usually supports a maximum wind speed of 37 kt (19 m/sec). At 121800Z, satellite intensity analysis determined that Cary's intensity was 35 kt (17 m/sec). Subsequent satellite intensity analysis, six hours later, indicated that Cary had winds of 45 kt (23 m/sec). Based on these intensity estimates the first warning on Tropical Storm Cary was issued at 130000Z with winds of 50 kt (26 m/sec) gusting to 65 kt (33 m/sec). Post-analysis revealed that Cary most probably had an intensity of 40 kt (21 m/sec) at the time of the first warning, and had reached tropical storm intensity six hours earlier at 121800Z.

The synoptic feature that dominated the low-level steering flow was the subtropical

ridge to the north. With Cary embedded in the monsoon trough east of Super Typhoon Betty (09W), the initial forecast reasoning was for Cary to track northwestward south of the ridge, closely paralleling the track of Betty (09W). The intensity was expected to increase at a normal rate, but the initial intensification and development of Cary was inhibited by Betty (09W) to the west. As Betty (09W) began to weaken as it crossed the Philippine Islands, Cary's upper-level outflow improved enough to allow development.

Satellite intensity analysis over the next 36-hours indicated that Cary developed rapidly to 90 kt (46 m/sec) at 140600Z. Post-analysis revealed that the satellite-derived intensity estimate ("T-number") was incorrect -

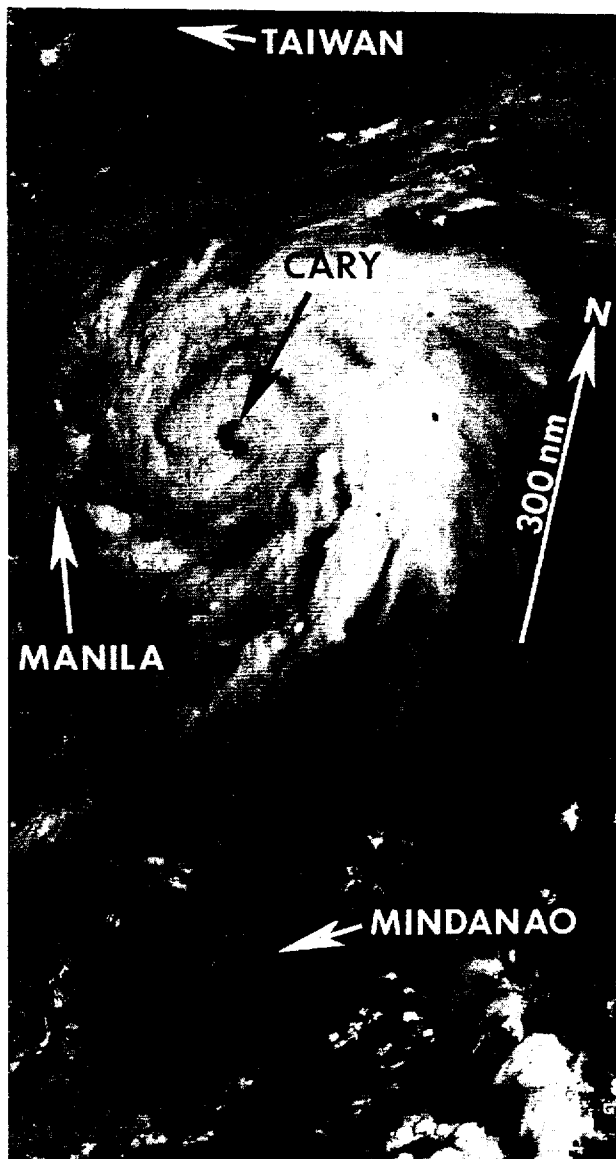


Figure 3-10-3. Typhoon Cary at near maximum intensity and approaching landfall on the island of Luzon (170036Z August DMSP visual imagery).

the diameter of the cold convective cover was misinterpreted as the diameter of a central dense overcast. Aircraft reconnaissance during the same period indicated that Cary was weakening (see Figure 3-10-1). Aircraft reconnaissance at 140029Z reported maximum winds of 50 kt (26 m/sec), however, a minimum sea-level pressure of only 1004 mb was reported, which normally supports only 21 kt (11 m/sec). Aircraft reconnaissance at 141151Z found 850 mb winds of 36 kt (19 m/sec) and an 850 mb height of only 1425 meters, which extrapolated to about

1000 mb surface pressure and surface winds of 30 kt (15 m/sec). The accuracy of the latter fix was especially questionable since the flight-level winds did not support the position in the vortex data message as being the low-level center. Additionally, the Aerial Reconnaissance Weather Officer indicated there was frequent lightning in all quadrants, possible multiple centers and that a penetration of the center was not feasible on this mission. Possibly the 850 mb fix (as indicated on Figure 3-10-2) should have been made about 18 nm (33 km) to the south as shown by the streamline analysis. Also, the excessive scatter (see Figure 3-10-1) of the intensity data acquired by different platforms during this phase of Cary's life is not often observed.

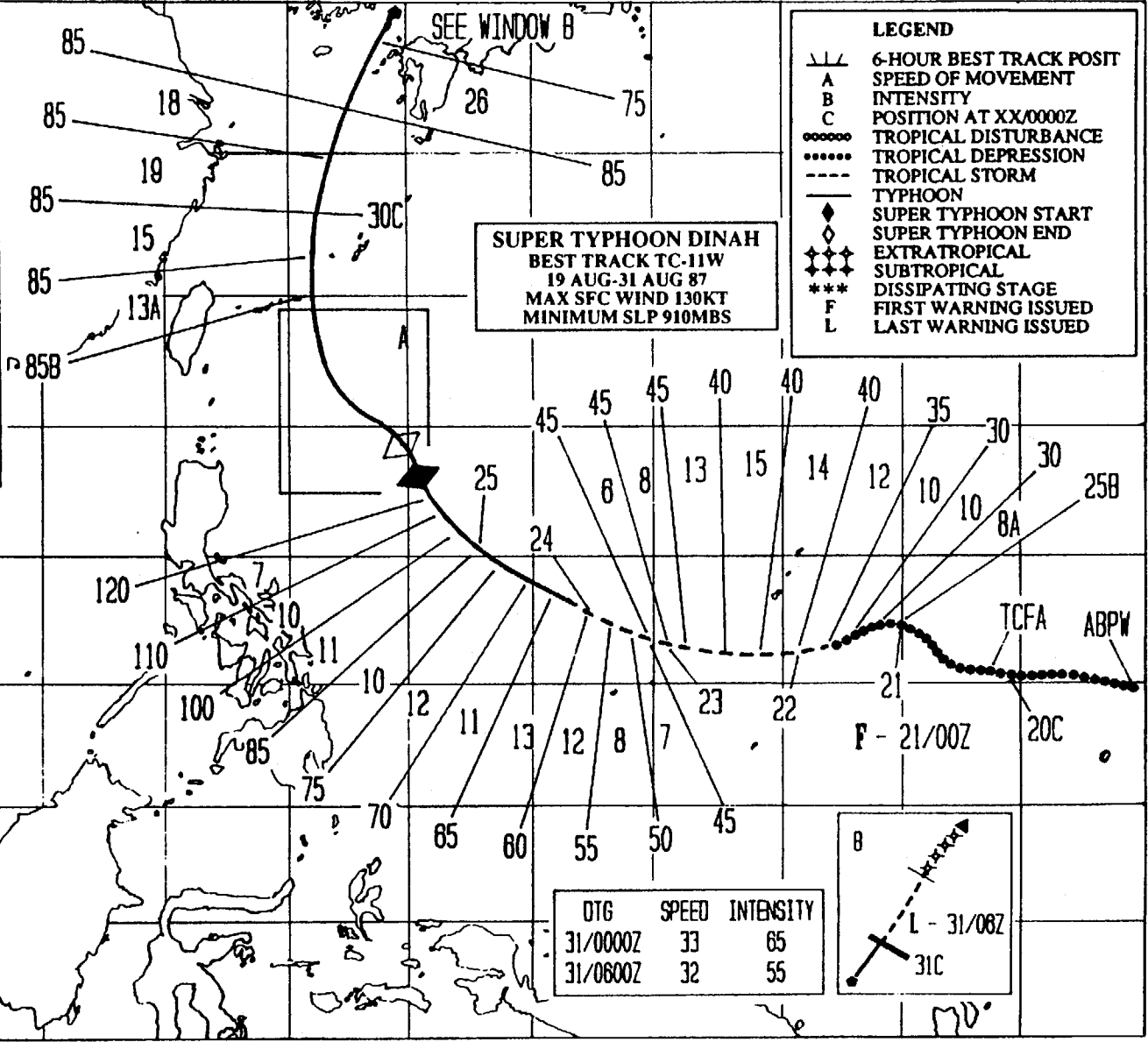
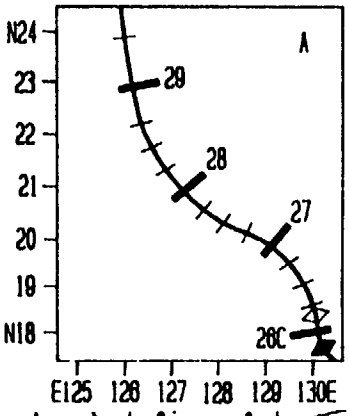
The last scheduled western North Pacific aircraft reconnaissance mission was flown on the 15th of August. At 151405Z, the maximum 700 mb winds reported were 61 kt (31 m/sec), and the 700 mb height was 3007 meters. This corresponds to about a 990 mb surface pressure and 46 kt (24 m/sec) winds. These values represented the strongest winds and lowest pressures found by aircraft reconnaissance on this system. Earlier Dvorak intensity estimates at 150600Z showed winds of 90 kt (46 m/sec). Post-analysis settled on a maximum wind of about 70 kt (41 m/sec) at 151800Z (see Figure 3-10-1).

Cary reached its maximum intensity of 85 kt (44 m/sec) at 170600Z, shortly before making landfall on eastern Luzon (Figure 3-10-3). The intensity dropped from 85 kt (44 m/sec) to 50 kt (26 m/sec) as Cary crossed the Philippine Islands. Extensive flooding was reported in the northern Philippine Islands. There were no reports of casualties.

Cary continued onward across the South China Sea and reintensified to 70 kt (36 m/sec) just southeast of the island of Hainan. The closest point of approach was 15 nm (28 km) to the south of Hainan at 211800Z. Cary then tracked toward the west through the Gulf of Tonkin and swept into northern Vietnam at 221200Z. The final warning was issued at that time. The dissipating system with its residual vorticity and moisture tracked northwestward over land into Burma before finally losing its identity on satellite imagery.

E 100 105 110 115 120 125 130 135 140 145 150 155 160
 N 35

DTG	SPEED	INTENSITY
28/0000Z	7	130
28/0800Z	8	125
28/1200Z	5	120
28/1800Z	5	115
27/0000Z	8	115
27/0800Z	4	115
27/1200Z	4	115
27/1800Z	4	115
28/0000Z	5	110
28/0600Z	4	110
28/1200Z	3	105
28/1800Z	8	95
29/0000Z	8	90
29/0600Z	11	90
29/1200Z	11	85

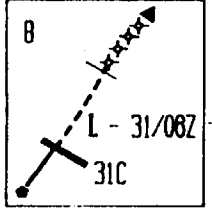


SUPER TYPHOON DINAH
 BEST TRACK TC-11W
 19 AUG-31 AUG 87
 MAX SFC WIND 130KT
 MINIMUM SLP 910MBS

LEGEND

- ▲ 6-HOUR BEST TRACK POSIT
- A SPEED OF MOVEMENT
- B INTENSITY
- C POSITION AT XX/0000Z
- TROPICAL DISTURBANCE
- TROPICAL DEPRESSION
- - - TROPICAL STORM
- TYPHOON
- ◆ SUPER TYPHOON START
- ◇ SUPER TYPHOON END
- ⊕ EXTRATROPICAL
- ⊗ SUBTROPICAL
- *** DISSIPATING STAGE
- F FIRST WARNING ISSUED
- L LAST WARNING ISSUED

DTG	SPEED	INTENSITY
31/0000Z	33	65
31/0600Z	32	55



70

EQ

S 5

SUPER TYPHOON DINAH (11W)

Super Typhoon Dinah (11W), the most destructive typhoon to strike Okinawa and the southern islands of Japan in the past 20 years, caused extensive damage to both Japanese civilian properties and U.S. military bases and assets.

Dinah was first observed on satellite imagery as a disorganized cluster of weak convection in the near-equatorial trough on 18 August. By the 19th, convection became better organized and the disturbance was noted on the Significant Tropical Weather Advisory (ABPW PGTW) issued at 190600Z. During the next

eighteen hours, Dinah developed a low-level circulation as it passed northwest of the island of Pohnpei and moved beneath moderate directional and speed divergence at the 200 mb level. The 200000Z satellite imagery indicated weak convective curvature and, as a result, a Tropical Cyclone Formation Alert was issued at 200427Z. During the next eighteen hours, satellite imagery indicated a considerable increase in convection which had become more centralized (see Figure 3-11-1). The system was assigned a Dvorak intensity number ("T-number") of 2.0 which corresponded to maximum sustained surface winds of 30 kt (15

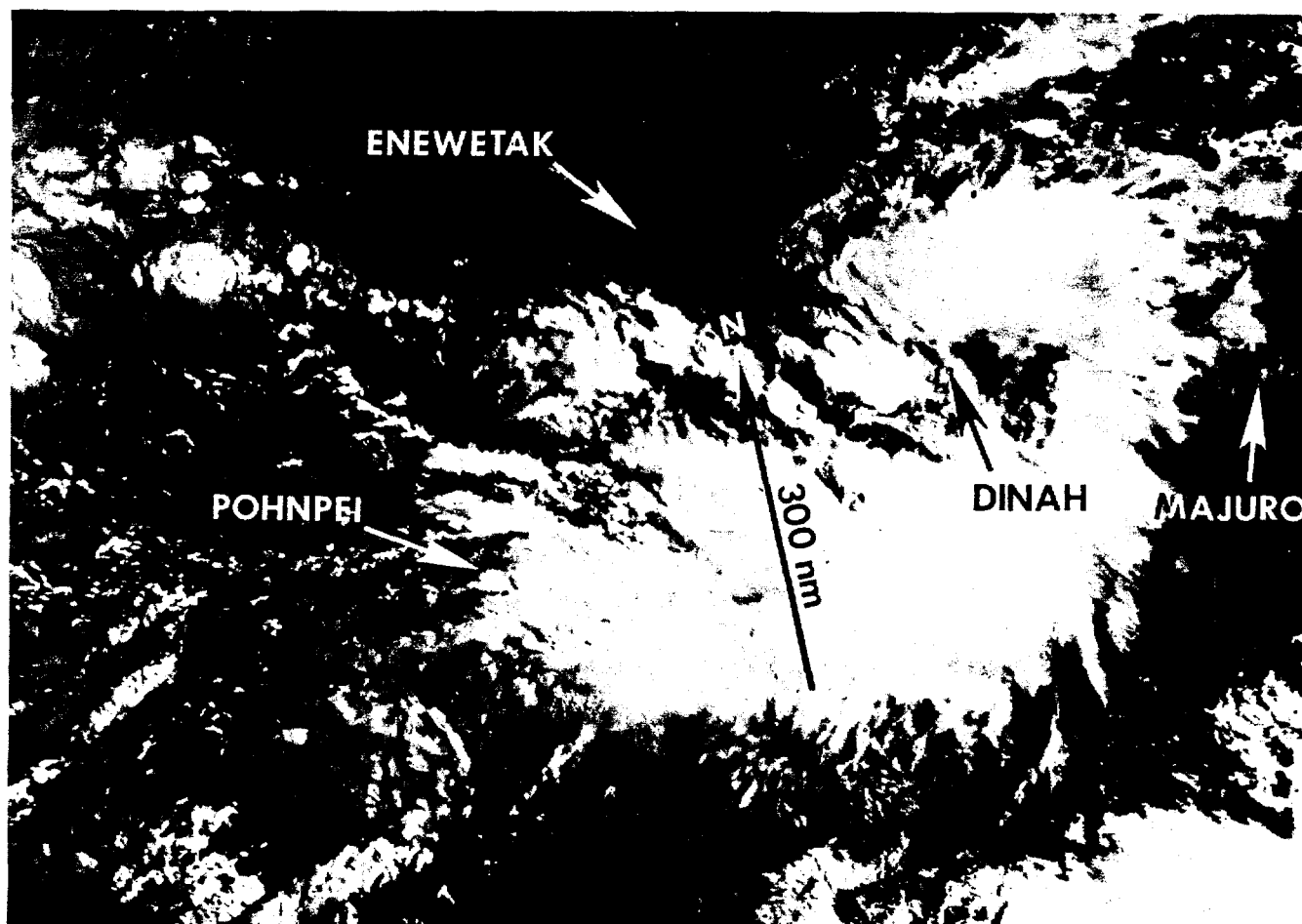


Figure 3-11-1. The initial development of Super Typhoon Dinah was first noted as a considerable increase in the amount of convection (202102Z August N(OAA visual imagery).

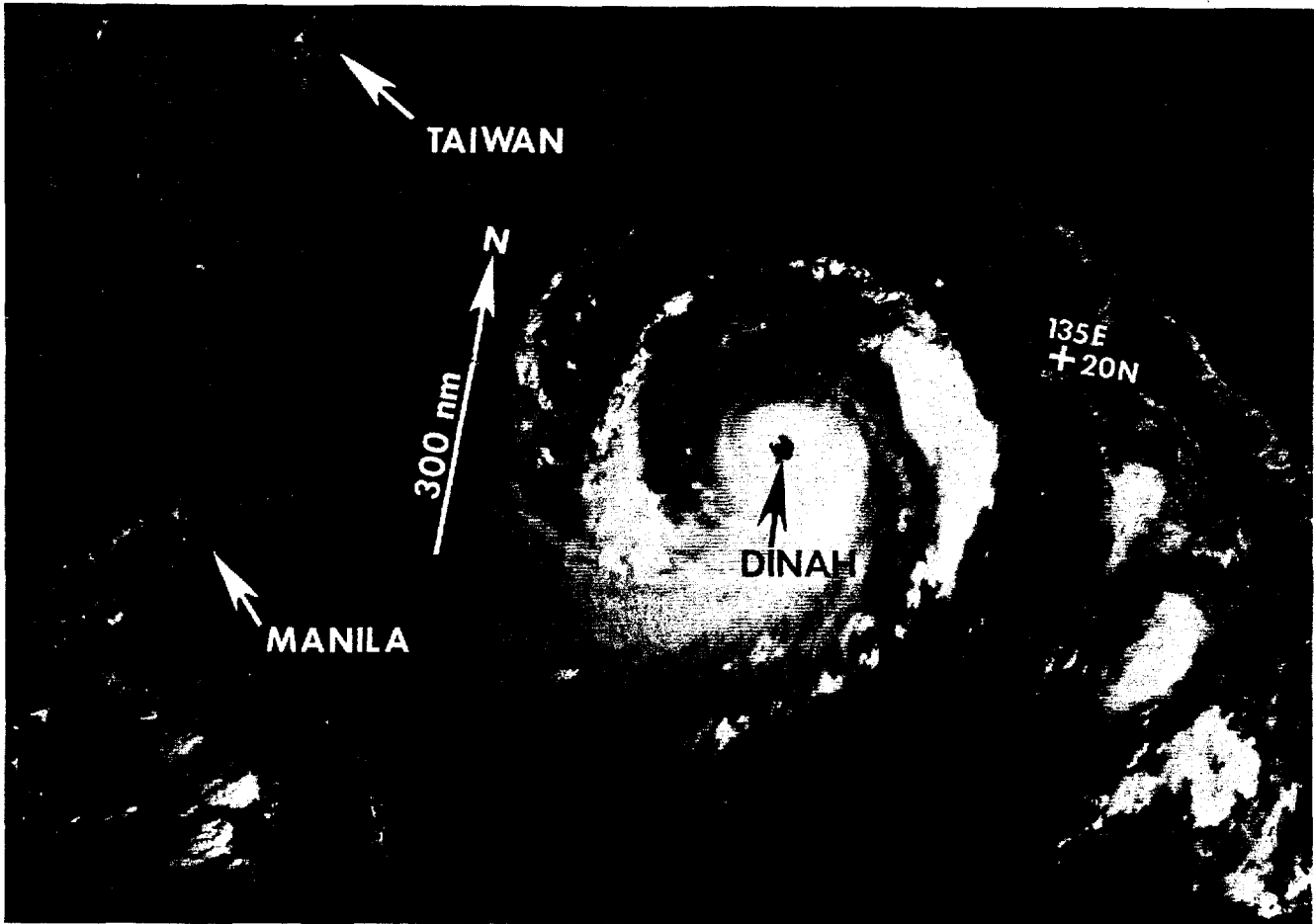


Figure 3-11-2. Super Typhoon Dinah in the Philippine Sea near maximum intensity (260054Z August DMSP visual imagery).

m/sec) and an estimated MSLP of 1000 mb. At 210000Z, the first warning was issued on Tropical Depression 11W when it was located 300 nm (556 km) east-southeast of Guam.

Between 210000Z and 211800Z, Tropical Depression 11W assumed a more westward track in response to the strengthening subtropical ridge to the north and moved beneath an upper-level anticyclone which had associated strong speed divergence southwest of the system. The increased outflow signature on satellite imagery allowed for a Dvorak intensity estimate of 35 kt (18 m/sec). Based on this estimation, Tropical Depression 11W was upgraded to Tropical Storm Dinah (11W) at 211800Z.

Over the next forty-eight hours, Dinah moved westward passing 120 nm (222 km) south of Guam at 220300Z with maximum sustained surface winds estimated at 40 kt (21 m/sec). Dinah did not intensify at the normal rate of one "T-number" per day. This was apparently due to 45 kt (23 m/sec) 200 mb winds over the cyclone which created an undesirable shearing environment. However, by 240000Z, Dinah had moved away from this unfavorable shearing environment and developed a good anticyclonic outflow pattern which was visible on satellite imagery. The 241200Z 200 mb streamline analysis confirmed this and indicated a good cyclonic outdraft directly over Dinah's center which became anticyclonic as it moved radially outward from

the center. During the first half of this period, Dinah tracked westward and then gradually turned more toward the west-northwest. JTWC forecasts correctly predicted the system's motion which was supported by the dynamic One-Way Interactive Tropical Cyclone Model (OTCM).

A Dvorak intensity analysis of satellite imagery at 240300Z estimated maximum sustained surface winds of 65 kt (33 m/sec) and an estimated MSLP of 980 mb. On the 240600Z warning, Tropical Storm Dinah was upgraded to typhoon status. At that time it was located 500 nm (926 km) west of Guam. Between 240600Z and 250600Z, Typhoon Dinah's outflow continued to increase with some restriction northwest through northeast of the cyclone which was associated with weak

short-wave troughs passing to the north. However, those minor restrictions did not inhibit Dinah from continuing to intensify at the normal Dvorak rate.

During the next twenty-four hours, Typhoon Dinah's intensity increased at a rate much faster than the normal one "T-number" per day and by 260000Z it reached super typhoon intensity (130 kt or 67 m/sec) at a location 500 nm (926 km) east of northern Luzon (see Figure 3-11-2). Dinah remained at super typhoon intensity for only a few hours but maintained maximum sustained surface winds of 110 kt (57 m/sec) or greater until 280600Z.

From 240600Z until 281200Z, Dinah basically tracked toward the northwest at an average forward speed of 11 kt (20 km/hr)

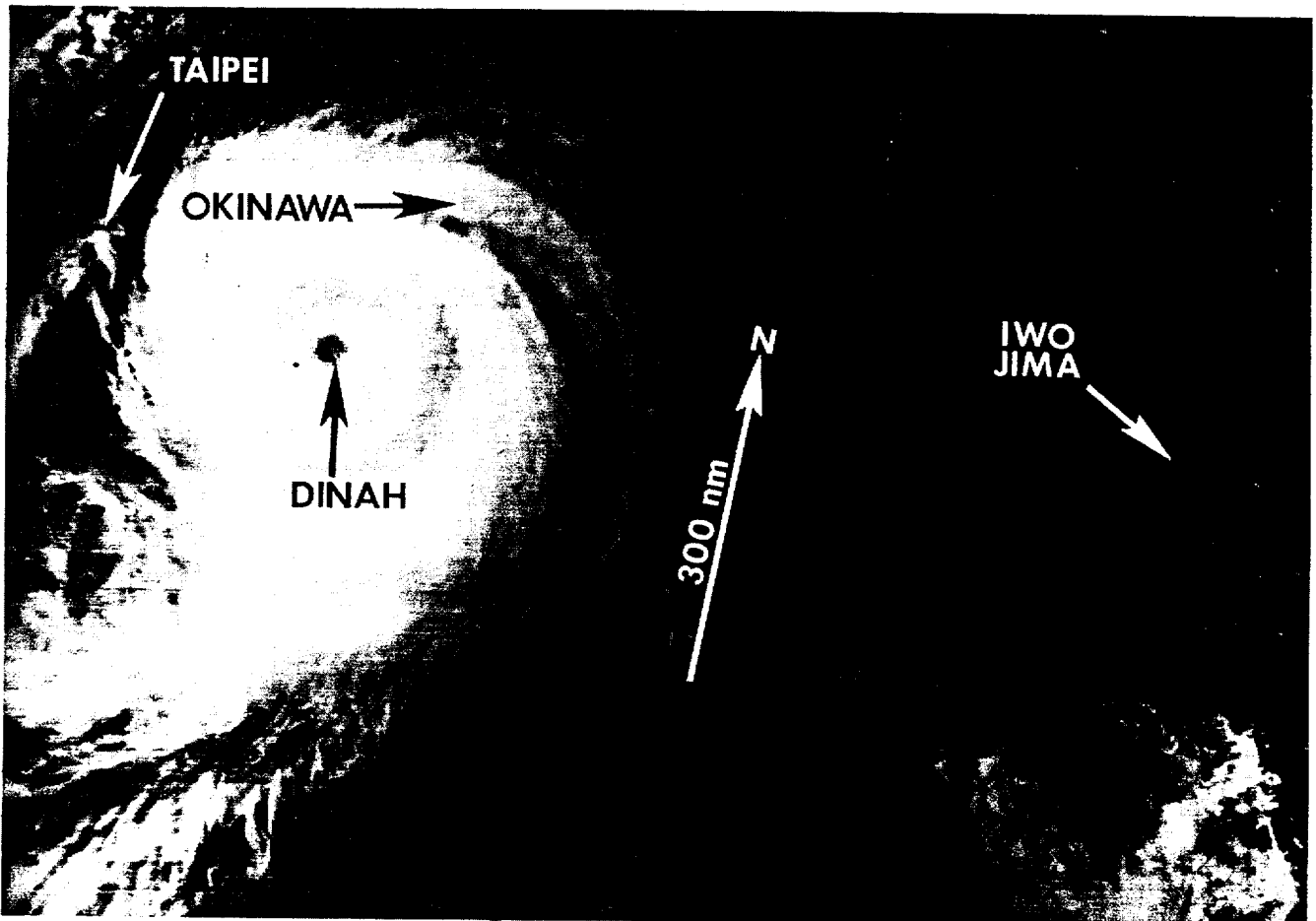


Figure 3-11-3. *Dinah during its dissipating stage passing to the west of Okinawa, Japan (290605Z August NORAD visual imagery).*

during the first twenty-four hour period, slowing to an average of 6 kt (11 km/hr) by 251800Z. The slower forward speed is typical of a very well-developed and very intense tropical cyclone as it approaches the axis of the subtropical ridge prior to recurvature.

After 281200Z, Typhoon Dinah made a turn toward a more northerly track as it moved around the western periphery of the subtropical high. During the next thirty-six hours, Dinah moved into unfavorable upper-level conditions in the form of impinging mid-level short-wave troughs moving northeastward across eastern China and Japan. As each short-wave trough passed north of Dinah, upper-level wind shear increased and the system's outflow became restricted. As a result, Dinah steadily weakened.

Although Dinah began to weaken after 281200Z (Figure 3-11-3), it still had maximum sustained surface winds of 85 kt (44 m/sec) as it passed 90 nm (167 km) west of Kadena Air Base (Figure 3-11-4) at 291500Z. It caused considerable damage to U.S. military facilities

on Okinawa. One person was killed and six people were injured. Trees were uprooted or broken off (Figure 3-11-5), utility poles and lines were blown down, and roofs and suffered structural damage. Total damage estimates to U.S. military facilities on Okinawa were in excess of \$1.3 million. Maximum sustained surface winds on Okinawa were 63 kt (32 m/sec) with gusts from 98 to 106 kt (50 to 55 m/sec). Minimum sea-level pressure observed was 983 mb at 291755Z. By 300000Z, Dinah was located 120 nm (222 km) northwest of Okinawa with maximum sustained surface winds estimated to be 85 kt (44 m/sec). A ship passing 30 nm (56 km) northeast of Dinah's center at that time reported sustained winds of 75 kt (39 m/sec) from the southeast and a sea-level pressure of 938.7 mb.

Dinah began to recurve by 300000Z, assumed a north-northeasterly track and accelerated while still maintaining maximum sustained surface winds of 85 kt (44 m/sec). At 301700Z, Typhoon Dinah passed 60 nm (111 km) northwest of Sasebo Naval Base in western

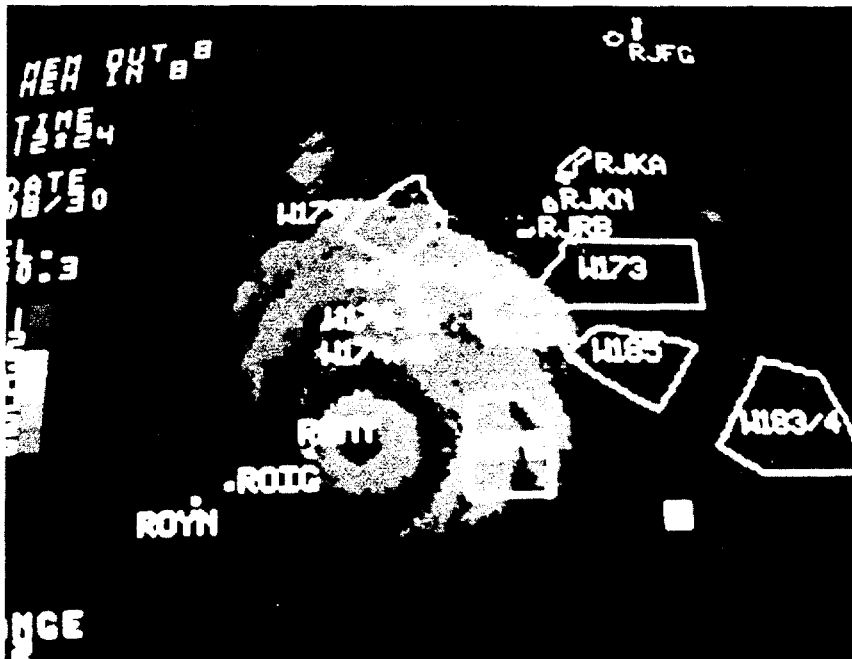


Figure 3-11-4. Radarscope photo of Dinah at 291224Z August (Photo courtesy of Detachment 8, 20 Weather Squadron, Kadena AB, Japan).

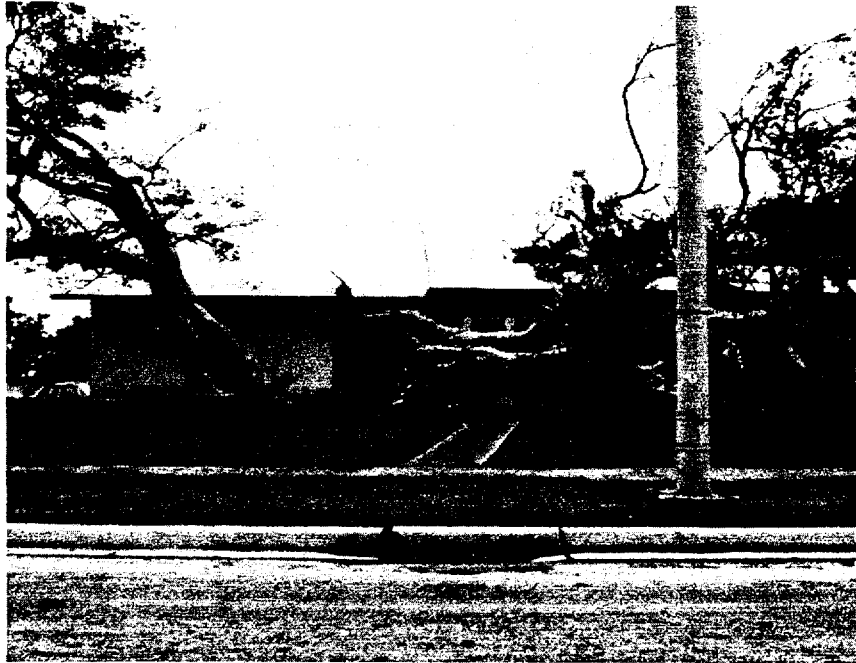


Figure 3-11-5. Trees on Okinawa were damaged and uprooted by the high winds associated with Dinah's passage (Photo courtesy of Detachment 8, 20 Weather Squadron, Kadena AB, Japan).

Japan where maximum sustained surface winds of 60 to 65 kt (31 to 33 m/sec) with gusts to 90 kt (46 m/sec) were observed. Extensive damage was caused by the storm surge and tidal action on seawalls and piers. A landing craft from the USS San Bernardino was destroyed when the seawall eroded and the pier collapsed. Damage also occurred to trees, utility lines and poles, and some building structures. Damage costs to the Japanese Sasebo Navy complex were in excess of \$6.7 million, making Dinah the worst tropical cyclone to strike southwest Japan in recent history.

By 310000Z, Dinah was becoming extratropical as it began to merge with a mid-latitude frontal system that extended southwestward across the Sea of Japan. It was

beneath the polar jet stream which had winds in excess of 90 kt (46 m/sec). Dinah was downgraded to a tropical storm as its convection sheared off to the northeast. The final warning was issued at 310600Z as the cyclone continued to accelerate toward the northeast at 33 kt (61 km/hr).

Throughout Dinah's life, JTWC consistently forecast recurvature and acceleration toward the northeast through the Sea of Japan. Forecast track errors were smaller than average. The dynamic aid OTCM performed extremely well during recurvature, while the objective aids Half Persistence and Climatology (HPAC) and climatology were used extensively as Dinah passed beneath the subtropical ridge.



Figure 3-11-5. Trees on Okinawa were damaged and uprooted by the high winds associated with Dinah's passage (Photo courtesy of Detachment 8, 20 Weather Squadron, Kadena AB, Japan).

Japan where maximum sustained surface winds of 60 to 65 kt (31 to 33 m/sec) with gusts to 90 kt (46 m/sec) were observed. Extensive damage was caused by the storm surge and tidal action on seawalls and piers. A landing craft from the USS San Bernardino was destroyed when the seawall eroded and the pier collapsed. Damage also occurred to trees, utility lines and poles, and some building structures. Damage costs to the Japanese Sasebo Navy complex were in excess of \$6.7 million, making Dinah the worst tropical cyclone to strike southwest Japan in recent history.

By 310000Z, Dinah was becoming extratropical as it began to merge with a mid-latitude frontal system that extended southwestward across the Sea of Japan. It was

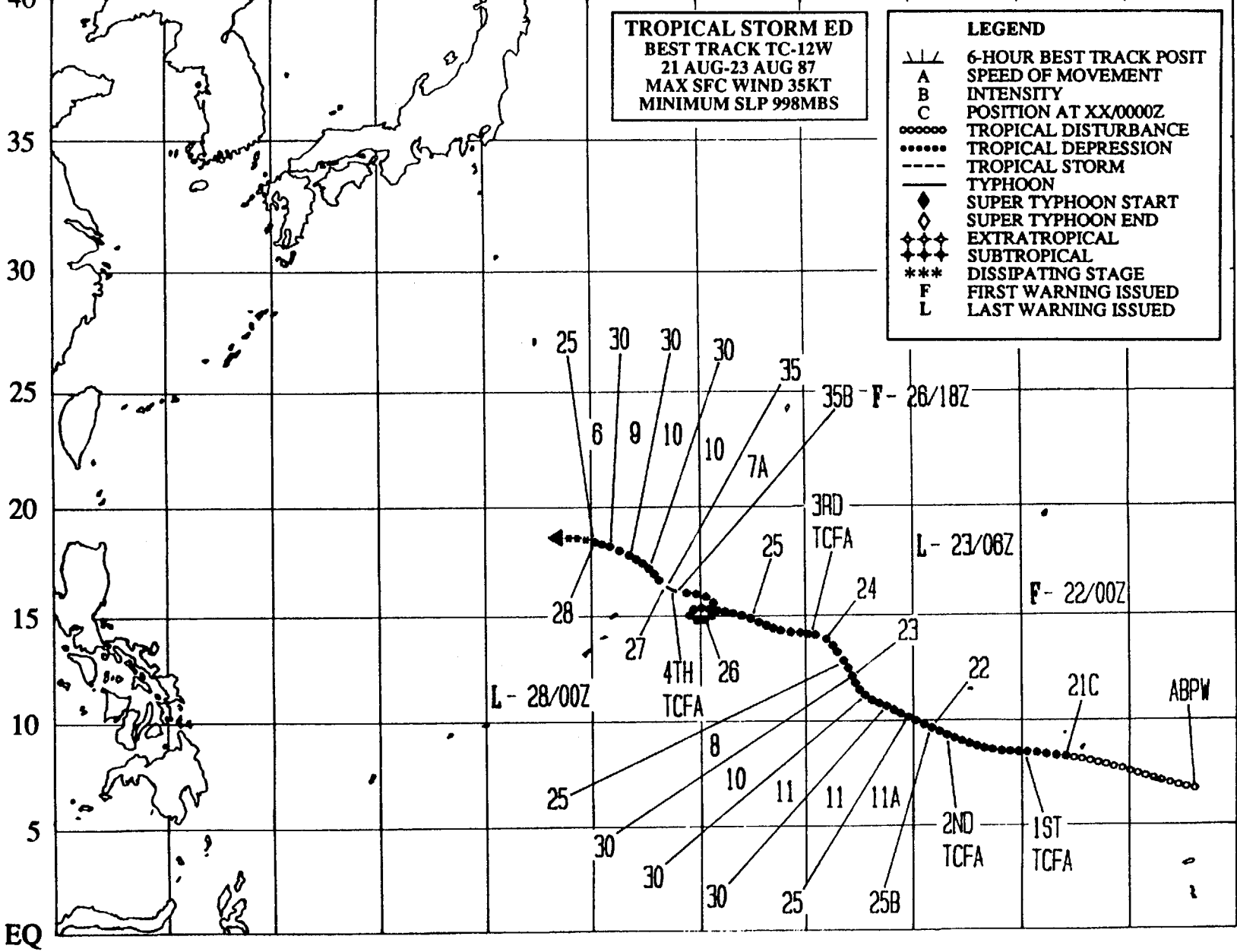
beneath the polar jet stream which had winds in excess of 90 kt (46 m/sec). Dinah was downgraded to a tropical storm as its convection sheared off to the northeast. The final warning was issued at 310600Z as the cyclone continued to accelerate toward the northeast at 33 kt (61 km/hr).

Throughout Dinah's life, JTWC consistently forecast recurvature and acceleration toward the northeast through the Sea of Japan. Forecast track errors were smaller than average. The dynamic aid OTCM performed extremely well during recurvature, while the objective aids Half Persistence and Climatology (HPAC) and climatology were used extensively as Dinah passed beneath the subtropical ridge.

E 120 125 130 135 140 145 150 155 160 165 170 175 E
 N 40

TROPICAL STORM ED
BEST TRACK TC-12W
21 AUG-23 AUG 87
MAX SFC WIND 35KT
MINIMUM SLP 998MBS

LEGEND	
—/—/—	6-HOUR BEST TRACK POSIT
A	SPEED OF MOVEMENT
B	INTENSITY
C	POSITION AT XX/0000Z
○○○○○	TROPICAL DISTURBANCE
●●●●●	TROPICAL DEPRESSION
-----	TROPICAL STORM
————	TYPHOON
◆	SUPER TYPHOON START
◇	SUPER TYPHOON END
◆◆◆◆	EXTRATROPICAL
◆◆◆◆	SUBTROPICAL
***	DISSIPATING STAGE
F	FIRST WARNING ISSUED
L	LAST WARNING ISSUED



TROPICAL STORM ED (12W)

Tropical Storm Ed (12W) was the third of four significant tropical cyclones that occurred during the month of August. Ed was a difficult system for JTWC to locate and forecast because of its fluctuations in intensity, speed and track direction, and its poorly defined cloud signature.

Ed formed during the third week of August in the western North Pacific monsoon trough about 90 nm (167 km) east of the island of Majuro in the Marshalls. It was first detected as an area of persistent convection with a

coincident weak low-level cyclonic circulation. This suspect area appeared on the Significant Tropical Weather Advisory (ABPW PGTW) at 200600Z. For the next 24-hours, the disturbance moved rapidly at a speed of 17 to 23 kt (32 to 43 km/hr) toward the west-northwest. Improved upper-level outflow and increased central convection prompted the first Tropical Cyclone Formation Alert (TCFA) at 210600Z.

At 212130Z, a second TCFA was issued to supersede the first TCFA, since the disturbance was moving out of the original alert

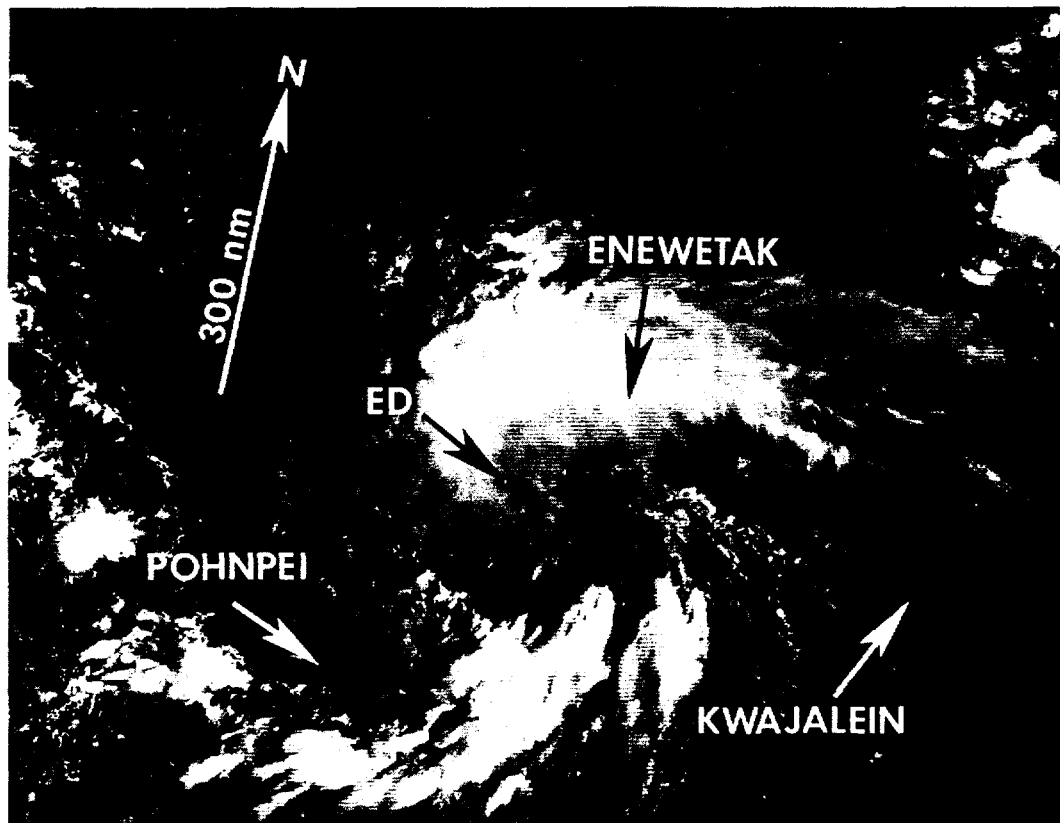


Figure 3-12-1. Formative stage of Tropical Storm Ed (212253Z August DMSP visual imagery).

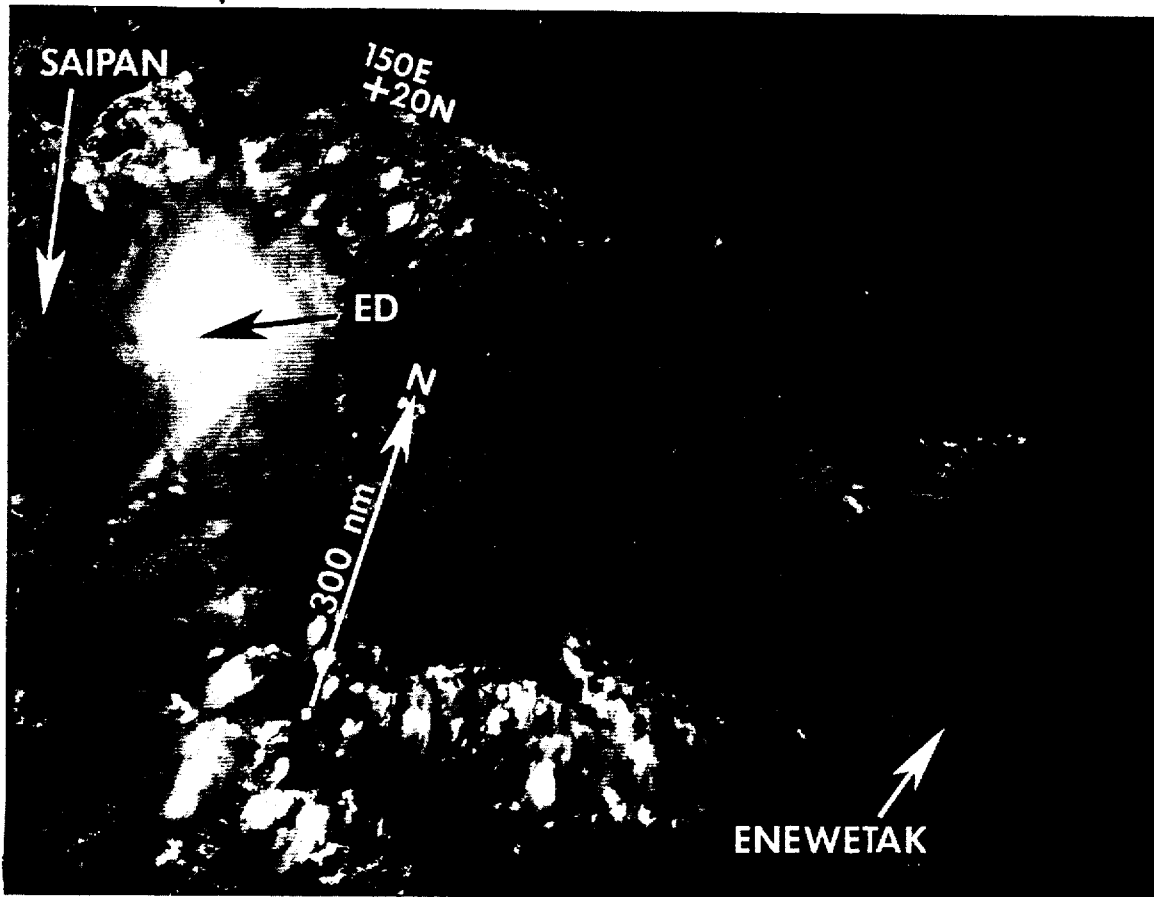


Figure 3-12-2. The regenerated Tropical Depression 12W shortly before it was upgraded once more to Tropical Storm Ed (262252Z August DMSP visual imagery).

area. The disturbance continued on a west-northwestward track at slightly lower speeds of 14 to 17 kt (26 to 32 km/hr).

Visual satellite imagery (Figure 3-12-1) showed tighter curvature of the convective cloud lines and increased cirrus outflow to the north. Also, drifting buoys in the area indicated surface wind speeds of 25 to 30 kt (13 to 15 m/sec). As a result, at 220000Z the second TCFA was upgraded to Tropical Depression 12W. Unexpectedly, thirty-hours later Tropical Depression 12W showed significantly decreased convection and system organization on satellite imagery. Consequently, a final warning was issued. The tropical disturbance was then placed on the ABPW PGTW and monitored for signs of future regeneration.

Ed did maintain its low-level identity even as Typhoon Dinah (11W), which was further to the west, was increasing the vertical shear aloft over it. Finally, a ragged central dense overcast persisted and the system's upper-level outflow redeveloped. The third TCFA followed at 240800Z. However, by 250600Z, the TCFA was cancelled when the upper-level outflow from Super Typhoon Dinah (11W), located to the west, increased its shearing effect on Ed which caused the convection to significantly decrease.

At 262030Z, a fourth TCFA was issued when cloudiness associated with the disturbance flared-up again. Satellite intensity analysis (Dvorak, 1984) estimated the intensity of the system at 35 kt (18 m/sec). This TCFA was

almost immediately upgraded as Tropical Depression 12W, with a valid time of 261800Z, based on the receipt of a new satellite picture, which indicated that the disturbance had been developing more rapidly than previously expected (see Figure 3-12-2).

The regenerated Tropical Depression 12W was further upgraded to tropical storm intensity at 270000Z. This upgrade was based on the Dvorak satellite intensity analysis at 261800Z, that indicated 35 kt (18 m/sec) sustained surface winds. In addition, at

270600Z, Tropical Storm Ed's position was relocated on the warning due to the formation of a 60 nm (111 km) diameter central dense overcast from a central cold cover. As a result, Ed's center location was moved 45 nm (83 km) farther north. Later, at 271200Z, Tropical Storm Ed (12W) was relocated a second time when satellite fixes revealed that the system had moved 75 nm (139 km) further north than previously forecast. When the central convection was finally stripped away from the low-level circulation, the last warning was issued at 280000Z (see Figure 3-12-3).

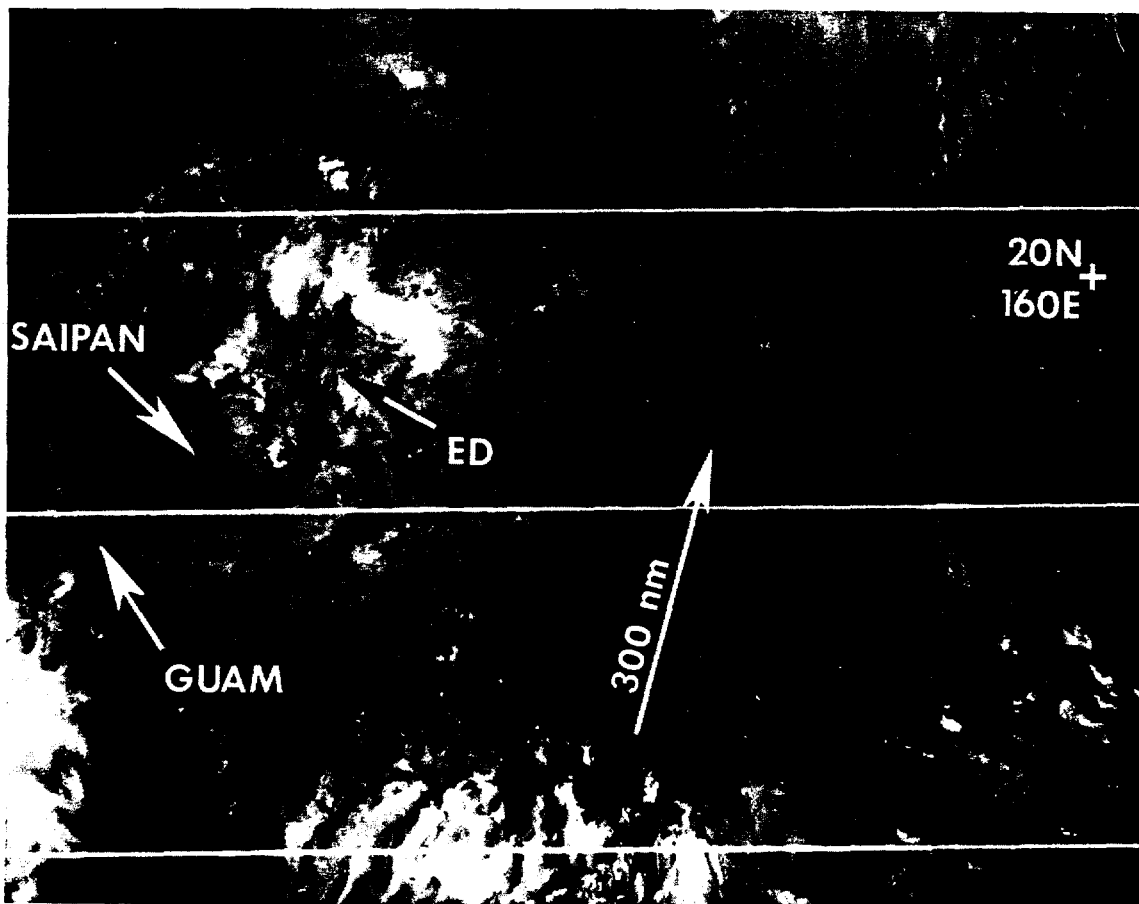


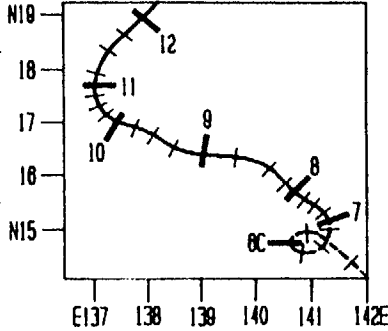
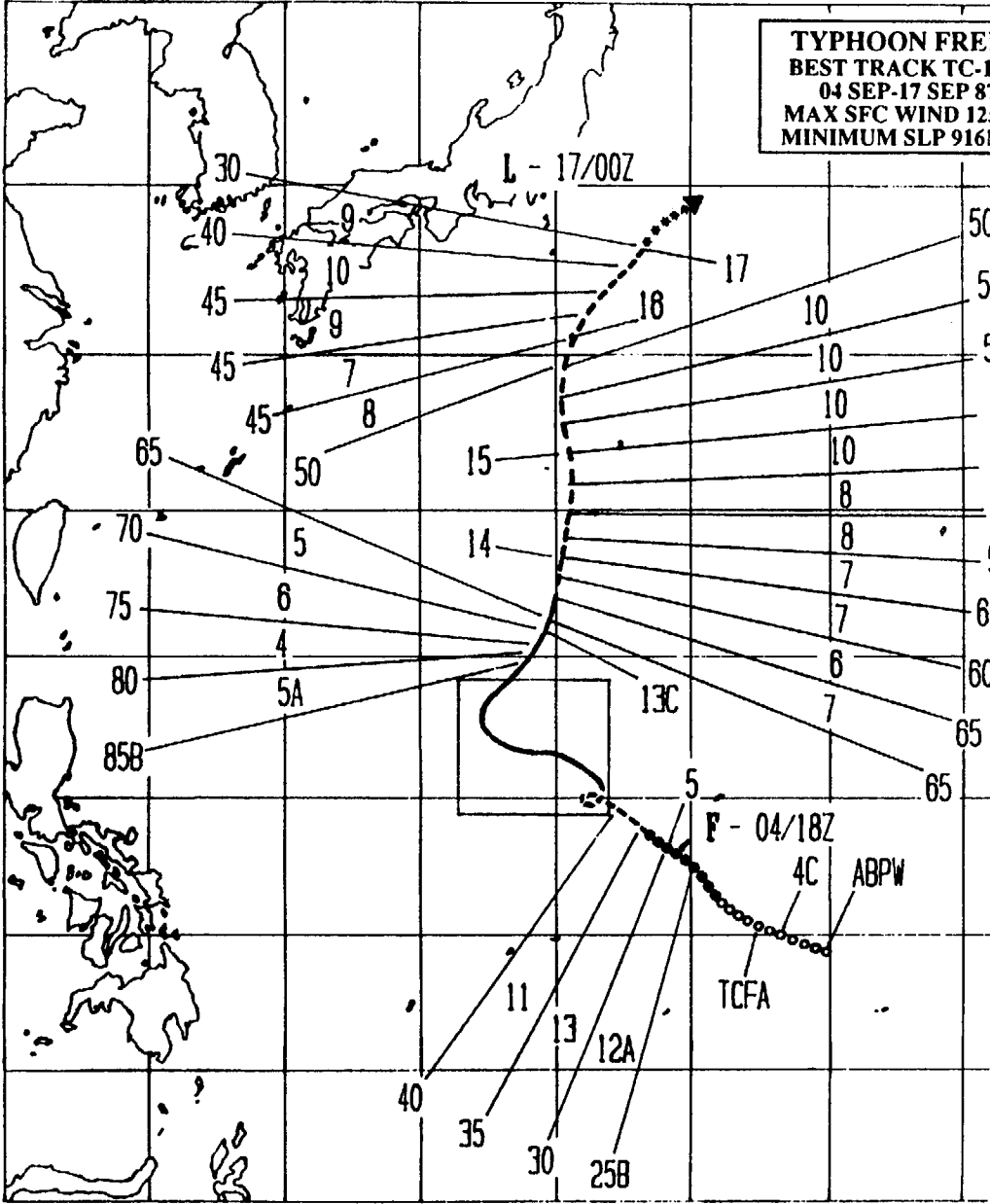
Figure 3-12-3. Tropical Storm Ed (12W) after the system had shed its central dense overcast (270445Z August NOAA visual imagery).

E 120 125 130 135 140 145 150 155 160 165 170 175 E
 N 40
 35
 30
 25
 20
 15
 10
 5
 EQ

TYPHOON FREDA
BEST TRACK TC-13W
 04 SEP-17 SEP 87
 MAX SFC WIND 125KT
 MINIMUM SLP 916MBS

LEGEND

- 6-HOUR BEST TRACK POSIT
- A SPEED OF MOVEMENT
- B INTENSITY
- C POSITION AT XX/0000Z
- TROPICAL DISTURBANCE
- TROPICAL DEPRESSION
- TROPICAL STORM
- TYPHOON
- ◆ SUPER TYPHOON START
- ◇ SUPER TYPHOON END
- ◆◆◆ EXTRATROPICAL
- ◆◆◆ SUBTROPICAL
- *** DISSIPATING STAGE
- F FIRST WARNING ISSUED
- L LAST WARNING ISSUED



DTG	SPEED	INTENSITY	DTG	SPEED	INTENSITY
05/1200Z	11	40	08/0000Z	8	100
05/1800Z	9	45	08/0600Z	4	110
08/0000Z	3	50	08/1200Z	4	115
08/0600Z	2	55	08/1800Z	3	120
08/1200Z	3	60	10/0000Z	3	125
08/1800Z	4	65	10/0600Z	3	125
07/0000Z	1	65	10/1200Z	1	120
07/0600Z	1	70	10/1800Z	2	115
07/1200Z	2	70	11/0000Z	2	110
07/1800Z	2	75	11/0600Z	2	105
08/0000Z	2	80	11/1200Z	4	100
08/0600Z	1	85	11/1800Z	4	95
08/1200Z	4	90	12/0000Z	4	90
08/1800Z	8	95	12/0600Z	5	85

80

TYPHOON FREDA (13W)

Freda was the first of seven significant tropical cyclones to develop during the month of September and the middle tropical cyclone (geographically) of three systems that developed at nearly the same time; namely Freda, Typhoon Gerald (14W) and Super Typhoon Holly (15W). During this three tropical cyclone outbreak, individual development and movement trends were very similar even though the systems were never closer together than 900 nm (1667 km). Freda was unusual because although it traversed less than 10 degrees of longitude while in warning status, it moved northward for almost twenty-five degrees of latitude. Freda's thirteen day life span and fifty warnings were WESTPAC records for 1987.



With the tropical disturbance just southeast of Guam, there was heightened concern about intensification as the system moved into an area of decreased vertical shear. During the night, infrared satellite images showed a flaring of convection, rapidly expanding cirrus outflow and a speedy displacement of the cloud system toward the west. Satellite analysis at 041745Z estimated maximum sustained surface winds of 30 kt (15 m/sec) and supported the issuance of the first warning on Tropical Depression 13W at 041800Z. (This was also the time JTWC went to warning on Tropical Depression 14W.) Within six hours, after the first visual satellite imagery provided a better look, Tropical Depression 13W was relocated 215 nm (398 km) east-southeast of the earlier expected position.

Freda developed in *Figure 3-13-1. First appearance of Freda's eye* an active monsoon trough. (061723Z September 1987 (OAA infrared imagery). The disturbance first appeared as a persistent cluster of convection in the eastern Caroline Islands on the 1st of September. Due to the persistent convective activity it was mentioned as a new suspect area on the 030600Z Significant Tropical Weather Advisory (ABPW PGTW). A low-level cyclonic circulation was apparent in the synoptic surface/gradient-level data beginning at 031200Z. By 040000Z, synoptic data indicated winds of 20 to 30 kt (10 to 15 m/sec). Satellite intensity analysis (Dvorak, 1984) estimated maximum sustained surface winds of 25 kt (13 m/sec). These data, plus a distinct gradient-level circulation and a 3 mb pressure fall over the past 24-hours (to a minimum of 1003 mb) supported a Tropical Cyclone Formation Alert issued at 040357Z.

Warning number two included the amplifying remarks:

Satellite imagery over the past six hours for Tropical Depression 13W indicate that the feature previously tracked on infrared imagery, has weakened, hence the system has been relocated. The latest visual imagery shows low-level cloud lines placing the low-level circulation center substantially further to the east than previously expected. This also indicates a slower forward speed.

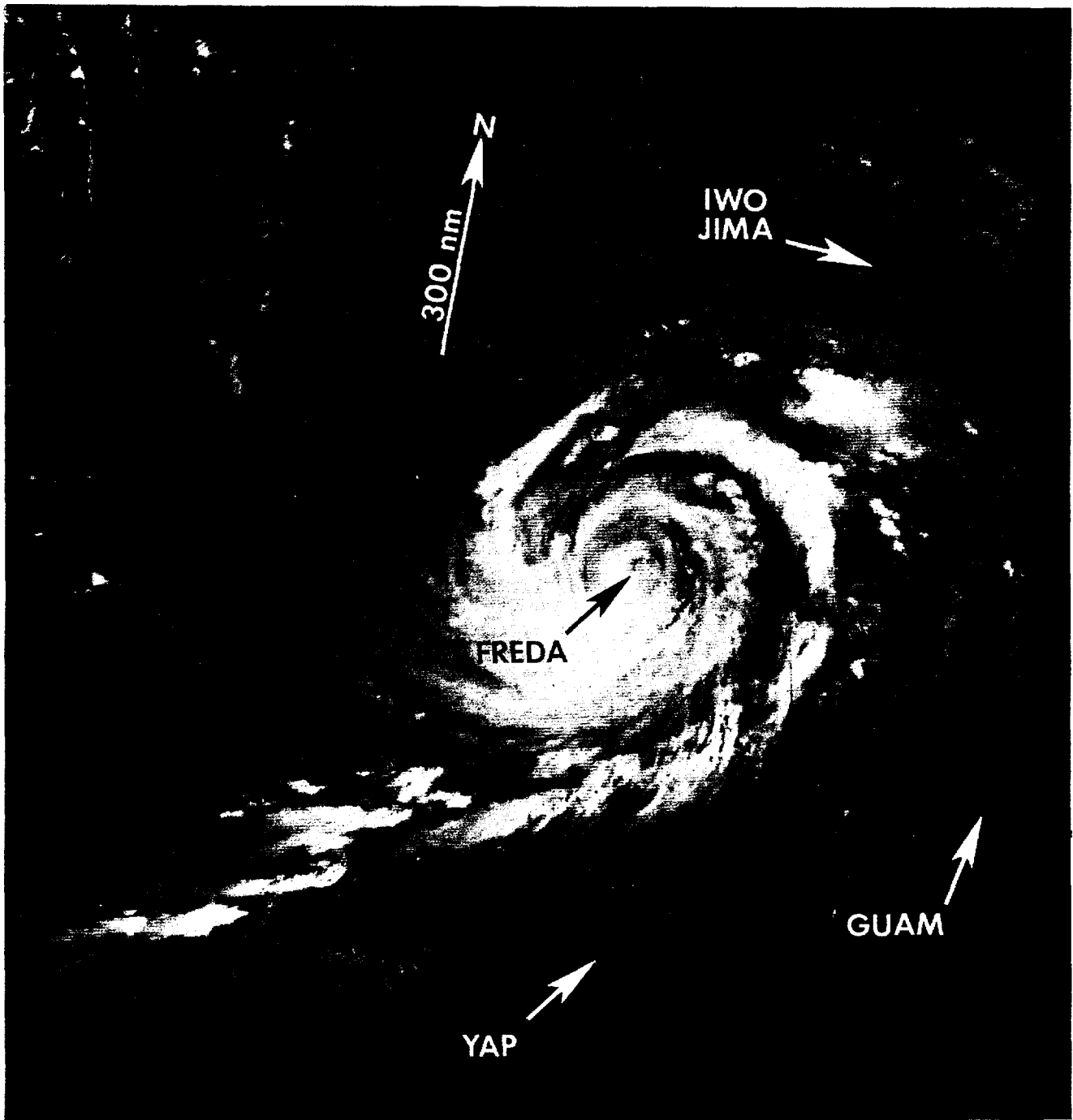


Figure 3-13-2. Typhoon Freda near maximum intensity. Note the elongation of the cloud system from east-northeast to west-southwest (110030Z September DMSP visual imagery).

Freda passed approximately 30 nm (56 km) southwest of Guam while moving northwestward at 14 kt (26 km/hr) with an estimated intensity of 25 to 30 kt (13 to 15 m/sec). Once past Guam, Freda developed rapidly and was upgraded to tropical storm intensity at 050600Z. (It was at this time that JTWC also began

warning on Tropical Depression 15W, thus creating the second three-storm warning situation of the year.)

Suddenly, twelve-hours later, Freda appeared to become quasi-stationary at a position approximately 250 nm (463 km) to the

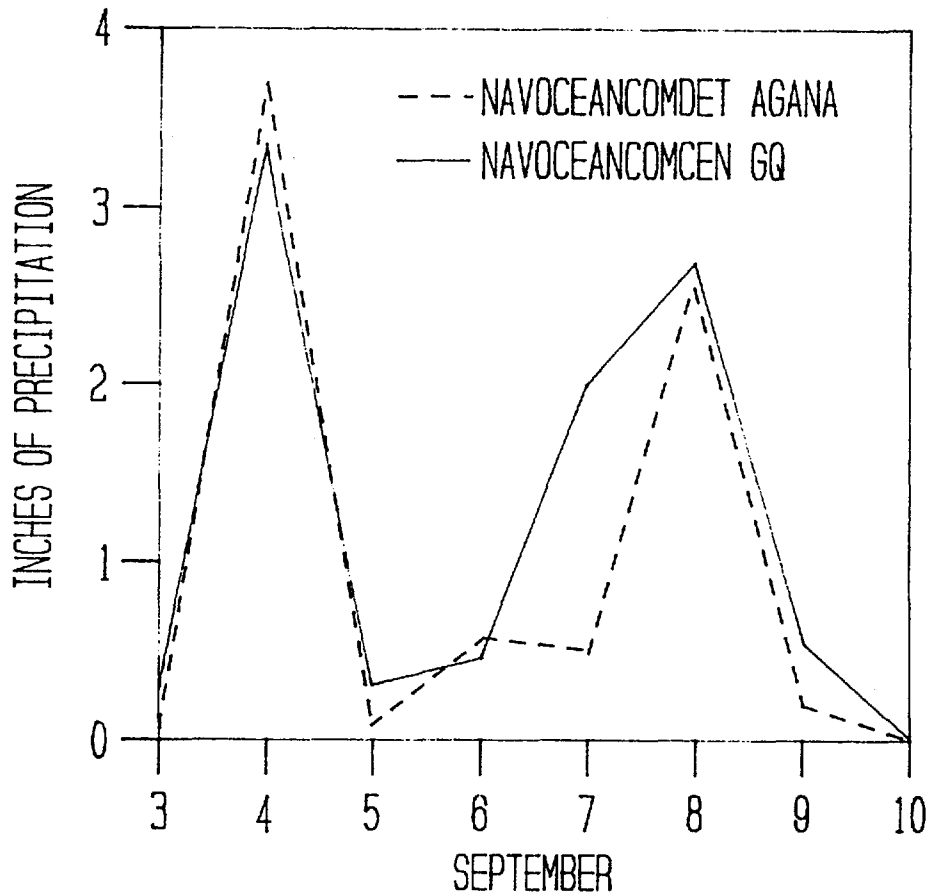


Figure 3-13-3. Plot of the daily amounts of precipitation at two recording stations on Guam as spiral convective arms from Freda passed over the island.

west-northwest of Guam. This was also the same time that Tropical Storm Gerald (14W) became quasi-stationary. The two systems were approximately 900 nm (1667 km) apart at that time.

With the appearance of a small ragged eye on satellite imagery at 061723Z (see Figure 3-13-1), Freda was upgraded to typhoon intensity. After executing a tight cyclonic loop, Freda began to move slowly westward on the 8th. Then, on the 10th, Freda slowed and started a tight turn toward the northeast. Concurrently with the track change, Freda reached an estimated peak intensity of 125 kt (64 m/sec), based on Dvorak satellite intensity analysis. Figure 3-13-2 shows Freda early on

the 11th as it rounds the western periphery of the subtropical ridge. Note the elongation of the cloud system into an east-northeast/west-southwest orientation. This asymmetry is a consequence of adjustments between the tropical cyclone and the ambient flow. (One day prior to Freda's change in track toward the north, Super Typhoon Holly (15W) also moved northward. At 091200Z, the two systems were approximately 1080 nm (2000 km) apart. Super Typhoon Holly (15W) had been steadily moving closer to Freda from the east prior to the northward bends in their tracks.)

During this prolonged northward trek, a consequence of the intense monsoonal trough and the absence of a strong subtropical ridge,

Freda started to slowly accelerate and weaken. At 1800Z on the 13th, Freda was downgraded to tropical storm intensity.

On the 16th, Freda began to interact with an eastward-moving, mid-level trough passing to the north of the system. This interaction resulted in a curved track toward the northeast. As a result, Freda missed the southeastern tip of Honshu by approximately

180 nm (333 km). Shortly thereafter, Freda began extratropical transition as vertical wind shear increased and the system entrained dry, cool, mid-latitude air. The last warning was issued by JTWC at 170000Z as the system accelerated toward the northeast.

Guam received two distinct heavy periods of rain over five days when Freda stalled to the west (Figure 3-13-3). Specifically

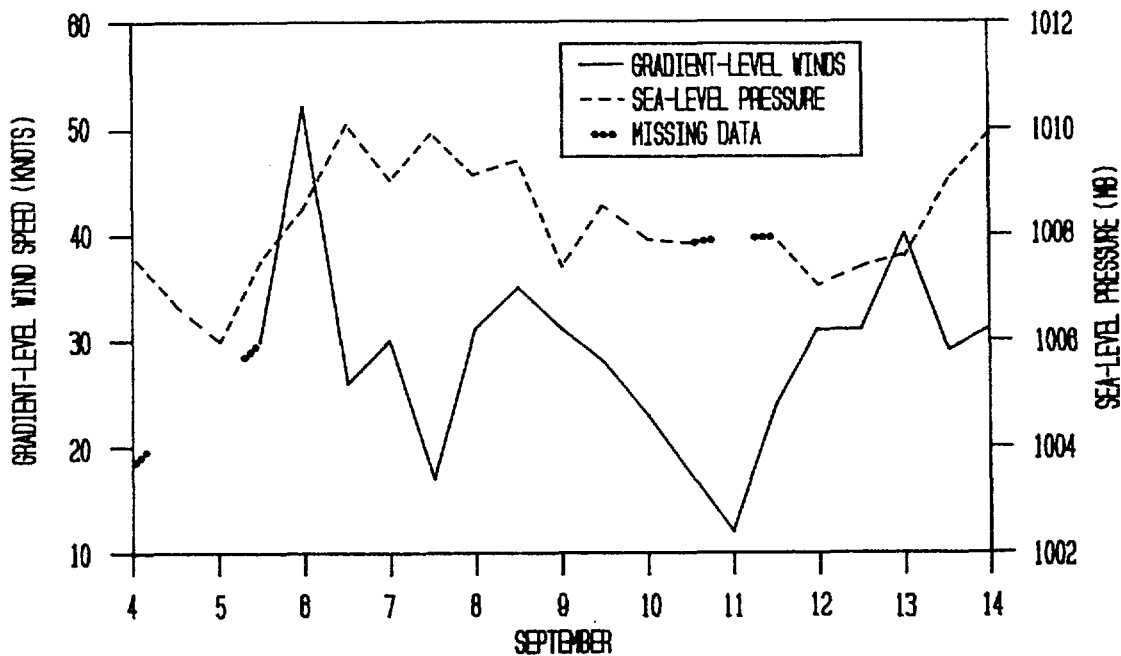
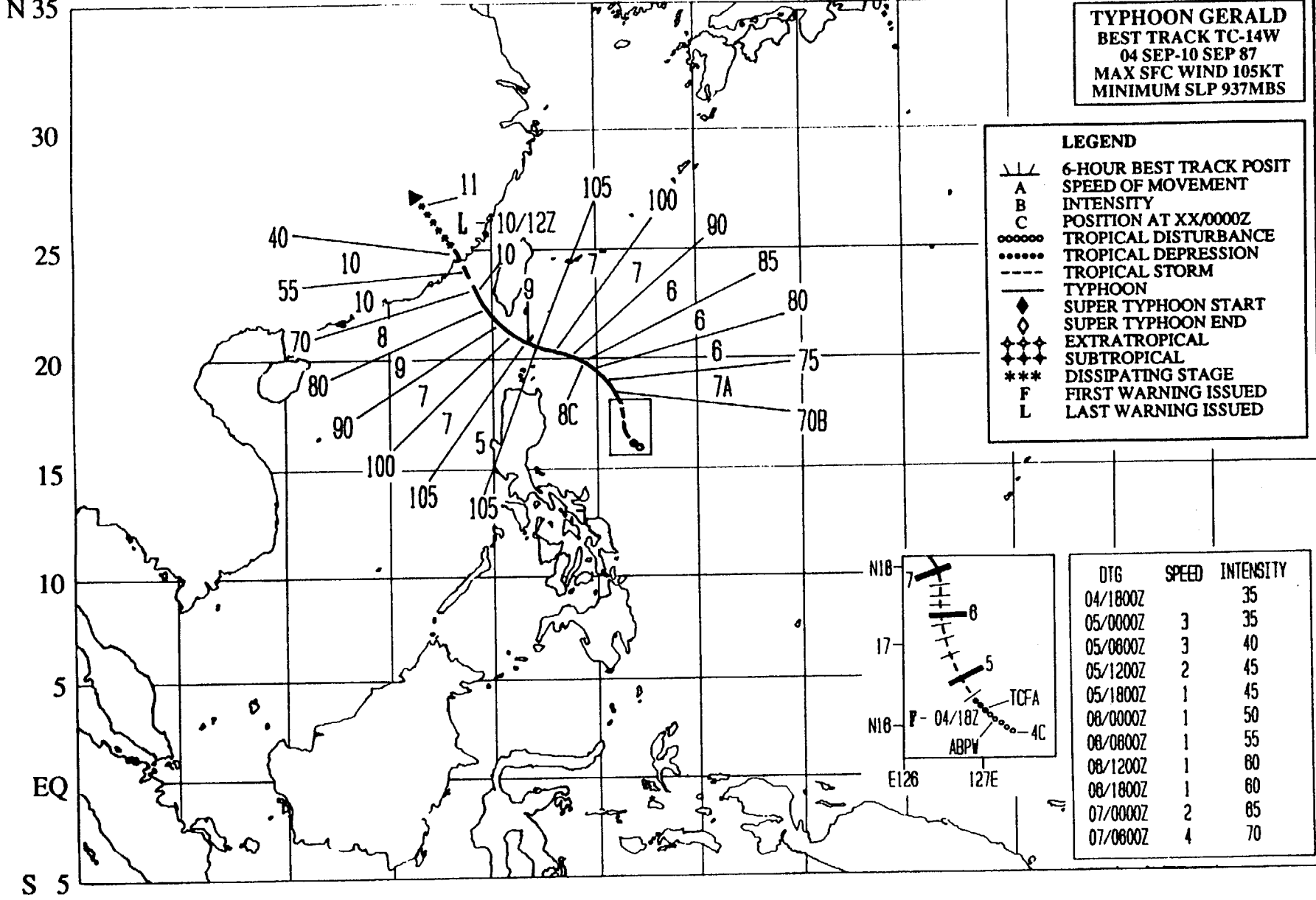


Figure 3-13-4. Gradient-level wind speeds and sea-level pressure on Guam as Freda stalled southwest of the island. The period of lighter winds from the 10th through the 11th was associated with the proximity of the zone of low-level speed convergence (convergent asymptote) between Freda and Super Typhoon Holly (15W).

on the 4th of September, when Freda was close by NAVOCEANCOMCEN/JTWC located on Nimitz Hill, Guam received 3.35 in (8.51 cm) of precipitation, and the Naval Oceanography Command Detachment at the Naval Air Station Agana, a few miles further north, received 3.75 in (10.93 cm). On the 8th, over 2.5 in (6.35 cm) of rain fell on Guam as convection associated with a spiral band passed overhead. Due to the proximity of Freda, and later Super Typhoon Holly (15W), Guam experienced periods of

gales from the south-southwest to west-southwest for nearly 10 days (from the 5th through the 14th) (Figure 3-13-4). The strongest observed winds reported during this period were the 40 kt (21 m/sec) southwesterly gradient-level winds at 121200Z. The resulting high seas and hazardous surf through the Marianas disrupted shipping, destroyed seawalls, damaged reefs, eroded beaches and stranded islanders; but fortunately no lives were lost.

E 100 105 110 115 120 125 130 135 140 145 150 155 160 E



98

S 5

TYPHOON GERALD (14W)

Typhoon Gerald developed in early September in an active monsoon trough at the same time that Typhoons Freda (13W) and Holly (15W) were intensifying further to the east. Gerald was unique in that it matured within the monsoon trough and did not detach from it. The most distinctive feature of Gerald was an unusually large eye.

After Typhoon Dinah (11W) moved northward through the East China Sea and became extratropical in the Sea of Japan, the minimum sea-level pressures (MSLPs) east of the Philippine Islands remained slightly lower (1005 mb) than the seasonal mean of 1007 mb. This below normal low-pressure area was not

mentioned as a suspect area on the Significant Tropical Weather Advisory (ABPW PGTW) until 020600Z September, when persistent convection appeared.

A Tropical Cyclone Formation Alert (TCFA) at 020830Z upgraded the suspect area in the Philippine Sea after a sudden flare-up of convection within the cloud system. Almost immediately the central convection fell apart as the poleward edge of the cirrus outflow flattened, restricted by the amplification of a mid-latitude trough to the north. Cancellation of the first TCFA on the monsoon depression area followed at 030800Z (Figure 3-14-1). The arrested development of the monsoon

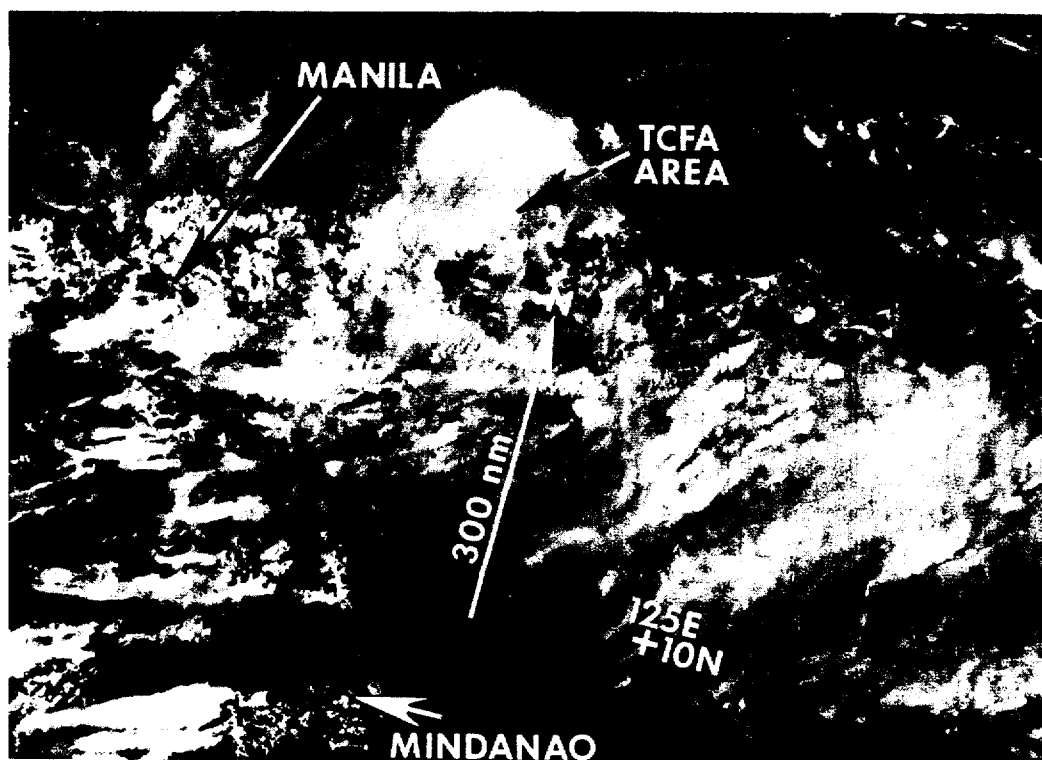


Figure 3-14-1. A broad band of cloudiness associated with the southwest monsoon extends eastward across the central Philippine Islands (030653Z September NOAA visual imagery).

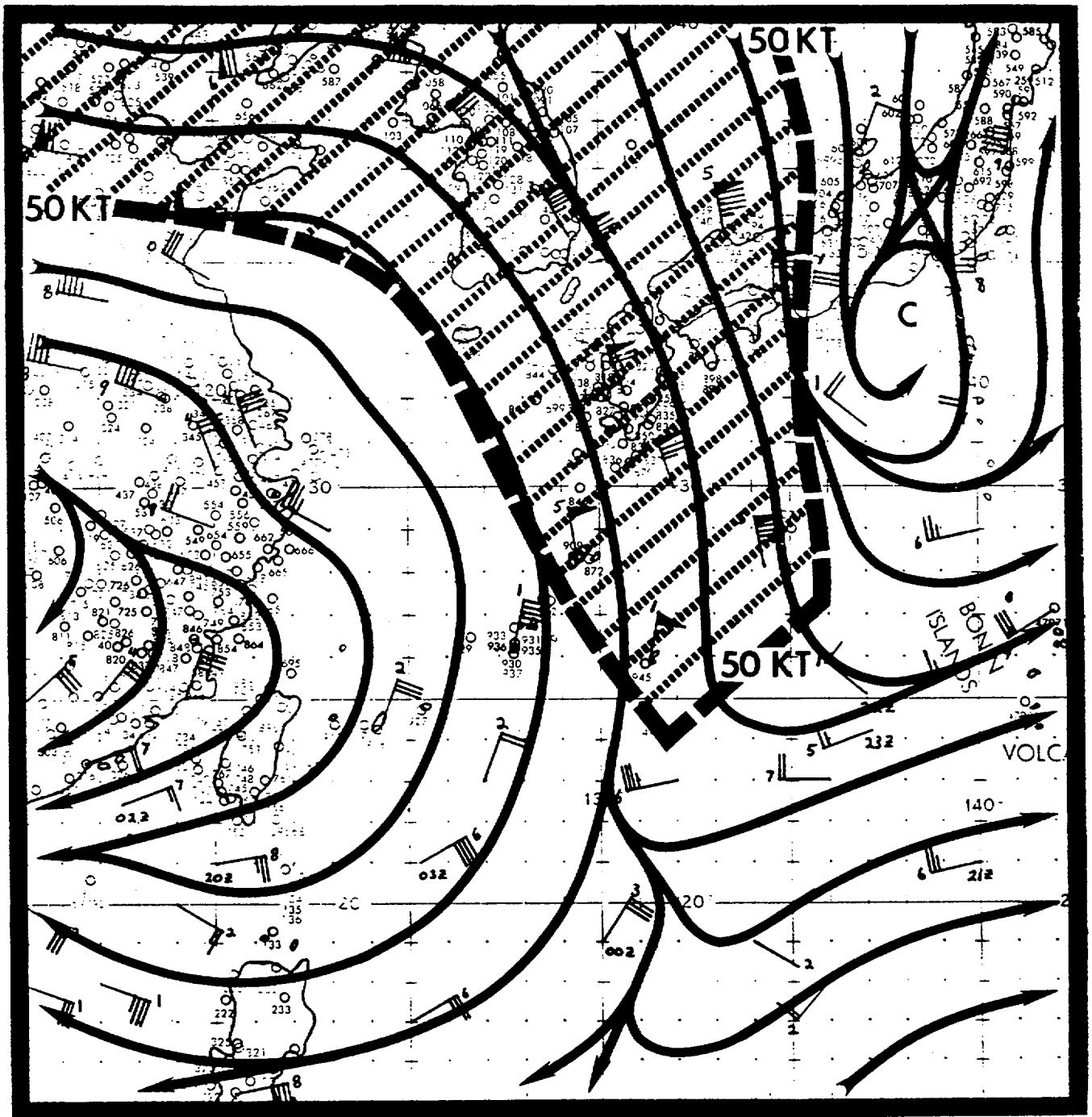


Figure 3-14-2. The 200 mb analysis at 040000Z September revealed a wind speed maximum across southwestern Japan.

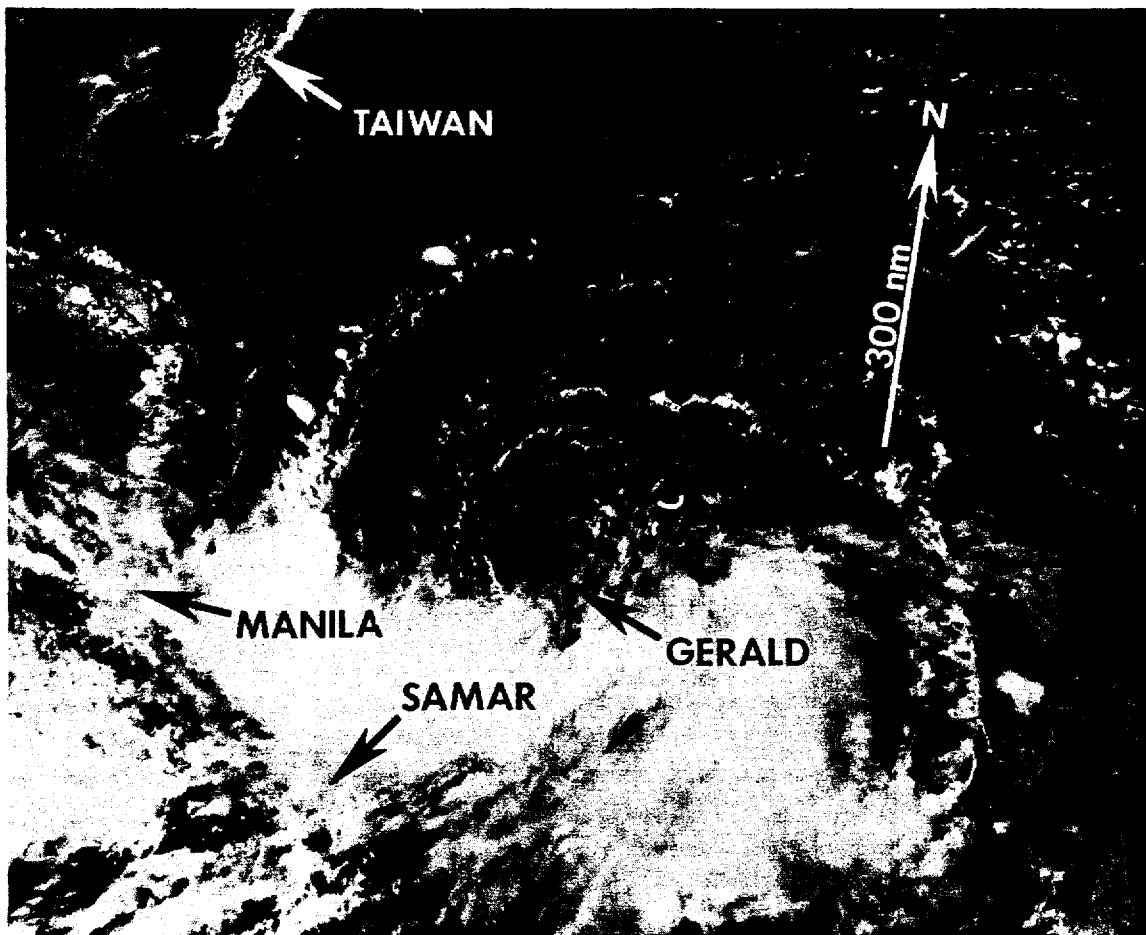


Figure 3-14-3. Due to northerly flow aloft, convection associated with the low-level circulation center was confined to the southern semicircle (040642Z September 9(OAA visual imagery)).

depression appears to be related to the movement of an upper-level wind maximum across the island of Kyushu, Japan. This resulted in an increase in northerly flow over the northern Philippine Sea (Figure 3-14-2). This increased upper-level wind shear was responsible for delaying Gerald's development beyond the monsoon depression stage.

At 040600Z, synoptic data obtained from drifting buoy and ship reports indicated the MSLP had dropped to 1003 mb with 25 to 30 kt (13 to 15 m/sec) winds near the circulation center. Satellite imagery also showed an exposed low-level circulation was displaced slightly to the north of a single major convective band (Figure 3-14-3). These data

prompted the issuance of a second TCFA at 041000Z. The first warning on Tropical Depression 14W followed at 041800Z, supported by a Dvorak intensity estimate of 30 kt (15 m/sec) and a drifting buoy report of a 1001 mb that revealed falling surface pressures.

Since Gerald was a shallow low-level circulation in an active monsoonal trough, its movement was erratic and difficult to forecast. During the period 040000Z to 071800Z, the primary numerical aid, the One-Way Interactive Tropical Cyclone Model (OTCM), was used by JTWC to forecast movement.

JTWC forecast Typhoon Gerald would slowly recurve to the east of Taiwan, however,

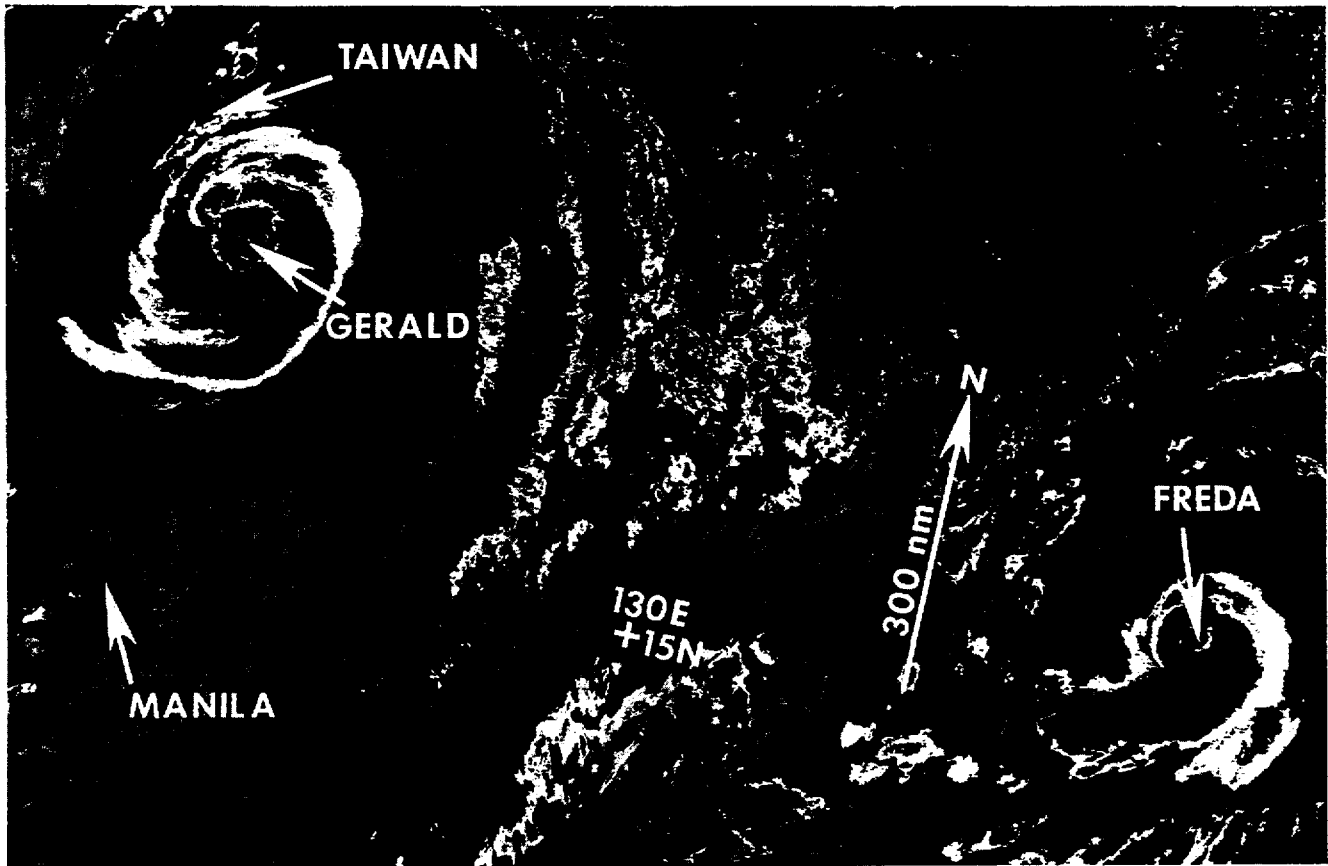


Figure 3-14-4. Typhoon Gerald at maximum intensity. The large eye is approximately 60 nm (111 km) in diameter. Prior to September, the 1987 season was characterized by an unusual number of 'midget' tropical cyclones. Typhoon Freda (13°W), which also has an eye, is located approximately 1000 nm (1852 km) east-southeast of Gerald (082111Z September DMSP enhanced infrared imagery).

northwestward movement up the monsoonal trough began on the 7th, as did acceleration and intensification. The 081800Z warning signalled a major change in the expected movement of Typhoon Gerald. The forecast indicated Gerald would pass through the Luzon Strait and make landfall on the southeast coast of mainland China.

Typhoon Gerald, with a large classic eye 60 nm (111 km) in diameter, reached its maximum intensity of 105 kt (54 m/sec) at 081800Z (Figure 3-14-4). Later, Gerald skirted the southwest coast of Taiwan (Figure 3-14-5). The mountainous terrain reduced low-level inflow and Gerald began to weaken (Figure 3-14-6). Gerald continued to weaken over the Formosa Straits and made landfall on the China

coast 50 nm (93 km) east-northeast of Amoy, a city about 245 nm (454 km) east-northeast of Hong Kong. The remnants of Gerald dissipated over land and were no longer apparent on either satellite imagery or synoptic data after 110000Z.

Typhoon Gerald caused extensive damage to Taiwan and China. In Taiwan, five people died and over \$10 million in damage was caused by heavy rain and flooding. Up to 16 inches (41 cm) of rain was reported in parts of the Zhejiang Province, China (south of Beijing). Flooding inundated more than 1,950 square miles (505,440 hectares) of farmland, causing widespread damage to crops valued at \$121 million. The Chinese death toll from Typhoon Gerald was 122.

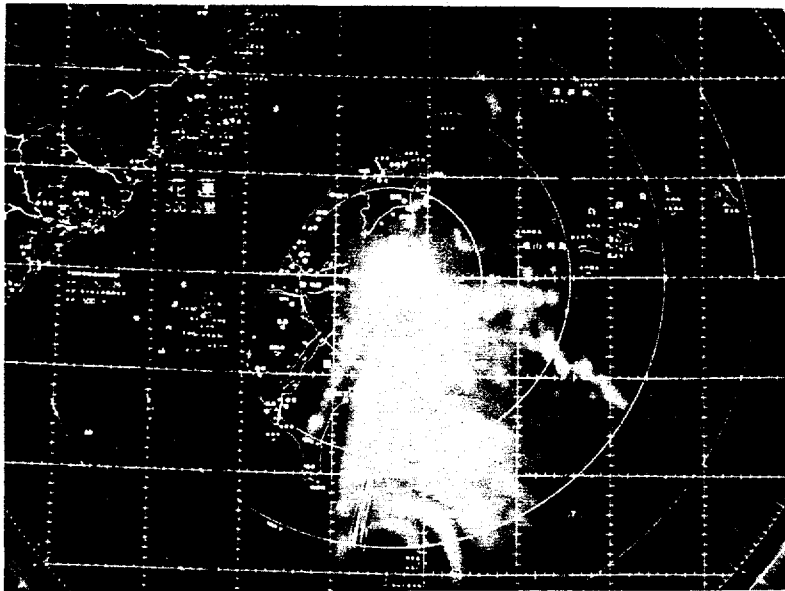


Figure 3-14-5. Radar presentation of the concentric rainbands of Typhoon Gerald as seen from Hualien, Taiwan (WMO 46699) at 090200Z September (Photograph courtesy of Central Weather Bureau, Taipei, Taiwan).

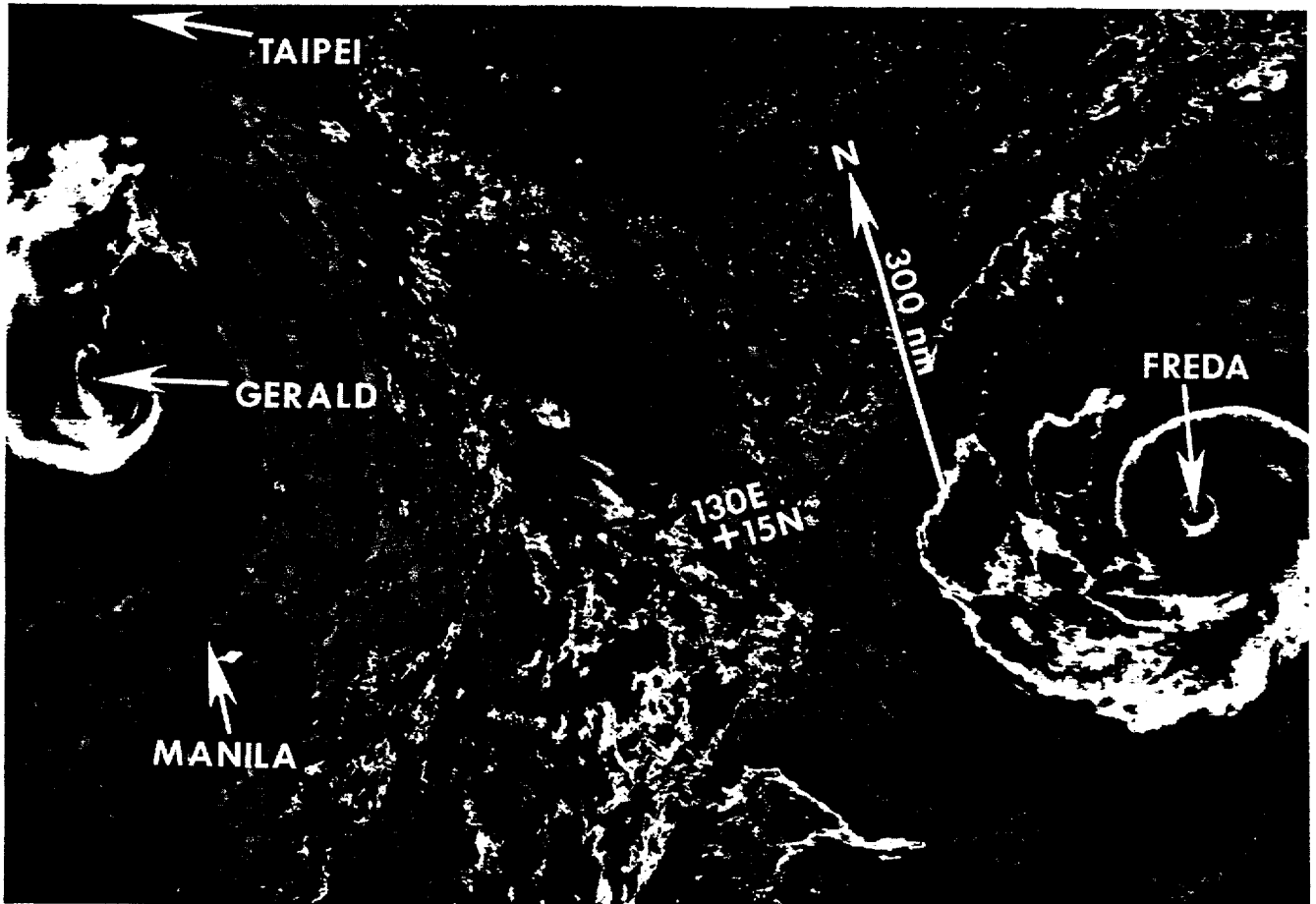
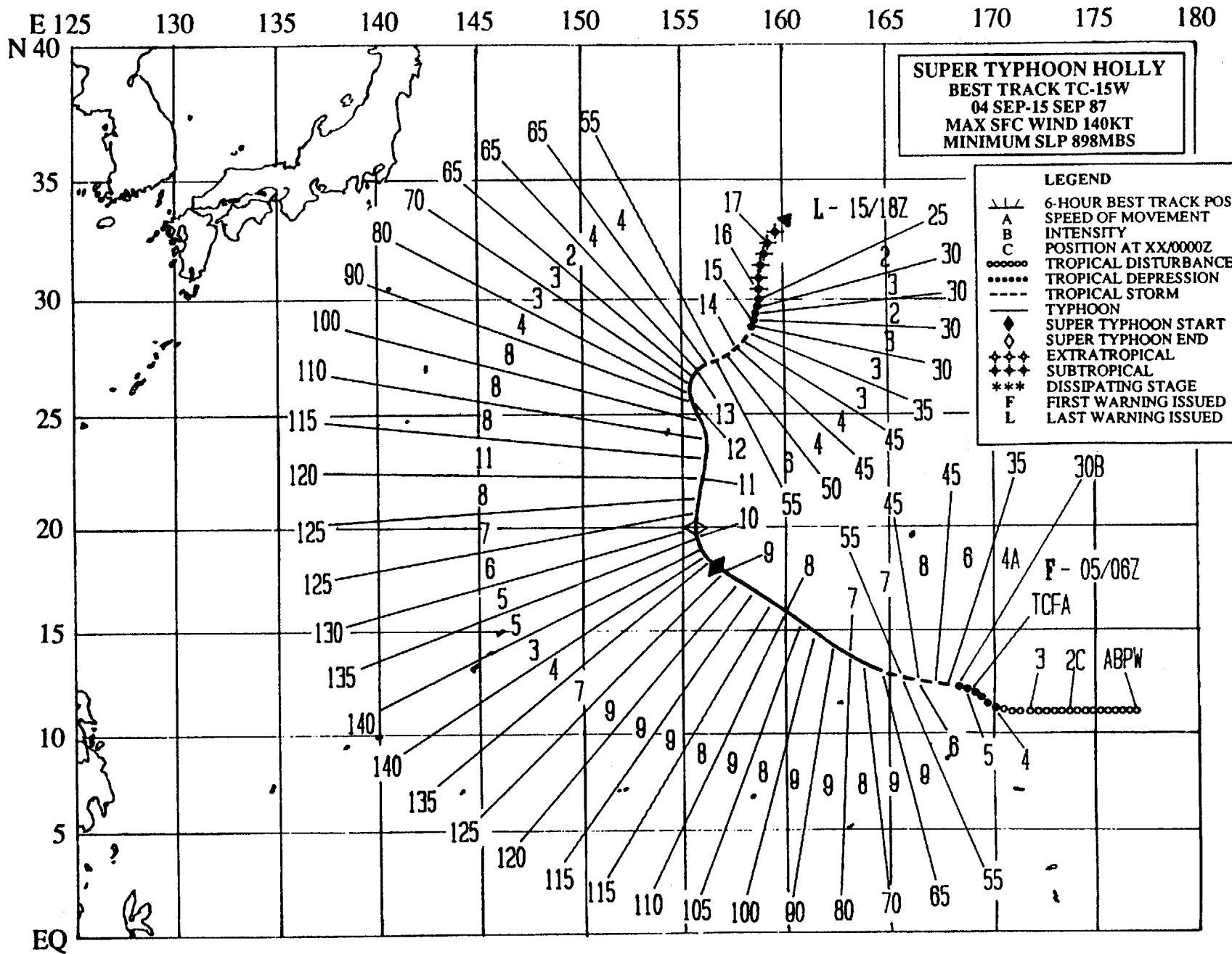


Figure 3-14-6. The effect of land interaction on Gerald's cloud pattern. This enhanced infrared image shows the distinct break in the central cloud mass to the north of the eye, which is related to lee-side subsidence over western Taiwan. This cloud-minimum area parallels the ridge line of mountainous central Taiwan (090956Z September DMSP infrared imagery).



SUPER TYPHOON HOLLY (15W)

In early September the active monsoonal trough spawned a three tropical cyclone outbreak. Super Typhoon Holly was one of the three. Typhoons Freda (13W) and Gerald (14W) were first warned on at 041800Z September, with Holly following 12-hours later. As these three systems matured, the monsoon trough became displaced well to the north of its "normal" location (see Figures 3-15-1 and 3-15-2). In fact, by the 11th of September, Holly, Typhoon Freda (13W) and the remains of Typhoon Gerald (14W) were all north of 15 degrees North Latitude as an anticyclonic circulation developed in low-latitudes just north of the island of Pohnpei in the eastern Caroline Islands. This anomalous low-latitude high pressure suppressed additional cyclogenesis for

the next four days (see Figure 3-15-3). Monsoonal troughing began to reappear on the 171200Z surface/gradient-level streamline analysis and was firmly re-established a day and a half later.

Holly began as a westward-moving area of persistent, but weakly organized, convection at the eastern end of the monsoon trough 560 nm (1037 km) east-northeast of Kwajalein and was first mentioned on the Significant Tropical Weather Advisory (ABPW PGTW) at 010600Z. As Holly developed over the next three days, satellite reconnaissance intensity estimates (Dvorak, 1984) of maximum sustained surface winds indicated an increase from 25 kt (13 m/sec) to 30 kt (15 m/sec). Vertical wind shear

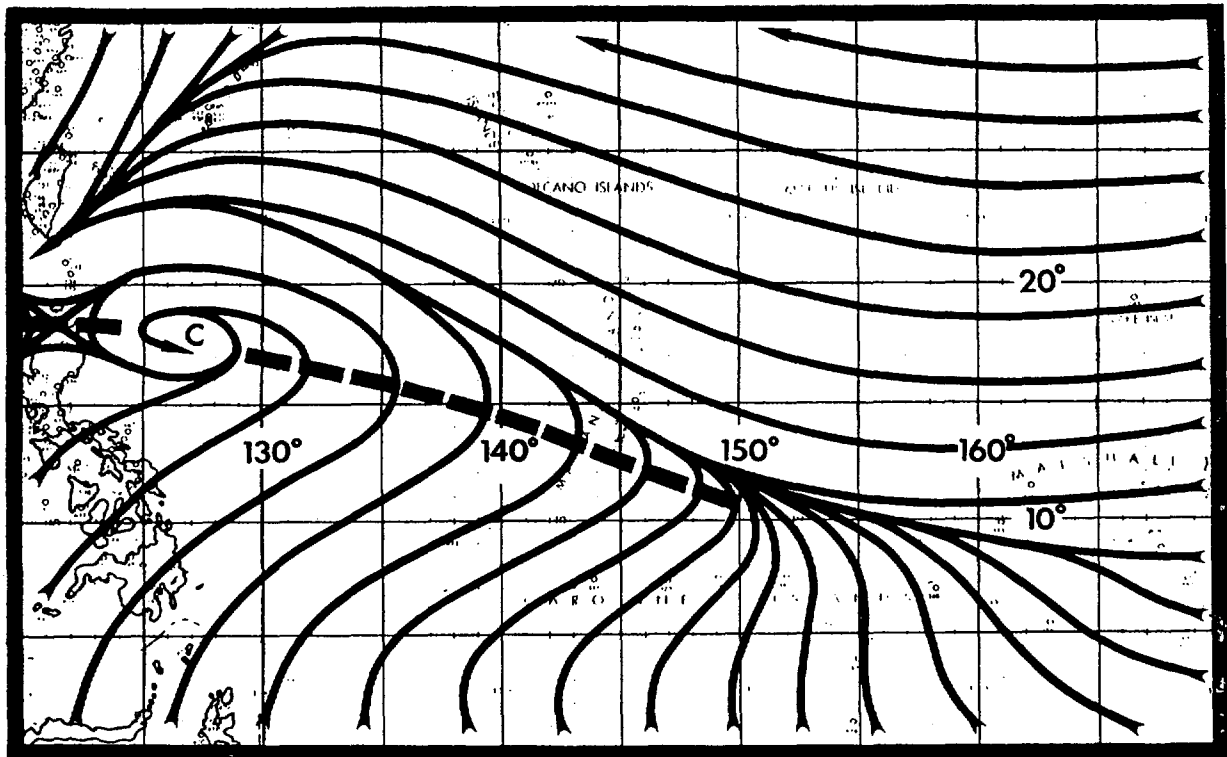


Figure 3-15-1. Gradient-level wind climatology for September (Sadler, et al, 1987).

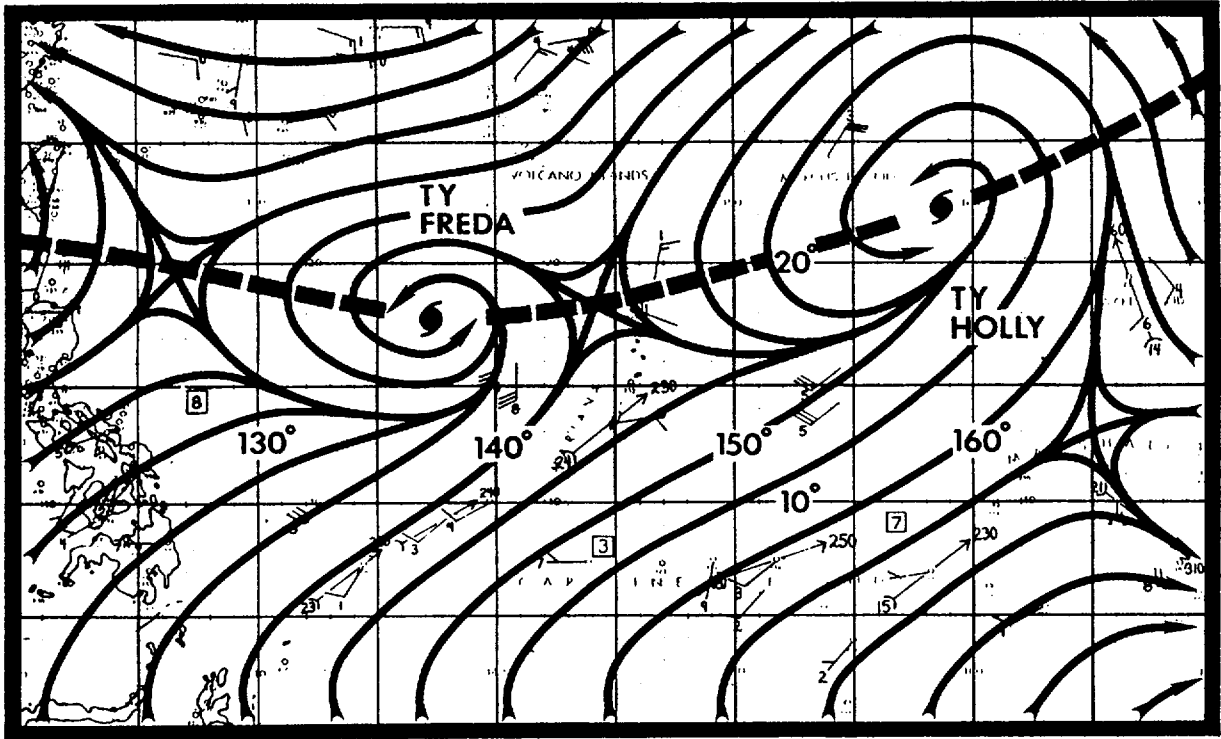


Figure 3-15-2. Low-level troughing is shown on this surface/gradient-level streamline analysis from 110000Z September well north of its climatological position (see Figure 3-15-1) due to the combined influences of Typhoons Freda (13°W) and Holly, and the remains of Typhoon Gerald (14°W).

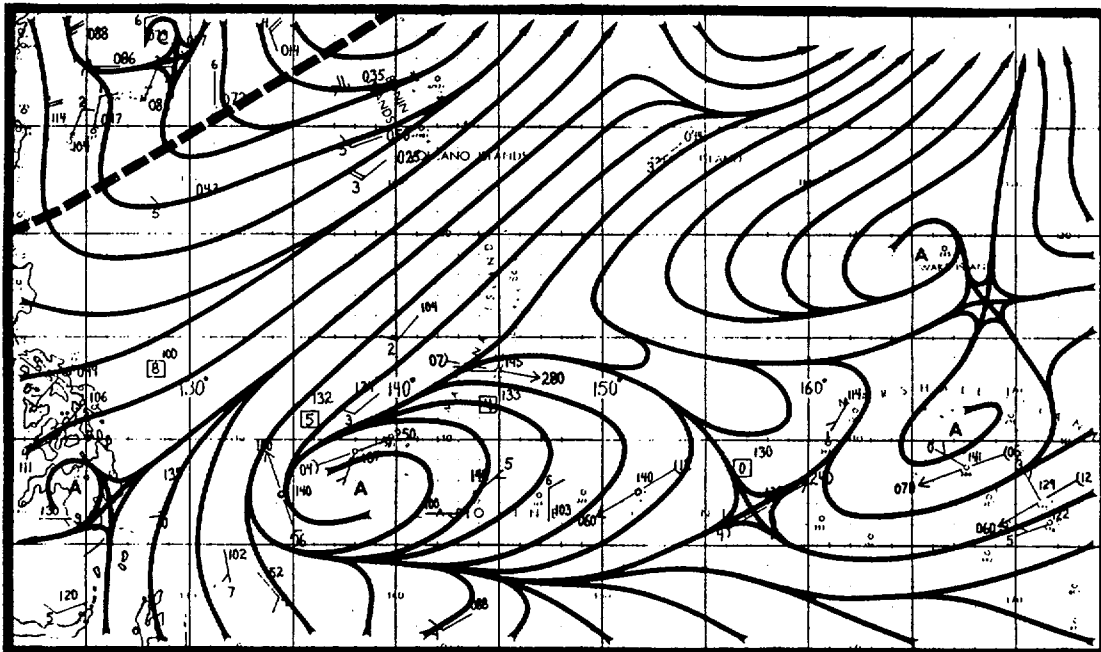


Figure 3-15-3. Ridging, shown as a band of anticyclones on this surface/gradient-level analysis for 161200Z September developed in latitudes normally expected to show monsoonal troughing. This appears to have been a key element in the suppression of further low-latitude tropical cyclone genesis through the 19th.

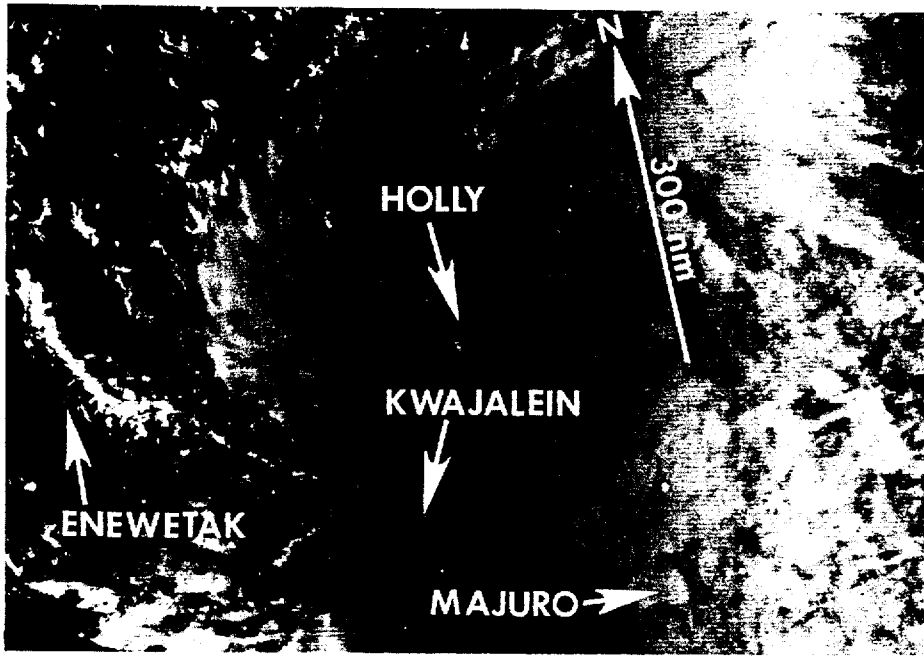


Figure 3-15-4. Holly near the time of its first warning (050721Z September DMSP visual imagery).

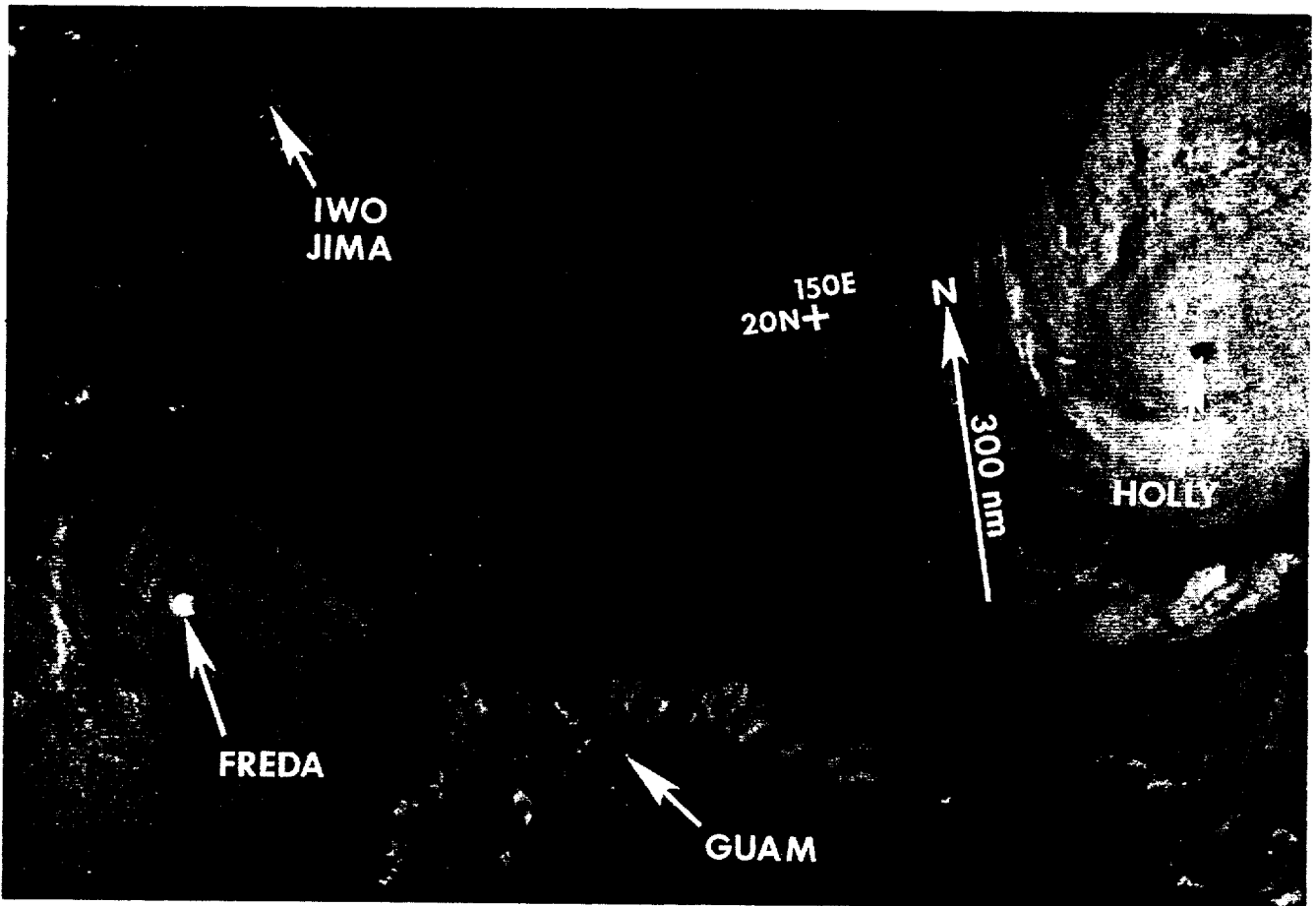


Figure 3-15-5. Super Typhoon Holly at peak intensity. Typhoon Freda (13W) appears to the left of Holly (091210Z September DMSP visual imagery).

over the system remained low (not more than 10 kt (5 m/sec)), favoring development. Surface/gradient-level streamline analysis at 040000Z showed moderate low-level cross-equatorial flow from the south into the disturbance. This was apparent from the southwesterly gradient-level winds at Truk (WMO 91334) and Pohnpei (WMO 91348) at 040000Z. Minimum sea-level pressures were 1006 mb in Holly with the mean environmental pressures near 1009 mb. This combination, together with indications that the deepest convection was consolidating about the low-level circulation center, supported the issuance of a Tropical Cyclone Formation Alert at 041930Z.

The first warning on Tropical Depression 15W followed at 050600Z. At that time, the maximum sustained surface winds were 30 kt (15 m/sec), with a forecast increase to 35 kt (18 m/sec) the next day. Satellite imagery on the 5th showed favorable upper-level outflow and a ragged central convective mass about 2 1/2 degrees in diameter (Figure 3-15-4). Associated convective bands southwest and east of the center implied a large-scale circulation and little competition for energy from Typhoon Freda (13W) to the west. As a consequence, Holly developed from 30 kt (15 m/sec) at the time of the first warning to 90 kt (46 m/sec) at the time of the ninth warning at 070600Z.

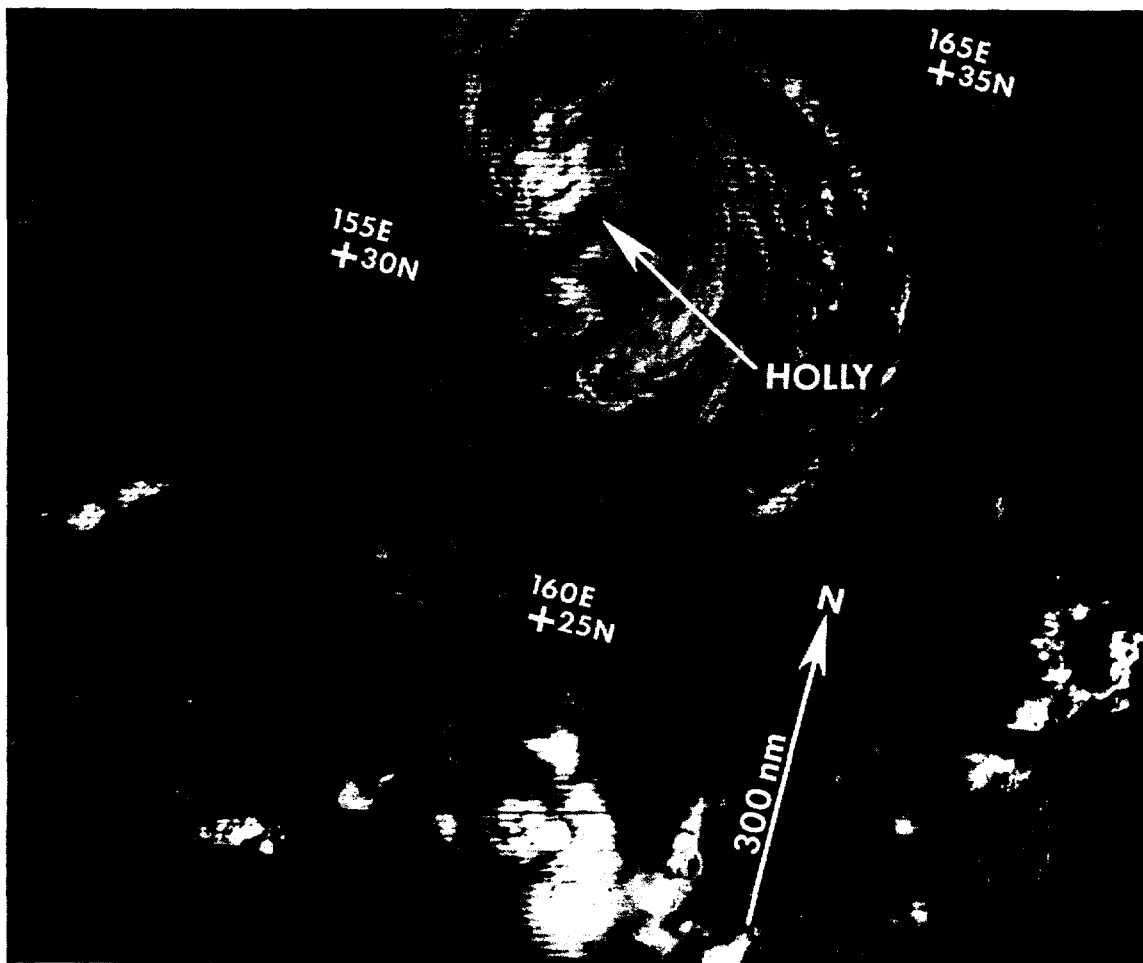
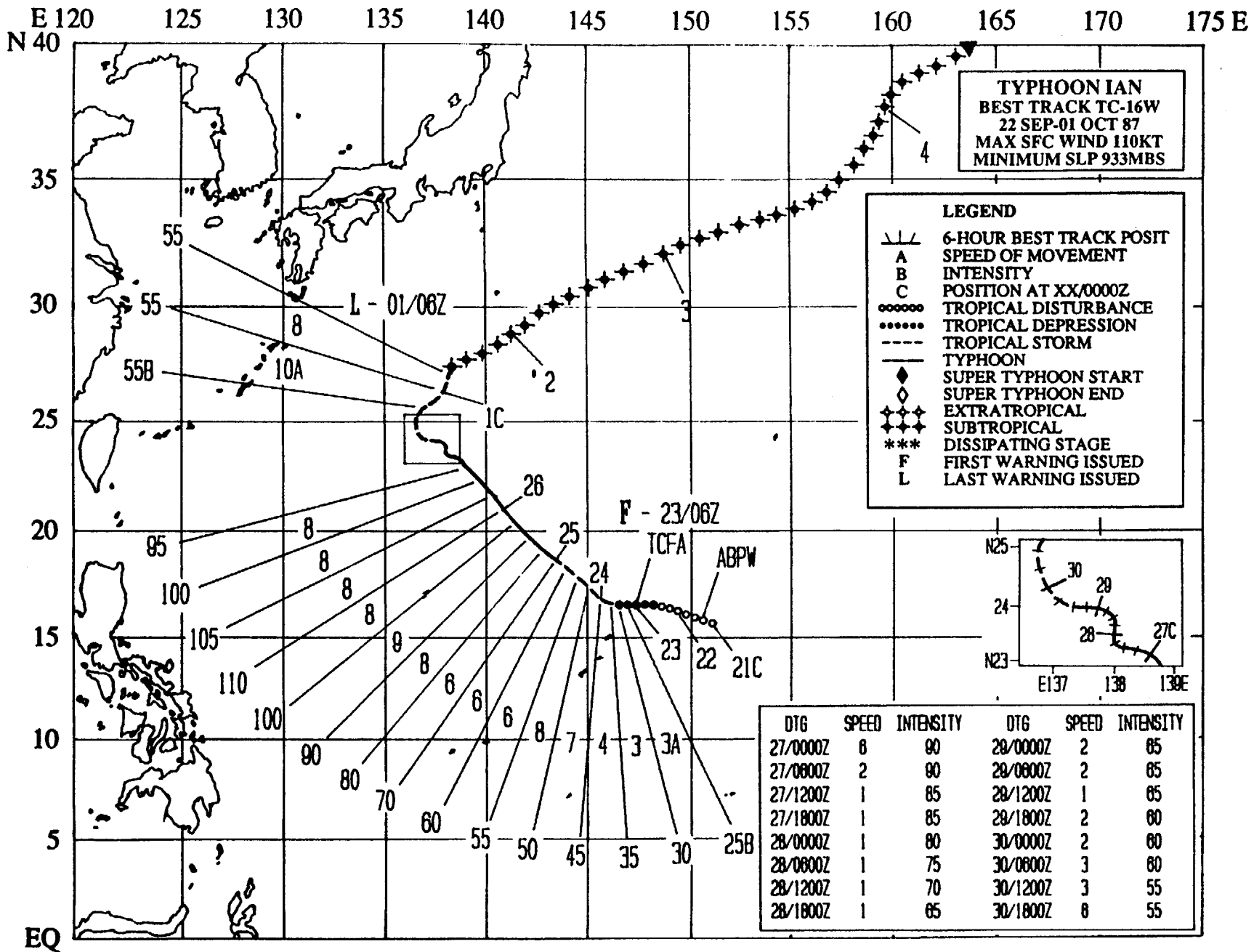


Figure 3-15-6. The subtropical remains of Holly (162227Z September DMSP visual imagery).

Holly's track abruptly changed from northwestward to northward at a position approximately 720 nm (1333 km) northeast of Guam. A maximum intensity of 140 kt (72 m/sec) was reached at 091200Z (Figure 3-15-5). Sparse upper-air and synoptic data did not clearly show a specific weakness in the subtropical ridge to the north of Holly. As a result, the early forecast tracks called for west-northwestward or westward movement. However, the relative movement and displacement of the monsoonal trough and the weakness of the subtropical ridge appear to have caused Holly's northward movement. (By the 10th, Typhoon Freda (13W) was about 950 nm (1759 km) to the west-southwest and

drifting slowly west-northwestward. No binary interaction was apparent between Holly and Typhoon Freda (13W).) With no strong mid-latitude systems approaching to provide stronger westerly or southwesterly steering flow, Holly (along with Typhoon Freda (13W)) drifted slowly northward in the active monsoon trough and weakened. Holly acquired subtropical characteristics after 140300Z, and retained 45 kt (23 m/sec) maximum sustained surface winds. Its remnants could still be located on satellite imagery through the 17th (Figure 3-16-6), with the final satellite fix obtained at 170600Z. No reports of damage or loss of life were attributed to Holly during its lifetime.



TYPHOON IAN (16W)

Typhoon Ian was the fourth of seven tropical cyclones to occur in the western North Pacific during September. Ian developed into a significant tropical cyclone six days after the second three-storm warning situation of the year involving Typhoons Freda (13W), Gerald (14W) and Super Typhoon Holly (15W) had ended on September 17th. Thirty-six hours after the first warning on Ian, it was joined by Tropical Depression 17W, which brought to seven the number of periods during 1987 that JTWC was warning on at least two systems at the same time. Even though, Tropical Depression 17W was a very short-lived system, Hurricane Peke (02C), which crossed the dateline (becoming Typhoon Peke (02C)), and Tropical Storm June (18W) soon took its place. This gave rise to the third three-storm warning situation of the year and the second to occur during September.

Forecasts verified extremely well on Typhoon Ian. The forecast track error statistics for all three verification times (i.e., 24-, 48- and 72-hours) were significantly less than the five-year average (see Chapter V, Tables 5-1A through 5-2B), though the 72-hour forecast error of 344 nm (637 km) exceeded the 1987

average. The reason for the poor 72-hour forecast errors was the unexpected slower movement of Ian between 270600Z and 290000Z when the system became nearly quasi-stationary while tracking generally toward the northwest. If this abnormal behavior had not occurred, JTWC's statistics on Ian would have been outstanding.

Ian began as a broad, poorly organized tropical disturbance 330 nm (611 km) to the east-northeast of Guam. Satellite analysts from Detachment 1, 1st Weather Wing (Det 1, 1WW) alerted the Typhoon Duty Officer to the presence of a persistent area of convection showing improved upper-level outflow. This was in the region where the monsoonal trough was attempting to become re-established after being disrupted by the previous three-storm situation. On 21 September at 0600Z, JTWC added the disturbance to its Significant Tropical Weather Advisory (ABPW PGTW) and listed its potential for development as poor due to the relatively high minimum sea-level pressures (MSLPs) evident in the trough at that time. Within 24-hours, the MSLPs decreased by 2 mb and the wind speeds increased another 5 kt (3 m/sec) to 25 kt (13 m/sec) (see Figure 3-16-1).



Figure 3-16-1. Ian, as a tropical disturbance with 25 kt (13 m/sec) maximum sustained winds at the surface (220007Z, September DMSP visual imagery).

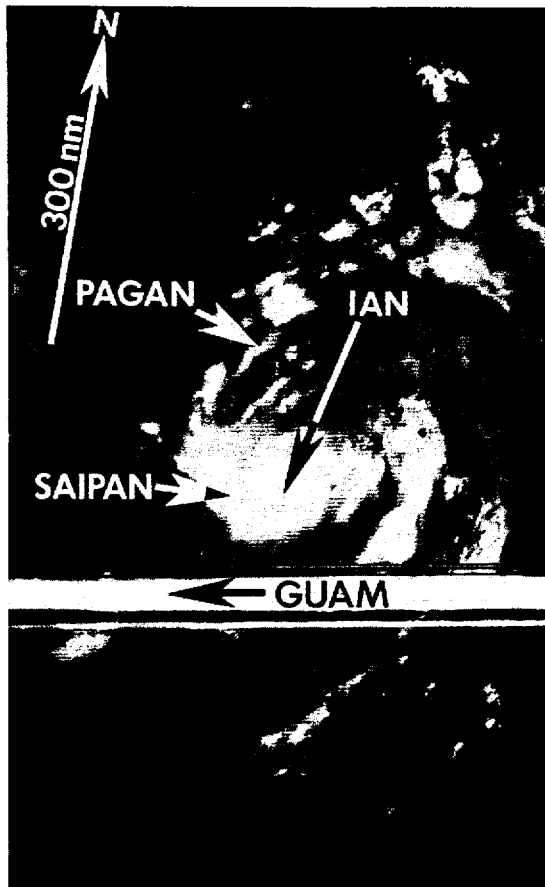


Figure 3-16-2. Curvature is evident in the convective cloud lines just prior to JTWC issuing a Tropical Cyclone Formation Alert at 230130Z (222346Z September DMSP visual imagery).

Ian continued its slow-paced development. Early on the 23rd, satellite imagery (see Figure 3-16-2) showed further intensification had taken place. Curvature became evident in the low-level cloud lines. Satellite intensity analysis (Dvorak, 1984) of imagery at 222346Z estimated 30 kt (15 m/sec) winds at the surface associated with this disturbance. JTWC promptly issued a Tropical Cyclone Formation Alert at 230130Z for the Mariana Islands north of Guam.

JTWC issued the first warning on Ian (as Tropical Depression 16W) at 230600Z, with an intensity of 25 kt (13 m/sec) and gusts to 35 kt

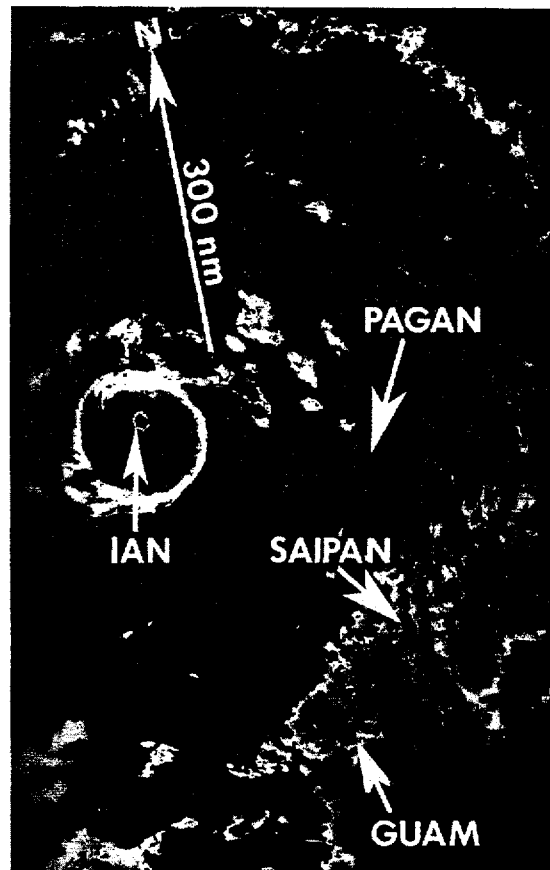


Figure 3-16-3. Typhoon Ian approximately 12-hours before reaching its maximum intensity of 110 kt (57 m/sec). Note the small circular eye and compact central dense overcast (251146Z September DMSP enhanced infrared imagery).

(18 m/sec), based on spiral bands of convection which became visible on visual and infrared satellite imagery. The system was upgraded to Tropical Storm Ian (16W) on the third warning (231800Z) as it progressed slowly westward into an area of low vertical wind shear.

At about that time, Ian began to develop at slightly greater than the normal Dvorak rate of one "T-number" per day. Wind speeds increased from 35 kt (18 m/sec) at 231800Z to 60 kt (31 m/sec) at 241800Z. Midway through this period, Ian turned from its westward course and began to move toward the northwest. Five radar fixes were obtained from Andersen Air

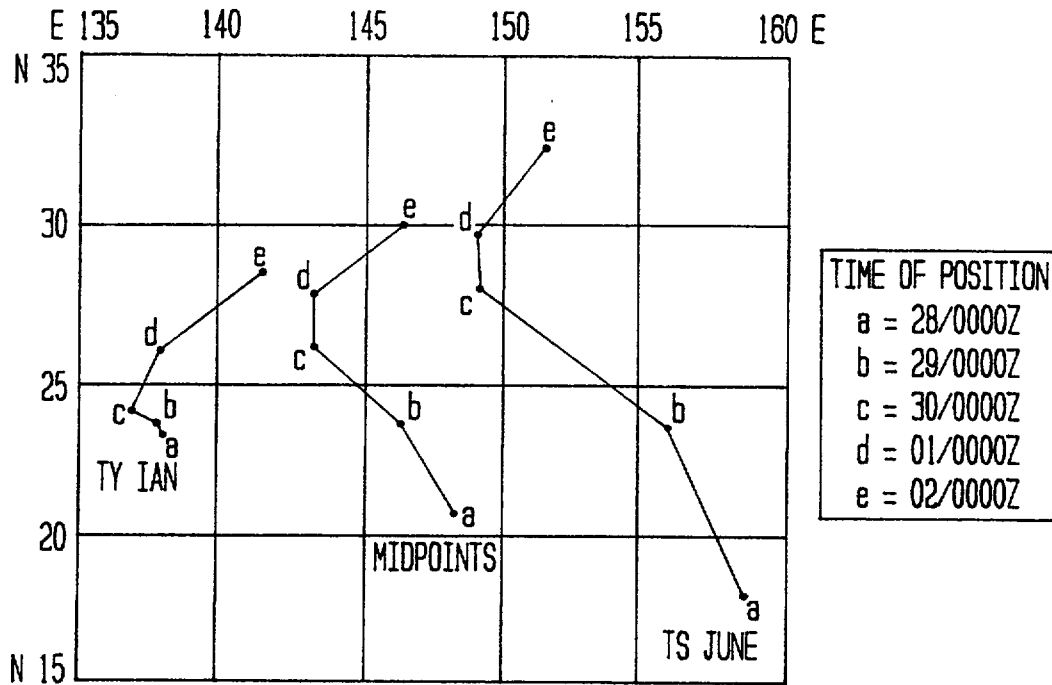


Figure 3-16-4. Plot of the slight binary interaction between Ian and June (18°W) showing their individual tracks and the path of the midpoints.

Force Base on Guam during this same time period. The center positions were based on the convective banding features. No eye feature was apparent on radar for any of the fixes.

Between 241800Z and 250000Z, Ian reached typhoon intensity as it moved steadily toward the northwest at 7 kt (13 km/hr). It intensified at a rate of 10 kt (5 m/sec) per six-hour interval (i.e., between warning times) from 241800Z through 260000Z (Figure 3-16-3). Note the small circular eye and the compact nature of the deepest convection. Ian reached its maximum intensity of 110 kt (57 m/sec) at 260000Z. It

was during this time of steady intensification that Tropical Depression 17W developed and then dissipated to the east of Ian. No binary interaction was apparent between them. A steady, slow decline followed. Twenty-four hours after Tropical Depression 17W had dissipated Ian slowed dramatically in forward speed as it approached a mid-latitude front lying just to the east of the Ryukyu Islands. Ian inched slowly northward between the times of 270600Z and 290000Z at a rate of less than 2 kt (4 km/hr). Its deep central convection decreased significantly. The movement of a mid-latitude shortwave north of Ian appeared to

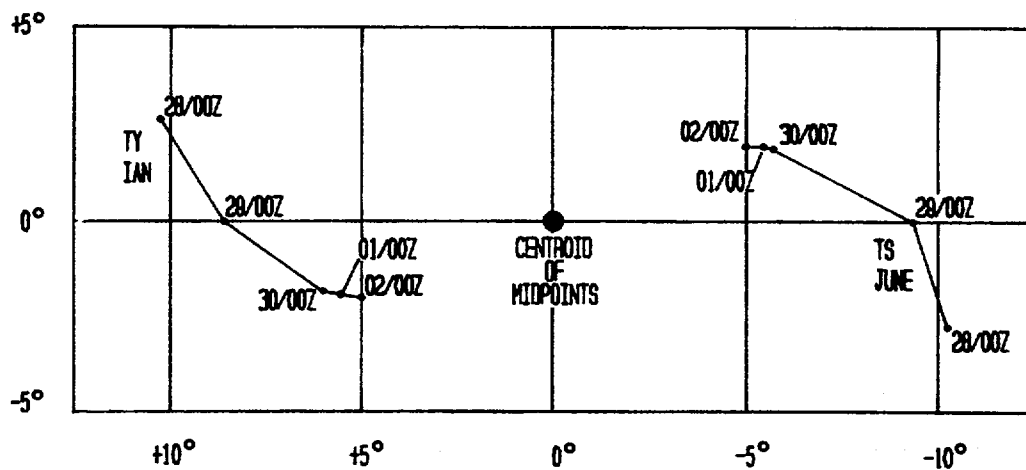


Figure 3-16-5. Plot of the center-relative movement about the midpoint centroid.

have suppressed it. Once this shortwave moved off toward the east on the 29th, Ian's upper-level outflow became aligned with the jet stream (which was above the lower level front) and the system began recurving south of Japan.

Meanwhile Tropical Storm June (18W), which began its development on the 28th, was moving rapidly northwestward at 18 to 20 kt (33 to 37 km/hr). Ian and June (18W) were close to one another at this stage (within 400 nm (741 km)) and eventually underwent a slight binary interaction between 300000Z September and 020000Z October. In Figure 3-16-4, the midway point is plotted for the times the two systems coexisted. Figure 3-16-5 shows a plot of the relative movement of each system with respect to the centroid position. As Ian and June (18W) moved northeastward and dissipated, the separation between their tracks decreased.

Ian continued to slowly weaken as this interaction took place, however JTWC forecasters and the Det 1, 1WW satellite analysts misread the changes to Ian on satellite imagery. Dvorak analysis at 010600Z October estimated Ian's intensity at 30 kt (15 m/sec), which supported a final warning and a downgrade to tropical depression intensity. Post-analysis indicates that Ian most probably transitioned to a subtropical system (rather than extratropical since the subtropical ridge was located to the north of Ian) and still had 55 kt (28 m/sec) winds at the time of the final warning.

The remnants of Ian continued to move northeastward after it transitioned to subtropical and finally dissipated 1200 nm (2222 km) to the east of Japan on the 4th of October. No damage or deaths were attributed to Ian.

TROPICAL DEPRESSION 17W

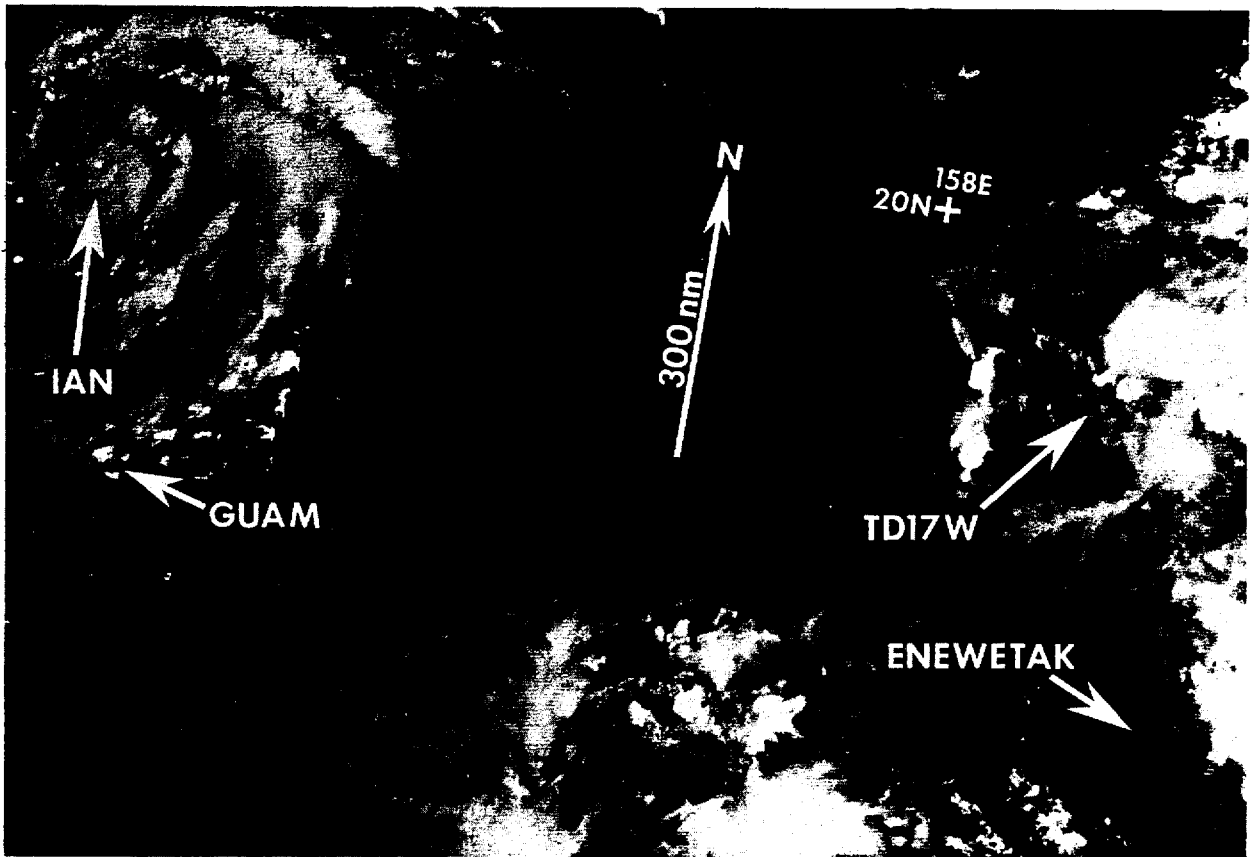


Figure 3-17-1. Tropical Depression 17W slowly developed from a tropical disturbance 250 nm (463 km) north of the Marshall Islands during the same period JTWC was warning on Typhoon Ian (16W). It was first detected on satellite imagery on the 23rd of September and mentioned on the Significant Tropical Weather Advisory (ABPW PGTW) as a new suspect area at 0600Z. JTWC issued a Tropical Cyclone Formation Alert nearly 24-hours later at 240330Z when this system displayed increased convective organization. Maximum sustained surface winds, at that time, were estimated at 15 to 25 kt (8 to 13 m/sec). The first warning on Tropical Depression 17W was issued at 241800Z based on satellite intensity estimate (Dvorak, 1984) of 35 kt (18 m/sec) winds at the surface. A well-established mid-level ridge was located to the northeast of Tropical Depression 17W. At the same time, an eastward-progressing, mid-latitude trough to the north was beginning to influence the system. This trough continued to suppress Tropical Depression 17W's development even after it had passed to the northeast of the disturbance. Concurrently, Typhoon Ian's (16W) upper-level outflow (at the left of the image) restricted Tropical Depression 17W's outflow in the northwest quadrant. This combination of factors appears to have stopped further intensification and induced dissipation over water. The last warning was issued on the 26th of September at 0600Z. The satellite image above shows Tropical Depression 17W shortly before the second warning was issued, while it was at its maximum intensity of 30 kt (15 m/sec) and 960 nm (1778 km) east-southeast of Typhoon Ian (16W). A partially exposed low-level circulation is visible slightly west of the heaviest convection (242305Z September DMSP visual imagery).

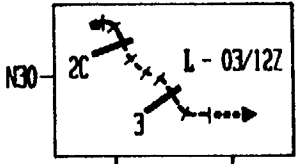
E 145 150 155 160 165 170 175 180 175 170 165 160 W

N 40

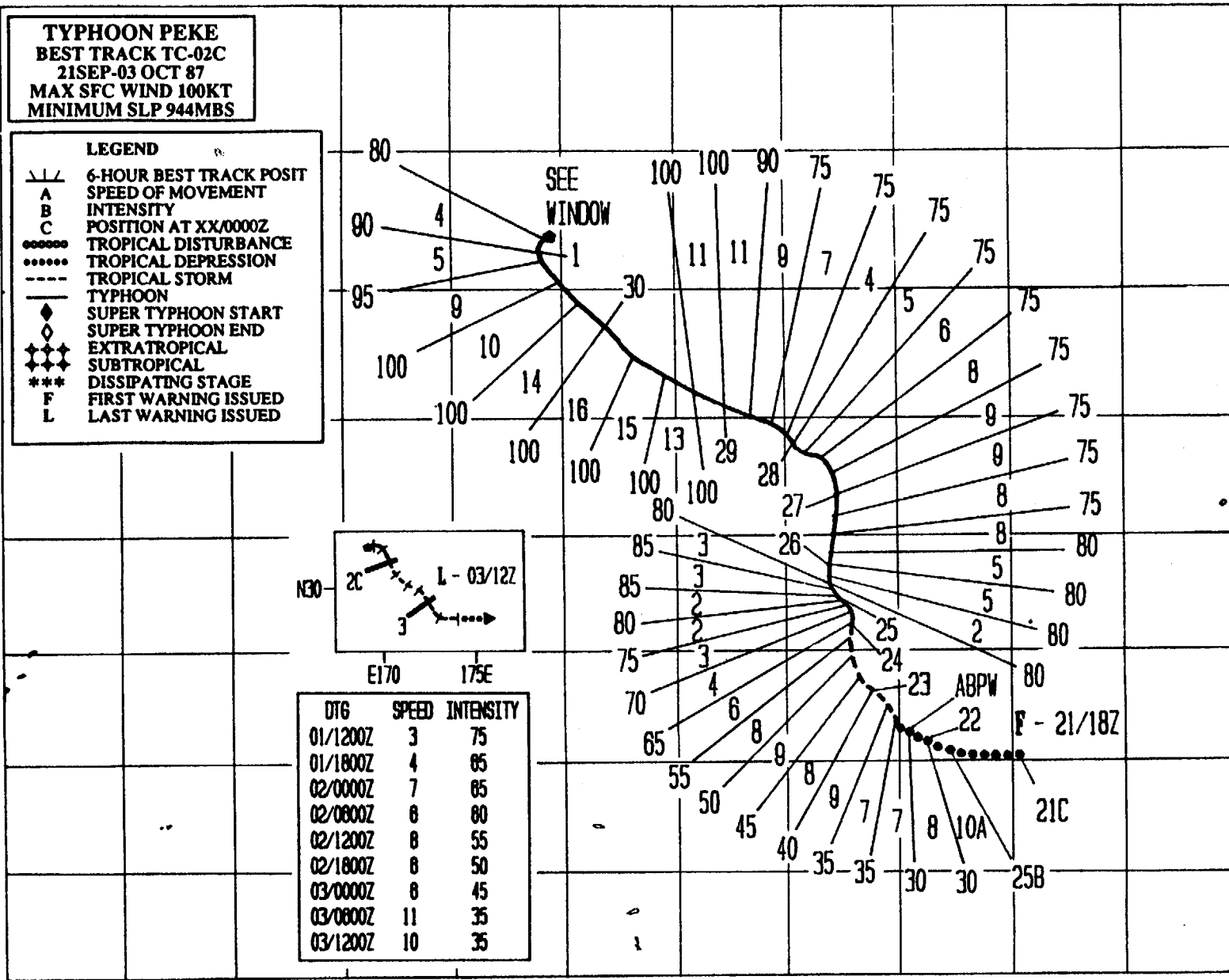
TYPHOON PEKE
BEST TRACK TC-02C
 21SEP-03 OCT 87
 MAX SFC WIND 100KT
 MINIMUM SLP 944MBS

LEGEND

- 6-HOUR BEST TRACK POSIT
- A SPEED OF MOVEMENT
- B INTENSITY
- C POSITION AT XX/0000Z
- TROPICAL DISTURBANCE
- TROPICAL DEPRESSION
- TROPICAL STORM
- TYPHOON
- ◆ SUPER TYPHOON START
- ◇ SUPER TYPHOON END
- ◆◆◆◆ EXTRATROPICAL
- ◆◆◆◆ SUBTROPICAL
- ◆◆◆◆ DISSIPATING STAGE
- *** FIRST WARNING ISSUED
- L LAST WARNING ISSUED



DTG	SPEED	INTENSITY
01/1200Z	3	75
01/1800Z	4	85
02/0000Z	7	85
02/0600Z	8	80
02/1200Z	8	55
02/1800Z	8	50
03/0000Z	8	45
03/0600Z	11	35
03/1200Z	10	35



106

EQ

TYPHOON PEKE (02C)

Typhoon Peke (02C) was the first hurricane during the past twenty years (since Typhoon Sara (28) in September 1967) to form in the central North Pacific and cross the dateline. Peke was the only significant tropical cyclone to cross the dateline north of the equator this year. The first twenty-five advisories were issued by the Central Pacific Hurricane Center (CPHC) in Honolulu, Hawaii (the Naval Western Oceanography Center at Pearl Harbor, Hawaii issued the corresponding warnings for the Department of Defense customers). The final twenty-three warnings were issued by JTWC.

Peke began as a broad area of convection about 480 nm (889 km) to the south-southeast of Johnston Island in the west central North Pacific on the 20th of September. The system tracked toward the west and increased in convection and organization over the next 24-hours. The upper-level outflow was initially restricted by an upper-level trough to the north of the system. The first advisory on Tropical Depression 02C was issued by CPHC at 211800Z. Satellite imagery indicated a low-level cyclonic circulation with spiral banding. This developed after the tropical cyclone had moved toward the west past the restricting influence of the upper-level trough to the north.

Over the next 18-hours, the amount of convection continued to increase. Upper-level outflow was unrestricted to the south and was becoming less restricted to the north, prompting the upgrade to Tropical Storm Peke (02C). During this time, Peke changed its track from westward to northwestward in response to a mid-level weakness in the subtropical ridge. It continued to intensify at a normal rate (Dvorak, 1984) and began to track more toward the north. CPHC upgraded the system to Hurricane Peke (02C) at 231800Z based on the formation of a banding-type eye, but Dvorak intensity post-analysis indicated that the system most probably did not reach hurricane intensity for another 6- to 12-hours. Peke continued to intensify and reached a first peak, of 85 kt (44 m/sec), at 250000Z.

Peke continued moving northward until 270600Z. After which time, it tracked toward the west-northwest in response to the strong mid-level flow around the subtropical ridge lying to the north of the system. CPHC issued their last advisory on Hurricane Peke (02C) at 271800Z September. It was approximately 30 nm (56 km) to the east of the dateline when JTWC issued its first warning (warning number 26) and redesignated the system as Typhoon Peke (02C) at 280000Z. Peke crossed the dateline at 280600Z. After having maintained a steady 75 kt (39 m/sec) intensity for over 36-hours, it began to re-intensify. Peke reached its second peak intensity (of 100 kt (51 m/sec)) between 290600Z and 291200Z, as upper-level outflow to the north improved.

Shortly afterward, JTWC was issuing warnings on three western North Pacific systems. Typhoon Ian (16W) was over 2000 nm (3704 km) to the west, and having little effect directly on Peke. About 1000 nm (1852 km) to the west of Peke, Tropical Storm June (18W) was beginning to organize (Figure 3-02C-1). Peke, together with Typhoon Ian (16W) and Tropical Storm June (18W), modified the environment and forced the subtropical ridge axis even further north to beyond 35 degrees North Latitude.

Earlier, as Peke crossed the dateline, it accelerated over a 48-hour period from near 7 kt (13 km/hr) forward speed to about 16 kt (30 km/hr). At that time, Peke began to entrain drier air into its central region. Satellite imagery at 291800Z indicated that a banding eye was present instead of an eye within a central dense overcast. Peke maintained its intensity and was still at 100 kt (51 m/sec) at 301200Z, when the system began to decelerate. At that time, recurvature was forecast along with rapid weakening due to strong westerly flow aloft. Peke became nearly quasi-stationary at 010600Z October, prior to recurvature. Within six hours, Peke was recurving toward the north-northeast and had steadily weakened from 100 kt (51 m/sec) at 301200Z September to 75 kt (39 m/sec) at 011200Z October. Over

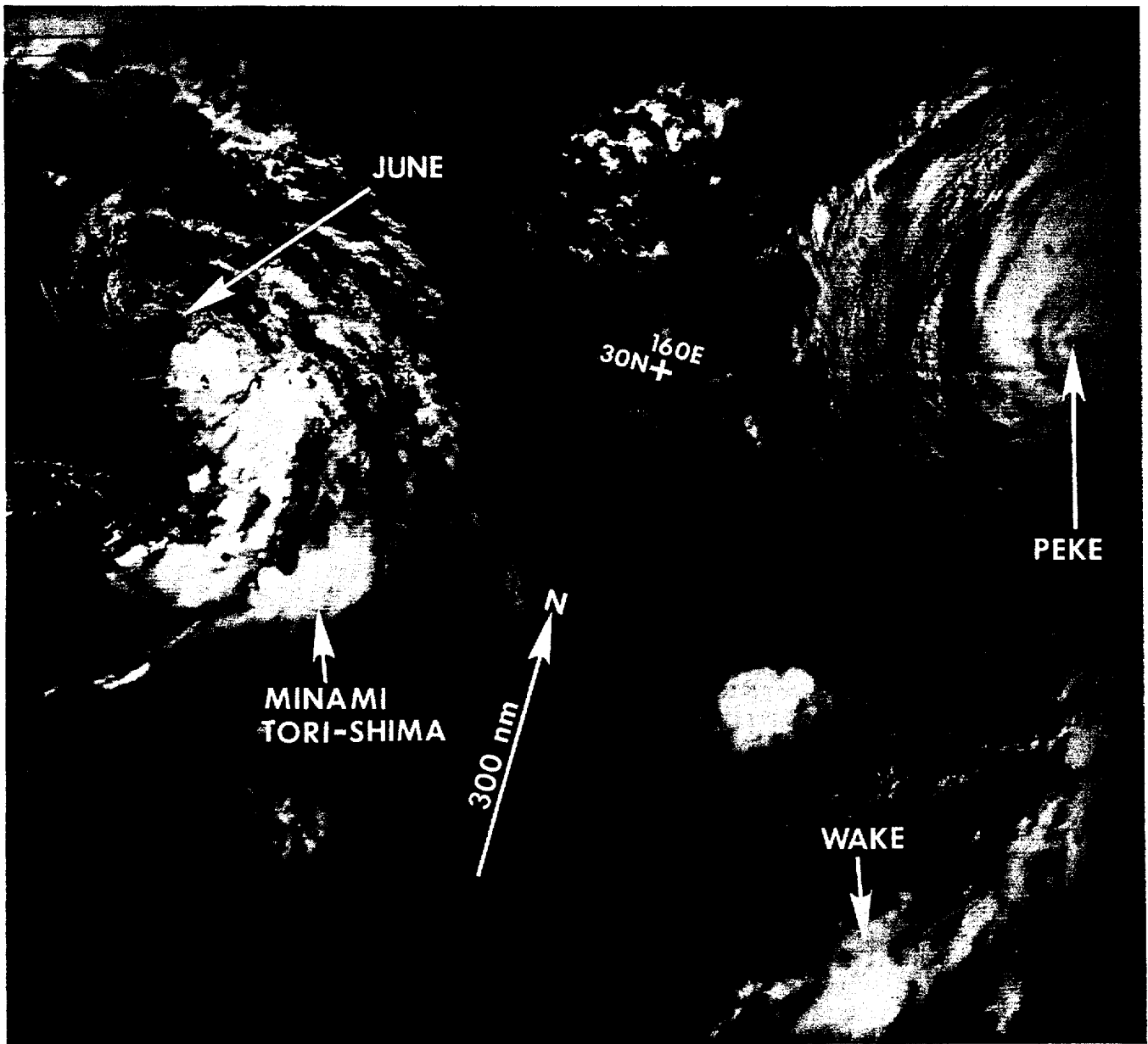


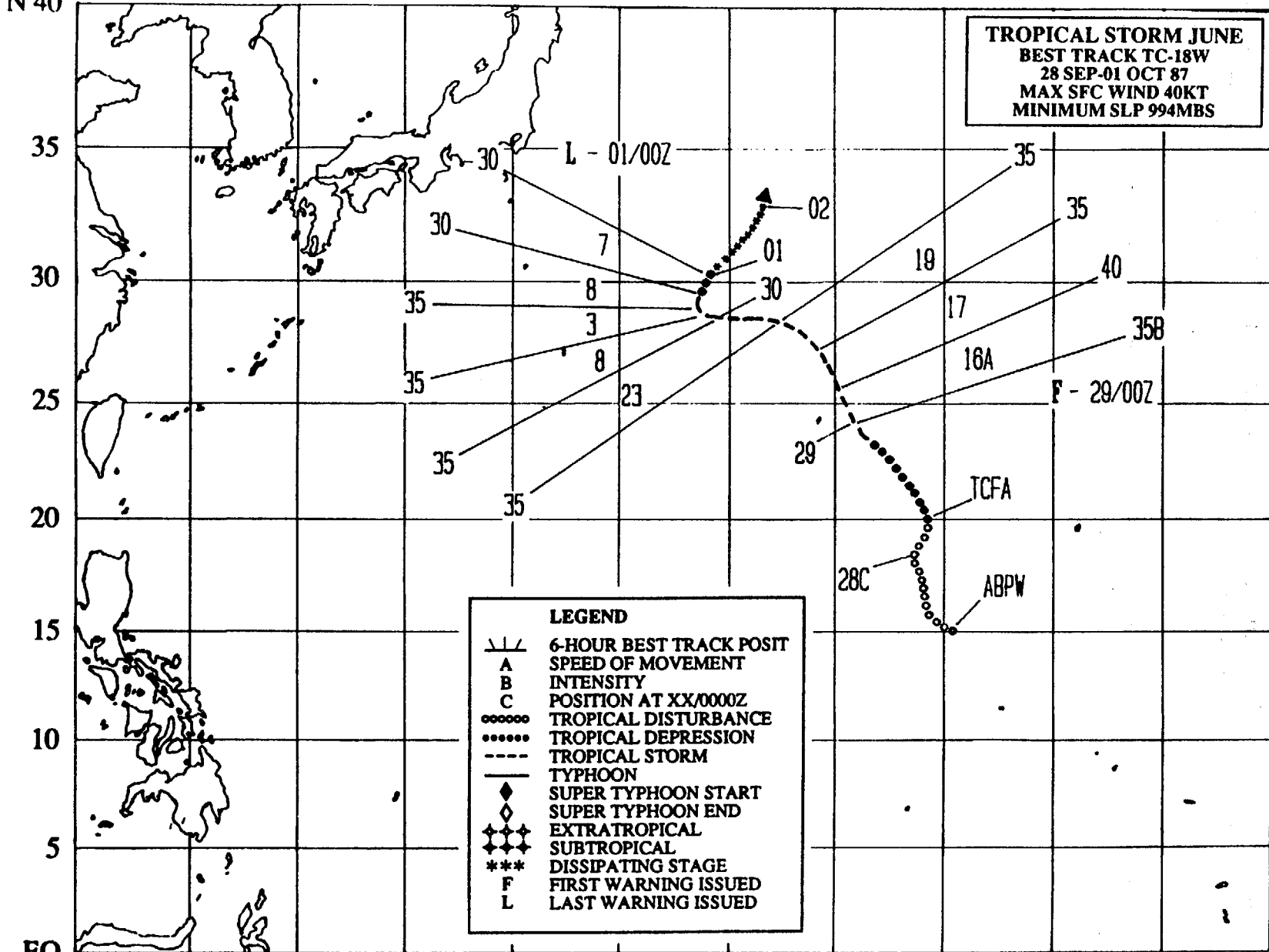
Figure 3-02C-1. Typhoon Peke (02C) with Tropical Storm June (18W) to the west (302243Z September DMSP infrared imagery).

the next day, Peke weakened even more, to 55 kt (28 m/sec), but instead of tracking toward the north-northeast, the low-level drifted toward the southeast, while the upper-level tracked toward the south-southeast in response to weak steering flow and increasing vertical wind shear. The last warning on Tropical Depression 02C was

issued by JTWC at 031200Z. The remnants of Peke moved erratically over the next three and one half days in response to weak steering flow, first tracking toward the east, then toward the northwest and finally back toward the southeast until it could no longer be identified on satellite imagery.

E 120 125 130 135 140 145 150 155 160 165 170 175 E
 N 40

TROPICAL STORM JUNE
BEST TRACK TC-18W
28 SEP-01 OCT 87
MAX SFC WIND 40KT
MINIMUM SLP 994MBS



LEGEND

- ||| 6-HOUR BEST TRACK POSIT
- A SPEED OF MOVEMENT
- B INTENSITY
- C POSITION AT XX/0000Z
- oooooo TROPICAL DISTURBANCE
- TROPICAL DEPRESSION
- TROPICAL STORM
- TYPHOON
- ◆ SUPER TYPHOON START
- ◇ SUPER TYPHOON END
- ◆◆◆◆ EXTRATROPICAL
- ◆◆◆◆ SUBTROPICAL
- *** DISSIPATING STAGE
- F FIRST WARNING ISSUED
- L LAST WARNING ISSUED

110

EQ

TROPICAL STORM JUNE (18W)

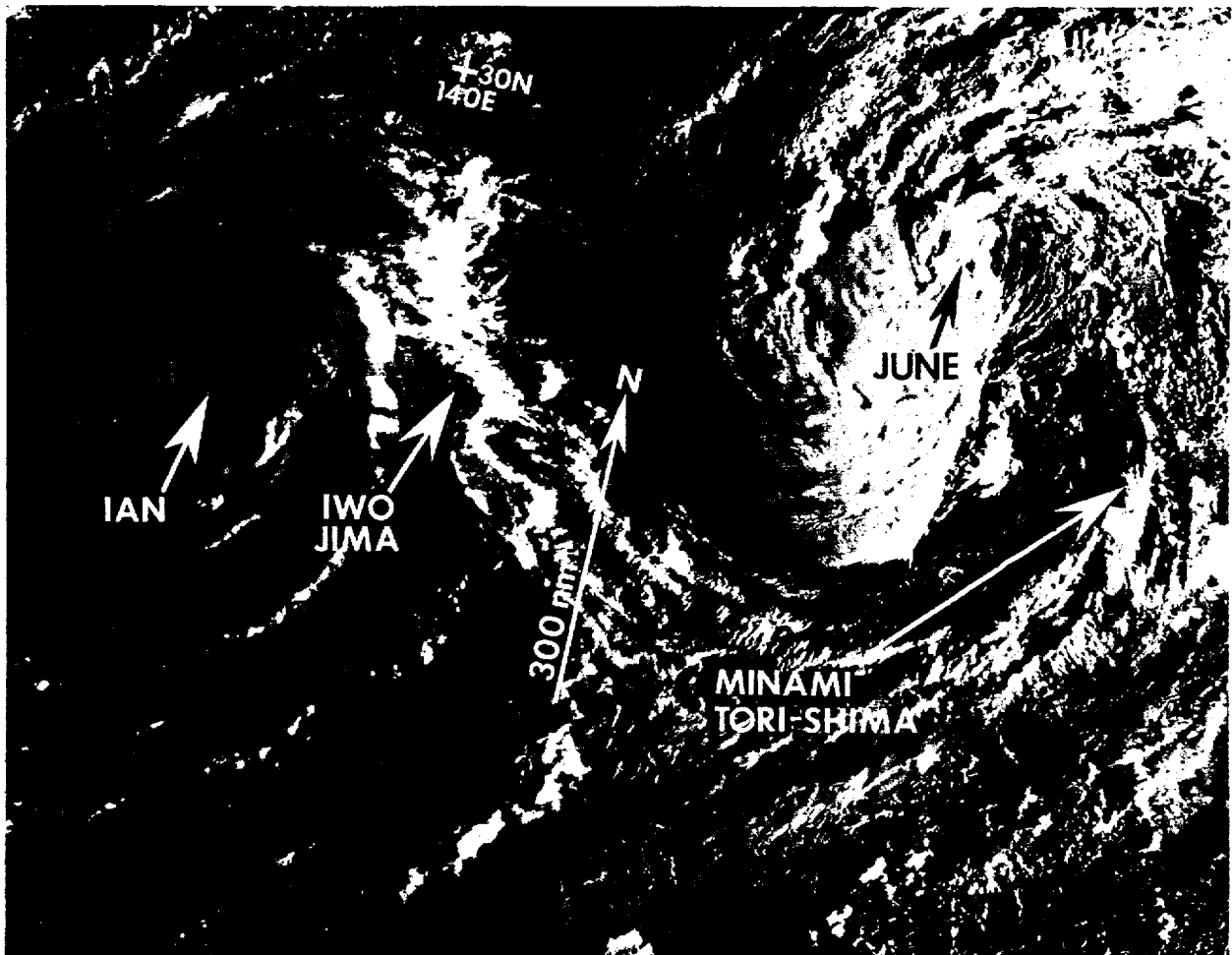
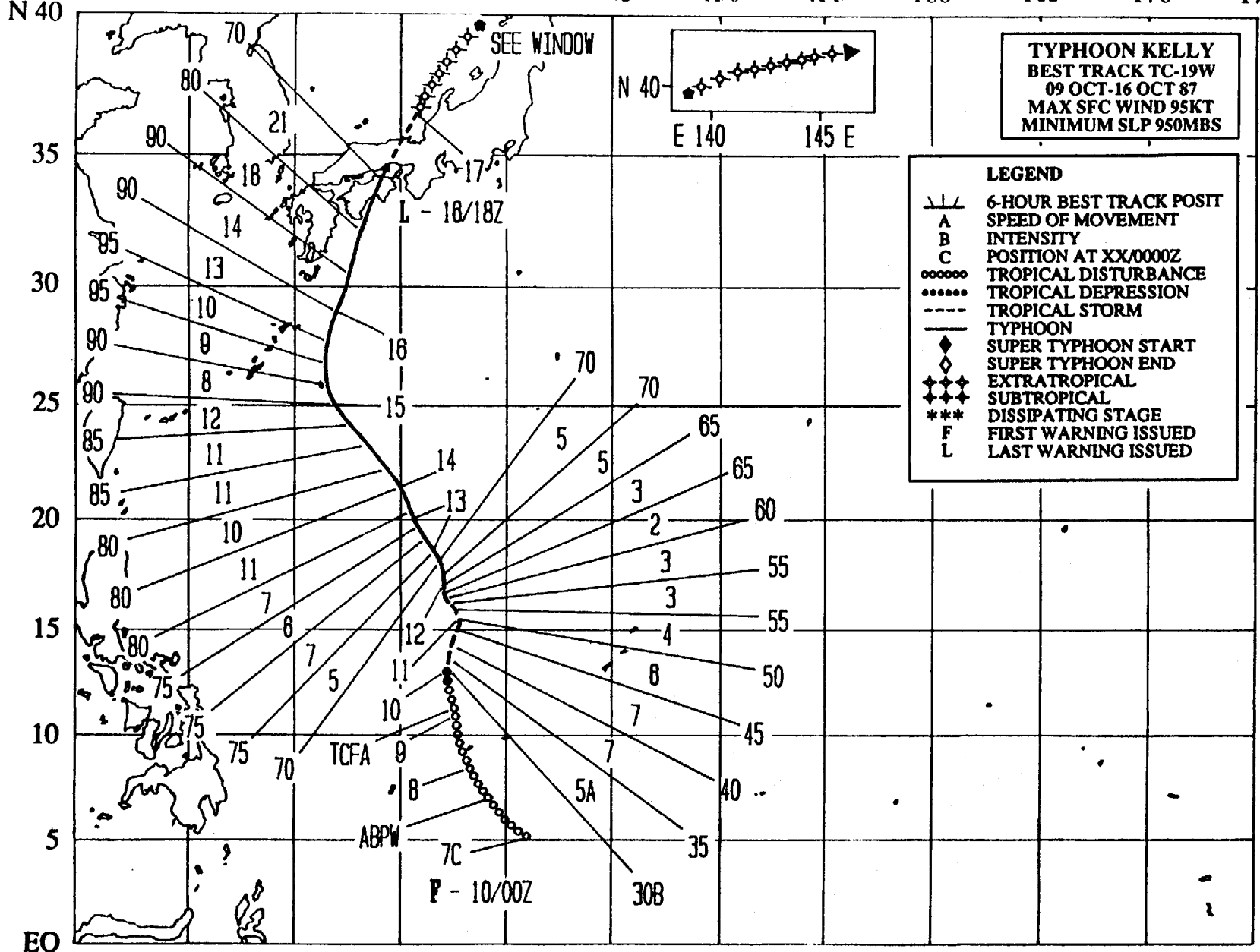


Figure 3-18-1. Tropical Storm June (18W) was the seventh and final tropical cyclone to occur in the western North Pacific during the month of September. It followed in the wake of Tropical Depression 17W. June was of significance due to the fact that, as it developed, two other tropical cyclones were also being warned on by JTWC. June struggled to develop for four days and was first noted as a suspect area on the Significant Tropical Weather Advisory (ABPWPGTW) on September 27th at 0600Z. At 280600Z, JTWC issued a Tropical Cyclone Formation Alert based on increased convective organization and satellite intensity estimates (Dvorak, 1984) of 25 kt (13 m/sec). During the next 18-hours, the convection associated with June increased significantly north of the partially exposed low-level circulation center. This, plus a satellite intensity analysis of 35 kt (18 m/sec), prompted the first warning, at 290000Z. Throughout its existence, June's upper-level outflow was restricted in the west quadrant due to the strength of Typhoon Ian's (16W) outflow. The final warning on June was issued on the 1st of October at 0000Z when the increased vertical wind shear finally stripped away the central cloudiness. The low-level remnants continued to track toward the northeast and were detected on satellite imagery until the 2nd of October. The above image shows June approximately 12-hours after reaching its peak intensity of 40 kt (21 m/sec) (292016Z September DMSP visual imagery).

E 120 125 130 135 140 145 150 155 160 165 170 175 E



TYPHOON KELLY (19W)

Typhoon Kelly was the first of two significant tropical cyclones to develop during the month of October. It moved steadily on a northward track, reaching its maximum intensity at the point of recurvature near 28 degrees North Latitude. Kelly made landfall on the Japanese island of Shikoku about 100 nm (185 km) southwest of Osaka with typhoon-force winds, then crossed west central Honshu, the main Japanese island, before moving into the Sea of Japan.

After an outbreak of three tropical cyclones in early September, an acimatological surface ridge developed in the low latitudes which proved to be unfavorable for tropical cyclones genesis for about six days. A similar occurrence took place during the first week of October with Typhoon Ian (16W), Tropical Storm June (18W) and Typhoon Peke (02C). The strong surface ridge was the primary synoptic feature in an area normally dominated by the monsoon trough. The existence of a low-latitude ridge during the height of the tropical cyclone season appeared to be a readjustment mechanism for the unusual northward displacement of the active monsoon trough to 25 degrees North Latitude associated with both multiple-storm outbreaks.

On 6 October cross-equatorial flow returned to the low latitudes from the southern Philippine Islands to the area south of the island of Pohnpei in the eastern Caroline Islands, allowing the monsoonal trough to re-establish itself along 5 degrees North Latitude. Moonlight visual satellite imagery on 7 October indicated a circulation was developing 190 nm (352 km) south of the island of Yap (Figure 3-19-1). The 071400Z Significant Tropical Weather Advisory (ABPW PGTW) mentioned the area and classified its potential for development into a significant tropical cyclone as fair, based on an initial satellite intensity

estimate (Dvorak, 1984) of 25 kt (13 m/sec) surface winds and supporting synoptic data.

Over the next 36-hours, the surface pressures at Yap and Koror (WMO 91408) were closely monitored for indications of possible development. Surface pressures at Yap dropped 1.5 mb per day, reaching a minimum of 1005 mb at 090600Z (see Figure 3-19-2).

Visual satellite imagery on 8 October indicated the low-level circulation center was displaced approximately 200 nm (370 km) south of the main convective band. As a result, satellite fixes at night, based only on infrared imagery, were unable to accurately locate the low-level center through the high cirrus shield.

A Tropical Cyclone Formation Alert was issued on the tropical disturbance at 090330Z, based on increased cirrus outflow and

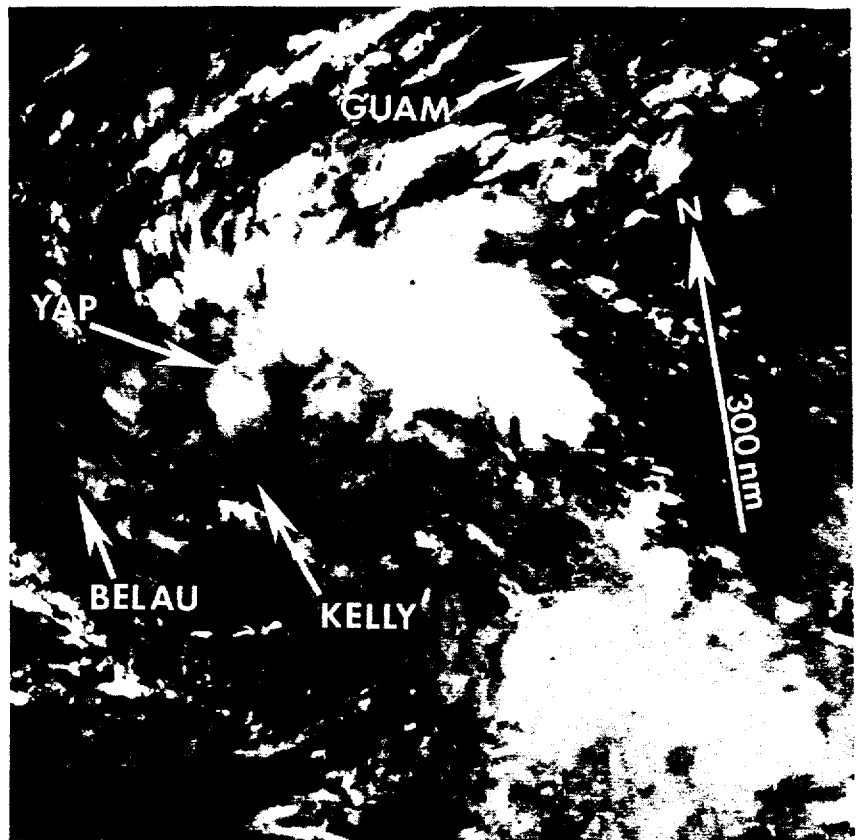


Figure 3-19-1. Moonlight visual imagery showing Typhoon Kelly at an early stage of development (071243Z October DMSP visual imagery).

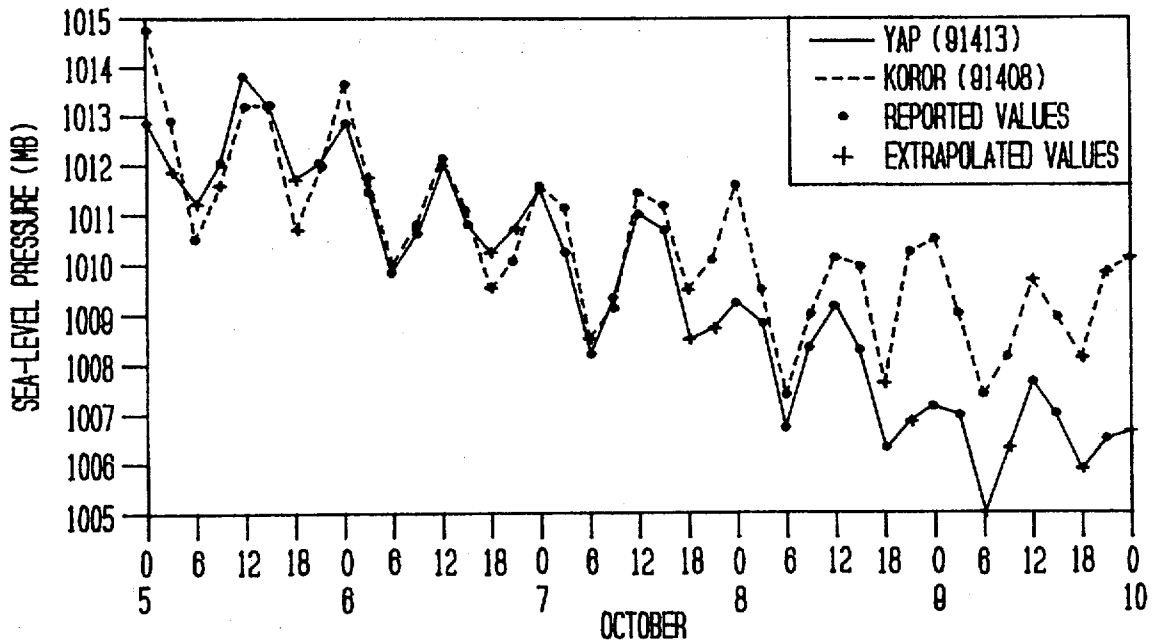


Figure 3-19-2. A plot of the surface pressures for Yap and Koror for the time period 050000Z to 100000Z October (missing values are extrapolated for continuity purposes). Although pressures were dropping at both stations, the lower surface pressures and more rapid falls at Yap indicated the low pressure center was passing close by.

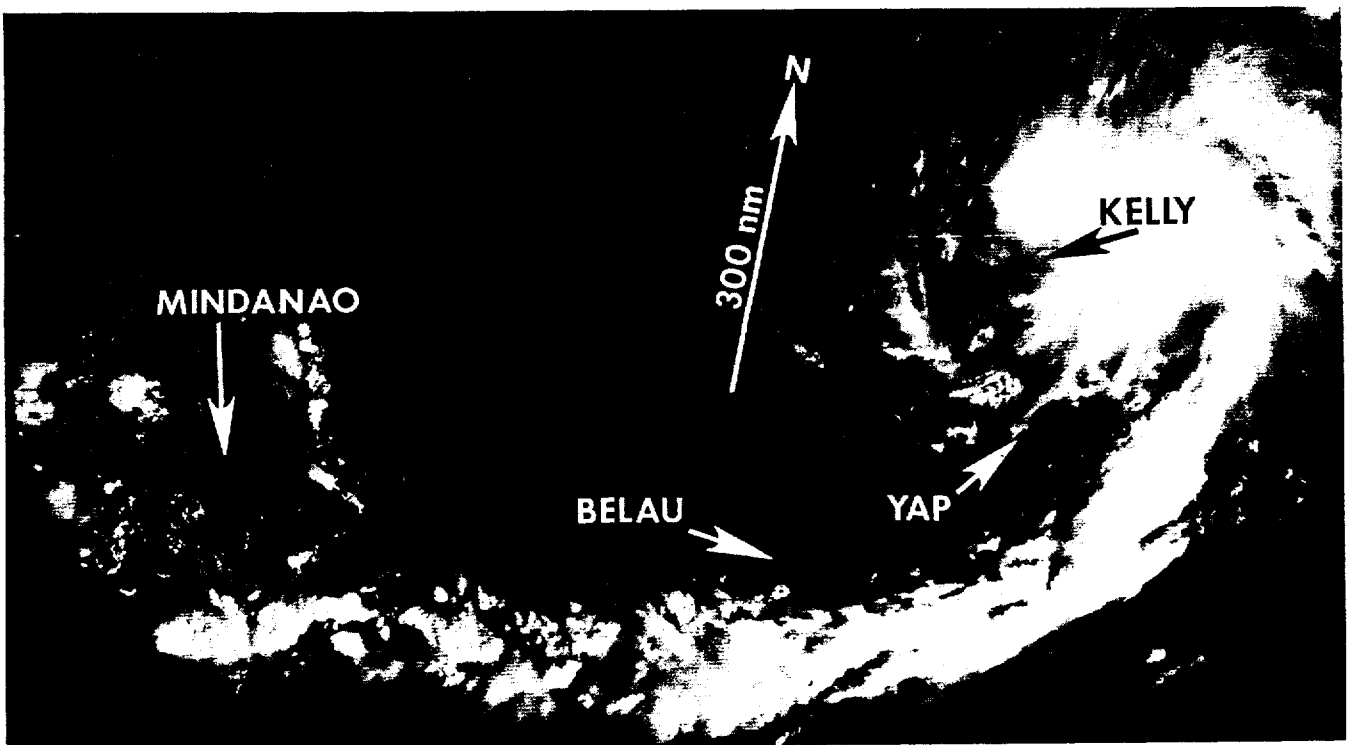


Figure 3-19-3. The low-level circulation center located west of the convective cloud mass is partially obscured by cirrus blow-off. A convective band south of Kelly identifies an area of intense convergence which extended as far west as the island of Mindanao (100043Z October DMSP visual imagery).

persistent convection around the exposed low-level circulation center. Satellite imagery over the next 24-hours showed a steady increase in the amount of convection within the cloud system. The first warning on Tropical Depression 19W was issued at 100000Z, supported by a satellite intensity estimate of 30 kt (15 m/sec). At the time of the first warning, the low-level center was still located about 60 nm (111 km) west of the dense convection (see Figure 3-19-3).

A 35 kt (18 m/sec) ship report 30 nm (56 km) north-northwest of the circulation center at 101200Z supported the earlier upgrade to tropical storm and previous satellite estimates that Kelly had attained tropical storm intensity. The low-level center position remained 95 nm (176 km) southwest of the upper-level circulation center at that time. This separation between the low- and upper-level positions

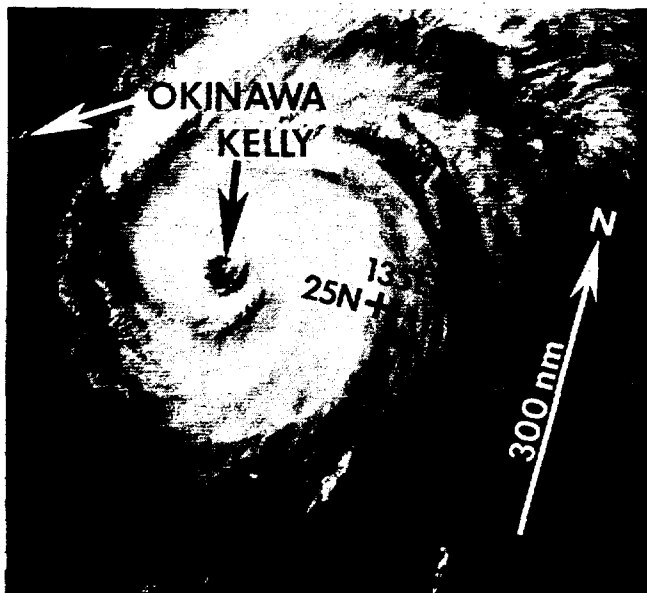


Figure 3-19-4. Typhoon Kelly approximately twelve hours prior to its reaching its maximum intensity of 95 kt (49 m/sec) (150042Z October DMSP visual imagery).

resulted in initial position relocations on the 101200Z and 101800Z warnings.

Once the low- and upper-level centers became aligned on the 11th, Kelly slowly intensified. Minimal typhoon intensity of 65 kt (33 m/sec) was reached at 120000Z. Kelly's intensity peaked at 95 kt (49 m/sec) near the point of

recurvature at 151200Z (Figure 3-19-4).

By that time, Typhoon Kelly posed a serious threat to Japan. As it began to slow its forward speed and recurve near the 28th parallel, the forecast question was whether the system would continue to track northward across Japan or recurve south of Japan. Synoptic data at 150000Z indicated the upper-level westerly winds south of Japan were nearly zonal, which would tend to steer Kelly toward the east-northeast, favoring the south of Honshu scenario. This reasoning prevailed and recurvature south of Japan was forecast. By 160000Z however, a mid-level long-wave trough, anchored near the Yellow Sea, deepened as an intense short wave came in phase with the trough axis. Consequently, the steering flow ahead of the trough shifted from westerly to south-southwesterly and Kelly continued its course across Japan instead of recurving sharply northeastward.

Typhoon Kelly weakened only slightly as it began to assume extratropical characteristics on the 16th. Synoptic reports indicated Kelly did not dissipate as rapidly as implied from satellite imagery. Upper-air reports at Shiono, Japan (WMO 47778) revealed that Kelly still packed winds of 95 kt (49 m/sec) at the 850 mb level at 161200Z.

Eventually, Typhoon Kelly made landfall on the southern coast of the island of Shikoku. At least 13,000 homes were flooded and another 30 were badly damaged by mudslides triggered by as much as 20 inches (51 cm) of rain. Wind gusts were reported as high as 120 kt (62 m/sec) as typhoon-force winds battered southern Japan. At least eight people were killed.

After crossing the islands of Shikoku and Honshu, Kelly moved offshore and became extratropical over the Sea of Japan. Later, Misawa Air Base (WMO 47580), located near the northern tip of Honshu, reported maximum surface winds of 32 kt (16 m/sec) and a surface pressure of 985 mb as the extratropical low passed between the islands of Honshu and Hokkaido at 171200Z. The residual circulation of Typhoon Kelly was no longer visible on satellite imagery after 180300Z.

SUPER TYPHOON LYNN (20W)

Super Typhoon Lynn was the third tropical cyclone of 1987 to produce maximum sustained surface winds of 140 kt (72 m/sec) with gusts to 170 kt (87 m/sec) and the second to attain an estimated minimum sea-level pressure (MSLP) of 898 mb (only Super Typhoons Betty (09W) and Nina (22W) were lower with a MSLP of 891 mb). It was also the fifth super typhoon of the year. Lynn, during its latter stages, also had a devastating impact on Taiwan and caused some concern in the Hong Kong area, as well.

Lynn began as a broad, poorly organized area of convection in the monsoon trough about 200 nm (370 km) north-northeast of Kwajalein Atoll in the Marshall Islands. After the convection had persisted for 24-hours, it was added as a new suspect area to the Significant Tropical Weather Advisory (ABPW

PGTW) at 150600Z. Maximum sustained surface winds were estimated at 15 to 20 kt (8 to 10 m/sec); the MSLP was estimated to be 1008 mb. Over the next 18-hours, upper-level outflow and the amount of convection increased significantly as the MSLP decreased to 1001 mb. For these reasons, a Tropical Cyclone Formation Alert was issued at 160030Z, when the system was located about 360 nm (667 km) north-northwest of the island of Pohnpei in the eastern Caroline Islands. Six hours later at 160600Z, the first warning on Tropical Storm Lynn (20W) was issued, based on the satellite intensity estimate (Dvorak, 1984) of 35 kt (18 m/sec). Until 171800Z, Lynn had been moving toward the west along the southern periphery of the subtropical ridge. Before reaching tropical storm intensity, Lynn had been moving at speeds in excess of 20 kt (37 km/hr). But as it began to intensify, it decelerated. By 161200Z,

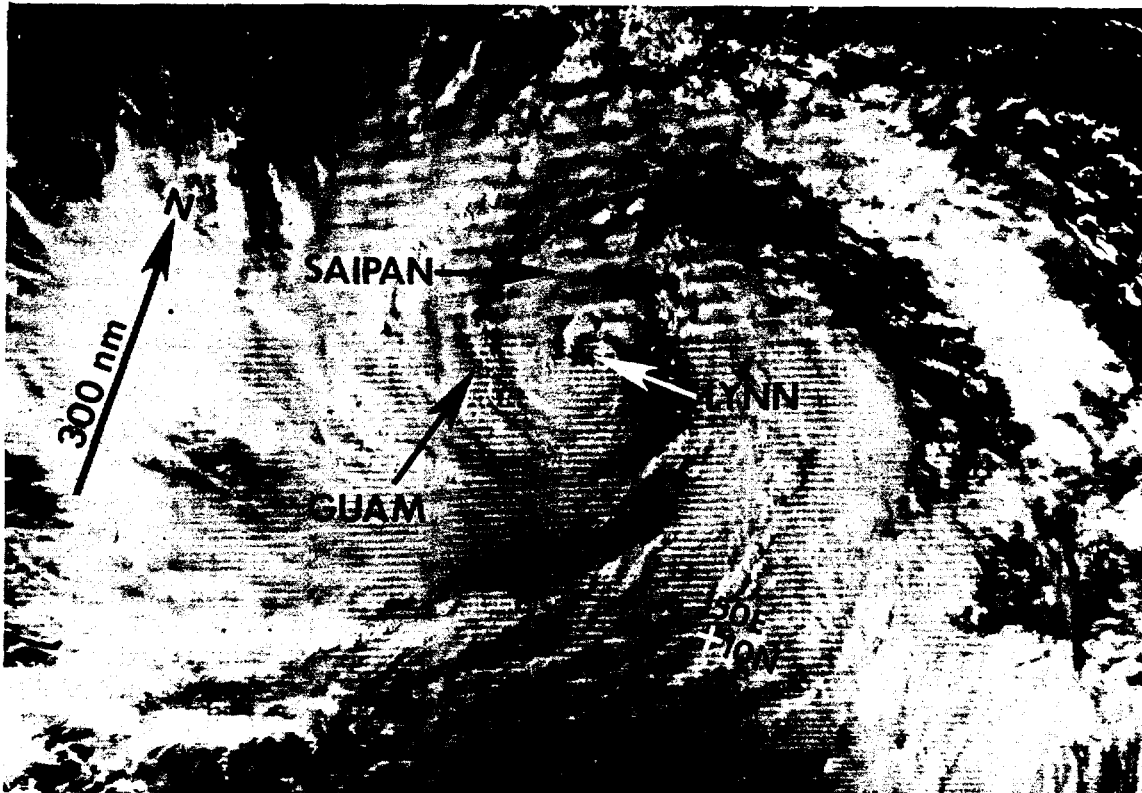


Figure 3-20-1. Tropical Storm Lynn (20W), shortly before being upgraded to typhoon intensity (180528Z October NOAA visual imagery).

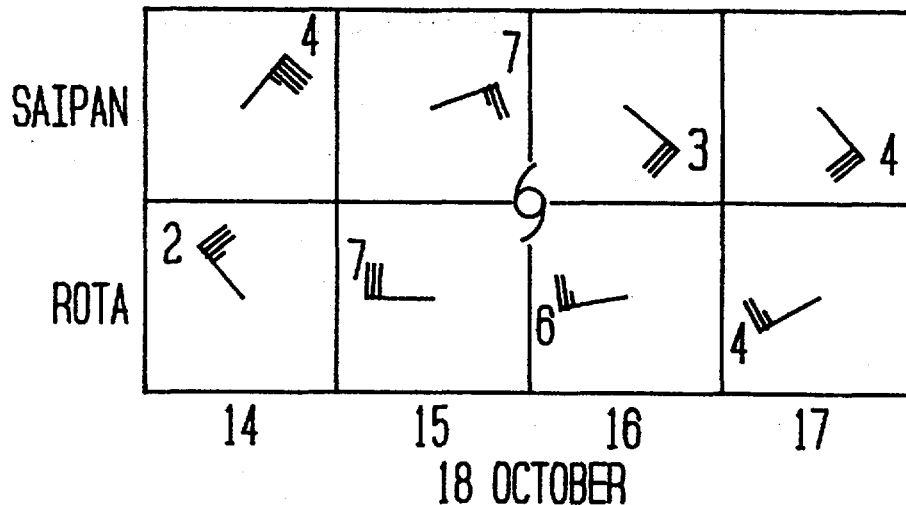


Figure 3-20-2. HAN/DAR observations for the islands of Saipan and Rota. These observations illustrate the closest point of approach of Typhoon Lynn to Saipan and Rota was between 181500Z and 181600Z.

Lynn was moving at a speed of only 6 kt (11 km/hr). At 180600Z, it was upgraded to typhoon status when visual and infrared satellite imagery, plus radar observations from Andersen Air Force Base on Guam, indicated Lynn had formed an eye 20 nm (37 km) in diameter (see Figure 3-20-1). Satellite analysis at that time estimated Lynn's intensity at 65 kt (33 m/sec). (Post-analysis on the system indicated that Lynn was most probably a typhoon at 180000Z.)

As it intensified, Typhoon Lynn was starting to track toward the west-northwest, away from Guam towards the island of Saipan. Consequently, JTWC amended its 180600Z warning which had forecast a more westward track. At 181200Z, Typhoon Lynn made its closest point of approach (CPA) to Guam when it tracked 75 nm (139 km) to the northeast of the island. Maximum sustained surface winds recorded on the island were 36 kt (19 m/sec) with a peak gust of 57 kt (29 m/sec) at Agana (WMO 91212). A maximum rainfall accumulation of 6.08 inches (154.4 mm) was recorded at Andersen Air Force Base (WMO 91218).

Lynn's approach had a profound effect on the island of Guam. Apra Harbor on the west side of Guam was closed after four U.S.

Navy ships sortied to open waters. Military airfields evacuated aircraft and secured some aircraft in hangars. All commercial flights to and from Guam were cancelled on 18 October. Most villages on Guam reported flooding in low-lying areas, broken windows, and power and water outages. The power outages were caused mainly by the high winds which knocked vegetation onto power lines, and required several days for Guam Power Authority to repair. Perhaps the most serious damage from Typhoon Lynn was to local agriculture.

At 181500Z, Lynn made its CPA to the island of Tinian - 15 nm (28 km) southwest of the island. The automatic weather station observations at Rota, 53 nm (98 km) south-southwest of Tinian, and at Saipan, 5 nm (9 km) to the northeast of Tinian, for 181500Z and 181600Z recorded Lynn's passage (see Figure 3-20-2). Maximum sustained surface winds of 45 kt (23 m/sec), with a peak gust of 65 kt (33 m/sec) were recorded on Saipan. All commercial airline flights to and from Saipan were cancelled. Schools and government offices on Saipan were closed on 19 and 20 October. The islands of Saipan and Rota both experienced island-wide power outages on the evening of 18 October.

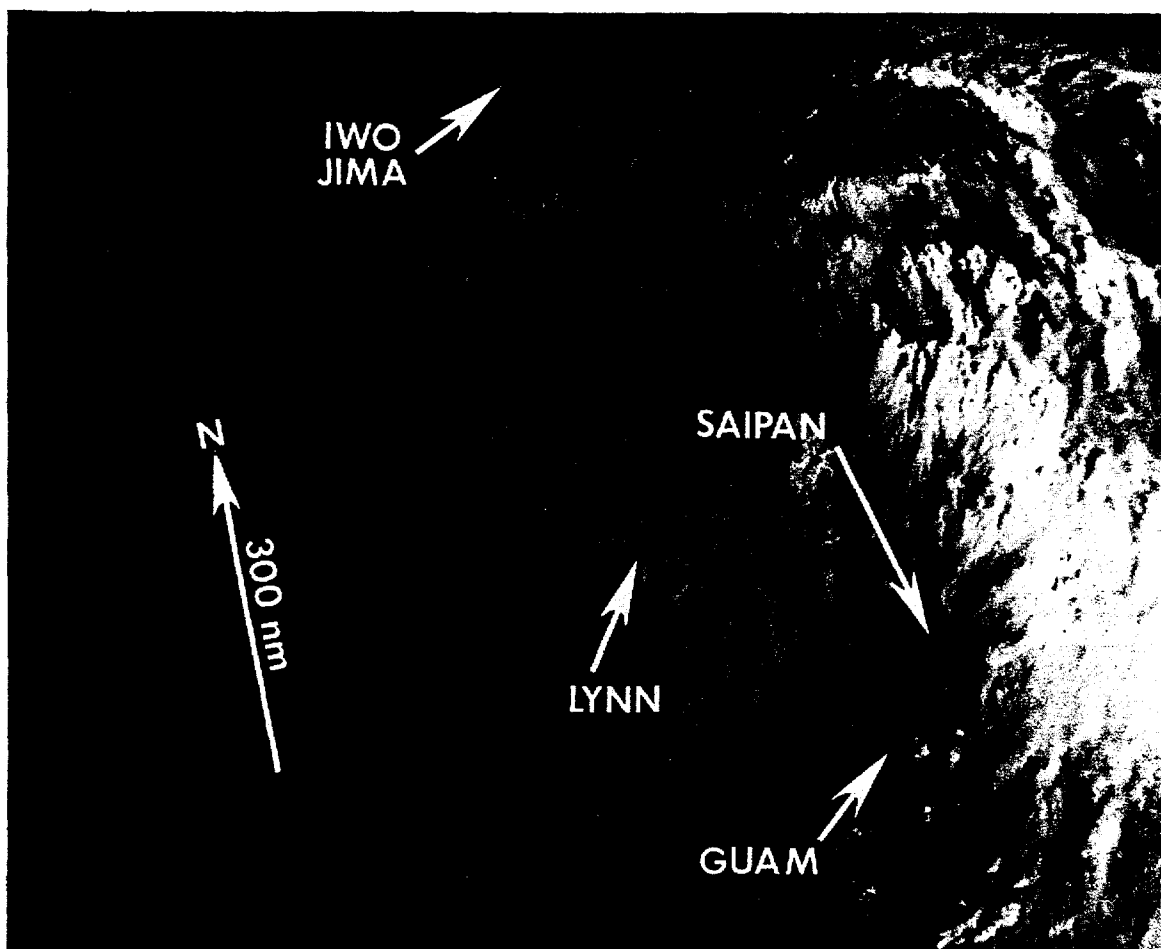


Figure 3-20-3. Super Typhoon Lynn at its maximum intensity of 140 kt (72 m/sec) (192240Z October NOAA visual imagery).

Once past the Marianas, Lynn intensified rapidly from 80 kt (41 m/sec) to its peak intensity of 140 kt (72 m/sec), reaching super typhoon intensity (130 kt or 67 m/sec) shortly after 191800Z. Super Typhoon Lynn maintained its 140 kt (72 m/sec) intensity (Figure 3-20-3) until 210000Z.

As Lynn began weakening after 210000Z, its track became westerly. Prior to that time, the forecast track had been west-northwesterly to northwesterly. Numerical guidance provided by the One-Way Interactive Tropical Cyclone Model (OTCM) appeared to be accurate. The 210600Z warning echoed this guidance, however Lynn persisted on its westward track. A closer look at the lower-tropospheric and deep-layer mean flow fields

north of the typhoon provided a clue as to why Lynn was not behaving as expected. Because of Lynn's synoptic size cyclonic circulation, the integrated effect on the low- and mid-level steering flow was to eliminate the narrow subtropical ridge. Perhaps, OTCM interpreted the large-scale storm-induced circulation as being the synoptic steering flow and therefore, did not detect the narrow subtropical ridge. In contrast, Lynn was large enough to be resolved by the Navy Operational Global Atmospheric Prediction System (NOGAPS) and European Center for Medium-Range Weather Forecasting (ECMWF) numerical models, which in turn provided more accurate forecast guidance. The next warning (number 22 at 211200Z) put the forecast back "on track" and OTCM became the less-favored alternate scenario.

A close encounter by a merchant vessel on 22 October provided testimony to the fury of the typhoon. Excerpts from the ship's log include:

"Sea and swell were of height and steepness that we couldn't turn around anymore ... Seas are approximately 2 1/2 times the bridge height and breaking all around us. At 1000 we recorded the lowest barometric pressure of 969 HPA", (approximately 75 nm (139 km) from the center of Typhoon Lynn, at that time). "During passage of "Lynn" visibility was reduced to 000.0 mtr. Wind above comprehension ... our ears on the bridge were popping due to pressure change with pitching of vessel."

At 240000Z, Lynn was tracking through the Luzon Strait, moving toward the northwest. From 24 through 26 October, it devastated portions of Taiwan (Figure 3-20-4). The island received high winds because of the strong pressure gradient between Lynn's low central pressure and the large high pressure area over mainland China. These high winds, caused rapid orographic lifting along the steep mountains of Taiwan, producing torrential precipitation. Although the center of Lynn passed 110 nm (204 km) to the southwest of Taiwan, it produced heavy weather over the northernmost parts of the island. News services reported 68 inches (173 cm) of rainfall on the capital city of Taipei from 24 to 26 October! In Taipei, torrential rainshowers caused landslides that smashed houses and killed 14 people. Over 2,200 people were stranded by floodwaters from

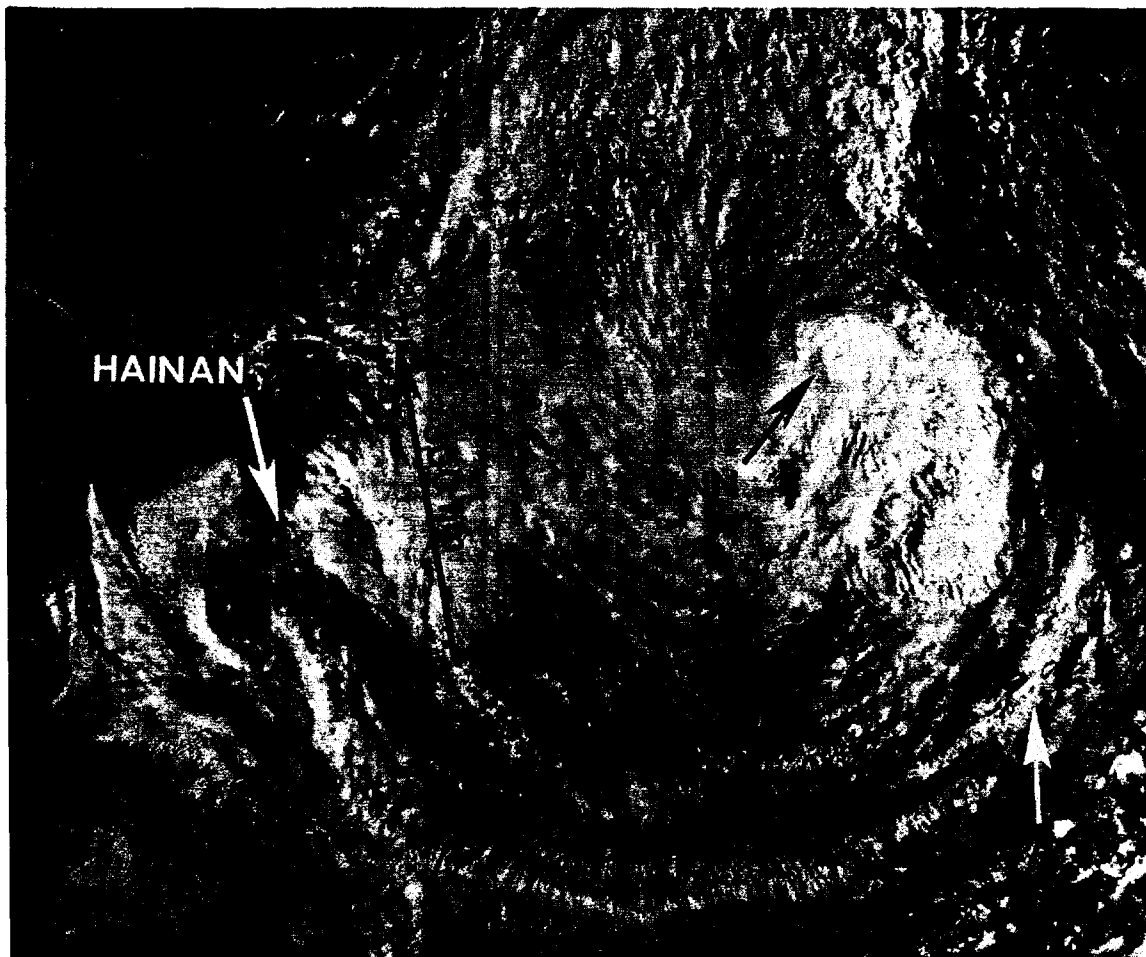


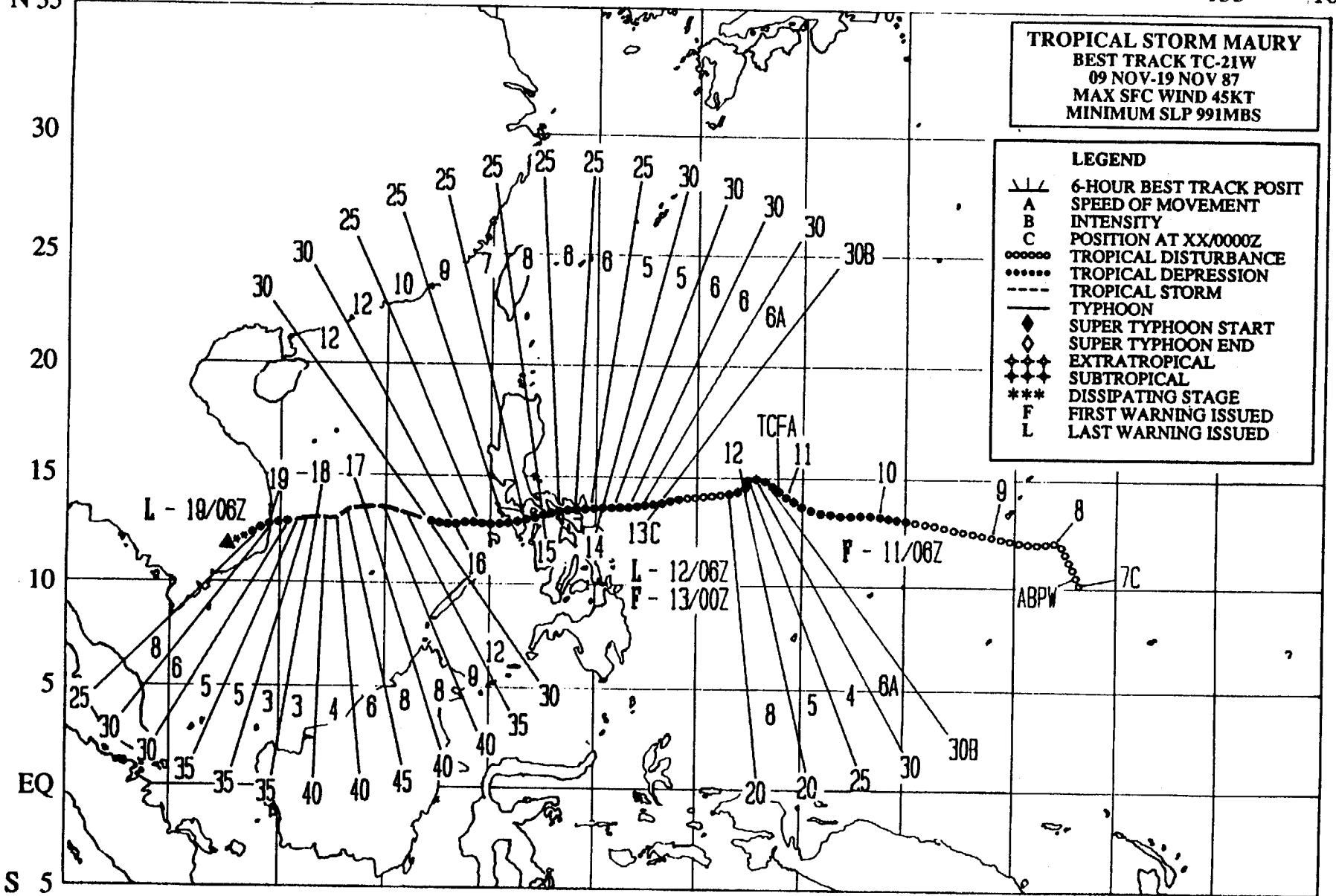
Figure 3-20-4. Tropical Storm Lynn during its rapid weakening phase (250013Z October NOAA visual imagery).

the Keelung River in Taipei making travel impossible. The Central Weather Bureau in Taipei reported 84 kt (43 m/sec) maximum sustained surface winds on 24 October and 61 kt (31 m/sec) maximum sustained surface winds on 25 October. The port city of Keelung reported over five million dollars worth of damage from Lynn. Lynn created 20 ft (6.1 meter) high waves at Hengchun on the extreme southern tip of Taiwan and nine children were swept away. The result of Lynn's passage was Taiwan's worst flooding in 40 years; 42 people perished and 18 were reported missing.

Visual and infrared satellite imagery at 260300Z, indicated that Lynn was being sheared apart. Subsequent satellite imagery showed the low-level circulation center moving

toward the west-southwest away from the convective mass. At 270000Z, the final warning was issued on Tropical Depression 20W (Lynn). Although the tropical cyclone had lost its central convection, the remaining low-level circulation center still had an impact on the Hong Kong area. The wind speeds and precipitation amounts the Hong Kong area received were higher than expected. The strong pressure gradient between the residual low offshore and the high over mainland China fostered gales along the south coast. The Hong Kong (WMO 45005) 280000Z upper-air sounding revealed maximum winds of 55 kt (28 m/sec) from the east-southeast, at 900 and 850 mb. The low tracked south of Hong Kong, into the Pearl River Estuary and eventually dissipated over land.

E 100 105 110 115 120 125 130 135 140 145 150 155 160 E



122

S 5

TROPICAL STORM MAURY (21W)

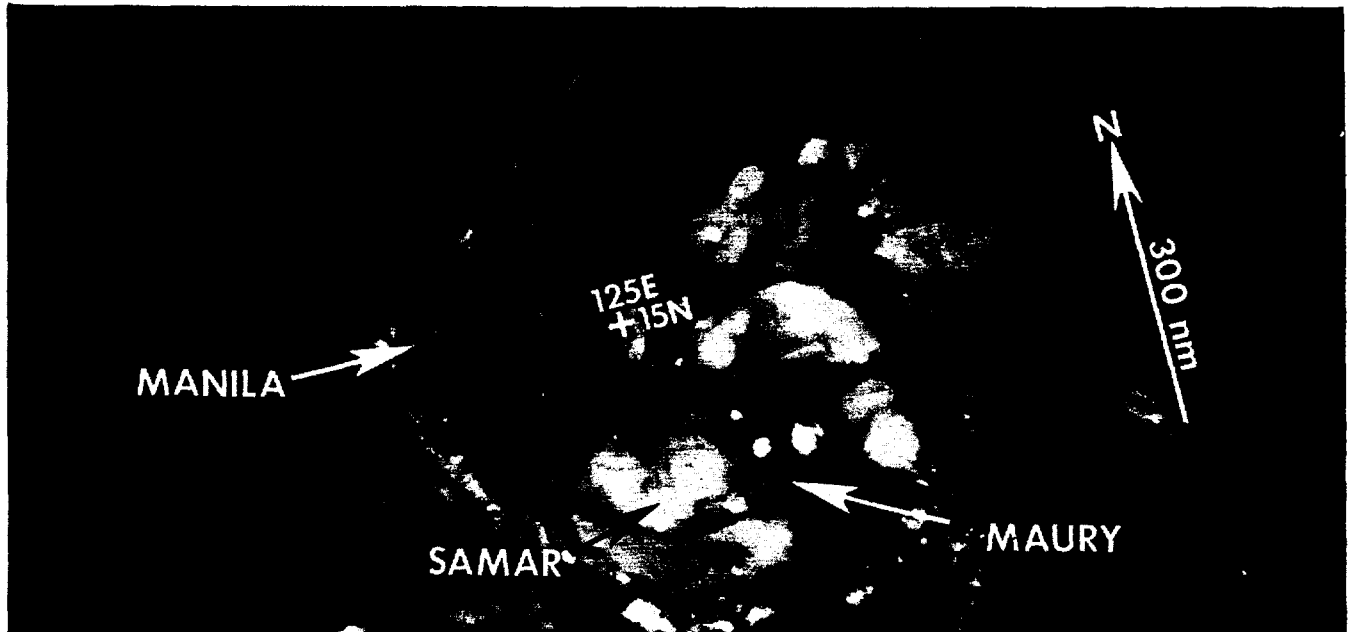
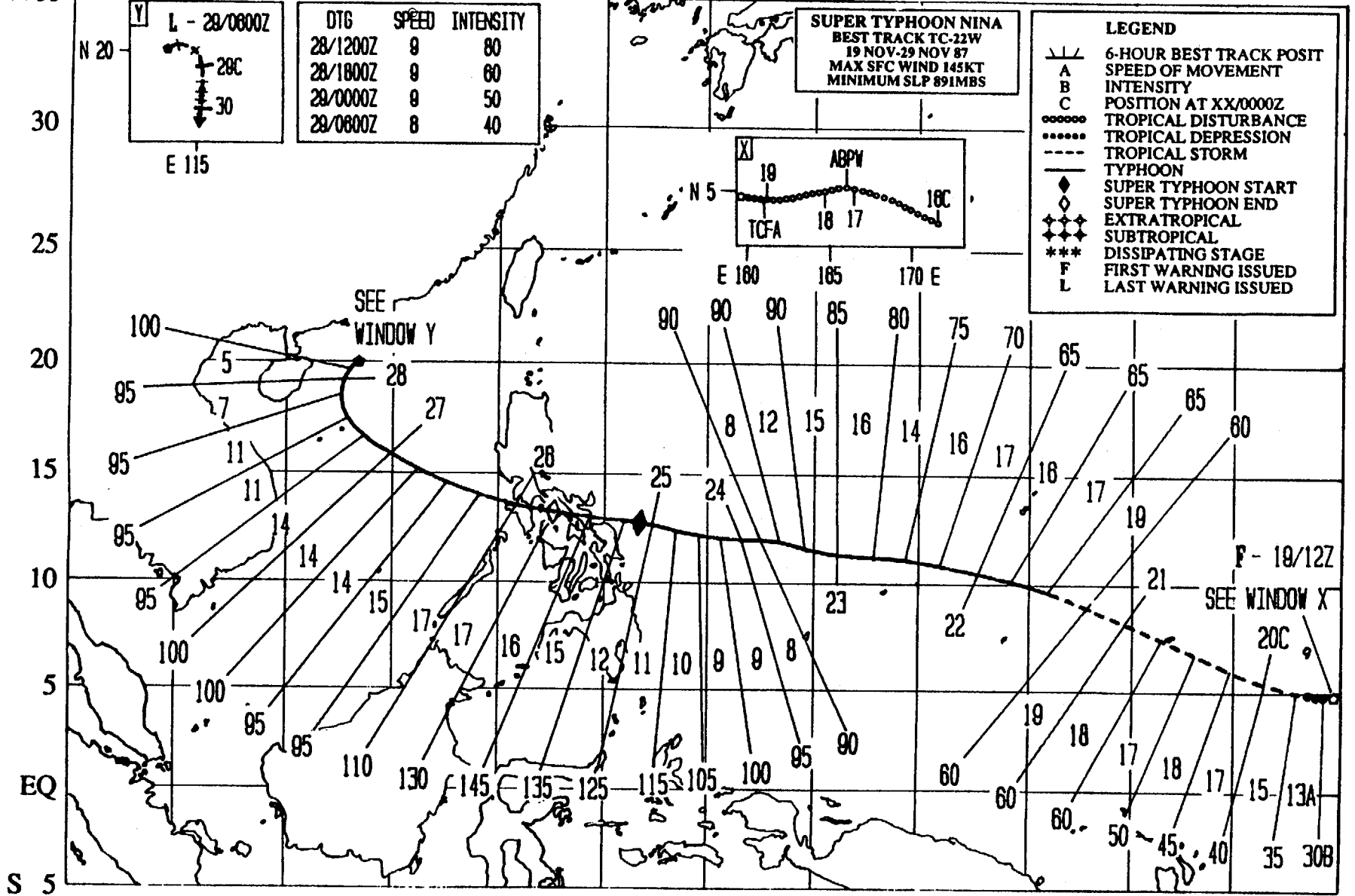


Figure 3-21-1. Tropical Storm Maury was a relatively weak, but persistent, tropical cyclone that tracked westward across the Philippine and South China Seas. It was the first of three significant tropical cyclones to form in November and the second system of the year to regenerate over water. Tropical Storm Maury formed in early November in the western North Pacific near-equatorial trough about 300 nm (556 km) to the southeast of Guam. It was first detected as an area of deep convection with a well-defined, low-level circulation center but a poor upper-level outflow and was first mentioned on the Significant Tropical Weather Advisory (ABPW PGTW) at 070600Z. Due to unfavorable vertical shear, the system appeared to have a poor chance for further development and showed little sign of intensification over the next three days. However, the central convection did increase. At 110130Z, a Tropical Cyclone Formation Alert (TCFA) was issued. The first warning on Tropical Depression 21W followed at 110600Z, based upon the presence of a central dense overcast and satellite intensity estimates (Dvorak, 1984) of 30 kt (15 m/sec). Tropical Depression 21W maintained its organization and convection over the next 6- to 9-hours, but began to slow and weaken, as an eastward-moving, low- to mid-level trough passed to the north. At 120000Z, JTWC issued a final warning, but continued to monitor the remnants for possible regeneration. With the trough in the polar westerlies displaced to the east, the convection in the remnants of Tropical Depression 21W flared-up, prompting the issuance of a second TCFA at 130330Z. Almost immediately, an abbreviated warning (the first of the year) was issued (at 130530Z) as the cloud system gained in organization. Over the next 12-hours, the regenerated Tropical Depression 21W maintained its organization, but remained below tropical storm intensity (see above image). By 131800Z, as it approached the Philippine Islands, Tropical Depression 21W showed signs of becoming less organized, as the central convection diminished. Prior to Tropical Depression 21W crossing the Philippine Islands, JTWC altered its forecast philosophy from 'dissipating over land', to 'regeneration' in the South China Sea. As Tropical Depression 21W entered the South China Sea, the deep convection increased significantly. Dvorak satellite intensity analysis at 161200Z estimated maximum surface winds of 35 kt (18 m/sec), prompting JTWC to upgrade Tropical Depression 21W to Tropical Storm Maury (21W). Maury tracked westward across the South China Sea and reached the maximum intensity of 45 kt (23 m/sec) at 170600Z. Later, it made landfall on the southeast coast of Vietnam 25 nm (46 km) north of Cam Ranh Bay at 190400Z. The final warning was issued at 190600Z as Maury dissipated over land. No reports of severe damage or loss of life were received (131009Z November DMSR infrared imagery).

E 100 105 110 115 120 125 130 135 140 145 150 155 160 E



124

SUPER TYPHOON NINA (22W)

Super Typhoon Nina was the most intense and most destructive tropical cyclone to develop in the western North Pacific in 1987. During its track toward the west, it devastated the Truk Atoll in the eastern Caroline Islands, decimated the north central Philippine Islands and then executed a final dramatic loop in the South China Sea south of Hong Kong. Nina was the second of three significant tropical cyclones to develop during November.

Nina developed in low latitudes just west of the dateline. At 150000Z, satellite intensity analysis (Dvorak, 1984) estimated a cloud system center had maximum sustained surface winds of 25 kt (13 m/sec). For two days this disturbance showed marked diurnal fluctuations in convection. It was first mentioned on the 170600Z Significant Tropical Weather Advisory (ABPW PGTW) as a system with fair potential to develop into a significant tropical cyclone. The system displayed good upper-level outflow and increasing convection over a broad area.

A Tropical Cyclone Formation Alert was issued at 190100Z as deep convection consolidated in the center of the tropical disturbance. Synoptically, the system appeared to be well-established in the low levels up to 400 mb (Figure 3-22-1) with 25 to 30 kt (13 to 15 m/sec) easterlies aloft. With speed and directional divergence aloft, Nina continued its rapid organization. At 191200Z, the first warning was issued on Tropical Depression 22W. By that time, Nina had formed a curved band of convection. Satellite imagery (Figure 3-22-2) suggested unrestricted upper-level outflow over the system; however, the upper-level rawinsonde reports showed that the anticyclonic circulation (at 200 mb) was displaced to the east of the center of cirrus outflow (Figure 3-22-3).

At the time of the first warning, working plots of satellite fix positions indicated Nina was slowing down its west-northwestward movement. (To the contrary, post-analysis revealed that Nina did not slow down while intensifying but actually accelerated slightly.

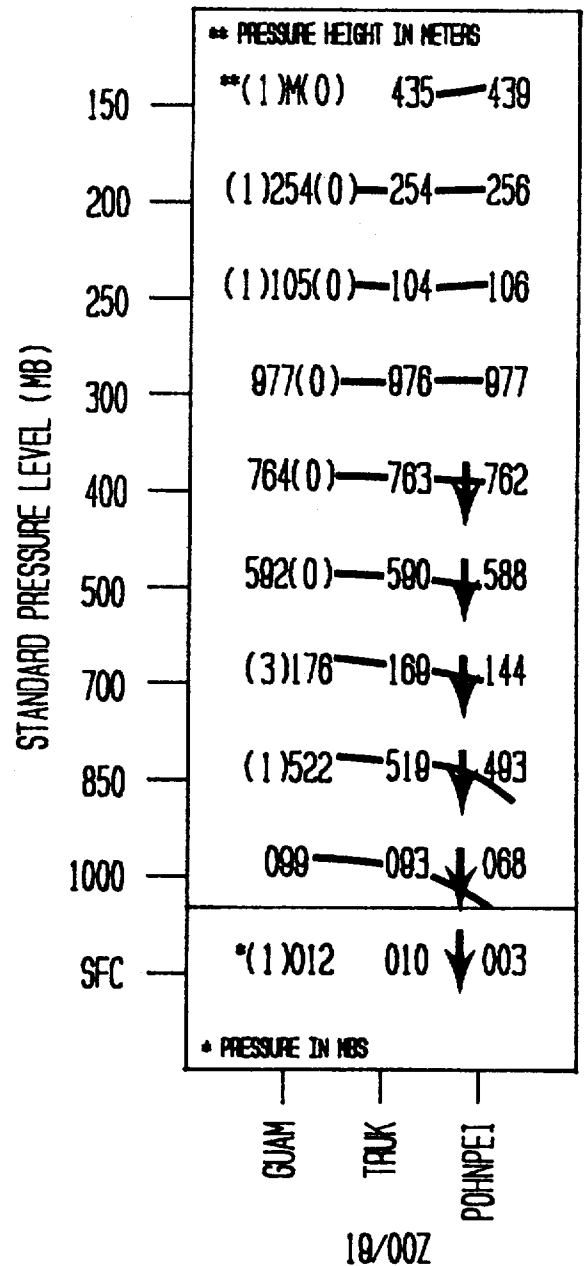


Figure 3-22-1. Heights of the standard pressure levels and surface pressure at Pohnpei (WMO 91348), Truk (WMO 91334) and Guam (WMO 91217) at 190000Z. At this time, Nina was 230 nm (426 km) southeast of the island of Pohnpei. In comparison with Truk and Guam, the lower heights at Pohnpei (WMO 91348) at the 400 mb level and below are due to the approaching tropical cyclone.

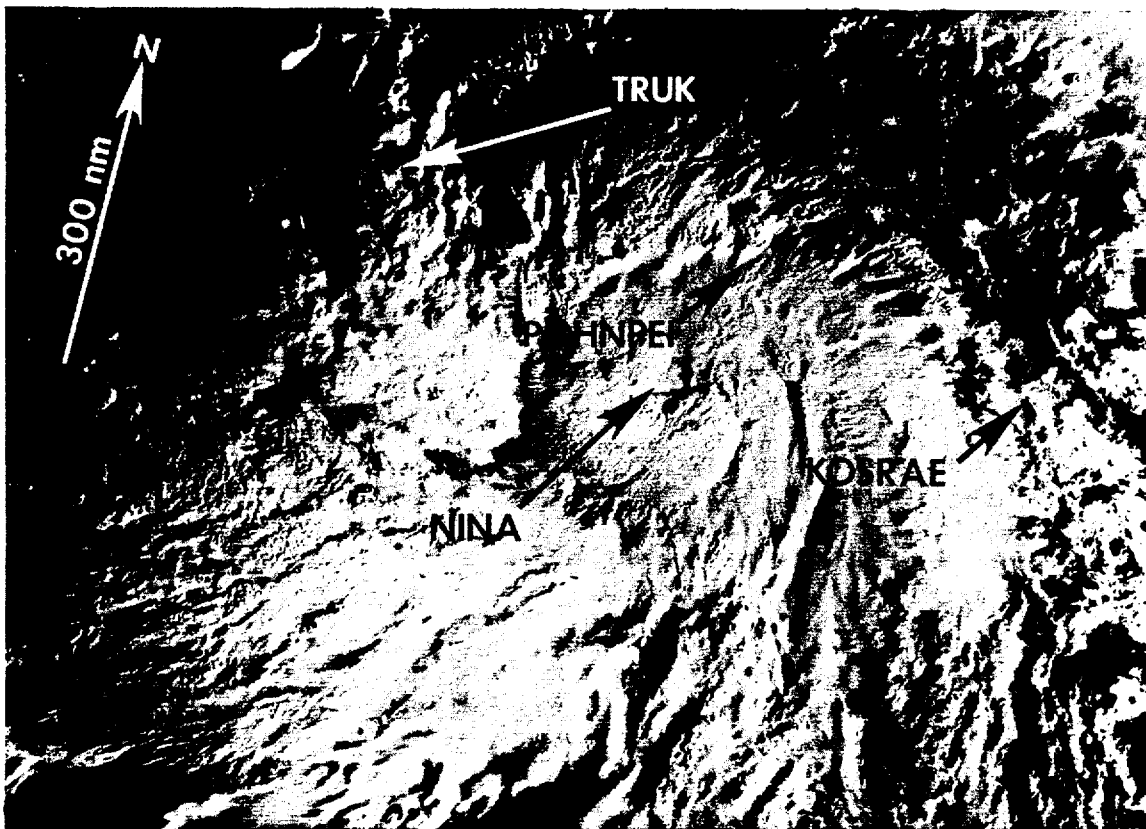


Figure 3-22-2. Satellite imagery indicating improving organization in the central convection and good upper-level outflow associated with the tropical disturbance that was to become Nina (191457Z November DMSP visual imagery).

This acceleration along the working best track would greatly affect the forecast movement. For example, if a cyclone is moving at 2 kt (4 km/hr) faster than forecast, it will travel in 72-hours an additional 144 nm (267 km).

Nina continued to intensify and accelerate. By the time of the second warning at 191800Z, Nina was upgraded to tropical storm intensity. More rapid westward movement was supported by upper-level data at Guam (WMO 91217), Truk (WMO 91334) and Pohnpei (WMO 91348), which indicated 30 kt (15 m/sec) easterly mid-level flow during this time (Figure 3-22-4). At 201600Z, Nina passed 40 nm (74 km) south of Moen Island in the Truk Atoll while moving west-northwestward at 18 kt (33 km/hr). Satellite intensity analysis estimated winds between 45 and 50 kt (23 to 26 m/sec). Maximum winds reported at Moen Island were 60 kt (31 m/sec) with gusts up to 80 kt (41 m/sec). (Note: The difference in intensity may be due to the fact that winds in

the right front quadrant of a tropical cyclone are a combination of its kinetic energy and the vector addition of its forward movement.) The lowest pressure recorded was 987 mb, which correlates (Atkinson and Holliday, (1977)) to 50 kt (26 m/sec).

Nina passed the Truk Atoll during the early morning hours on the 21st of November. Civil Action Teams reported that five people were killed, 38 seriously injured, and most of the more than 40,000 residents were homeless and without electrical power. The Truk Atoll was declared a federal disaster area in order to compensate for the \$30 to \$40 million in damage to housing, businesses and agriculture. In addition, U. S. Armed Forces airlifted supplies into the ravaged islands.

After Nina passed the Truk Atoll, it slowly decelerated. The rate of intensification also slowed. Nevertheless, Nina was upgraded to typhoon intensity at 211200Z. Nina passed

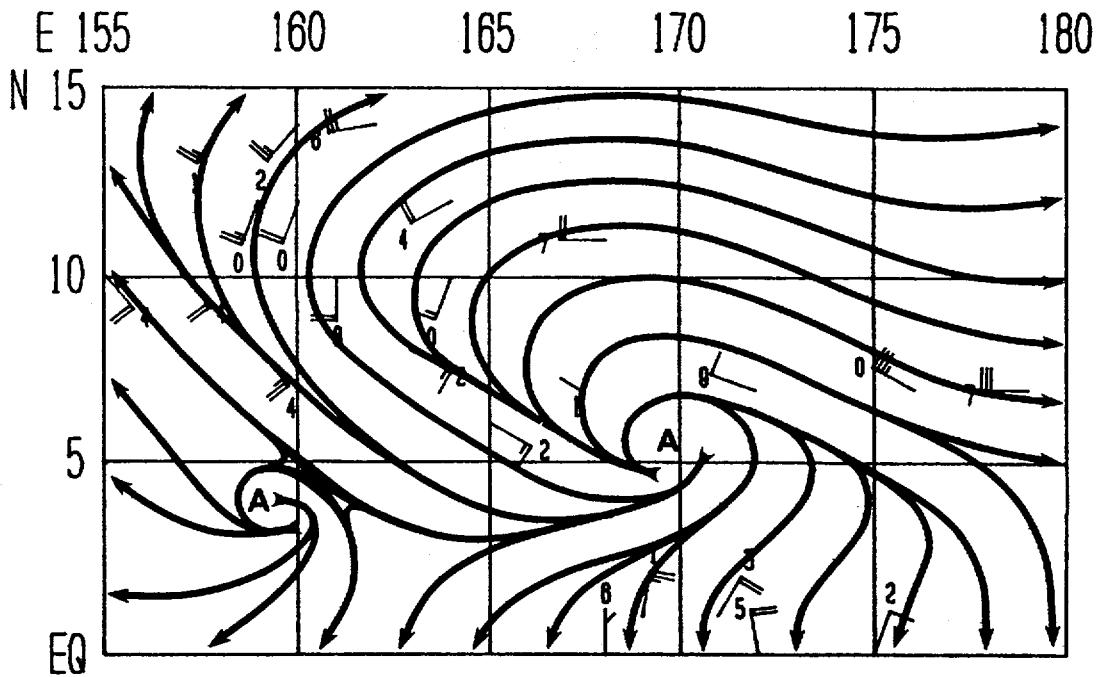


Figure 3-22-3. Synoptic data at 191200Z, showing the center of the upper-level anticyclonic circulation at 200 mb located considerably east of the center of the cirrus outflow associated with Tropical Depression 22W.

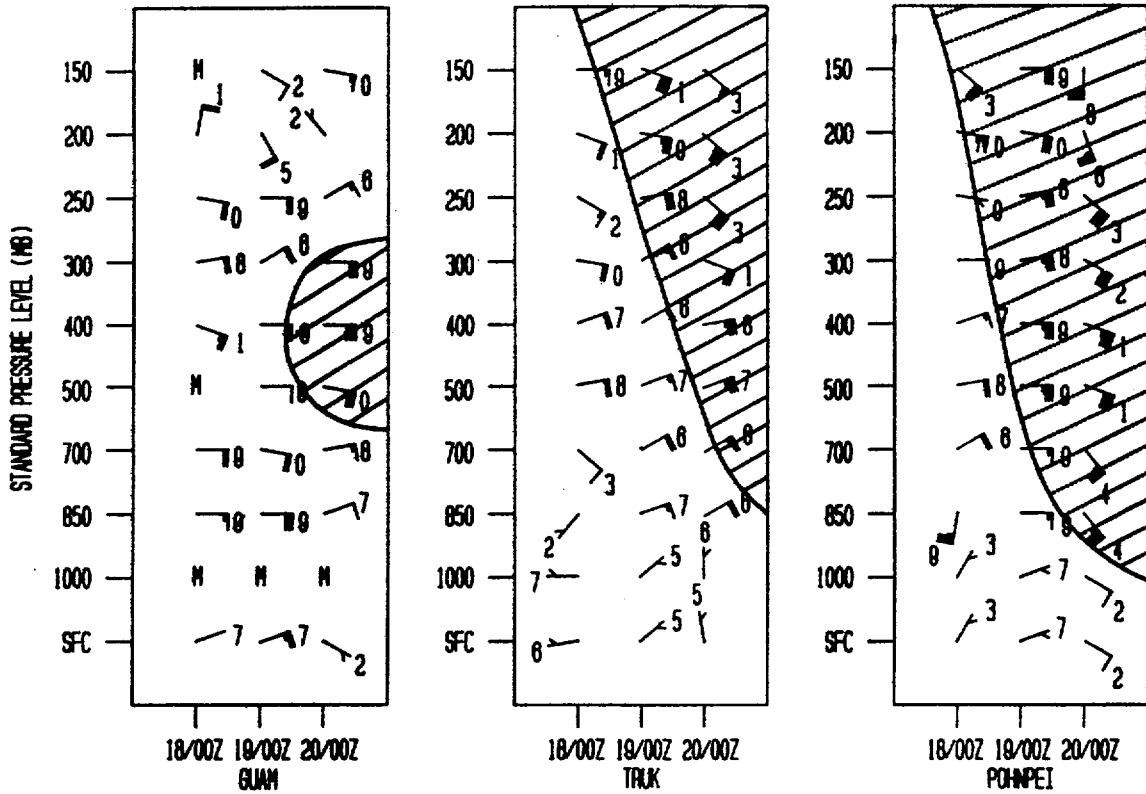


Figure 3-22-4. Upper-air winds and heights at standard pressure levels for Guam (WMO 91217), Truk (WMO 91334) and Pohnpei (WMO 91348) for the period 180000Z to 200000Z. Notice the 30 kt (15 m/sec) mid-level easterlies which would support the rapid movement of Nina toward the west.

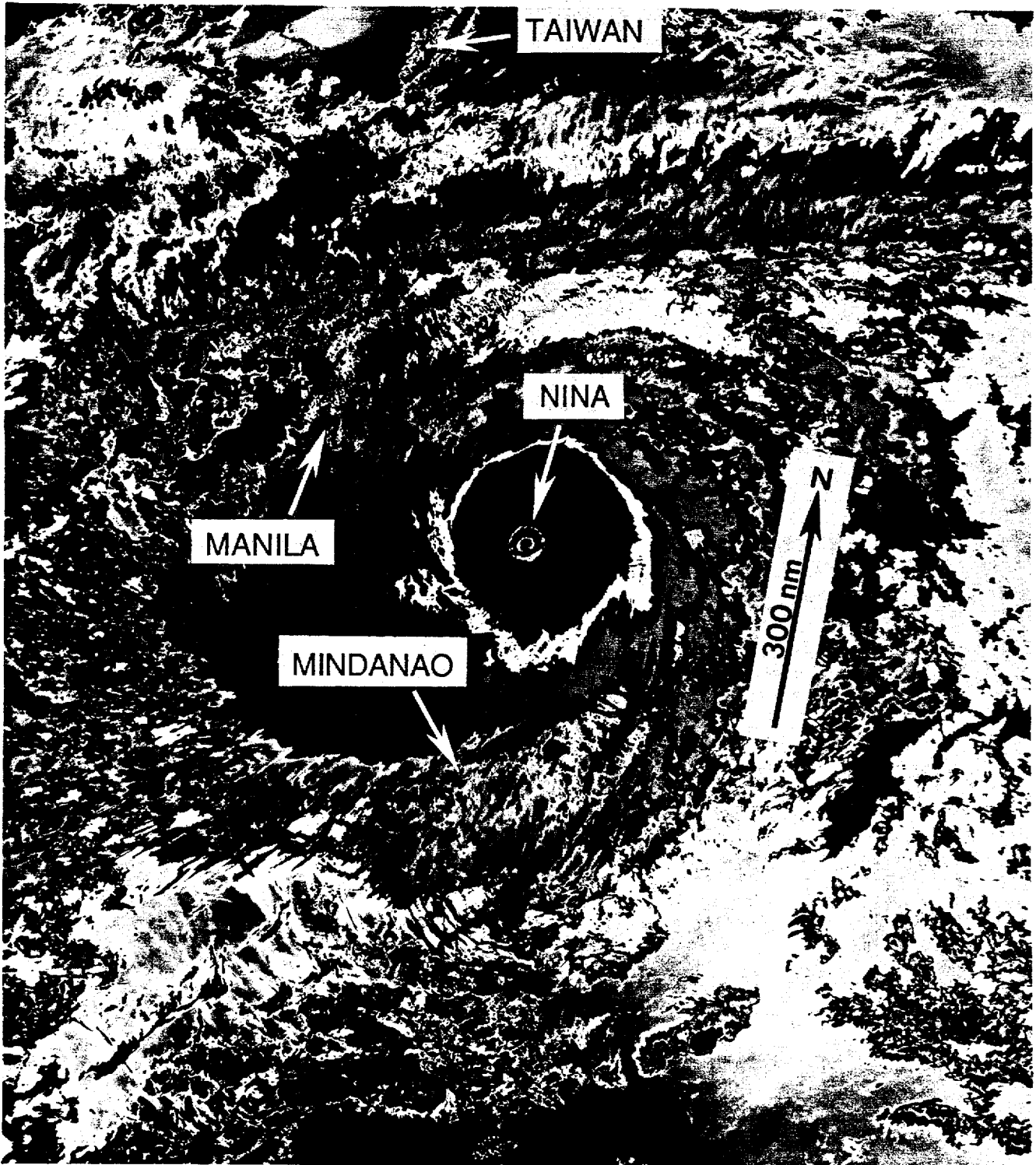


Figure 3-22-5. Satellite imagery showing the well-defined eye of Super Typhoon Nina as it approached the Philippine Islands (250701Z November NOAA visual imagery).

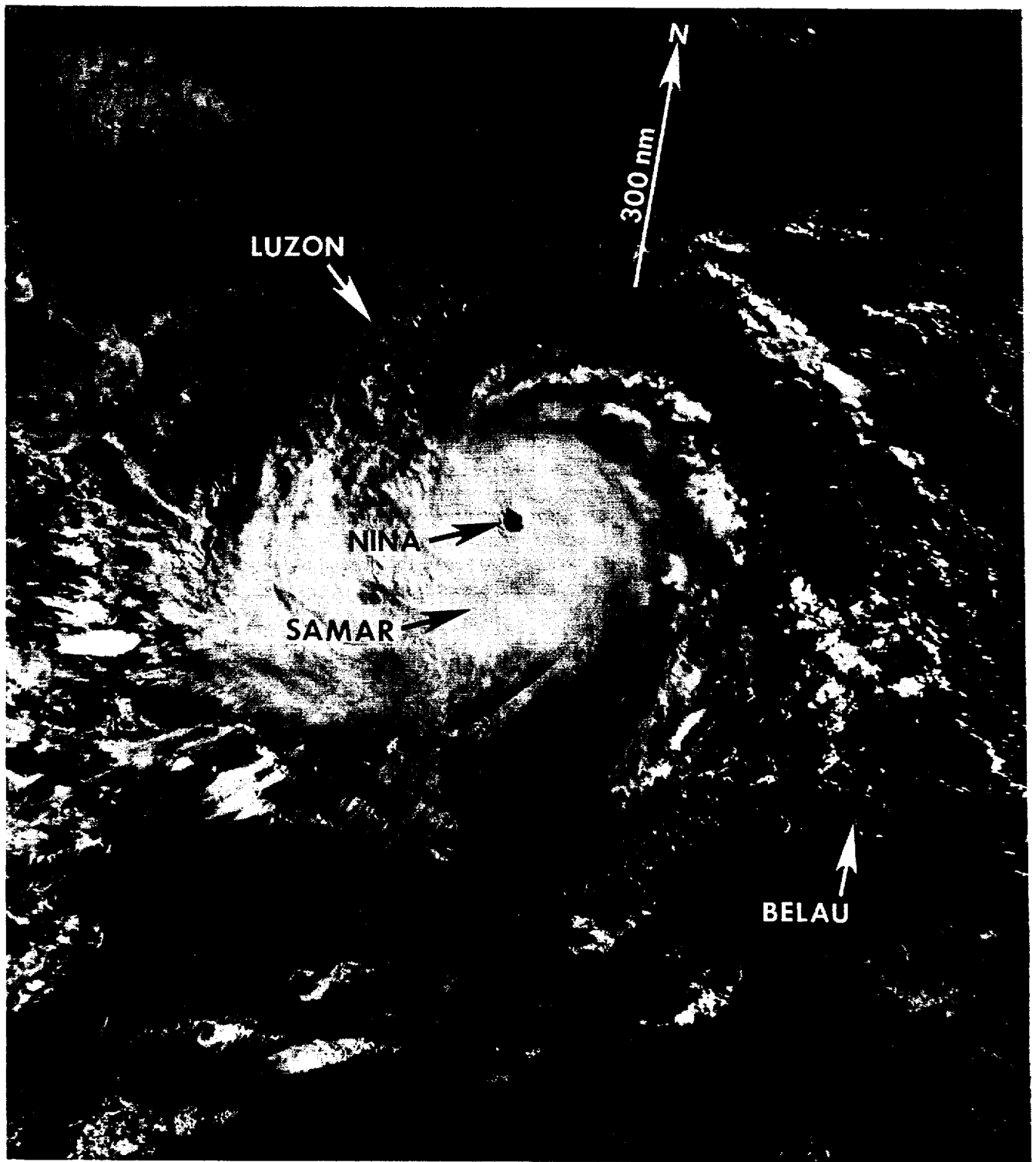


Figure 3-22-6. Matching infrared image for visual in Figure 3-22-5 (250701Z November NOAA infrared imagery).

Prognostic Reasoning

<u>DTG</u>	<u>Direction</u>	<u>Guidance</u>	<u>Speed</u>
260000Z	WNW for 36-hrs then NW	OTCM & COSMOS	Decelerating
261200Z	WNW 12- to 18- hrs then NW	Break in 400 mb ridges	-----
Alternate scenario:	Recurve in 48- to 72-hrs	OTCM	-----
2nd alternate scenario:	Move west	CSUM	-----
270000Z	WNW for 48-hrs	NE surge interaction, ECMWF & NORAPS & HPAC	Slowly decelerating
Alternate scenario:	West	-----	-----
271200Z	NW then West	NE surge, NORAPS & NOGAPS & ECMWF	-----
280000Z	North for 27-hrs then West	NE surge, 700 & 400 mb progs & HPAC	-----
281200Z	ENE	Strong mid- to upper-level westerly flow & CSUM	Accelerating
290000Z	ENE	Strong mid- to upper- level southwesterly flow	Accelerating

Figure 3-22-7. Abbreviated Prognostic Reasoning for the 260000Z through 290000Z November time period.

60 nm (111 km) north of the island of Ulithi and 95 nm (176 km) north of Yap at 221000Z and 221600Z, respectively. Later, on November 25th, an overflying Navy aircraft observed moderate flood damage to the Ulithi's agricultural areas. Twenty percent of the buildings had received structural damage. No damage was reported on Yap.

Nina began to slowly accelerate and rapidly intensify (Holliday and Thompson,

1979), dropping approximately 4 mb per six hours, as it approached the Philippine Islands. Beginning at 241200Z, Nina began to explosively deepen (Holliday and Thompson), dropping approximately 8 mb per six hours. Nina displayed a symmetrical eye that was 18 nm (33 km) in diameter (Figures 3-22-5 and 3-22-6). Nina slammed into the southern tip of Luzon at 251500Z with maximum winds estimated at 145 kt (75 m/sec) with gusts to 175

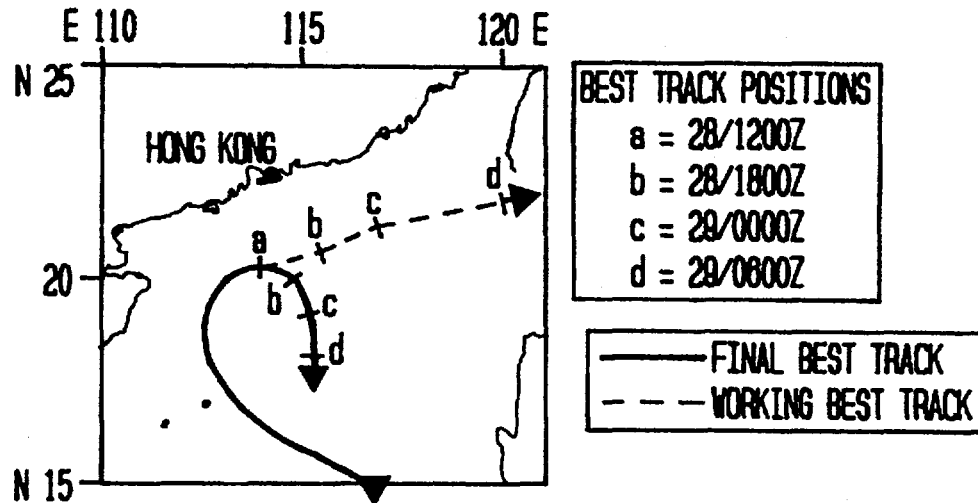


Figure 3-22-8. Difference between the working and final best tracks as Nina was sheared apart by the strong surge of the Northeast Monsoon.

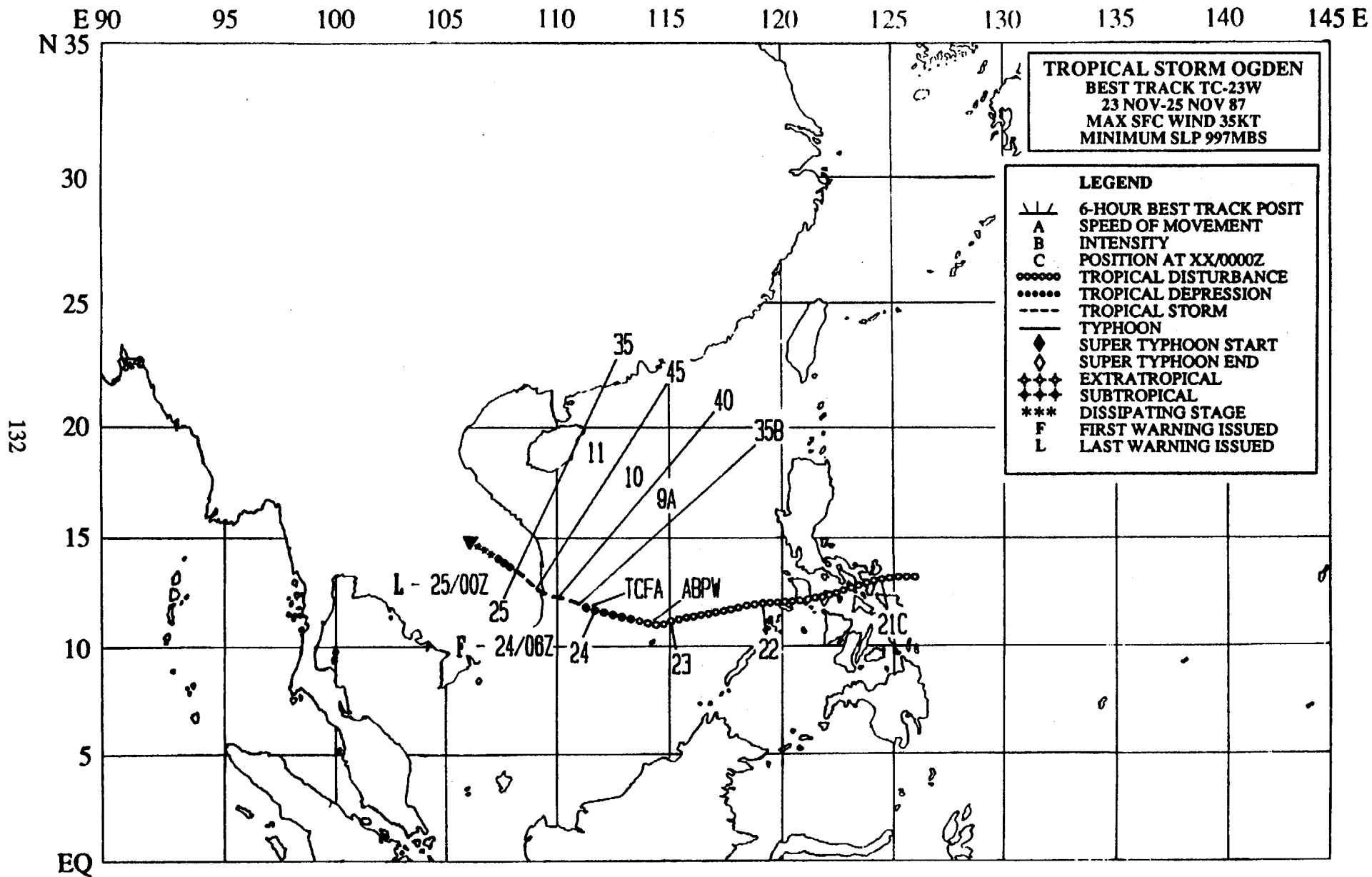
kt (90 m/sec). At least 687 people perished in the north central Philippine Islands. As with the Truk Atoll, Nina struck at night. Philippine authorities declared a state of emergency for 18 provinces that were battered by Nina. Overall more than 500,000 people were either rendered homeless, evacuated, or lost their sources of income. Croplands were heavily damaged. News sources reported that Nina was the most destructive typhoon to hit the Philippine Islands in nearly 20 years.

Nina traversed between the islands of Luzon and Mindoro and entered the South China Sea with 95 kt (49 m/sec) winds. Although satellite imagery could not detect an eye, land-based radar continued to track the cloud covered eye. Shortly thereafter, Nina was packing 100 kt (51 m/sec) winds.

Once Nina was in the South China Sea, the forecast philosophy attempted to keep up with the changing synoptic situation. Figure 3-22-7 provides an abbreviated look at the specifics of each prognostic reasoning message for the 260000Z through 290000Z November time period. Basically what initially appeared to be straight-forward, wasn't! The decoupling of Nina's lower- and upper-level circulations developed into a complex event; culminating in the 270000Z prognostic reasoning message,

which became a classic example of being wrong for all the right reasons. The net result was a very tense situation for Hong Kong and the southern China coast.

As the system began to move northward, an eye became visible at 280300Z. Within 6- to 12-hours, Nina was sheared apart by the shallow, but strong, low-level surge in the northeast monsoon flow and strong westerly winds at the mid- and upper-levels. During the shearing, the deep convection, which was poorly defined and being positioned as an upper-level circulation by satellite, accelerated east-northeastward along the quasi-stationary front. As a consequence, the forecast philosophy embraced a cloud system moving rapidly through the Luzon Strait and becoming extratropical. (Post-analysis found that the low-level most probably separated from the upper-level circulation center at 280600Z. This resulted in a 340 nm (630 km) difference at 24-hours between the working best track and the final best track points as seen in Figure 3-22-8.) The upper-level cloudiness did move east-northeastward; however, the low-level circulation center executed an anticyclonic loop and headed slowly southward with the monsoonal flow. The residual low-level vorticity and cloudiness rapidly dissipated over the South China Sea.



TROPICAL STORM OGDEN (23W)

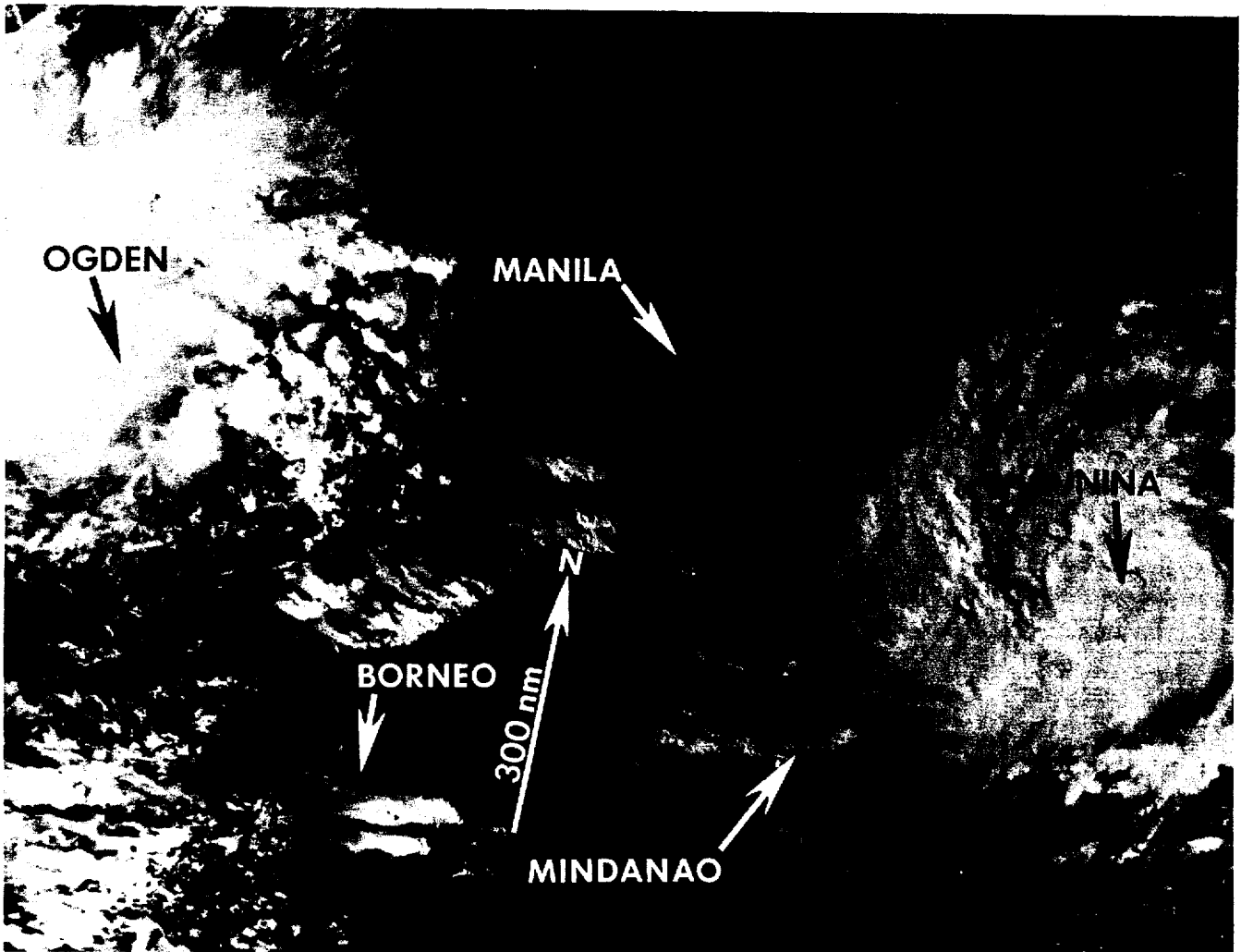
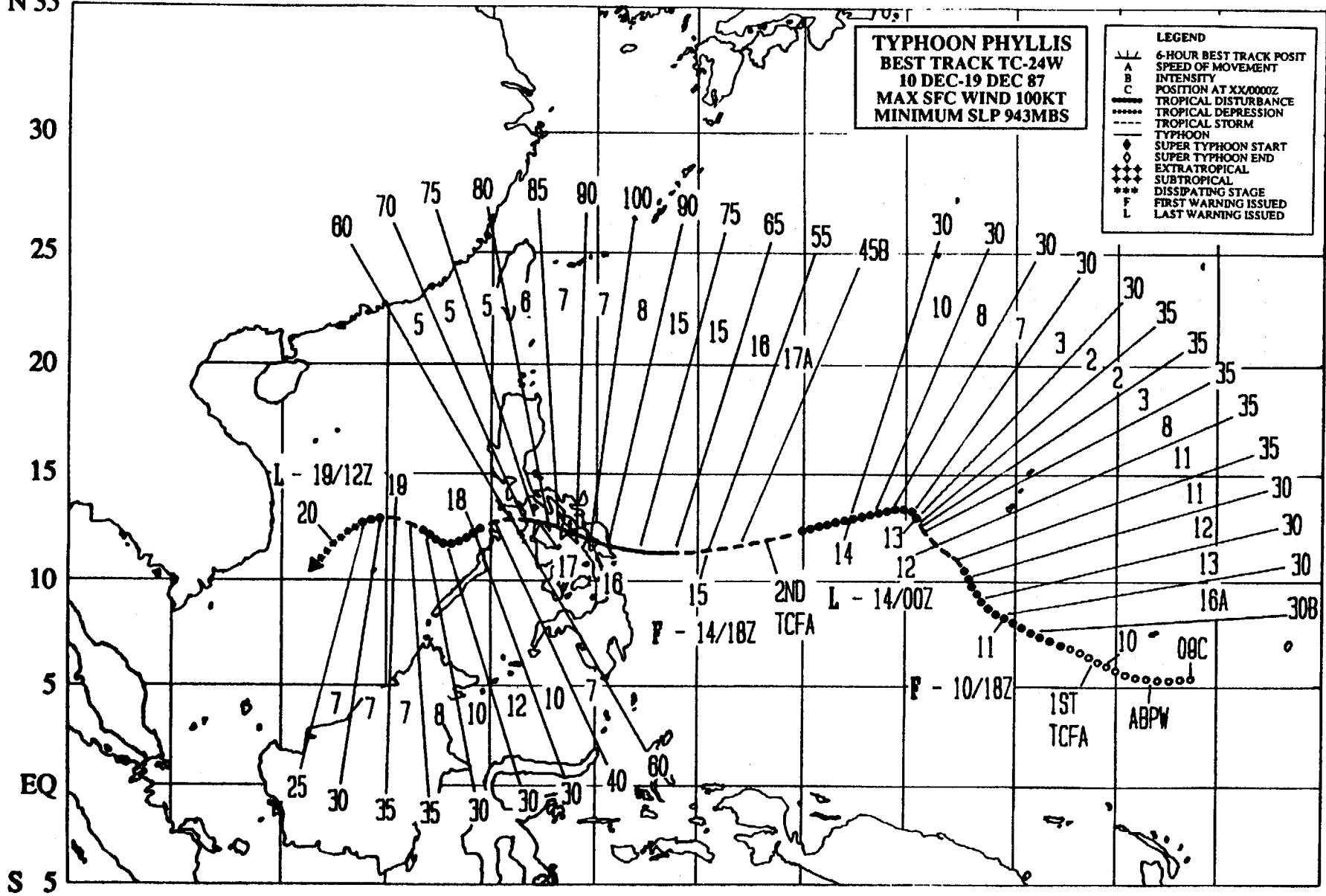


Figure 3-23-1. The third significant tropical cyclone of November, Tropical Storm Ogden, developed into a tropical storm in the South China Sea and quickly made landfall over southern Vietnam. Ogden was first detected late on November 20th as a poorly organized area of convection just east of the Philippines. Once in the South China Sea, the development of spiralling low-level cloud lines led to the system's first mention on the Significant Tropical Weather Advisory (ABPW PGTW) at 230600Z. At 240400Z, a Tropical Cyclone Formation Alert (TCFA) was issued based on the improved low-level cloud organization and synoptic reports of a closed surface circulation with maximum winds of 15 to 25 kt (8 to 13 m/sec). Shortly thereafter, Dvorak intensity analysis of satellite imagery estimated 30 kt (15 m/sec) winds which prompted the first warning on Tropical Depression 23W at 240600Z (see image above). At 241800Z, Ogden reached a maximum intensity of 45 kt (23 m/sec) just prior to making landfall. Ogden made landfall on the east coast of Vietnam 18 nm (33 km) south of Tuy Hoa at 241900Z. The final warning was issued at 250000Z as the system moved inland and dissipated (240712Z November NOAA visual imagery).

E 100 105 110 115 120 125 130 135 140 145 150 155 160 E



134

S 5

TROPICAL STORM PHYLLIS (24W)

Typhoon Phyllis was the only significant tropical cyclone to develop in the western North Pacific in December and the third to regenerate over water in 1987 (reference Tropical Storms Ed (12W) and Maury (21W)). It struck the central Philippine Islands three weeks after Super Typhoon Nina (22W) and added further misery to that ravaged nation.

Phyllis began as an area of weakly organized convection in the eastern Caroline Islands 150 nm (278 km) southeast of the Truk Atoll. It was mentioned for the first time on the 091030Z December Significant Tropical Weather Advisory (ABPW PGTW) after

exhibiting a rapid increase in the amount and organization of convection. The potential development was listed as fair due to the pre-existence of a low-level circulation and unrestricted upper-level outflow.

A Tropical Cyclone Formation Alert (TCFA) was issued the next day at 100230Z when a satellite intensity estimate (Dvorak, 1984) indicated 25 kt (13 m/sec) winds at the surface. The first warning, on Tropical Depression 24W, came at 101800Z as the estimate of the surface winds increased to 30 kt (15 m/sec) and the associated deep convection became more centralized. At that time, Tropical

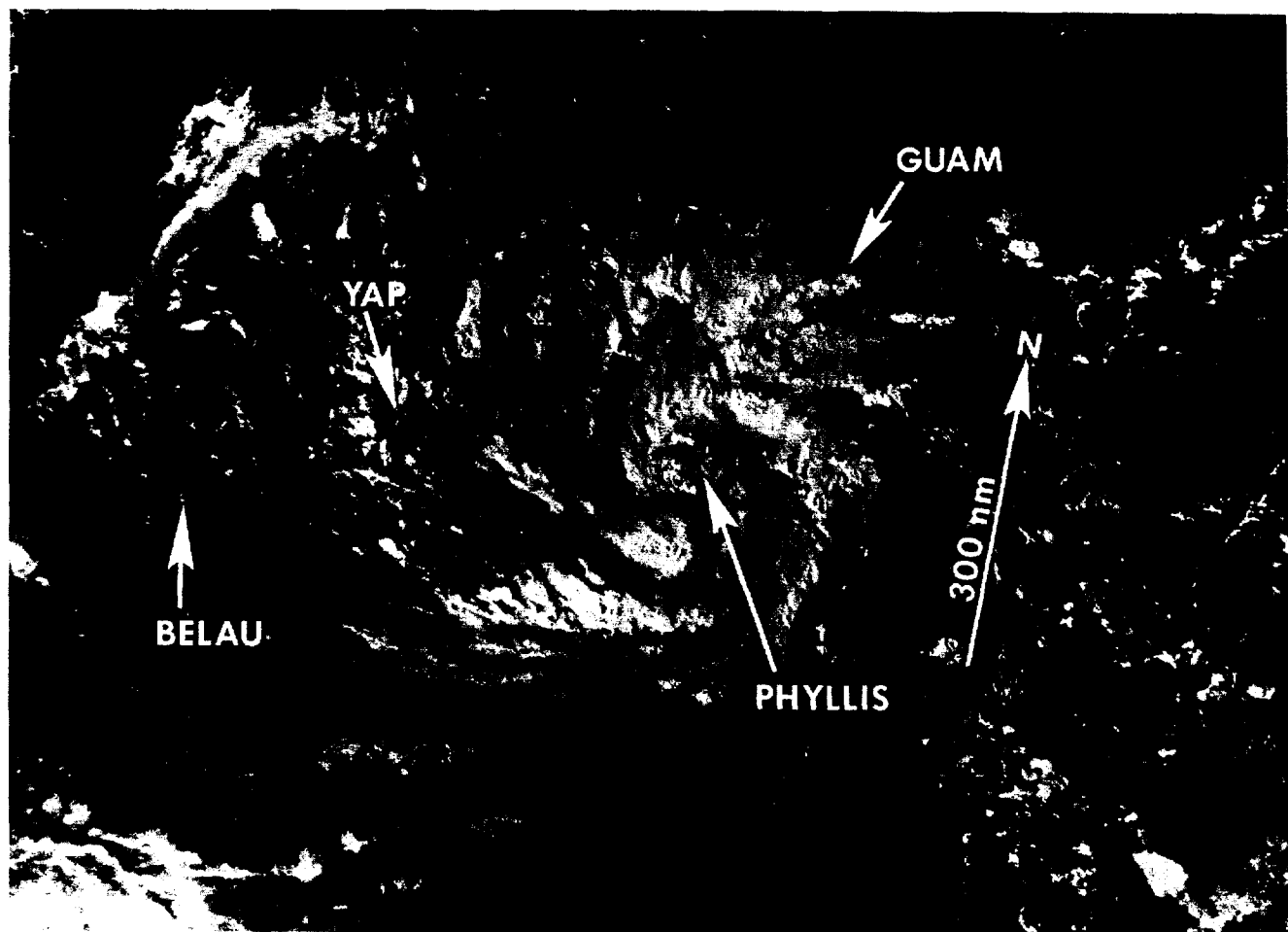


Figure 3-24-1. The well-defined, low-level circulation center of Tropical Depression 24W is revealed by the spiral convective bands of cloudiness (110547Z December NOAA visual imagery).

Depression 24W was located 370 nm (685 km) south-southeast of Guam and was moving toward the northwest. Twenty-four hours later, it made its closest point of approach to Guam (210 nm (389 km) to the southwest) and was upgraded to a tropical storm based on the development of a large cloud system and improved upper-level outflow in the southwest quadrant (see Figure 3-24-1). Early dissipation was forecast (beginning with the third warning at 110600Z). The approach of an eastward-moving, mid-latitude trough would increase the vertical wind shear. As the short wave moved eastward from mainland China, Phyllis slowed

its forward motion until 130600Z, then abruptly changed course and accelerated toward the west-southwest. After downgrading the tropical cyclone to a tropical depression at 130000Z, the final warning followed at 140000Z. The displacement of central convection to the northeast of the low-level circulation center and the entrainment of cooler, drier air appeared to have started an irreversible weakening process.

However, within 18-hours (once the vertical wind shear decreased), Phyllis began to reestablish its central convection under a favorable upper-level outflow pattern. This

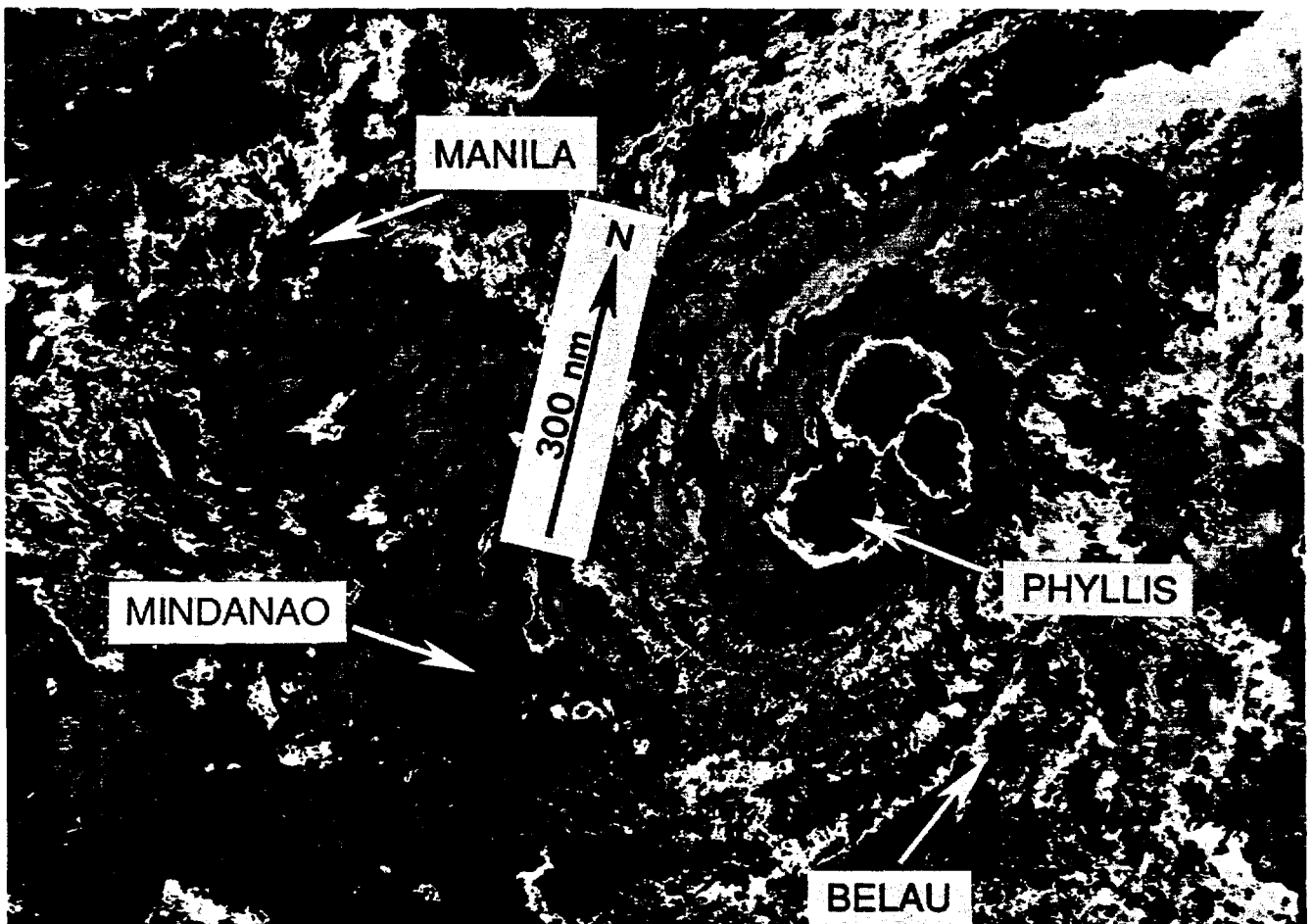


Figure 3-24-2. Tropical Storm Phyllis shortly after regeneration (142136Z December DMSP infrared imagery).

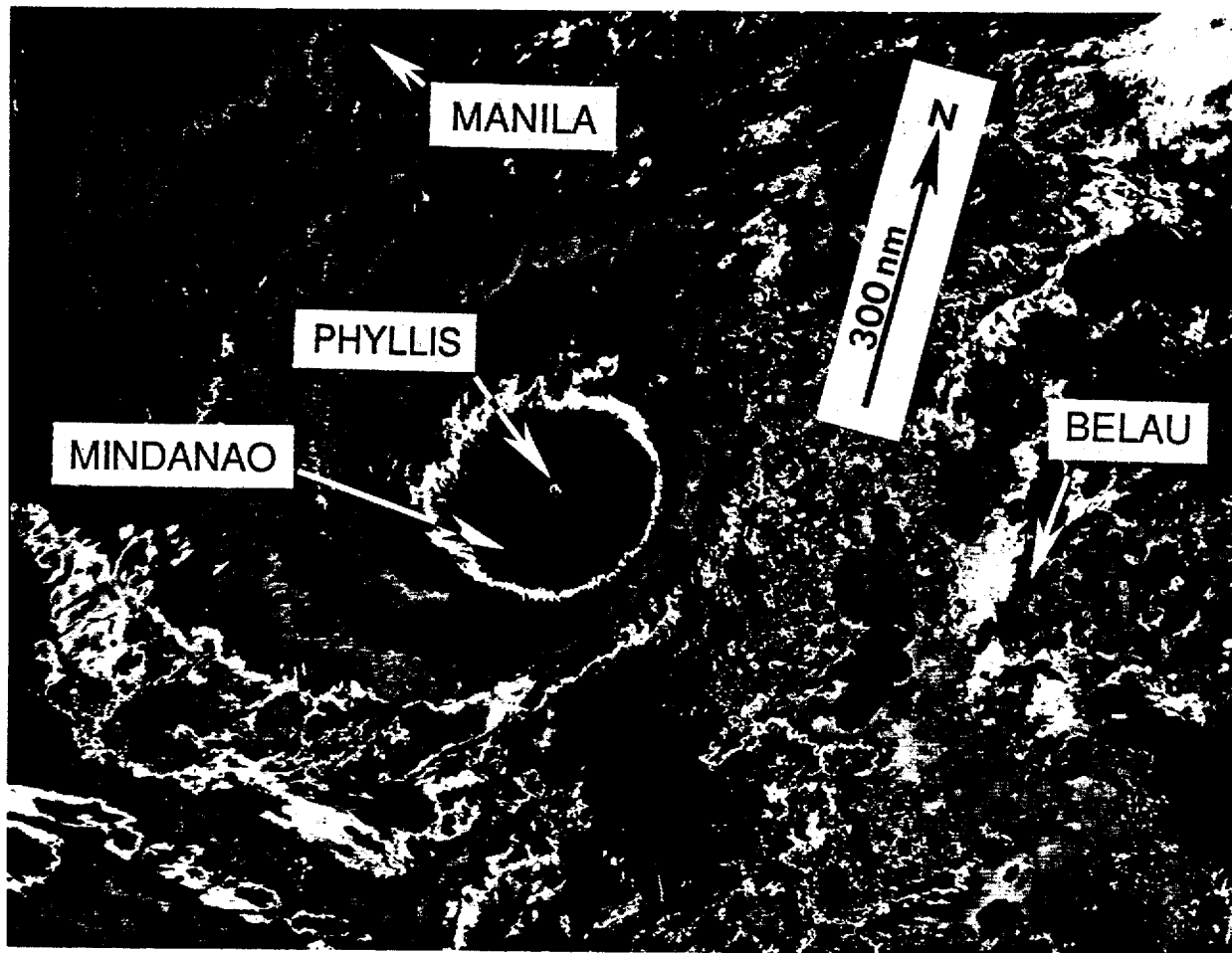


Figure 3-24-3. Tightly wrapped, small eye of Typhoon Phyllis during landfall on the island of Samar (152123Z December DMSP infrared imagery).

resulted in the issuance of a second TCFA at 141630Z. The (first regenerated) warning followed at 141800Z (as warning number 15 on the system) based on the satellite intensity estimate of 45 kt (23 m/sec) (see Figure 3-24-2). Intensification continued until 150000Z when Phyllis peaked at 100 kt (51 m/sec) while making landfall on the island of Samar in the central Philippine Islands (Figure 3-24-3). Phyllis left ten people dead and thirteen more were listed as missing when a ferry boat sank off of northern Samar.

After peaking, Phyllis weakened slowly for 24-hours while traversing the central Philippine Islands. Weakened by the frictional effects of the surrounding mountainous island terrain, Phyllis entered the South China Sea and was downgraded to a tropical depression at 180000Z. The forecast to dissipate within 48-hours over water was basically correct, however, the tropical cyclone did briefly reintensify to 35 kt (18 m/sec) on the 19th. No other reports of deaths or serious damage were received.

3. NORTH INDIAN OCEAN TROPICAL CYCLONES

Eight significant tropical cyclones developed in the North Indian Ocean during 1987. That set a new all-time record and surpassed the previous high of seven systems in 1979. This was in sharp contrast with 1986 when only three significant tropical cyclones were observed. The long-term mean is approximately four per year. These eight systems (all of tropical storm intensity) developed during the Spring and Fall transition periods (i. e., the intervals of weak opposing wind flow between the Northeast and Southwest Monsoons). Tables 3-5 and 3-6 provide a summary of information for 1987 and comparison with earlier years.

TABLE 3.5 NORTH INDIAN OCEAN
1987 SIGNIFICANT TROPICAL CYCLONES

TROPICAL CYCLONE	PERIOD OF WARNING	CALENDAR DAYS OF WARNING	NUMBER OF WARNINGS ISSUED	MAXIMUM SURFACE WINDS-KT (M/S)	ESTIMATED MSLP - MB
TC 01B	01 FEB - 03 FEB	3	11	55 (28)	984
TC 02B	02 JUN - 05 JUN	4	12	55 (28)	983
TC 03A	05 JUN - 09 JUN	5	18	50 (26)	987
TC 04B	15 OCT - 16 OCT	2	3	45 (23)	991
TC 05B	31 OCT - 03 NOV	4	14	40 (21)	994
TC 06B	11 NOV - 13 NOV	3	6	50 (26)	987
TC 07A	08 DEC - 11 DEC	4	14	45 (23)	991
TC 08B	18 DEC - 19 DEC	2	5	35 (18)	997
1987 TOTALS:		26*	83		

*Overlapping days are counted only once in sum.

TABLE 3-6. FREQUENCY OF NORTH INDIAN OCEAN TROPICAL CYCLONES

YEAR	JAN	FEB	MAR	APR	MAY	JUN	JUL	AUG	SEP	OCT	NOV	DEC	TOTAL
1971*	-	-	-	-	-	0	0	0	0	1	1	0	2
1972*	0	0	0	1	0	0	0	0	2	0	1	0	4
1973*	0	0	0	0	0	0	0	0	0	1	2	1	4
1974*	0	0	0	0	0	0	0	0	0	0	1	0	1
1975	1	0	0	0	2	0	0	0	0	1	2	0	6
1976	0	0	0	1	0	1	0	0	1	1	0	1	5
1977	0	0	0	0	1	1	0	0	0	1	2	0	5
1978	0	0	0	0	1	0	0	0	0	1	2	0	4
1979	0	0	0	0	1	1	0	0	2	1	2	0	7
1980	0	0	0	0	0	0	0	0	0	0	1	1	2
1981	0	0	0	0	0	0	0	0	0	1	1	1	3
1982	0	0	0	0	1	1	0	0	0	2	1	0	5
1983	0	0	0	0	0	0	0	1	0	1	1	0	3
1984	0	0	0	0	1	0	0	0	0	1	2	0	4
1985	0	0	0	0	2	0	0	0	0	2	1	1	6
1986	1	0	0	0	0	0	0	0	0	0	2	0	3
1987	0	1	0	0	0	2	0	0	0	1	2	2	8

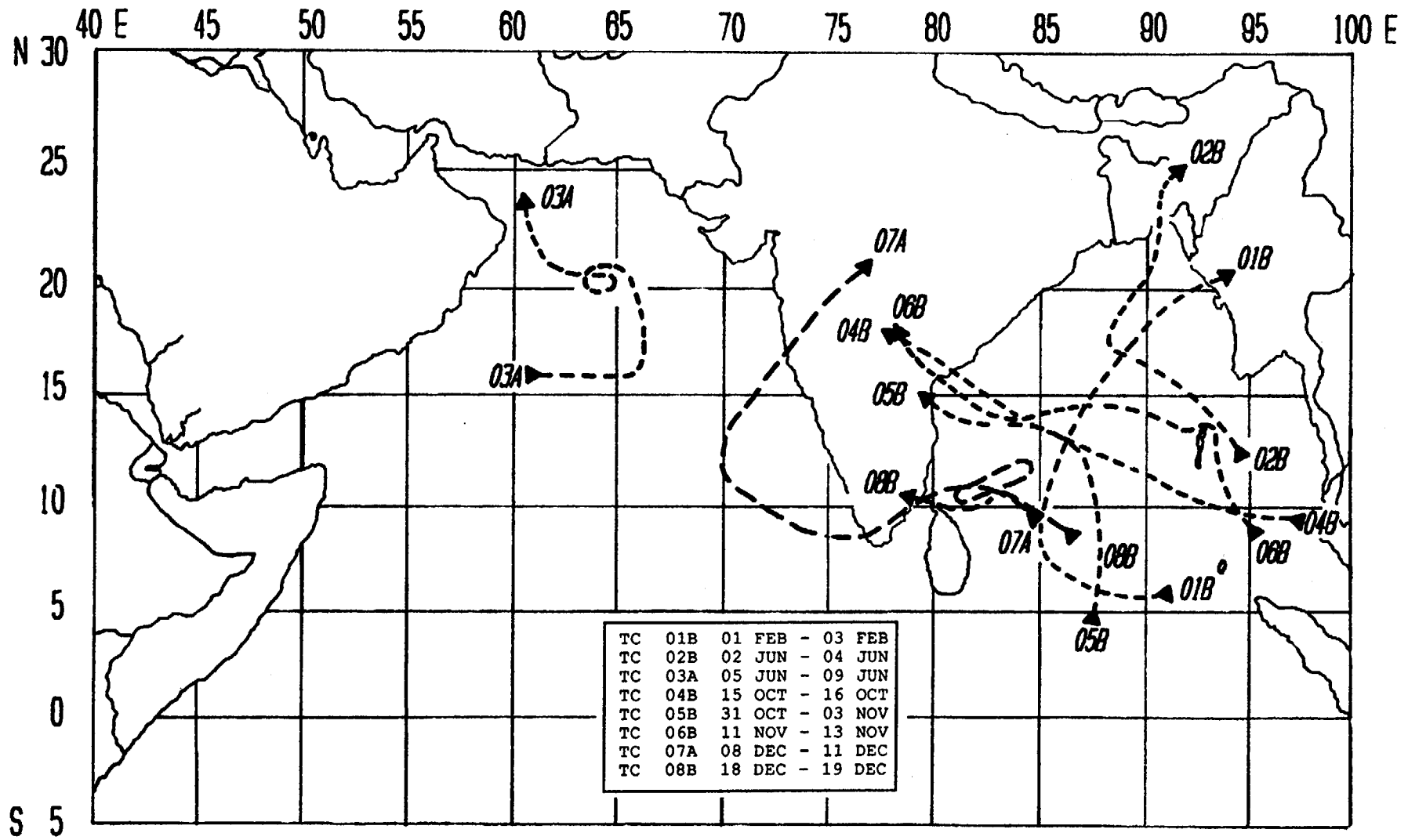
(1975-1987)

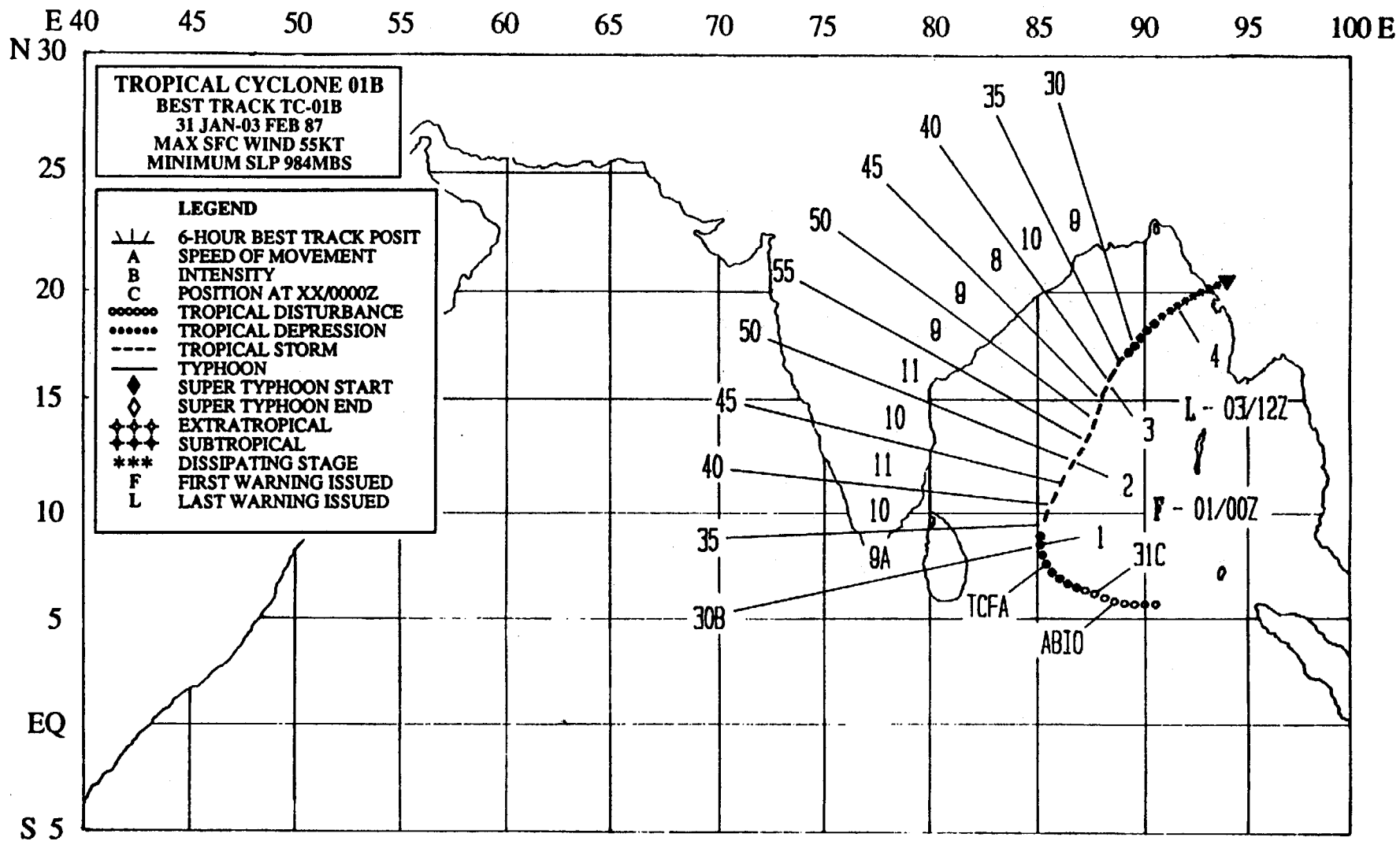
AVERAGE	0.2	0.1	0.0	0.1	0.7	0.5	0.0	0.1	0.2	1.0	1.5	0.5	4.7
CASES	2	1	0	1	9	6	0	1	3	13	19	6	61

* JTWC WARNING RESPONSIBILITY BEGAN ON 4 JUN 71 FOR THE BAY OF BENGAL, EAST OF 90 DEGREES EAST LONGITUDE. AS DIRECTED BY CINCPAC, JTWC ISSUED WARNINGS ONLY FOR THOSE TROPICAL CYCLONES THAT DEVELOPED OR TRACKED THROUGH THAT PORTION OF THE BAY OF BENGAL. COMMENCING WITH THE 1975 TROPICAL CYCLONE SEASON, JTWC'S AREA OF RESPONSIBILITY WAS EXTENDED WESTWARD TO INCLUDE THE WESTERN PORTION OF THE BAY OF BENGAL AND THE ENTIRE ARABIAN SEA.

FORMATION ALERTS: 7 OF 8 FORMATION ALERTS DEVELOPED INTO SIGNIFICANT TROPICAL CYCLONES. TROPICAL CYCLONE FORMATION ALERTS WERE ISSUED FOR ALL OF THE SIGNIFICANT TROPICAL CYCLONES THAT DEVELOPED IN 1987, EXCEPT TROPICAL CYCLONE 03A.

WARNINGS:	NUMBER OF CALENDAR WARNING DAYS:	26
	NUMBER OF CALENDAR WARNING DAYS WITH TWO TROPICAL CYCLONES:	1
	NUMBER OF CALENDAR WARNING DAYS WITH THREE TROPICAL CYCLONES:	0





140

TROPICAL CYCLONE 01B

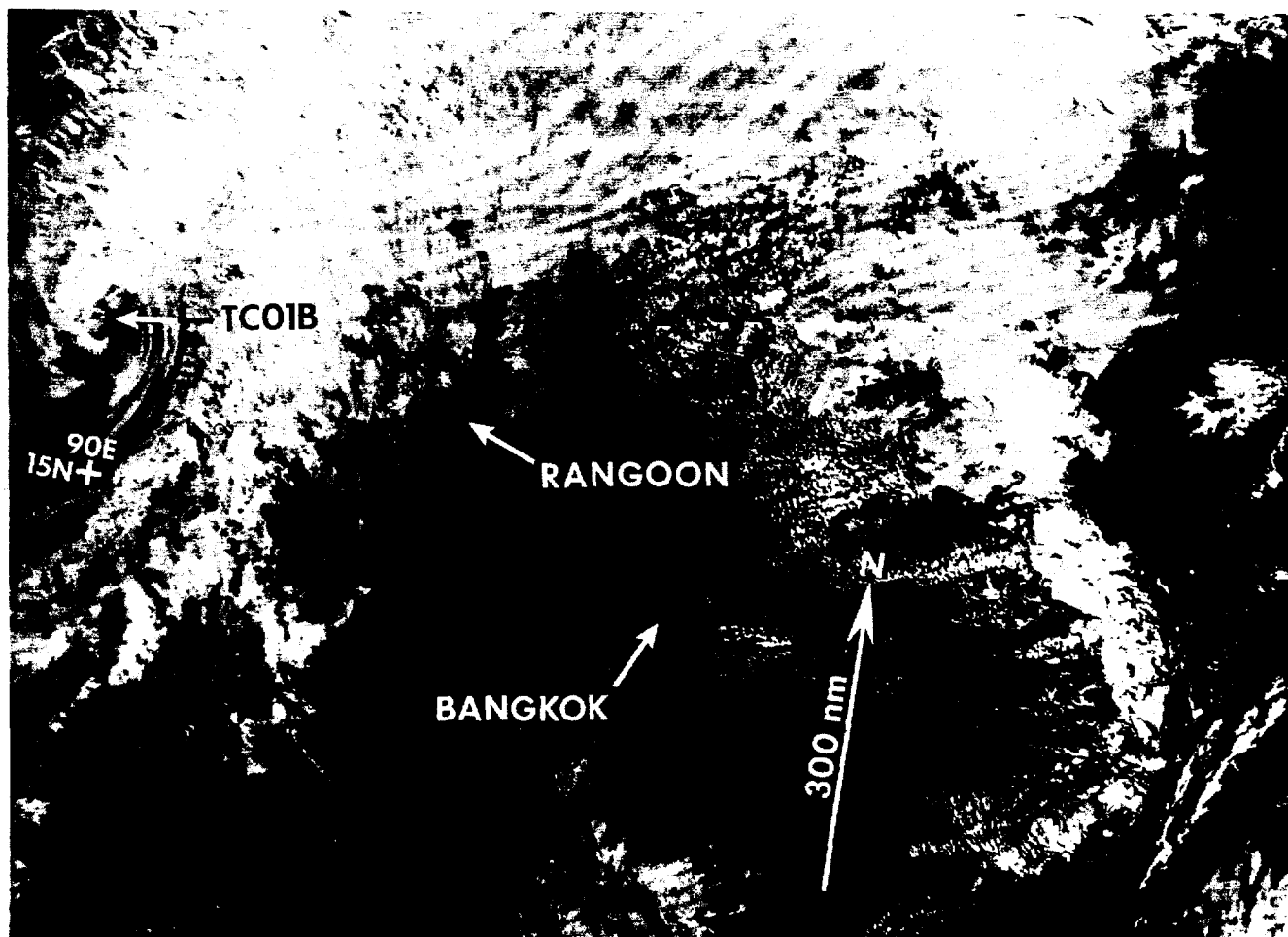
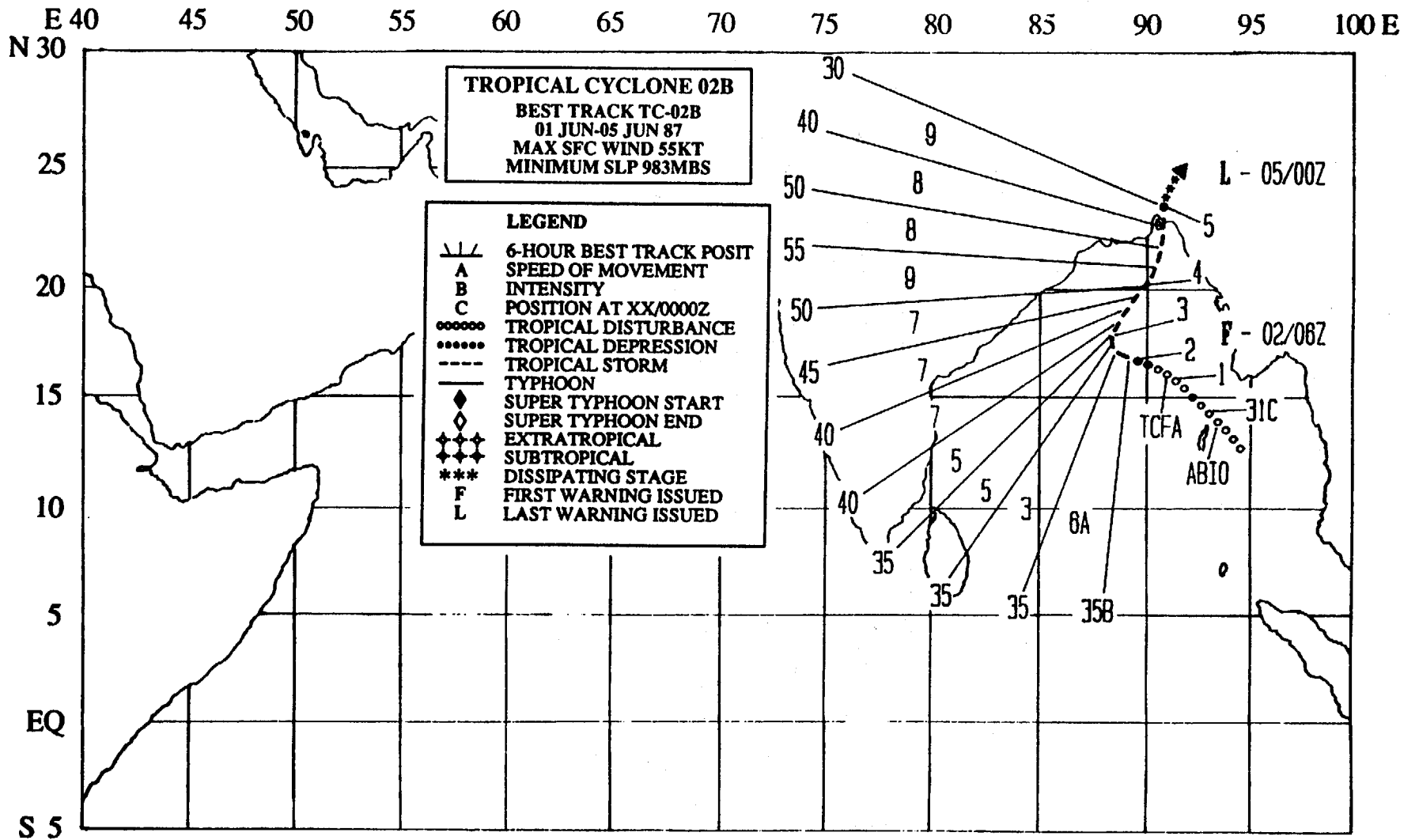


Figure 3-01B-1. Tropical Cyclone 01B was the first significant tropical cyclone to form in the Bay of Bengal during 1987. It was detected as an amorphous area of convection about 500 nm (926 km) east of Sri Lanka on the 29th of January and was noted on the 301800Z Significant Tropical Weather Advisory (ABIO PGTW). Satellite imagery at that time showed upper-level anticyclonically curved outflow over a weak, low-level circulation. Within the next 24-hours, the organization and amount of convection steadily increased. A Tropical Cyclone Formation Alert was issued at 311900Z. Satellite imagery showed convective banding had continued to increase, but sparse synoptic data showed no low surface pressures. At 0000Z on February 1st, the first warning was issued with the appearance of a central dense overcast and unrestricted outflow in all quadrants. The system then tracked steadily northeastward. The intensity peaked at 55 kt (28 m/sec) at 020600Z as the system began interaction with upper-level southwesterlies, which sent a long plume of cirrus northeastward across Burma. A partially exposed low-level circulation center became apparent at 030000Z, as increased vertical wind shear from the southwesterlies aloft stripped away the central cloudiness. Six hours later the low-level vortex was fully exposed (see above imagery). At 031200Z, JTWC issued the final warning on the 30 kt (15 m/sec) weakening tropical cyclone. The remnants of Tropical Cyclone 01B continued to track toward the northeast and dissipation occurred after it made landfall on February 4th over the northwest coast of Burma (030805Z February NOAA visual imagery).



TROPICAL CYCLONE 02B

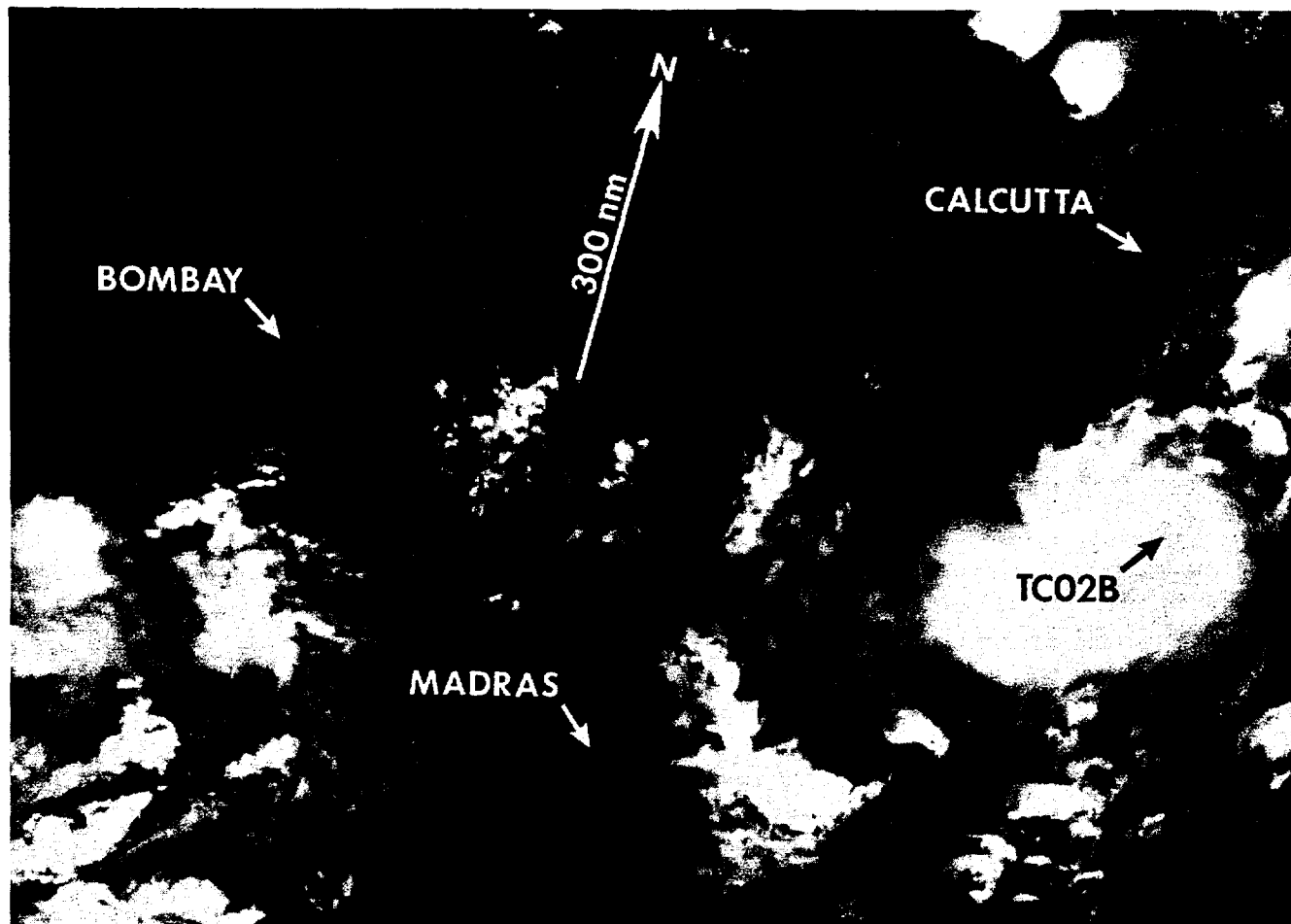


Figure 3-02B-1. Tropical Cyclone 02B was the second significant tropical cyclone to form in the Bay of Bengal. It was detected on satellite imagery as an area of organizing convection about 220 nm (407 km) southwest of Rangoon, Burma and was first mentioned as a new suspect area on the 301800Z May Significant Tropical Weather Advisory (ABIO PGTW). The development of strong central convection prompted a Tropical Cyclone Formation Alert on June 1st at 0600Z. The first tropical cyclone warning followed a day later at 020600Z as a result of continued development. The forecast track toward the northwest, which agreed closely with the Half Persistence and Climatology (HPAC) guidance, changed during the subsequent 24-hours, as mid-level ridging caused Tropical Cyclone 02B to assume a recurvature track toward the northeast (see above imagery). The One-Way Interactive Tropical Cyclone Model (OTCM), correctly predicted this recurvature toward the northeast; however, the guidance was discounted due to the previous poor performance of the model in this region. At 040600Z, Tropical Cyclone 02B reached its maximum intensity of 55 kt (28 m/sec) and developed a ragged eye. This intensity was maintained until the system made landfall over Bangladesh at 041200Z. Rapid dissipation followed. No reports of damage or loss of life were received (030421Z June DMSP visual imagery).

TROPICAL CYCLONE 03A

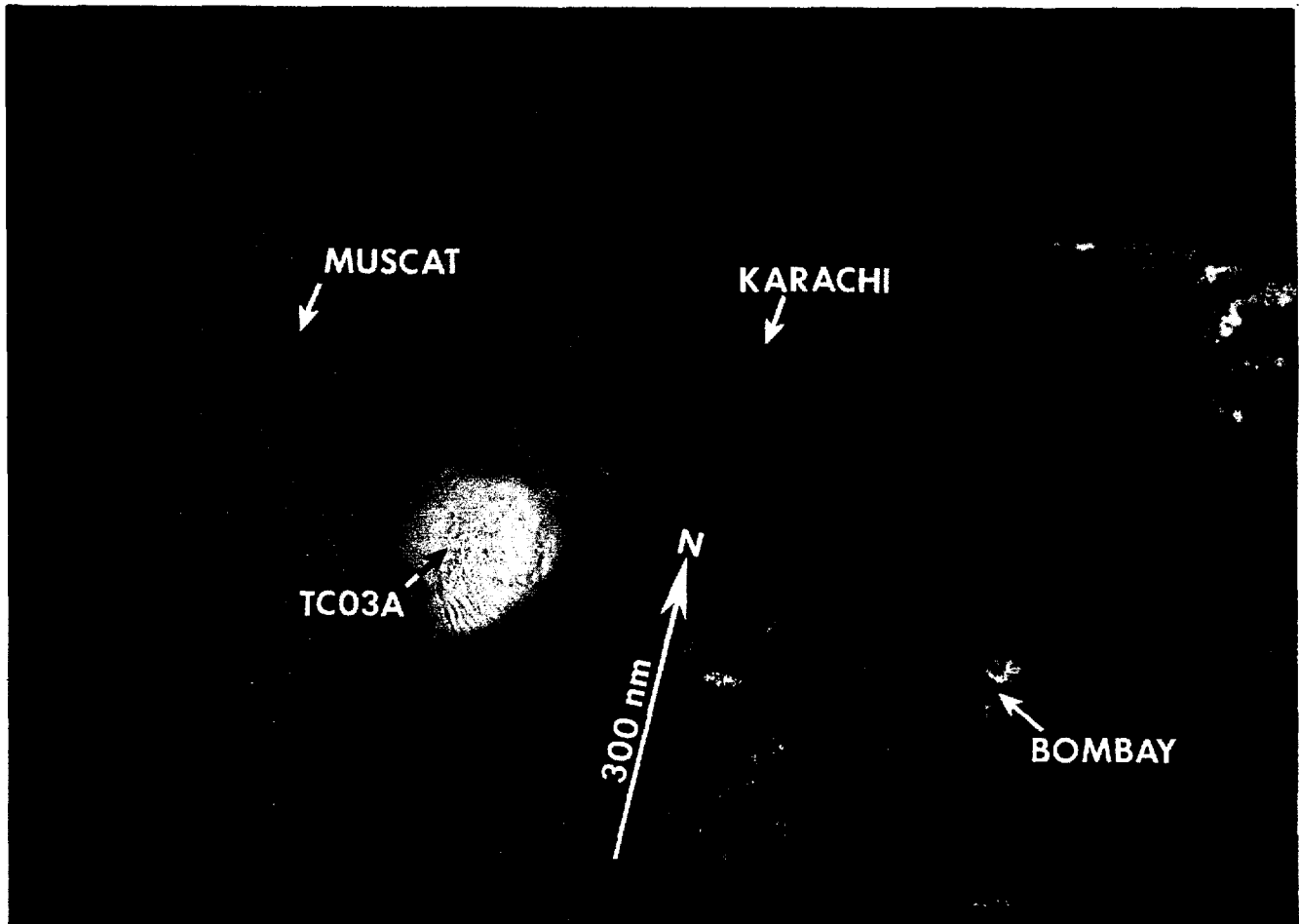
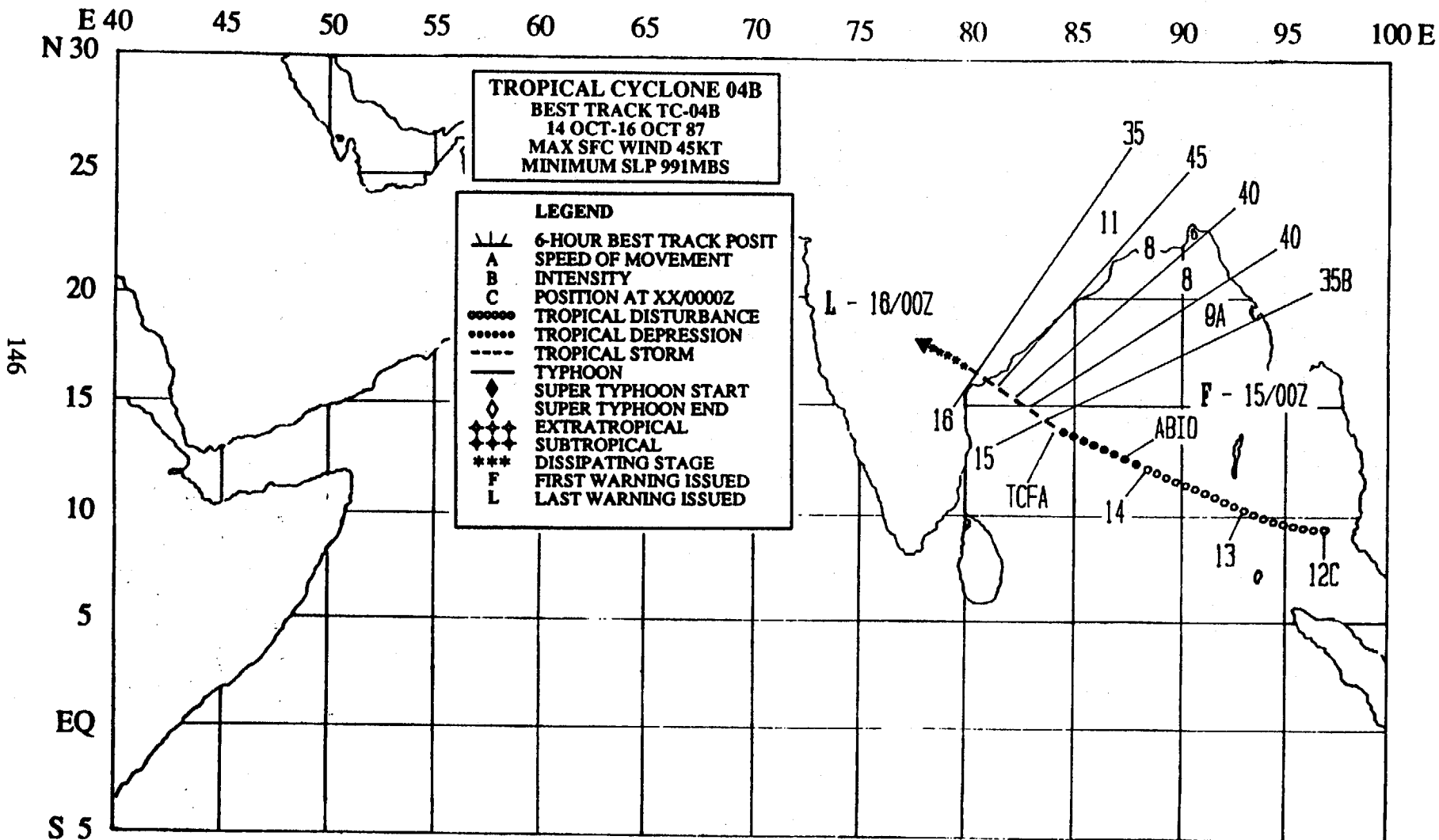


Figure 3-03A-1. Tropical Cyclone 03A began on June 4th as a monsoon depression with the supporting convection displaced from the low-level circulation center. Throughout the life of Tropical Cyclone 03A, brisk southwesterly flow dominated the low-levels with an overlying tropical easterly jet in the upper-levels. The low pressure center developed 250 nm (463 km) southeast of central Oman and moved slowly eastward along the edge of the low-level southwesterlies. An expanded radius of over 30 kt (15 m/sec) winds in the south semicircle resulted from interaction between the tropical cyclone and the already brisk monsoonal flow. JTWC issued its first warning at 050600Z without a preceding Tropical Cyclone Formation Alert, due to the rapid consolidation of convection around an exposed low-level circulation center. Post-analysis indicated the system had actually reached tropical storm intensity 18-hours earlier. Tropical Cyclone 03A reached a maximum intensity of 50 kt (26 m/sec) at 060000Z shortly before it abruptly changed its track toward the north. This intensity was maintained until 080000Z when the track became westerly. The final warning was issued at 091200Z as the system rapidly weakened due to increased vertical wind shear. Cloudiness associated with the remains of the low-level circulation flared up for a short time between 110400Z (see above imagery) and 111200Z; however, complete dissipation over water occurred within the next 24-hours (110501Z June DMSP visual imagery).



TROPICAL CYCLONE 04B

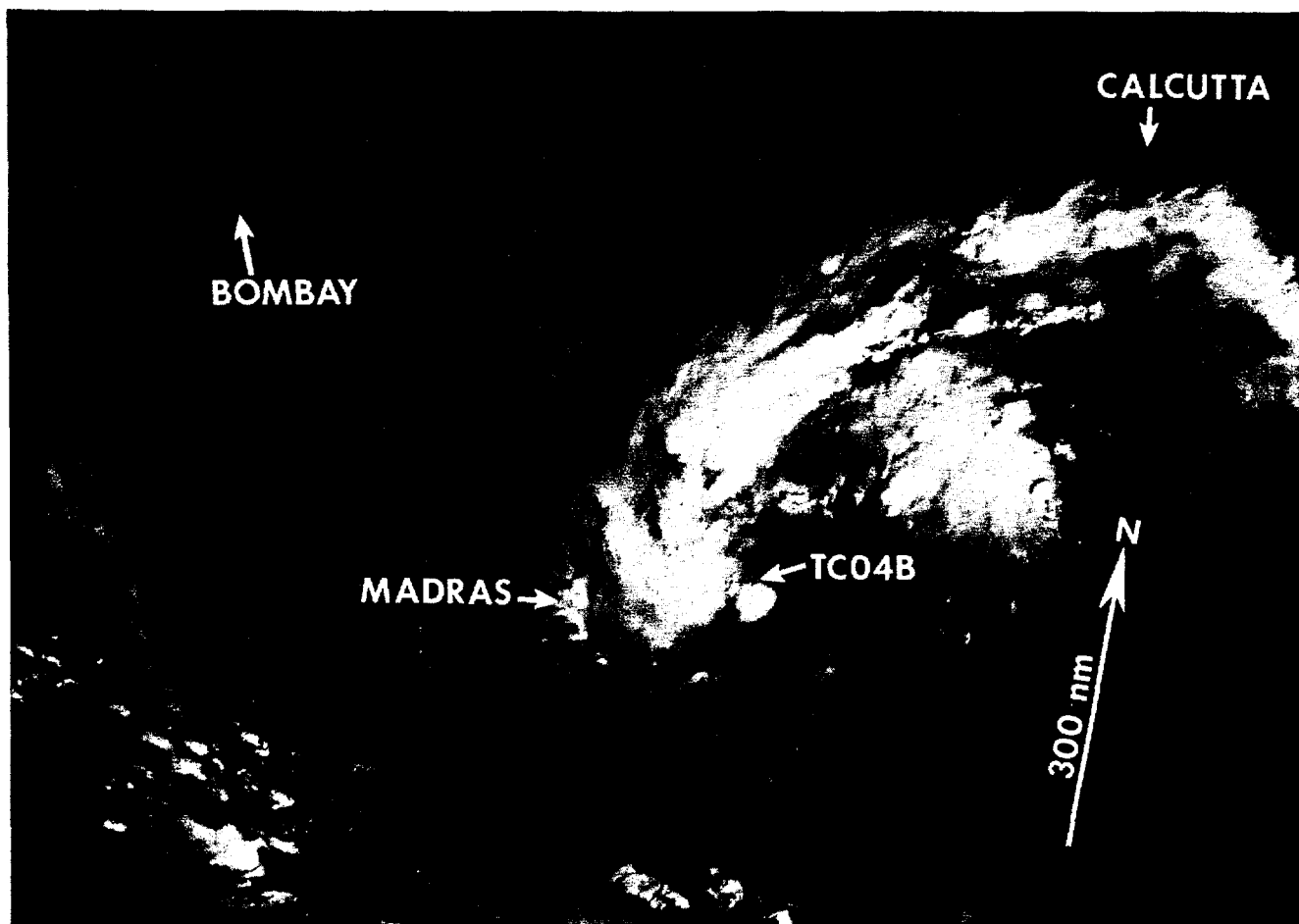


Figure 3-04B-1. Tropical Cyclone 04B began as a monsoon depression in the Andaman Sea on the 12th of October and tracked toward the west-northwest. By 13 October at 0600Z, the cloud system had separated from the general monsoonal cloudiness. At that time, JTWC added the system to its Significant Tropical Weather Advisory (ABIO PGTW), and indicated its potential for continued development was fair. At 142030Z, JTWC issued a Tropical Cyclone Formation Alert based on the appearance of a central dense overcast and an associated higher Dvorak intensity estimate of 30 kt (15 m/sec). The first warning followed at 150000Z as a result of a Dvorak estimate of 35 kt (18 m/sec) surface winds (see above imagery). This first warning, which indicated landfall within the next 12- to 24-hours, was also designated as the final warning. However, this forecast proved to be overly optimistic. At 151800Z, Tropical Cyclone 04B peaked at 45 kt (23 m/sec) and a second warning was issued. This was necessary because Tropical Cyclone 04B was on track, but still over water. At 160000Z, Tropical Cyclone 04B was finalled for a second time as it moved inland and weakened (150408Z October DMSP visual imagery).

TROPICAL CYCLONE 05B

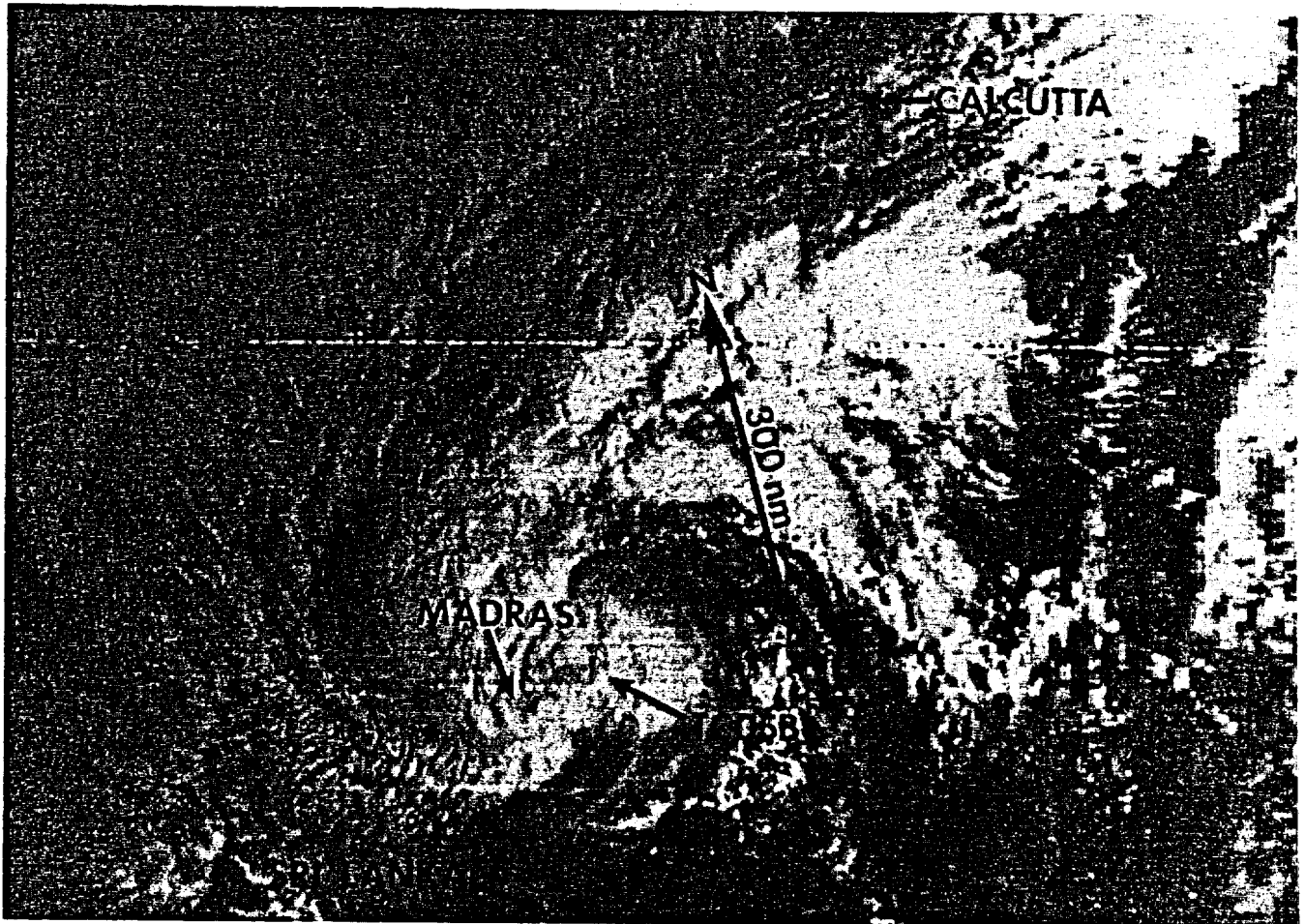
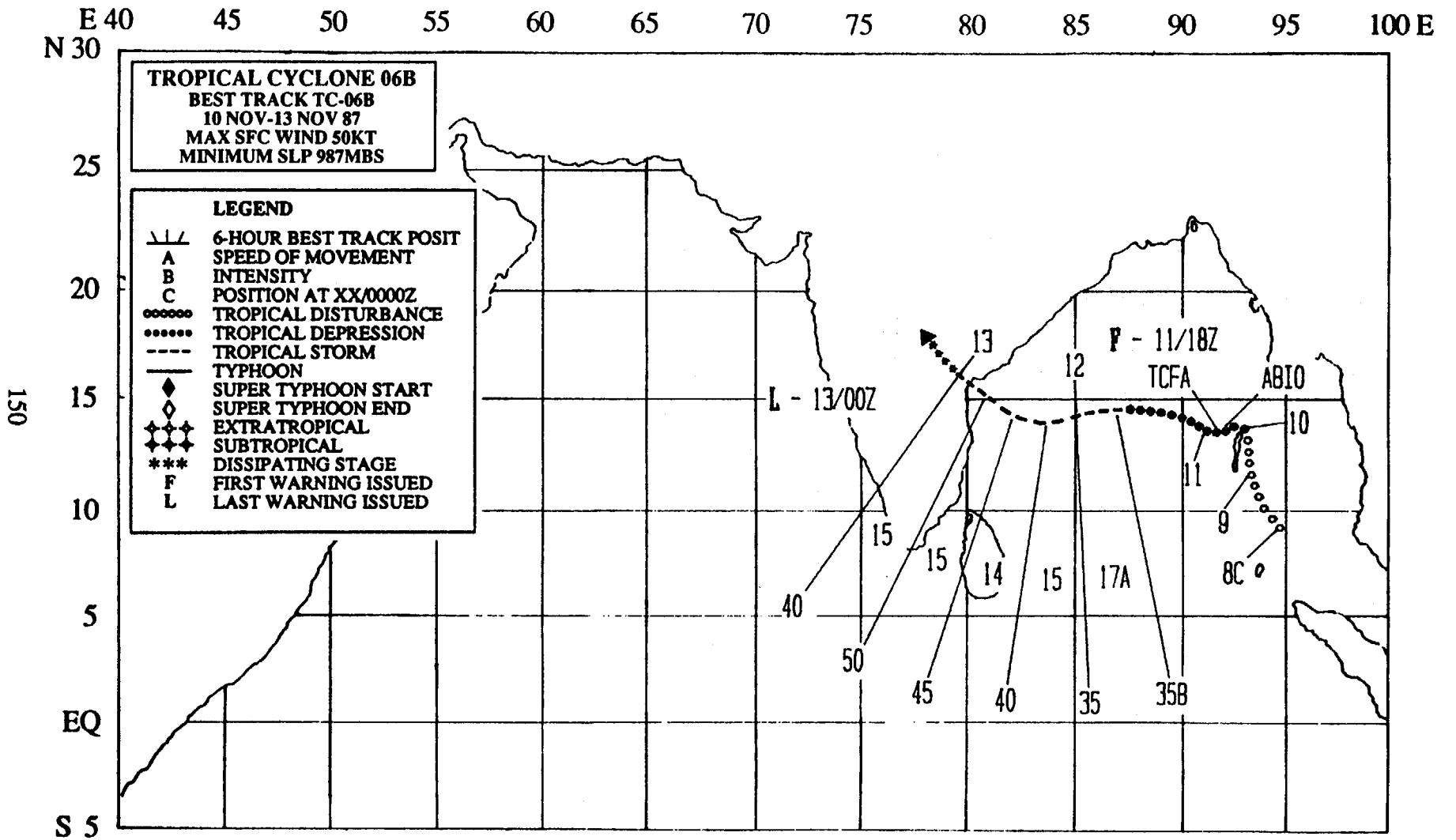


Figure 3-05B-1. Tropical Cyclone 05B spawned from the monsoon trough over the southern Bay of Bengal midway between Sri Lanka and northern Sumatra in late October. Its detection on satellite imagery resulted in the reissuance of the Significant Tropical Weather Advisory (SBIO PGTW) at 300300Z and assignment of a fair potential for development. Intensification continued and a Tropical Cyclone Formation Alert was issued at 301557Z. The first warning was issued at 310000Z. Tropical Cyclone 05B moved toward the north and was initially forecast to continue moving northward, then turn northeastward, crossing southern Bangladesh and northern Burma. Instead, it assumed a northwestward track and slowed in forward speed. Once the system began to take a definite track toward the northwest, the forecast philosophy was changed and the One-Way Tropical Cyclone Model (OTCM) guidance was followed with excellent results. The peak intensity of 55 kt (28 m/sec) was reached at 1200Z on the 1st of November and maintained until the system was close inshore as evidenced by the well-defined convective cloud band on the satellite image above. Issuance of the final warning occurred at 030600Z as Tropical Cyclone 05B was dissipating over land (020221Z November NOAA visual imagery).



TROPICAL CYCLONE 06B

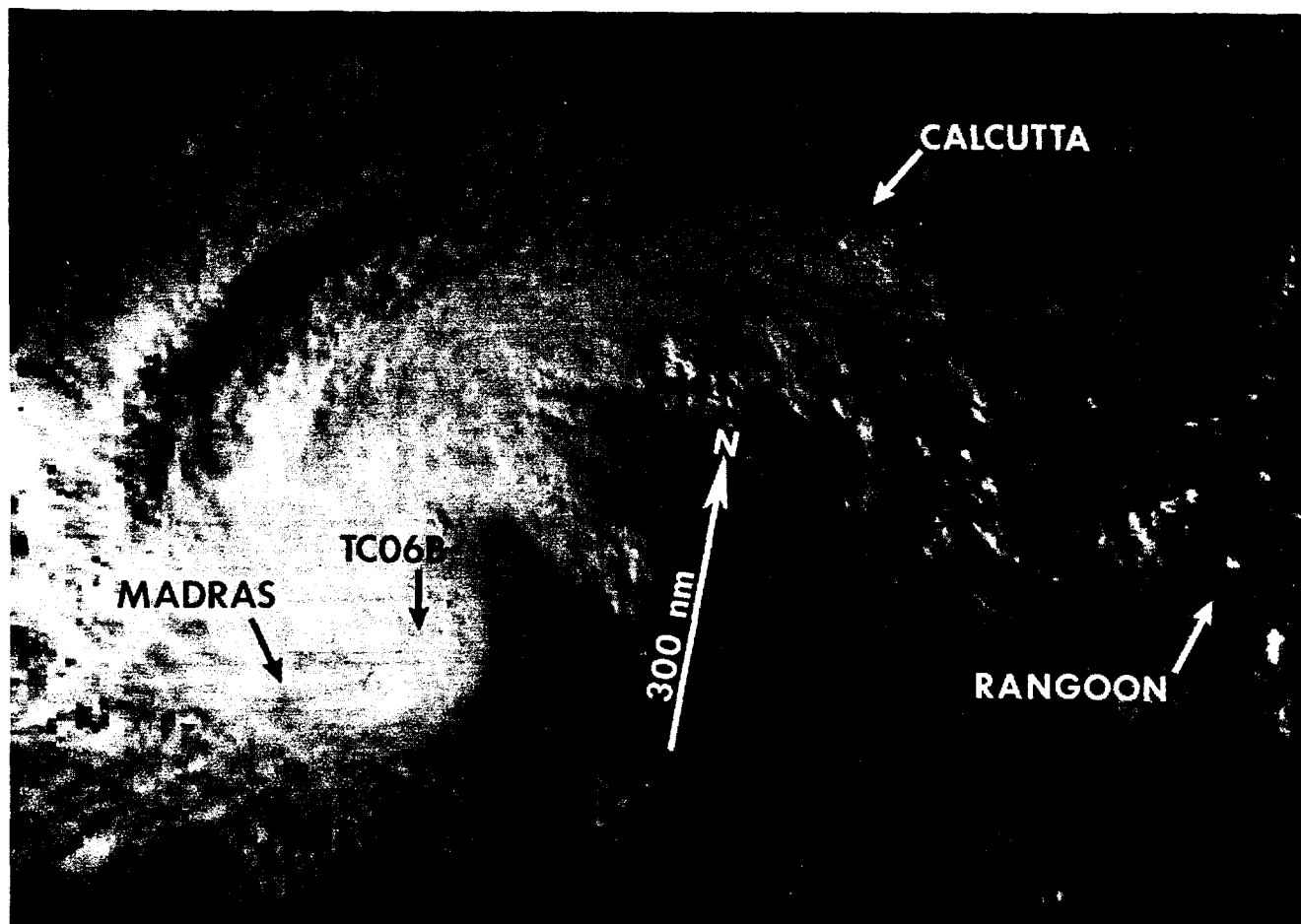
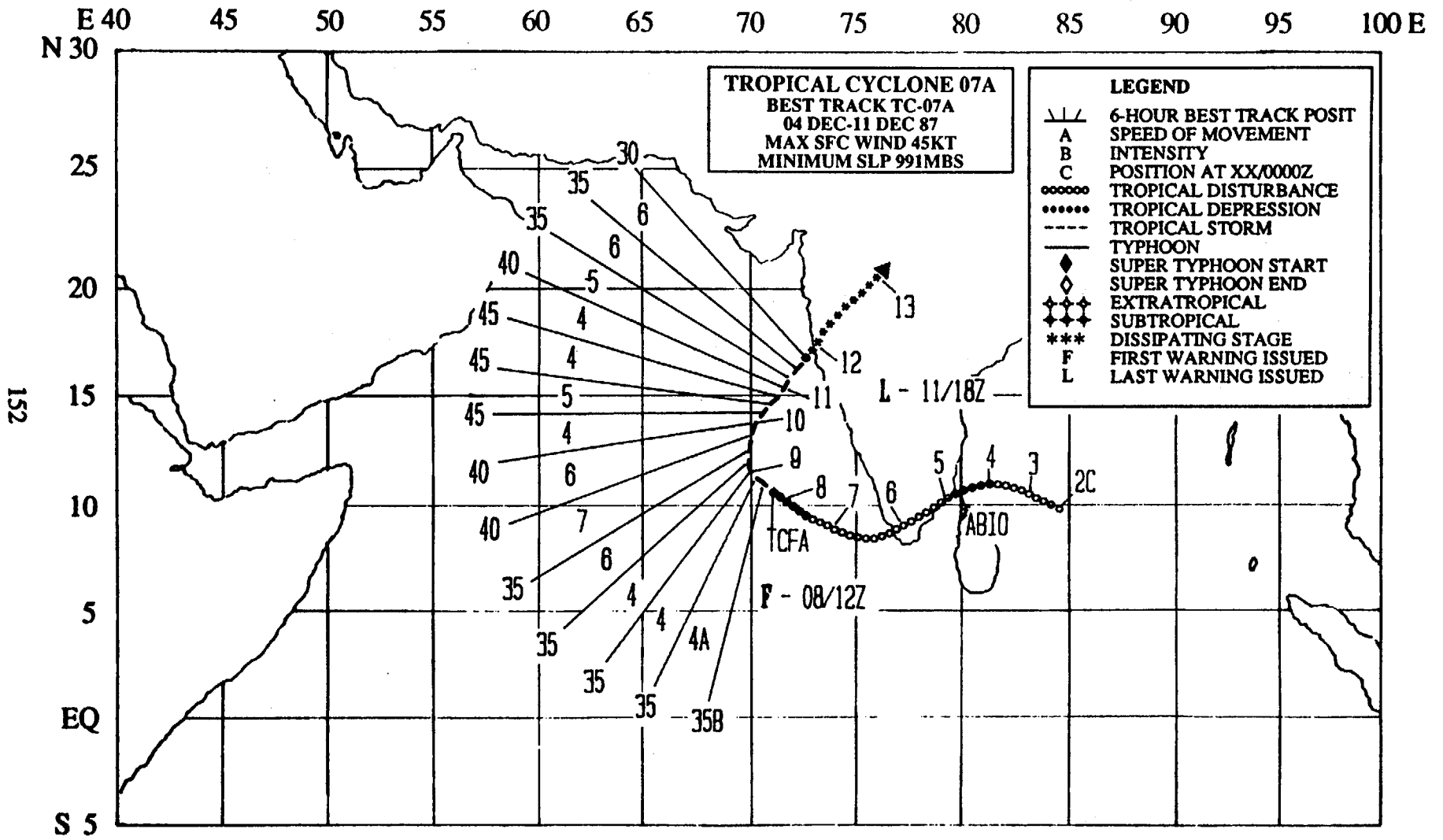


Figure 3-06B-1. Tropical Cyclone 06B became evident on satellite imagery on 8 November as a weakly organized area of convection in the northern Andaman Sea. Initially, it was associated with a broad band of monsoonal cloudiness which extended from the southern India eastward to the central Andaman Sea. First mention of the suspect area occurred on the Significant Tropical Weather Advisory (ABIO PGTW) at 101800Z. Sparse synoptic data implied a closed, low-level cyclonic circulation and associated upper-level divergent flow. As the tropical cyclone's organization increased, a Tropical Cyclone Formation Alert was issued at 102027Z (see above imagery), followed by the first warning at 111800Z. Tropical Cyclone 06B reached a peak intensity of 50 kt (26 m/sec) at 121800Z (see above imagery) as it turned northwestward. Four hours later it made landfall and rapidly weakened while moving into the Eastern Ghats mountains along the coast. The final warning was issued at 130000Z (120929Z November NOAA visual imagery).



TROPICAL CYCLONE 07A

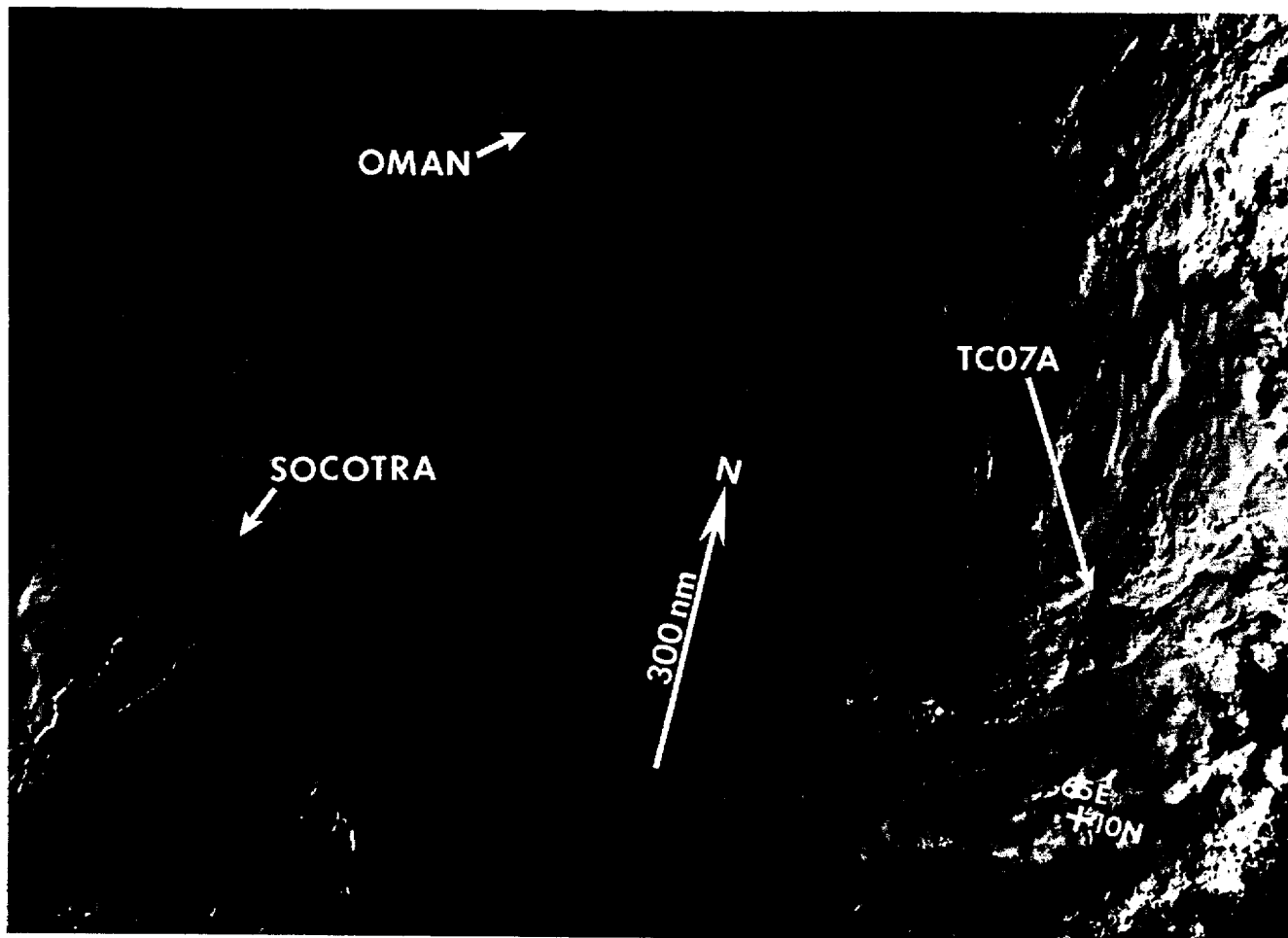
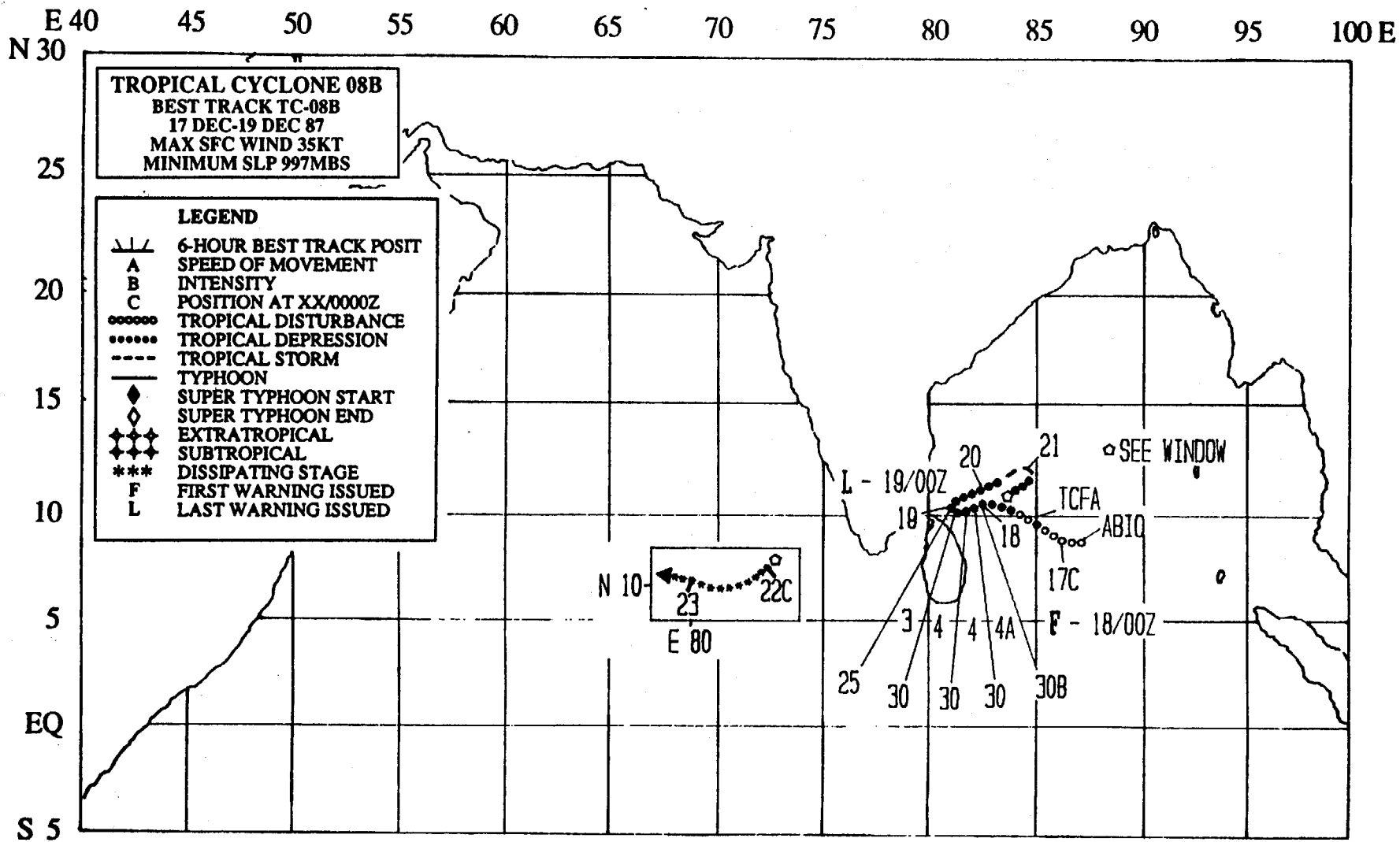


Figure 3-07A-1. Tropical Cyclone 07A was the first significant tropical cyclone in the Arabian Sea during the month of December since 1980. It also marked the first time since 1979 that seven significant tropical cyclones have occurred in the North Indian Ocean. Tropical Cyclone 07A initially developed as an exposed low-level circulation on December 2nd. It slowly intensified, reaching an intensity of 30 kt (15 m/sec) shortly before making landfall on the southeast coast of India at 041900Z, 150 nm (278 km) south of the city of Madras. No warnings were issued on this tropical depression in the Bay of Bengal, however it was mentioned on the 041800Z Significant Tropical Weather Advisory (ABIO PGTW) as having poor potential to develop into a significant tropical cyclone due to its proximity to land. Synoptic data indicated the disturbance maintained its identity as it tracked across the southern tip of India. Once the system moved out over water it reintensified in the Arabian Sea, JTWC issued a Tropical Cyclone Formation Alert at 080930Z. The first warning followed a few hours later at 081200Z, with winds of 35 kt (18 m/sec) based on a satellite intensity analysis (Dvorak, 1984). A maximum intensity of 45 kt (23 m/sec) was reached at 101200Z prior to Tropical Cyclone 07A recurving northward through a break in the subtropical ridge. It then headed toward the western coast of India where increasing vertical wind shear on the 11th weakened Tropical Cyclone 07A before it made landfall at 120000Z, 90 nm (167 km) south of Bombay. No reports of extensive damage or loss of life were received. The above stored data mosaic shows the system just prior to reaching maximum intensity (100202Z December DMSP visual imagery).



154

TROPICAL CYCLONE 08B

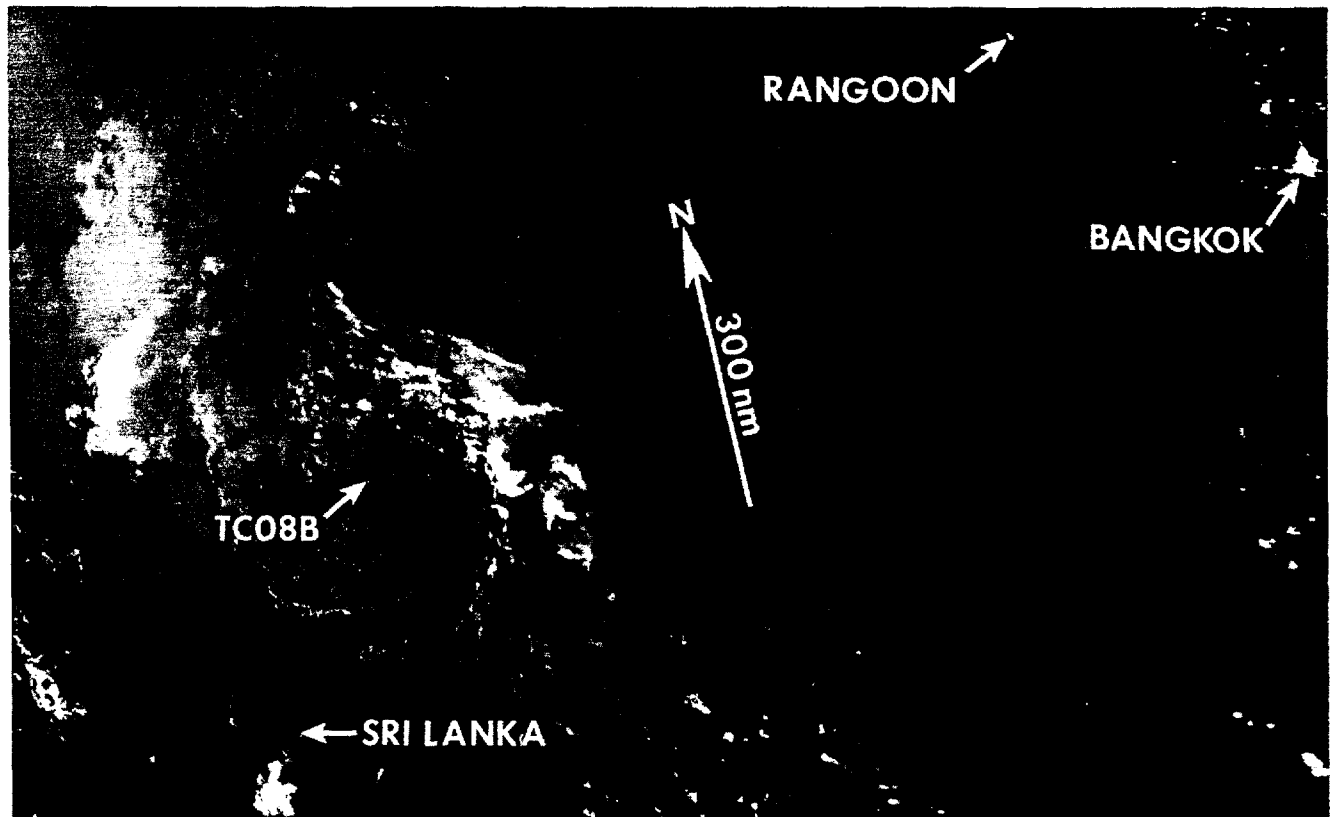


Figure 3-08B-1. Tropical Cyclone 08B was the record-setting eighth significant tropical cyclone to develop in the North Indian Ocean in 1987 and the second system to occur in December. It began as a rapidly organizing tropical disturbance 375 nm (695 km) east of Sri Lanka on the 16th. Tropical Cyclone 08B was mentioned for the first time on the 161800Z Significant Tropical Weather Advisory (ABIO PGTW) and was classified as having fair potential to develop into a significant tropical cyclone based on a low-level cyclonic circulation evident in the synoptic data and an improving upper-level outflow pattern. A Tropical Cyclone Formation Alert (TCFA) was issued the following day at 170800Z when it became apparent the system was increasing in the amount of convection and in organization. Satellite intensity analysis (Dvorak, 1984) estimated 25 kt (13 m/sec) winds at the surface, at that time. The first warning on Tropical Cyclone 08B came six hours later when it developed a central dense overcast and the satellite intensity estimate reached 30 kt (15 m/sec). Tropical Cyclone 08B was initially forecast to move inland near Madras, India and dissipate within 48-hours; however, the system slowed dramatically on the 18th. It changed course at 190000Z and headed toward the northeast. JTWC issued a final warning at 190000Z when it appeared the upper- and lower-level centers had become displaced by strong vertical shear. The exposed low-level circulation center maintained its identity during the subsequent 24-hour period and re-developed its central convection. A second TCFA was issued at 200630Z as the remnants of Tropical Cyclone 08B tracked northeastward and improved in organization. No further warnings were issued, however, despite several satellite intensity estimates of 35 kt (18 m/sec) on the 20th because JTWC believed the intensity was at, or below, warning criteria and not expected to develop further. On the 21st, the tropical cyclone began to weaken and looped unexpectedly back toward the Indian subcontinent (see above imagery). It made landfall on the 23rd on the Indian coast, 165 nm (306 km) south of Madras, India. No reports of major damage or loss of life were received (211229Z December DMSP visual imagery).

CHAPTER IV - SUMMARY OF SOUTH PACIFIC AND SOUTH INDIAN OCEAN TROPICAL CYCLONES

1. GENERAL

The JTWC area of responsibility (AOR) was expanded on 1 October 1980 -- to include the southern hemisphere from 180 degrees Longitude westward to the east coast of Africa. Details on tropical cyclones in this region for July 1980 to June 1982 are contained in Diercks et al, (1982). For the July 1982 through June 1984 period, reference the NOCC/JTWC TECH NOTE 86-1. As in earlier reports, data on tropical cyclones forming in, or moving into, the South Pacific Ocean east of 180 degrees Longitude, which is the Naval Western Oceanography Center's (NAVWEST-OCEANCEN) AOR, are included for completeness. JTWC provides the sequential

numbering for all South Pacific and South Indian Ocean significant tropical cyclones. The current convention (as stated in USCINCPACINST 3140.1 (series)) for labelling tropical cyclones that develop in the South Indian Ocean (west of 135 degrees East Longitude) is to add the suffix "S" to the assigned tropical cyclone number, while those originating in the South Pacific Ocean (east of 135 degrees East Longitude) receive a "P" suffix. The "P" suffix also applies to significant tropical cyclones which form east of 180 degrees Longitude in the South Pacific Ocean. Also, it should be noted that to encompass the southern hemisphere tropical cyclone season, which

TABLE 4-1. SOUTH PACIFIC AND SOUTH INDIAN OCEANS 1987 SIGNIFICANT TROPICAL CYCLONES

TROPICAL CYCLONE	PERIOD OF WARNING	CALENDAR DAYS OF WARNING	NUMBER WARNINGS ISSUED	MAXIMUM SURFACE WINDS - KT (M/S)	ESTIMATED MSLP - MB
01S -----	01 AUG - 03 AUG	3	4	40 (21)	994
02P OSEA	22 NOV - 25 NOV	4	7	55 (28)	984
03P PATSY	14 DEC - 18 DEC	5	8	55 (28)	984
04P RAJA	23 DEC - 01 JAN	10	18	90 (46)	953
05P SALLY	28 DEC - 04 JAN	8	16	65 (33)	976
06S -----	07 JAN - 09 JAN	3	5	45 (23)	991
07S -----	10 JAN - 12 JAN	3	5	55 (28)	984
08P TUSI	16 JAN - 20 JAN	5	10	100 (51)	943
09S ALININA	16 JAN - 20 JAN	5	8	75 (39)	967
09S ALININA*	22 JAN - 23 JAN	2	4	65 (33)	976
10S CONNIE	17 JAN - 20 JAN	4	6	55 (28)	984
11P IRMA	19 JAN - 20 JAN	2	3	30 (15)	1000
12S DAMIEN	01 FEB - 05 FEB	5	9	50 (26)	987
13P -----	04 FEB - 05 FEB	2	4	40 (21)	994
14P UMA	05 FEB - 09 FEB	5	9	80 (41)	963
15P JASON	07 FEB - 13 FEB	7	13	65 (33)	976
16P VELI	08 FEB - 09 FEB	2	3	30 (15)	1000
17S CLOTILDA	11 FEB - 16 FEB	6	11	50 (26)	987
18S ELSIE	22 FEB - 25 FEB	4	7	60 (31)	980
19P -----	28 FEB - 01 MAR	2	3	40 (21)	994
20P WINI	01 MAR - 06 MAR	6	9	65 (33)	976
21S DAODO	03 MAR - 15 MAR	13	25	75 (39)	967
22P YALI	08 MAR - 12 MAR	5	8	65 (33)	976
23P KAY	08 APR - 16 APR	9	17	65 (33)	976
24S -----	23 APR - 26 APR	4	8	75 (39)	967
25P ZUMAN	23 APR - 26 APR	4	8	55 (28)	984
26S -----	24 APR - 26 APR	3	5	45 (23)	991
27P BLANCHE	22 MAY - 25 MAY	4	7	55 (28)	984
28S -----	25 JUN - 27 JUN	3	5	35 (18)	997

1987 TOTALS: 94 ** 245

* REGENERATED

** OVERLAPPING DAYS INCLUDED ONLY ONCE IN SUM.

NOTE: NAMES OF CYCONES GIVEN BY REGIONAL WARNING CENTERS (NANDI, BRISBANE, DARWIN, PERTH AND MAURITIUS) AND ARE APPENDED TO JTWC WARNINGS, WHEN AVAILABLE.

TABLE 4-2.

FREQUENCY OF CYCLONES BY MONTH AND YEAR

YEAR	JUL	AUG	SEP	OCT	NOV	DEC	JAN	FEB	MAR	APR	MAY	JUN	TOTAL
(1959 - 1978) AVERAGE*	-	-	-	0.4	1.5	3.6	6.1	5.8	4.7	2.1	0.5	-	24.7
1981	0	0	0	1	3	2	6	5	3	3	1	0	24
1982	1	0	0	1	1	3	9	4	2	3	1	0	25
1983	1	0	0	1	1	3	5	6	3	5	0	0	25
1984	1	0	0	1	2	5	5	10	4	2	0	0	30
1985	0	0	0	0	1	7	9	9	6	3	0	0	35
1986	0	0	1	0	1	1	9	9	6	4	2	0	33
1987	0	1	0	0	1	3	6	8	3	4	1	1	28
(1981 - 1987) AVERAGE	0.4	0.1	0.1	0.6	1.4	3.4	7.0	7.3	3.9	3.4	0.7	0.1	28.6
CASES	3	1	1	4	10	24	49	51	27	24	5	1	200

occurs from January through April, the limits of each tropical cyclone year are defined as 1 July to 30 June. Thus, the 1987 southern hemisphere tropical cyclone year is from 1 July 1986 to 30 June 1987. (This is in contrast to the

convention of labelling northern hemisphere tropical cyclones which is based on the calendar year - 1 January to 31 December - to include the seasonal activity from May through December.)

TABLE 4-3. YEARLY VARIATION OF TROPICAL CYCLONES BY OCEAN BASIN

YEAR	SOUTH INDIAN (105 E WESTWARD)	AUSTRALIAN (105 E - 165 E)	SOUTH PACIFIC (165 E EASTWARD)	TOTAL
(1959 - 1978) AVERAGE*	8.4	10.3	5.9	24.7
1981	13	8	3	24
1982	12	11	2	25
1983	7	6	12	25
1984	14	14	2	30
1985	14	15	6	35
1986	14	16	3	33
1987	9	8	11	28
(1981 - 1987) AVERAGE	11.9	11.1	5.6	28.6
CASES	83	78	39	200

* (GRAY, 1979)

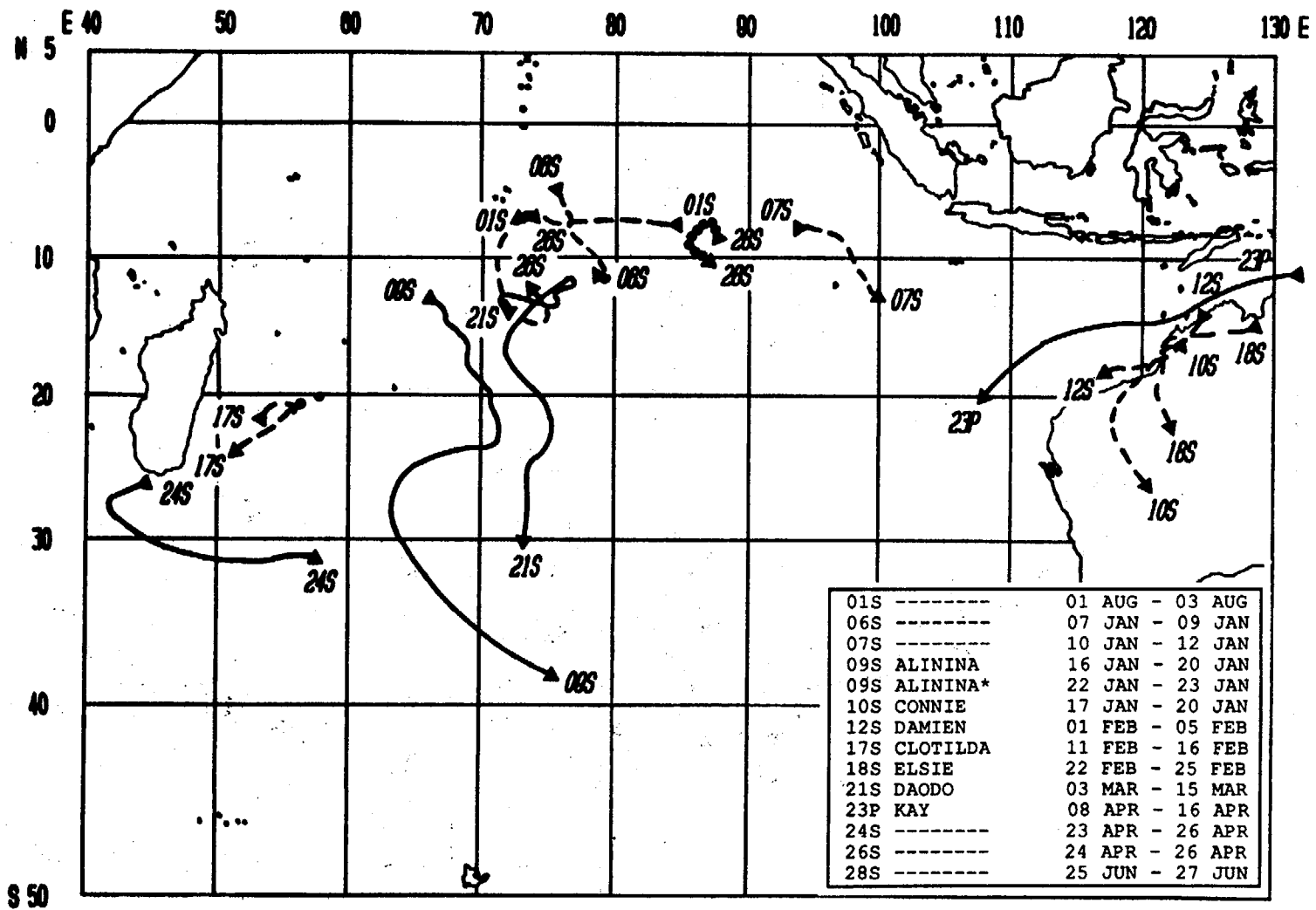
TABLE 4-4. MAXIMUM SUSTAINED SURFACE WINDS VERSUS MINIMUM SEA-LEVEL PRESSURE (ATKINSON AND HOLLIDAY, 1977)

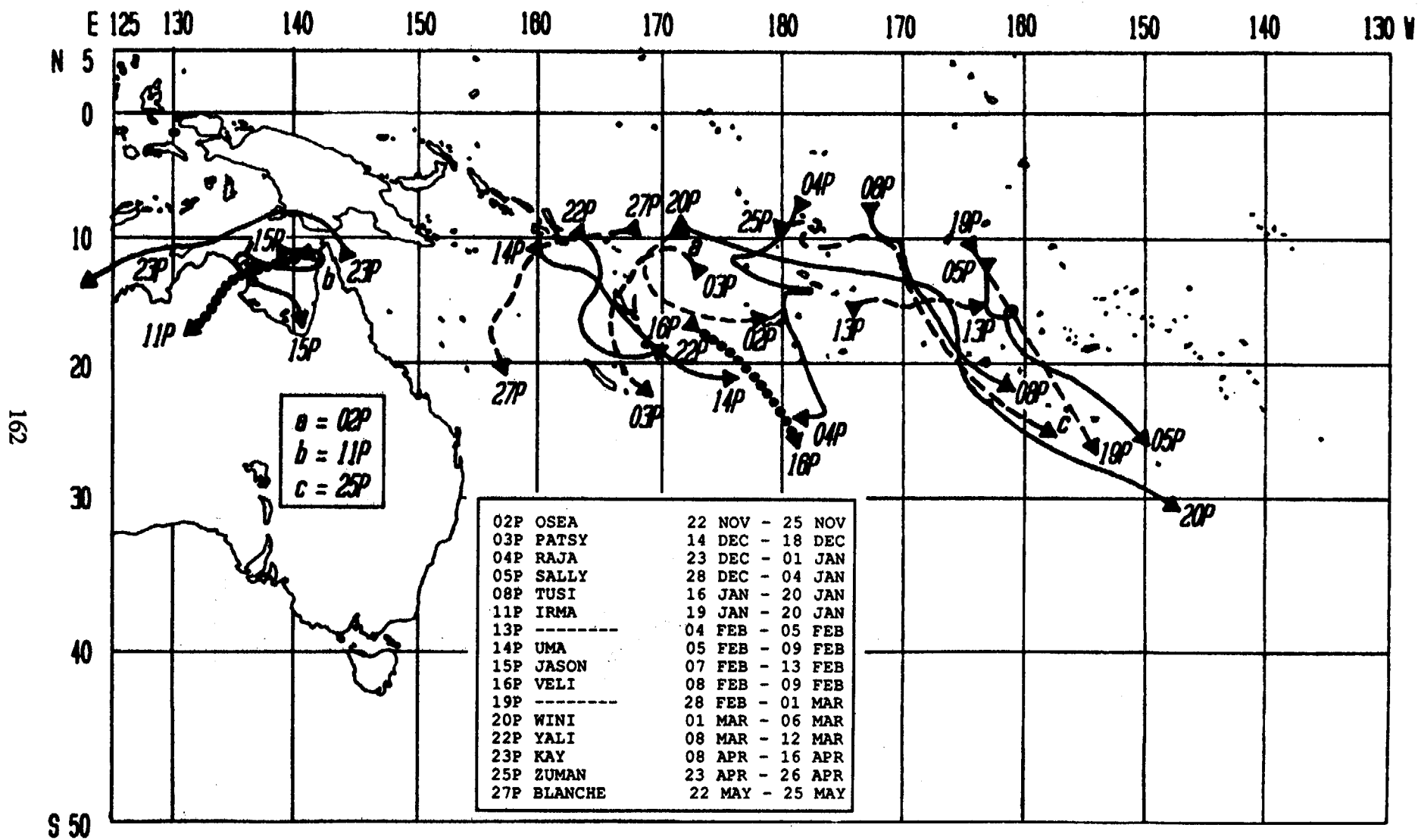
MAXIMUM SUSTAINED SURFACE WIND (KT)	EQUIVALENT MINIMUM SEA-LEVEL PRESSURE (MB)
30.....	1000
35.....	997
40.....	994
45.....	991
50.....	987
55.....	984
60.....	980
65.....	976
70.....	972
75.....	967
80.....	963
85.....	958
90.....	954
95.....	948
100.....	943
105.....	938
110.....	933
115.....	927
120.....	922
125.....	916
130.....	910
135.....	904
140.....	898
145.....	892
150.....	885
155.....	879
160.....	872
165.....	865
170.....	858

2. SOUTH PACIFIC AND SOUTH INDIAN OCEAN TROPICAL CYCLONES

The 1987 year (1 July 1986 through 30 June 1987) was active, with 28 significant tropical cyclones (see Table 4-1) reaching warning status. This did not exceed the total of 33 tropical cyclones for 1986 (1 July 1985 - 30 June 1986). Eleven tropical cyclones occurred in the South Pacific, east of 165 degrees East Longitude, which is about twice the long-term mean. The Australian area (105 to 165 degrees East Longitude) accounted for eight tropical cyclones compared to the climatological mean of 10.3 - two less than normal. Nine tropical cyclones developed in the South Indian Ocean, which is about one more than the long-term mean of 8.4 cyclones (see Tables 4-2 and 4-3). Meteorological satellite surveillance of tropical cyclones has been updating climatologies since the early 1960s. (This meteorological watch from space detects tropical cyclones that might have previously gone undetected over the conventional data sparse oceanic areas.) Thus, tropical cyclone climatologies should continue to benefit from increased surveillance from space in some areas, for example, the South Indian Ocean.

Caveat: Intensity estimates for southern hemisphere tropical cyclones are derived primarily from satellite imagery evaluation (Dvorak, 1984) and from intensity estimates reported by other regional centers. Only, in extremely rare instances are the intensity estimates based on surface observational data. Estimates of the minimum sea-level pressure are usually derived from the Atkinson and Holliday (1977) relationship between the maximum sustained one-minute surface wind and the minimum sea-level pressure (Table 4-4). This relationship has been shown to be representative for tropical cyclones in the western North Pacific and is also used by the Australian regional warning centers to provide intensity estimates. However, since these pressure estimates are usually based on wind intensities that were derived from interpretation of satellite imagery, considerable caution should be exercised when using these resultant pressure values in future tropical cyclone work.





CHAPTER V - SUMMARY OF FORECAST VERIFICATION

1. ANNUAL FORECAST VERIFICATION

a. Western North Pacific Ocean

The positions given for warning times and those at the 24-, 48- and 72-hour forecast times were verified against the final best track positions at the same valid times. The (scalar) forecast, along-track and cross-track errors (illustrated in Figure 5-1) were then calculated for each tropical cyclone and are presented in Tables 5-1A, 5-1B, 5-1C and 5-1D. Figures 5-2A through 5-2C provide, respectively, the frequency distributions of forecast errors in 30 nm increments for 24-, 48-, and 72-hour forecasts of all 1987 tropical cyclones in the western North Pacific. A summation of the mean forecast errors, as calculated for all tropical cyclones in each year, is shown in Table 5-2A. Table 5-2B includes along-track and cross-track errors for 1987. A comparison of the annual mean forecast errors for all tropical cyclones as compared to those tropical cyclones that reached typhoon intensity can be seen in Table 5-3. The mean forecast errors for 1987 as compared to the ten previous years are graphed in Figure 5-3.

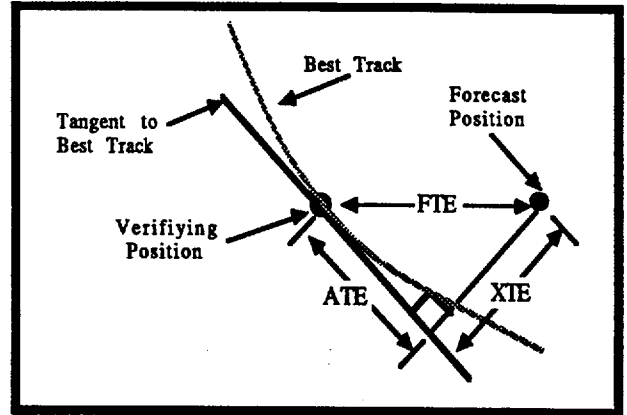
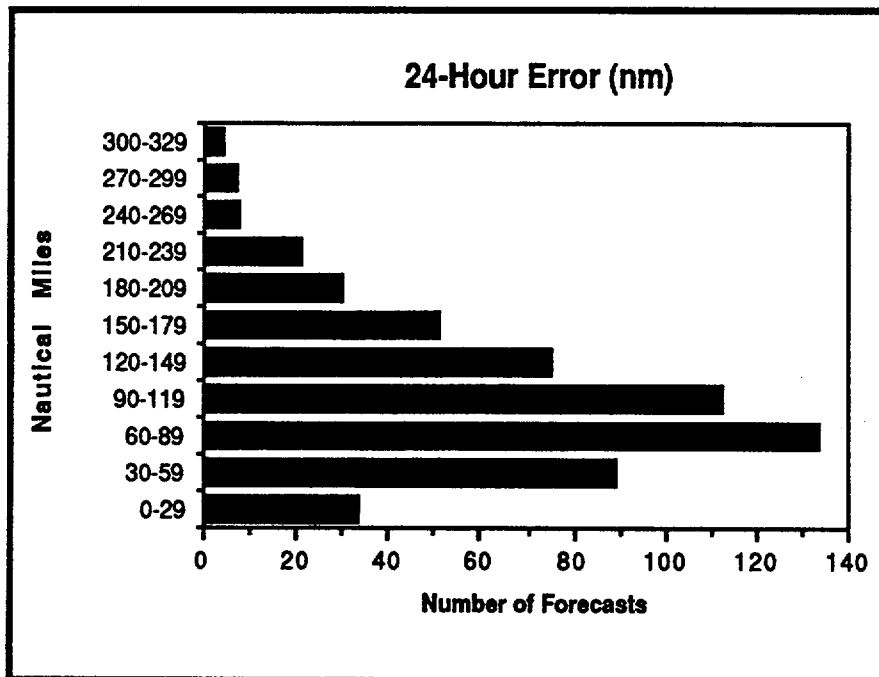


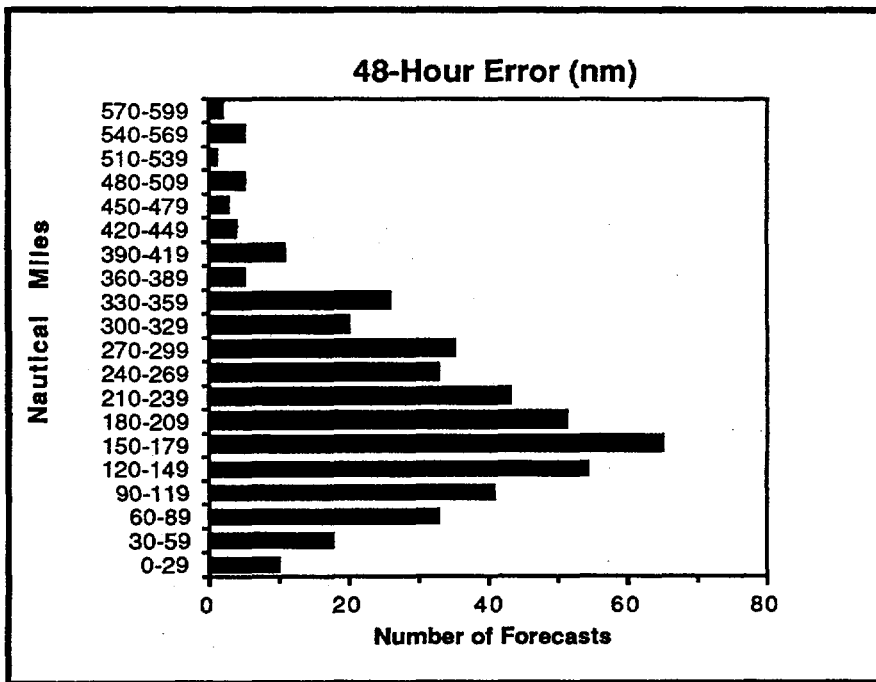
Figure 5-1. Definition of cross-track error (XTE), along-track error (ATE), and forecast track error (FTE). In this example, the XTE is positive (to the right of the Best Track) and the ATE is negative (behind or slower than the Best Track)..



FORECAST ERRORS (NM)

	24-HOUR
MEAN:	107
MEDIAN:	106
STANDARD DEVIATION:	60
CASES:	563

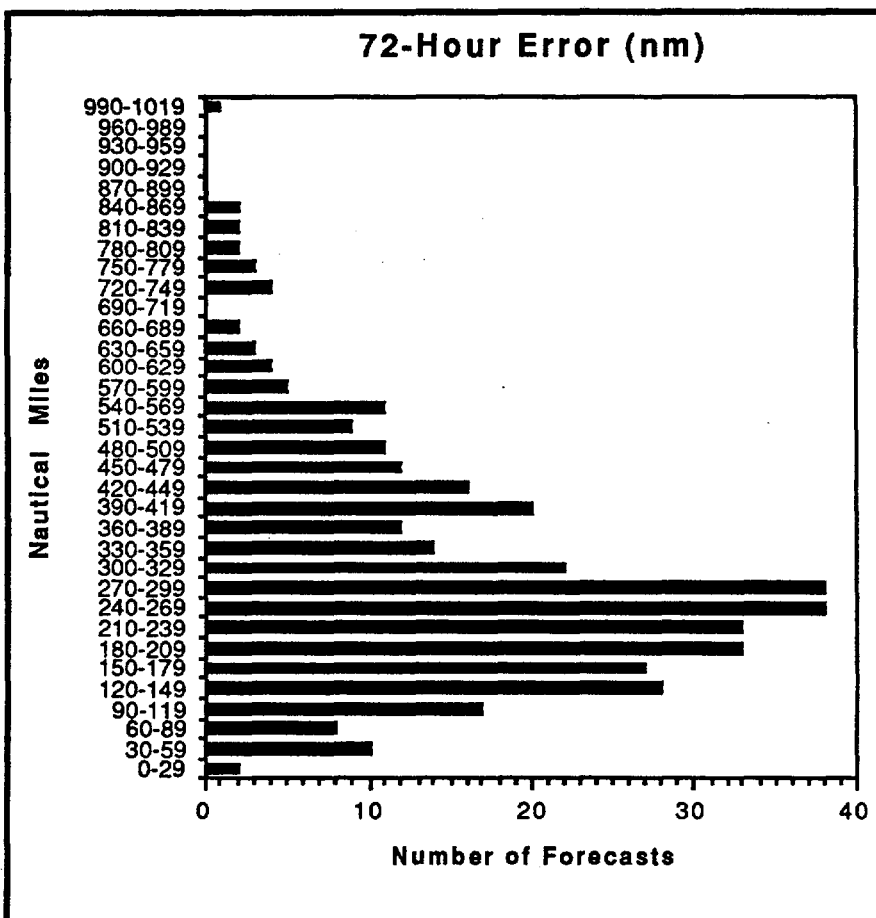
Figure 5-2A. Frequency distribution of the 24-hour forecast errors in 30 nm (56 km) increments for all significant tropical cyclones in the western North Pacific during 1987.



FORECAST ERRORS (NM)

	<u>48-HOUR</u>
MEAN:	204
MEDIAN:	202
STANDARD DEVIATION:	111
CASES:	465

Figure 5-2B. Frequency distribution of the 48-hour forecast errors in 30 nm (56 km) increments for all significant tropical cyclones in the western North Pacific during 1987.



FORECAST ERRORS (NM)

	<u>72-HOUR</u>
MEAN:	303
MEDIAN:	299
STANDARD DEVIATION:	171
CASES:	389

Figure 5-2C. Frequency distribution of the 72-hour forecast errors in 30 nm (56 km) increments for all significant tropical cyclones in the western North Pacific during 1987.

TABLE 5-1A. INITIAL POSITION ERROR SUMMARY FOR
THE WESTERN NORTH PACIFIC OCEAN
SIGNIFICANT TROPICAL CYCLONES OF 1987
(ERRORS IN NM)

TROPICAL CYCLONE	ERROR	NUMBER OF WARNINGS
(01W) TY ORCHID	17	23
(02W) TS PERCY	19	9
(03W) TS RUTH	13	5
(04W) TY SPERRY	16	17
(05W) STY THELMA	18	33
(06W) TY VERNON	33	21
(07W) TY WYNNE	15	39
(08W) TY ALEX	15	22
(09W) STY BETTY	7	31
(10W) TY CARY	15	39
(11W) STY DINAH	19	41
(12W) TS ED	33	11
(13W) TY FRED A	16	50
(14W) TY GERALD	20	24
(15W) STY HOLLY	23	43
(16W) TY IAN	14	33
(17W) TD 17W	21	7
(02C) TY PEKE	19	23
(18W) TS JUNE	33	9
(19W) TY KELLY	16	27
(20W) STY LYNN	17	44
(21W) TS MAURY	27	29
(22W) STY NINA	17	39
(23W) TS OGDEN	26	4
(24W) TY PHYLLIS	16	34

MEAN 18 TOTAL 657*

* DOES NOT INCLUDE DISSIPATED OR EXTRATROPICAL WARNINGS.

TABLE 5-1B. 24-HOUR FORECAST ERROR SUMMARY FOR
THE WESTERN NORTH PACIFIC OCEAN
SIGNIFICANT TROPICAL CYCLONES OF 1987
(ERRORS IN NM)

TROPICAL CYCLONE	FORECAST ERROR	ALONG-TRACK ERROR		CROSS-TRACK ERROR		NUMBER OF WARNINGS
		ABS MAG	BIAS	ABS MAG	BIAS	
(01W) TY ORCHID	41	72	-47	46	5	19
(02W) TS PERCY	69	47	*	37	*	8
(03W) TS RUTH	141	133	*	46	*	3
(04W) TY SPERRY	119	107	-85	41	30	15
(05W) STY THELMA	146	93	-77	92	50	31
(06W) TY VERNON	119	72	1	79	-48	18
(07W) TY WYNNE	107	69	-66	69	-39	36
(08W) TY ALEX	111	47	-19	90	-45	20
(09W) STY BETTY	91	57	-43	59	49	30
(10W) TY CARY	93	66	7	51	36	36
(11W) STY DINAH	96	63	-21	59	17	38
(12W) TS ED	120	55	*	97	*	10
(13W) TY FRED A	81	49	0	54	-29	47
(14W) TY GERALD	97	51	-31	69	-37	20
(15W) STY HOLLY	122	56	-5	100	-61	34
(16W) TY IAN	82	66	5	39	-32	27
(17W) TD 17W	81	66	*	30	*	3
(02C) TY PEKE	145	117	-105	71	-72	18
(18W) TS JUNE	65	130	*	90	*	2
(19W) TY KELLY	110	75	-22	68	-38	25
(20W) STY LYNN	89	59	-4	58	-7	41
(21W) TS MAURY	107	45	29	89	-5	19
(22W) STY NINA	138	121	-105	46	0	36
(23W) TS OGDEN	99	38	*	91	*	2
(24W) TY PHYLLIS	129	80	16	86	10	25
TOTALS	107	71	-30	64	-8	563

* Indicates too few cases (< 10) to compute the median error (BIAS)

ABS MAG = Absolute Magnitude. BIAS is the median (middle value) of the sample. Specifics on along-track and cross-track error components follows:

1. The Along-Track error component is a measure of how far a warning position was displaced left or right of the best track position. The sample consists of two parts: the absolute magnitude (distance) and the bias (negative values (minus sign) were left of track and positive values (plus sign) were right of track).

2. The Cross-Track error component is a measure of how far the warning position was displaced ahead or behind the best track position. The sample consists of two parts: The absolute magnitude (distance) and the bias (negative values (minus sign) were behind or slow and positive values (plus sign) were ahead or fast).

TABLE 5-1C.

48-HOUR FORECAST ERROR SUMMARY FOR
THE WESTERN NORTH PACIFIC OCEAN
SIGNIFICANT TROPICAL CYCLONES OF 1987
(ERRORS IN NM)

TROPICAL CYCLONE	FORECAST ERROR	ALONG-TRACK ERROR		CROSS-TRACK ERROR		NUMBER OF WARNINGS
		ABS MAG	BIAS	ABS MAG	BIAS	
(01W) TY ORCHID	158	116	-69	94	13	15
(02W) TS PERCY	116	110	*	18	*	4
(03W) TS RUTH	---	---	---	---	---	0
(04W) TY SPERRY	242	197	-201	122	119	12
(05W) STY THELMA	311	240	-179	160	73	28
(06W) TY VERNON	180	107	-6	130	-98	14
(07W) TY WYNNE	218	153	-156	124	-30	30
(08W) TY ALEX	204	129	-129	143	-120	16
(09W) STY BETTY	197	99	-95	147	144	26
(10W) TY CARY	163	102	6	106	99	33
(11W) STY DINAH	172	126	-23	98	19	34
(12W) TS ED	219	181	*	78	*	6
(13W) TY FREDA	181	84	-10	150	-99	42
(14W) TY GERALD	163	82	-47	121	-15	18
(15W) STY HOLLY	275	128	0	229	-202	33
(16W) TY IAN	201	164	69	83	-58	23
(17W) TD 17W	---	---	---	---	---	0
(02C) TY PEKE	310	271	-275	126	-93	11
(18W) TS JUNE	66	53	*	31	*	2
(19W) TY KELLY	183	138	-60	99	-43	21
(20W) STY LYNN	184	127	-3	117	-18	39
(21W) TS MAURY	162	86	70	123	26	13
(22W) STY NINA	235	181	-164	94	55	32
(23W) TS OGDEN	---	---	---	---	---	0
(24W) TY PHYLLIS	171	104	35	110	8	13
TOTALS	204	134	-58	127	-12	465

TABLE 5-1D.

72-HOUR FORECAST ERROR SUMMARY FOR
THE WESTERN NORTH PACIFIC OCEAN
SIGNIFICANT TROPICAL CYCLONES OF 1987
(ERRORS IN NM)

TROPICAL CYCLONE	FORECAST ERROR	ALONG-TRACK ERROR		CROSS-TRACK ERROR		NUMBER OF WARNINGS
		ABS MAG	BIAS	ABS MAG	BIAS	
(01W) TY ORCHID	234	150	-100	143	79	11
(02W) TS PERCY	206	167	*	53	*	4
(03W) TS RUTH	---	---	---	---	---	0
(04W) TY SPERRY	421	325	*	258	*	9
(05W) STY THELMA	479	419	-270	174	90	24
(06W) TY VERNON	224	133	*	145	*	10
(07W) TY WYNNE	332	228	-207	198	-86	30
(08W) TY ALEX	330	254	-245	182	-97	12
(09W) STY BETTY	257	176	-178	165	136	17
(10W) TY CARY	248	75	2	222	218	28
(11W) STY DINAH	222	154	-6	123	3	30
(12W) TS ED	278	238	*	115	*	5
(13W) TY FREDA	327	177	6	222	-190	34
(14W) TY GERALD	193	135	-31	129	57	14
(15W) STY HOLLY	455	240	-35	342	-299	31
(16W) TY IAN	344	252	122	191	-52	21
(17W) TD 17W	---	---	---	---	---	0
(02C) TY PEKE	247	181	*	148	*	5
(18W) TS JUNE	264	167	*	205	*	1
(19W) TY KELLY	289	216	-159	134	-39	17
(20W) STY LYNN	298	191	27	192	-18	31
(21W) TS MAURY	183	102	101	140	47	12
(22W) STY NINA	279	196	-191	151	93	30
(23W) TS OGDEN	---	---	---	---	---	0
(24W) TY PHYLLIS	196	164	24	76	64	13
TOTALS	303	198	-78	186	-13	389

TABLE 5-2A. ANNUAL MEAN FORECAST ERRORS FOR THE WESTERN NORTH PACIFIC

YEAR	24-HOUR		48-HOUR		72-HOUR	
	FORECAST	RIGHT ANGLE	FORECAST	RIGHT ANGLE	FORECAST	RIGHT ANGLE
1971	111	64	212	118	317	117
1972	117	72	245	146	381	210
1973	108	74	197	134	253	162
1974	120	78	226	157	348	245
1975	138	84	288	181	450	290
1976	117	71	230	132	338	202
1977	148	83	283	157	407	228
1978	127	75	271	179	410	297
1979	124	77	226	151	316	223
1980	126	79	243	164	389	287
1981*	123	75	220	119	334	168
1982*	113	67	237	139	341	206
1983*	117	72	259	152	405	237
1984*	117	66	233	137	363	231
1985*	117	66	231	134	367	214
1986	121	**	261	**	394	**
1987	107	**	204	**	303	**

* THE TECHNIQUE FOR CALCULATING RIGHT-ANGLE ERROR WAS REVISED IN 1981; THEREFORE, A DIRECT CORRELATION IN RIGHT-ANGLE STATISTICS CANNOT BE MADE FOR THE ERRORS COMPUTED BEFORE 1981 AND THE ERRORS COMPUTED SINCE 1981.

** IN 1986, THE RIGHT-ANGLE ERROR WAS REPLACED BY CROSS-TRACK ERROR (SEE FIGURE 5-1 FOR THE DEFINITION OF CROSS-TRACK ERROR).

TABLE 5-2B. 1987 MEAN FORECAST, ALONG-TRACK AND CROSS-TRACK ERRORS FOR THE WESTERN NORTH PACIFIC OCEAN (ERRORS IN NM).

TIMES:	FORECAST ERROR	ALONG-TRACK ERROR		CROSS-TRACK ERROR	
		ABS MAG	BIAS	ABS MAG	BIAS
24-HOUR	107	71	-30	64	-8
48-HOUR	204	134	-58	127	-12
72-HOUR	303	198	-78	186	-13

TABLE 5-3. ANNUAL MEAN FORECAST ERRORS FOR THE WESTERN NORTH PACIFIC (ERRORS ARE IN NAUTICAL MILES)

YEAR	24-HOUR ALL TYPHOON*		48-HOUR ALL TYPHOON*		72-HOUR ALL TYPHOON*	
1950-1958	170					
1959	117**		267**			
1960	177**		354**			
1961	136		274			
1962	144		287		476	
1963	127		246		374	
1964	133		284		429	
1965	151		303		418	
1966	136		280		432	
1967	125		276		414	
1968	105		229		337	
1969	111		237		349	
1970	104	98	190	181	279	272
1971	111	99	212	203	317	308
1972	117	116	245	245	381	382
1973	108	102	197	193	253	245
1974	120	114	226	218	348	357
1975	138	129	288	279	450	442
1976	117	117	230	232	338	336
1977	148	140	283	266	407	390
1978	127	120	271	241	410	459
1979	124	113	226	219	316	319
1980	126	116	243	221	389	362
1981	123	117	220	215	334	342
1982	113	114	237	229	341	337
1983	117	110	259	247	405	384
1984	117	110	233	228	363	361
1985	117	112	231	228	367	355
1986	121	117	261	261	394	403
1987	107	101	204	211	303	318

* FORECASTS WERE VERIFIED WHEN THE TROPICAL CYCLONE INTENSITIES WERE OVER 35 KT (18 M/SEC).

** FORECAST POSITIONS NORTH OF 35 DEGREES NORTH LATITUDE WERE NOT VERIFIED.

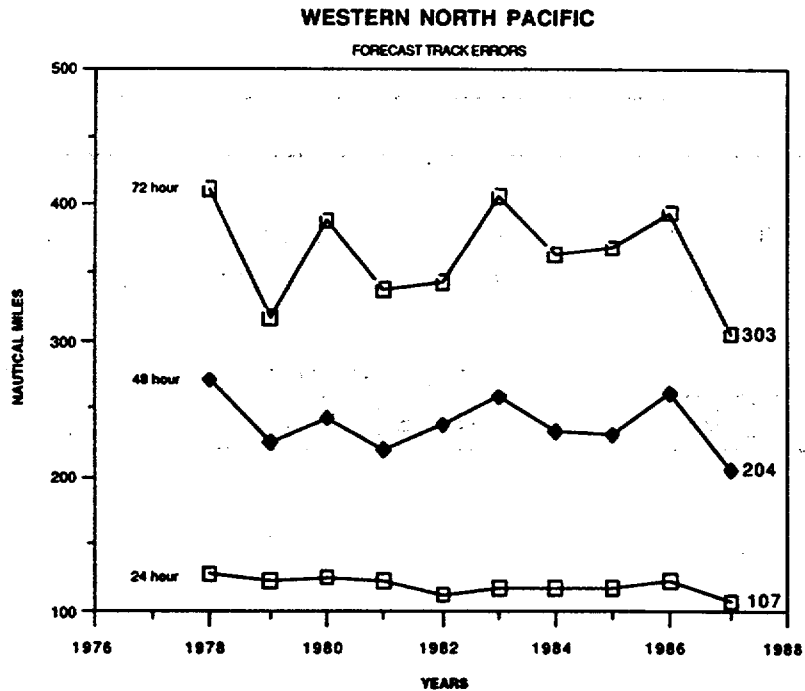


Figure 5-3. Annual mean forecast errors (in nm) for all significant tropical cyclones in the western North Pacific.

b. North Indian Ocean

The positions given for warning times and those at the 24-, 48-, and 72-hour valid times were verified for tropical cyclones in the North Indian Ocean by the same methods used for the western North Pacific. It should be noted that despite the record-setting eight North Indian Ocean tropical cyclones, these error statistics should not be taken as representative of any trend due to the small sample number.

Table 5-4 is the forecast along-track and cross-track error summary for the North Indian Ocean. Table 5-5A contains a summary of the annual mean forecast errors for each year. Table 5-5B includes along-track and cross-track errors for 1987. Forecast errors are plotted in Figure 5-4 (Seventy-two hour forecast errors were evaluated for the first time in 1979). There were no verifying 72-hour forecast in 1983 and 1985.

TABLE 5-4. 1987 FORECAST ERROR SUMMARY FOR THE NORTH INDIAN OCEAN SIGNIFICANT TROPICAL CYCLONES (ERRORS IN NM)

TROPICAL CYCLONES	ERROR	INITIAL POSITION NUMBER OF WARNINGS
TC 01B	23	11
TC 02B	33	12
TC 03A	62	18
TC 04B	12	3
TC 05B	31	14
TC 06B	16	4
TC 07A	38	14
TC 08B	123	5
MEAN	42	TOTAL 83

24-HOUR FORECASTS

TROPICAL CYCLONE	FORECAST ERROR	ALONG-TRACK ERROR		CROSS-TRACK ERROR	
		ABS MAG	BIAS	ABS MAG	BIAS
TC 01B	77	42	**	55	**
TC 02B	166	122	**	107	**
TC 03A	165	103	-95	116	-117
TC 04B	---	---	---	---	---
TC 05B	193	121	**	136	**
TC 06B	113	58	**	97	**
TC 07A	119	83	-84	75	-64
TC 08B	192	101	**	146	**
MEAN	144	91	-71	100	-50

48-HOUR FORECASTS

TROPICAL CYCLONE	FORECAST ERROR	ALONG-TRACK ERROR		CROSS-TRACK ERROR	
		ABS MAG	BIAS	ABS MAG	BIAS
TC 01B	90	26	**	55	**
TC 02B	72	37	**	52	**
TC 03A	183	106	57	124	-67
TC 04B	---	---	---	---	---
TC 05B	541	481	**	249	**
TC 06B	---	---	---	---	---
TC 07A	307	203	**	210	**
TC 08B	---	---	---	---	---
MEAN	205	125	-50	140	-91

72-HOUR FORECASTS

TROPICAL CYCLONE	FORECAST ERROR	ALONG-TRACK ERROR		CROSS-TRACK ERROR	
		ABS MAG	BIAS	ABS MAG	BIAS
TC 01B	254	165	**	192	**
TC 02B	72	63	**	36	**
TC 03A	208	144	-139	118	**
TC 04B	---	---	---	---	---
TC 05B	872	526	**	698	**
TC 06B	---	---	---	---	---
TC 07A	421	335	**	243	**
TC 08B	---	---	---	---	---
MEAN	305	219	-219	188	-63

** IF THERE WERE TEN OR LESS CASES, THE STATISTICAL PARAMETER BIAS WAS NOT COMPUTED, THOUGH EACH STATISTIC WAS INCLUDED IN THE FINAL TOTAL.

TABLE 5-5A. ANNUAL MEAN FORECAST ERRORS FOR THE NORTH INDIAN OCEAN

YEAR	24-HOUR		48-HOUR		72-HOUR	
	FORECAST	RIGHT ANGLE	FORECAST	RIGHT ANGLE	FORECAST	RIGHT ANGLE
1971*	232	--	410	---	---	---
1972*	224	101	292	112	---	---
1973*	182	99	299	160	---	---
1974*	137	81	238	146	---	---
1975	145	99	228	144	---	---
1976	138	108	204	159	---	---
1977	122	94	292	214	---	---
1978	133	86	202	128	---	---
1979	151	99	270	202	437	371
1980	115	73	93	87	167	126
1981**	109	65	176	103	197	73
1982**	138	66	368	175	762	404
1983**	117	46	153	67	---	---
1984**	154	71	274	127	388	159
1985**	123	51	242	109	---	---
1986	134	***	168	***	269	***
1987	144	***	205	***	305	***

* THE WESTERN BAY OF BENGAL AND ARABIAN SEA WERE NOT INCLUDED IN THE JTWC AREA OF RESPONSIBILITY UNTILL THE 1975 TROPICAL CYCLONE SEASON .

** THE TECHNIQUE FOR CALCULATING RIGHT-ANGLE ERROR WAS REVISED IN 1981 ; THEREFORE, A DIRECT CORRELATION IN RIGHT-ANGLE STATISTICS CANNOT BE MADE FOR THE ERRORS COMPUTED BEFORE 1981 AND THE ERRORS COMPUTED SINCE 1981.

*** IN 1986, THE RIGHT-ANGLE ERROR WAS REPLACED BY CROSS-TRACK ERROR (SEE FIGURE 5-1 FOR THE DEFINITION OF CROSS-TRACK ERROR).

TABLE 5-5B. 1987 MEAN FORECAST, ALONG-TRACK AND CROSS-TRACK ERRORS FOR THE NORTH INDIAN OCEAN (ERRORS IN NM).

TIMES:	FORECAST ERROR	ALONG-TRACK ERROR		CROSS-TRACK ERROR	
		ABS MAG	BIAS	ABS MAG	BIAS
24-HOUR	144	91	-71	100	-50
48-HOUR	205	125	-50	140	-91
72-HOUR	305	219	-219	188	-63

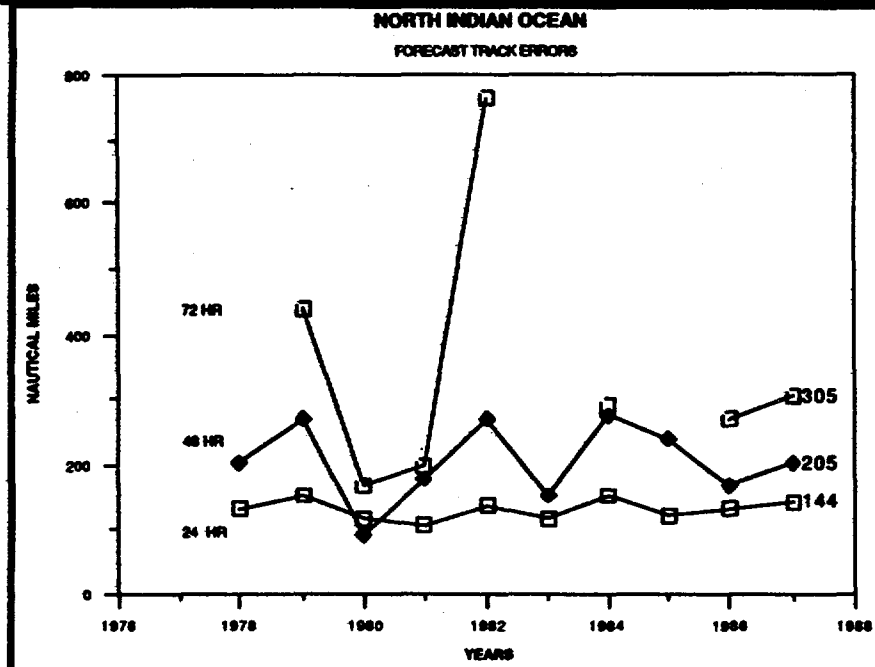


Figure 5-4. Annual mean forecast errors (in nm) for all tropical cyclones in the North Indian Ocean.

c. South Pacific and South Indian Oceans

The positions given for warning times and those at the 24-, 48-, and 72-hour valid times were verified for tropical cyclones in the Southern Hemisphere by the same methods used for the western North Pacific. It should be noted that due to the lack of verifying ground-

truth data, these error statistics should not be taken as representative of any trend. Table 5-6 is the forecast along-track and cross-track error summary for the Southern Hemisphere. Tables 5-7A and B contains a summary of the annual mean forecast errors for each year. Table 5-8 includes along- and cross-track errors for 1987. Forecast errors are plotted in Figure 5-5.

TABLE 5-6. 1987 FORECAST ERROR SUMMARY FOR THE SOUTH PACIFIC AND SOUTH INDIAN OCEAN SIGNIFICANT TROPICAL CYCLONES (ERRORS IN NM)

TROPICAL CYCLONE	NO OF WRNGS	INITIAL POS ER	NO OF WRNGS	FCST ERROR	24-HOURS		CROSS-TRACK		NO OF WRNGS	FCST ERROR	48-HOURS		CROSS-TRACK	
					ALONG-TRACK ABS MAG	BIAS	ABS MAG	BIAS			ALONG-TRACK ABS MAG	BIAS	ABS MAG	BIAS
TC 01S	4	25	3	90	56	**	57	**	1	196	49	**	190	**
TC 02P OSEA	6	33	4	141	125	**	61	**	2	292	248	**	145	**
TC 03P PATSY	6	42	4	160	67	**	135	**	2	340	141	**	296	**
TC 04P RAJA	18	35	16	171	117	-99	114	0	14	333	259	-177	176	21
TC 05P SALLY	16	41	14	139	62	-39	106	53	11	281	248	-129	97	-24
TC 06S	5	38	4	203	119	**	155	**	4	365	105	**	339	**
TC 07S	5	24	3	119	73	**	80	**	2	194	133	**	138	**
TC 08P TUSI	9	25	7	104	45	**	86	**	5	254	75	**	236	**
TC 09S ALININA	12	37	8	188	124	**	111	**	5	422	220	**	331	**
TC 10S CONNIE	6	15	5	92	34	**	80	**	4	201	58	**	183	**
TC 11P IRMA	3	13	1	17	12	**	12	**	0	---	---	---	---	---
TC 12S DAMIEN	9	35	7	138	62	**	111	**	5	135	118	**	49	**
TC 13P	3	36	2	139	53	**	125	**	0	---	---	---	---	---
TC 14P UMA	8	347	6	101	77	**	55	**	4	256	199	**	115	**
TC 15P JASON	12	27	8	120	109	**	35	**	2	369	344	**	129	**
TC 16P VELI	3	67	1	424	422	**	44	**	0	---	---	---	---	---
TC 17S CLOTILDA	10	51	7	109	61	**	86	**	6	227	151	**	154	**
TC 18S	7	11	6	147	76	**	120	**	4	369	140	**	304	**
TC 19P	3	5	1	332	325	**	69	**	0	---	---	---	---	---
TC 20P WINI	9	47	6	146	122	**	66	**	4	286	220	**	146	**
TC 21S DAODO	25	47	20	188	110	-86	136	-14	18	307	182	-38	204	0
TC 22P YALI	7	50	5	96	81	**	42	**	3	212	89	**	192	**
TC 23P KAY	17	25	12	90	50	-6	63	-24	12	166	105	1	113	-82
TC 24S	8	35	6	209	150	**	112	**	4	519	446	**	174	**
TC 25P ZUMAN	7	49	5	136	86	**	84	**	4	273	200	**	163	**
TC 26S	5	47	3	161	147	**	54	**	1	344	341	**	46	**
TC 27P BLANCHE	7	22	5	93	70	**	48	**	5	138	106	**	77	**
TC 28S	5	56	3	194	106	**	132	**	1	450	374	**	250	**
TOTALS	235	46	172	145	94	-57	90	13	123	280	195	-102	161	6

** THE STATISTICAL PARAMETER BIAS DOES NOT COMPUTE FOR INSTANCES OF TEN CASES, OR LESS.*

TABLE 5-7A. ANNUAL MEAN FORECAST ERRORS FOR THE SOUTHERN HEMISPHERE

YEAR	24-HOUR		48-HOUR	
	FORECAST	RIGHT ANGLE	FORECAST	RIGHT ANGLE
1981	165	119	315	216
1982	144	91	274	174
1983	154	84	288	150
1984	133	73	231	124
1985	138	78	242	133
1986	133	***	268	***
1987	145	***	280	***

TABLE 5-7B. 1987 MEAN FORECAST, ALONG-TRACK AND CROSS-TRACK ERRORS FOR THE SOUTHERN HEMISPHERE (ERRORS IN NM).

TIMES:	ALONG-TRACK ERROR			CROSS-TRACK ERROR	
	FORECAST ERROR	ABS MAG	BIAS	ABS MAG	BIAS
	24-HOUR	145	94	-57	90
48-HOUR	280	195	-102	161	6

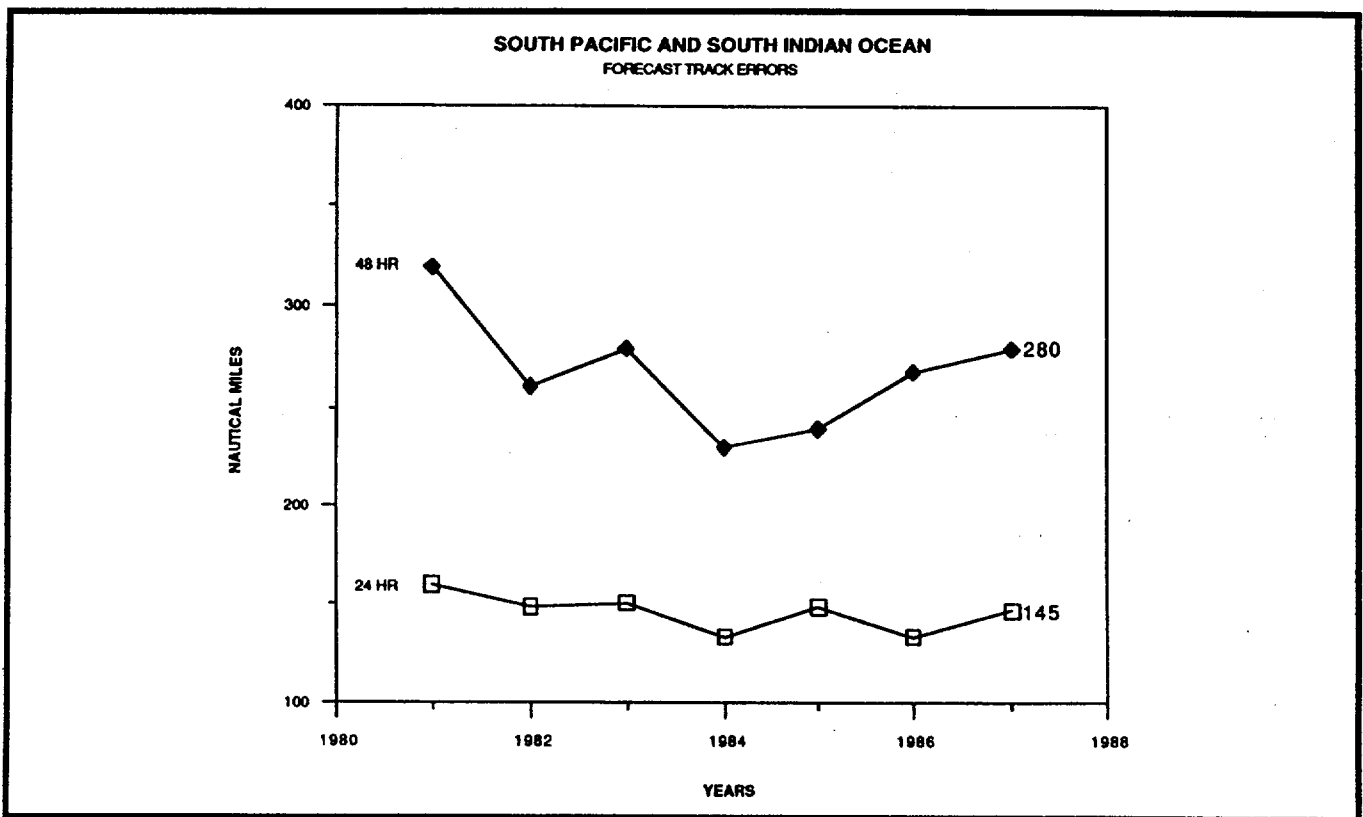


Figure 5-5. Annual mean forecast errors (in nm) for all tropical cyclones in the South Pacific and South Indian Oceans.

2. COMPARISON OF OBJECTIVE TECHNIQUES

a. General

Objective techniques used by JTWC are divided into five main categories:

- (1) extrapolation;
- (2) climatological and analog techniques;
- (3) model output statistics;
- (4) dynamic models; and
- (5) empirical and analytical techniques;

In September 1981, JTWC began to initialize its array of objective forecast techniques (described below) on the six-hour old preliminary best track position (an interpolative process) rather than the forecast (partially extrapolated) warning position, e.g. the 0600Z warning is now supported by objective techniques developed from the 0000Z preliminary best track position. This operational change has yielded several advantages:

*Techniques can now be requested much earlier in the warning development time line, i.e. as soon as the track can be approximated by one or more fix positions after the valid time of the previous warning;

*Receipt of these techniques is virtually assured prior to the development of the next warning; and

*Improved (mean) forecast accuracy. This latter aspect arises because JTWC now has more reliable approximation of the short-term tropical cyclone movement. Further, since most of the objective techniques are biased towards persistence, this new procedure optimizes their performance and provides more consistent guidance on short-term movement, indirectly yielding a more accurate initial position estimate as well as lowering 24-hour forecast errors.

b. Description of Objective Techniques

(1). XTRP -- Forecast positions for 24- and 48-hours are derived from the extension of a straight line which connects the most recent and 12-hour old preliminary best track positions.

(2). CLIM -- A climatological aid providing 24-, 48-, and 72-hour tropical cyclone forecast positions (and intensity changes in the western North Pacific) based upon the position of the tropical cyclone. The output is based upon data records from 1945 to 1981 for the western North Pacific Ocean and 1900 to 1981 for the North Indian Ocean.

(3). HPAC -- Forecast positions are generated from a blend of climatology and persistence. The 24-, 48- and 72-hour positions are equally weighted between climatology and persistence. Persistence is a straight line extension of a line connecting the current and 12-hour old positions. Climatology is based on data from 1945 to 1981 for the western North Pacific Ocean and 1900 to 1981 for the North Indian Ocean.

(4). TYAN -- An updated analog program which combines the earlier versions TYFN 75 and INJAN 74. The program scans a 30-year climatology with a similar history (within a specified acceptance envelope) to the current tropical cyclone. For the western North Pacific Ocean, three forecasts of position and intensity are provided for 24-, 48-, and 72-hours: RECR - a weighted mean of all tropical cyclones which were categorized as "recurving" during their best track period; STRA - a weighted mean of all accepted tropical cyclones which were categorized as moving "straight" (westward) during their best track period; TOTL - a weighted mean of all accepted tropical cyclones, including those used in the RECR and STRA forecast. For the North Indian Ocean, a single (total) forecast track is provided for the 12-hour intervals to 72-hours.

(5). COSMOS -- A model output statistics (MOS) routine based on the geostrophic steering at the 850-, 700-, and 500-mb levels. The steering is derived from the HATTRACK point advection model run on Global prognostic fields from the FLENUM-OCEANCEN's NOGAPS prediction system. The MOS forecast is then blended with the 6-hour past movement to generate the forecast track.

(6). Colorado State University Model (CSUM) -- A statistical method developed Matsumoto (1984) utilizes synoptic and persistence predictors by discretizing the forecast timeframe into three 24-hour time steps. Climatology is incorporated into the forecast via a stratification scheme based on the position of the tropical cyclone relative to the 500 mb subtropical ridge. Three sets of regression equations are used to determine the north-south and east-west displacements depending on whether the tropical cyclone is south, on or north relative to the ridge.

(7). One-way Interactive Tropical Cyclone Model (OTCM) -- A coarse-mesh, three-layer in the vertical, primitive equation model with a 205km grid spacing over a 6400 x 4700 km domain. The model's fields are computed around a bogused, digitized cyclone vortex using FLENUMOCEANCEN's Numerical Variational Analysis (NVA) or NOGAPS prognostic fields for the specified valid time. The past motion of the tropical cyclone is compared to initial steering fields and a bias correction is computed and applied to the model. FLENUMOCEANCEN's NOGAPS global prognostic fields are used at 12-hour intervals to update the model's boundaries. The resultant forecast positions are derived by locating the 850 mb vortex at six-hour intervals to 72-hours.

(8). TAPT -- An empirical technique which utilizes upper-tropospheric wind fields to estimate acceleration associated with the tropical cyclone's interaction with the mid-latitude westerlies. It includes guidelines for the duration of acceleration, upper-limits, and probable path of the cyclone.

(9). CLIPER -- A statistical

regression technique based on climatology, current intensity, position and past movement. This technique is used as a crude measure of real forecast skill when verifying forecast accuracy.

(10). THETA-E -- An empirically derived relationship between a tropical cyclone's minimum sea-level pressure (MSLP) and 700 mb equivalent potential temperature (Theta-E) was developed by Sikora (1976) and Dunnavan (1981). By monitoring MSLP and trends, the forecaster can evaluate the potential for sudden, rapid deepening of a tropical cyclone.

(11). WIND RADIUS -- Following an analytical model of the radial profiles of sea-level pressures and winds in mature tropical cyclones (Holland, 1980), a set of radii for 30-, 50-, and 100-knot winds based on the tropical cyclone's maximum winds have been produced to aid the forecaster in determining forecast wind radii.

(12). DVORAK -- An estimation of tropical cyclone's current and 24-hour forecast intensity is made from interpolation of satellite imagery (DVORAK, 1984) and provided to the forecaster. These intensity estimates are used in conjunction with other intensity-related data and trends to forecast tropical cyclone intensity.

JTWC uses HPAC, TAPT, TYAN78, COSMOS, OTCM and CSUM operationally to develop track forecasts.

c. Testing and Results

A comparison of selected techniques is included in Table 5-8 for all western North Pacific tropical cyclones, Table 5-9 for all North Indian Ocean tropical cyclones. In these tables, " x-axis " refers to techniques listed vertically. For example (Table 5-8) in the 507 cases available for a (homogeneous) comparison, the average forecast error at 24-hours was 118 nm (219 km) for TOTL and 120 nm (222 km) for RECR. The difference of 2 nm (4 km) is shown in the lower right. (Differences are not always exact, due to computational round-off which occurs for each of the cases available for comparison).

TABLE 5-8 1987 ERROR STATISTICS FOR SELECTED OBJECTIVE TECHNIQUES IN THE WESTERN NORTH PACIFIC OCEAN
24-HOUR MEAN FORECAST ERROR (MM)

	JTWC	CLIP	OTCM	CSUM	RECR	TOTL	COSM	HPAC	CLIM	XTRP
JTWC	563 107 107 0									
CLIP	541 107 128 21	582 133 133 0								
OTCM	544 106 103 -3	580 133 106 -27	584 104 106 0							
CSUM	503 107 98 -9	541 130 101 -29	543 103 102 -3	543 102 102 0						
RECR	472 105 114 9	503 131 120 -11	507 103 120 13	474 101 120 19	507 120 120 0					
TOTL	494 104 117 13	529 131 123 -8	533 106 123 17	499 101 124 23	507 120 118 -2	533 123 123 0				
COSM	540 107 106 -1	575 132 111 -21	578 106 111 5	539 102 110 8	503 120 111 -9	529 123 111 -12	579 111 111 0			
HPAC	541 107 112 5	577 132 115 -17	580 106 115 9	541 102 113 13	507 120 113 -7	532 123 114 -9	576 111 115 4	581 115 115 0		
CLIM	541 107 148 41	577 132 151 19	580 106 151 43	541 102 151 49	507 120 148 28	532 123 150 27	576 111 151 40	581 115 151 36	581 151 151 0	
XTRP	545 107 115 8	581 133 118 -13	584 106 118 12	543 102 116 14	507 120 116 -4	533 123 116 -7	579 111 118 7	581 113 118 3	581 151 116 -33	585 118 118 0

NUMBER OF CASES	X-AXIS TECHNIQUE ERROR
Y-AXIS TECHNIQUE ERROR	ERROR DIFFERENCE (Y-X)

48-HOUR MEAN FORECAST ERROR (MM)

	JTWC	CLIP	OTCM	CSUM	RECR	TOTL	COSM	HPAC	CLIM	XTRP
JTWC	465 204 204 0									
CLIP	450 204 368 56	511 276 276 0								
OTCM	449 204 187 -17	502 273 191 -82	503 191 191 0							
CSUM	413 203 191 -14	471 272 203 -69	465 191 202 11	471 203 203 0						
RECR	390 202 223 21	442 273 240 -33	435 190 237 47	411 203 241 38	444 239 239 0					
TOTL	410 203 240 37	465 272 232 -20	458 192 231 39	433 204 236 82	444 239 247 8	467 252 252 0				
COSM	447 203 204 1	504 274 221 -53	497 191 219 28	467 203 217 14	440 239 224 -15	463 252 224 -28	506 221 221 0			
HPAC	448 203 216 13	504 273 228 -45	499 192 227 35	469 203 228 25	444 239 226 -13	466 250 227 -23	503 221 228 7	508 228 228 0		
CLIM	448 203 271 68	506 273 282 9	499 192 282 90	469 203 283 80	444 239 276 37	466 250 281 28	503 221 281 60	508 228 282 54	508 282 282 0	
XTRP	432 204 232 48	510 276 265 -11	503 191 263 72	471 203 239 56	444 239 262 23	467 252 263 11	506 221 265 44	508 228 263 35	508 282 263 -19	512 265 265 0

JTWC - OFFICIAL JTWC FORECAST
CLIP - CLIPER (CLIMatology and Persistence)
OTCM - ONE-WAY TROPICAL CYCLONE MODEL
CSUM - COLORADO STATE UNIVERSITY MODEL
RECR - RECURVER ANALOG (TYAN 78)
TOTL - TOTAL ANALOG (TYAN 78)
COSM - COSMOS (Model Output Statistics)
HPAC - HALF CLIMATOLOGY AND PERSISTENCE BLEND
CLIM - CLIMATOLOGY
XTRP - 12-HR EXTRAPOLATION

72-HOUR MEAN FORECAST ERROR (MM)

	JTWC	CLIP	OTCM	CSUM	RECR	TOTL	COSM	HPAC	CLIM	XTRP
JTWC	389 303 303 0									
CLIP	377 304 388 84	433 389 389 0								
OTCM	351 304 288 -20	393 381 296 -83	393 296 296 0							
CSUM	341 308 289 -19	395 383 297 -86	362 300 290 -10	395 297 297 0						
RECR	340 306 381 75	382 395 394 -1	346 295 384 89	352 301 392 91	384 394 394 0					
TOTL	348 304 391 87	393 387 392 5	356 296 388 92	362 299 403 104	384 394 393 1	393 393 393 0				
COSM	374 302 334 32	428 388 354 -34	388 296 344 48	392 297 337 40	381 394 364 -30	392 393 362 -31	430 355 355 0			
HPAC	377 304 336 32	428 385 340 -45	388 297 330 33	392 296 340 44	384 394 346 -48	393 393 343 -50	426 354 339 -15	430 340 340 0		
CLIM	377 304 407 103	428 385 405 20	388 297 401 104	392 296 405 109	384 394 407 13	393 393 408 15	426 354 403 49	430 340 405 65	430 405 405 0	
XTRP	379 303 412 109	433 389 425 36	393 296 417 121	395 297 418 119	384 394 424 30	393 393 418 25	430 355 425 70	430 340 420 80	430 405 420 15	435 425 425 0

TABLE 5-9. 1987 ERROR STATISTICS FOR SELECTED OBJECTIVE TECHNIQUES IN THE NORTH INDIAN OCEAN
24-HOUR MEAN FORECAST ERROR (NM)

	JTWC		OTCM		CSUM		TOTL		HPAC		CLIM		XTRP	
JTWC	54	144												
	144	0												
OTCM	38	130	45	158										
	152	22	158	0										
CSUM	37	130	44	155	44	246								
	239	109	246	91	246	0								
TOTL	10	138	12	120	11	199	12	158						
	176	38	158	38	153	-46	158	0						
HPAC	38	130	45	158	44	246	12	158	45	138				
	140	10	138	-20	137	-109	147	-11	138	0				
CLIM	38	130	45	158	44	246	12	158	45	138	45	172		
	172	42	172	14	170	-76	165	7	172	34	172	0		
XTRP	38	130	45	158	44	246	12	158	45	138	45	172	45	141
	137	7	141	-17	140	-106	150	-8	141	3	141	-31	141	0

NUMBER OF CASES	X-AXIS TECHNIQUE ERROR
Y-AXIS TECHNIQUE ERROR	ERROR DIFFERENCE (Y-X)

48-HOUR MEAN FORECAST ERROR (NM)

	JTWC		OTCM		CSUM		TOTL		HPAC		CLIM		XTRP	
JTWC	25	205												
	205	0												
OTCM	9	220	26	419										
	450	230	419	0										
CSUM	10	217	25	413	28	481								
	468	251	477	64	481	0								
TOTL	2	102	7	216	6	395	7	388						
	399	297	388	172	379	-16	388	0						
HPAC	11	209	26	419	28	481	7	388	29	310				
	304	95	307	-112	309	-172	346	-42	310	0				
CLIM	11	209	26	419	28	481	7	388	29	310	29	322		
	376	167	314	-105	318	-163	325	-63	322	12	322	0		
XTRP	11	209	26	419	28	481	7	388	29	310	29	322	29	330
	265	56	330	-89	330	-151	391	3	330	20	330	8	330	0

JTWC - OFFICIAL JTWC FORECAST
OTCM - ONE-WAY TROPICAL CYCLONE MODEL
CSUM - COLORADO STATE UNIVERSITY MODEL
TOTL - TOTAL ANALOG (TYAN 78)
CLIM - CLIMATOLOGY
HPAC - HALF CLIMATOLOGY AND PERSISTENCE BLEND
XTRP - 12-HR EXTRAPOLATION

72-HOUR MEAN FORECAST ERROR (NM)

	JTWC		OTCM		CSUM		TOTL		HPAC		CLIM		XTRP	
JTWC	21	305												
	305	0												
OTCM	4	505	10	777										
	629	124	777	0										
CSUM	6	481	10	777	12	729								
	723	242	742	-35	729	0								
TOTL	0	0	1	72	1	203	1	339						
	0	0	339	267	339	136	339	0						
HPAC	7	440	10	777	12	729	1	339	13	425				
	356	-84	426	-351	412	-317	545	206	425	0				
CLIM	7	440	10	777	12	729	1	339	13	425	13	254		
	189	-251	242	-535	223	-506	385	46	254	-171	254	0		
XTRP	7	440	10	777	12	729	1	339	13	425	13	254	13	637
	572	132	656	-121	641	-88	706	367	637	212	637	383	637	0

TABLE 5-10. 1987 ERROR STATISTICS FOR SELECTED OBJECTIVE TECHNIQUES IN THE SOUTHERN HEMISPHERE
24-HOUR MEAN FORECAST ERROR (NM)

	JTWC		OTCM		TOTL		HPAC		CLIM		XTRP	
JTWC	172	145										
	145	0										
OTCM	100	141	111	136								
	138	-3	136	0								
TOTL	78	135	80	129	88	194						
	202	67	166	37	194	0						
HPAC	71	130	73	126	70	126	81	126				
	124	-6	119	-7	127	1	126	0				
CLIM	71	130	73	126	70	126	81	126	81	171		
	168	38	164	38	165	39	171	45	171	0		
XTRP	99	137	99	137	78	203	81	126	81	171	112	146
	148	11	133	-4	136	-67	118	-8	118	-53	146	0

48-HOUR MEAN FORECAST ERROR (NM)

	JTWC		OTCM		TOTL		HPAC		CLIM		XTRP	
JTWC	123	280										
	280	0										
OTCM	71	283	82	287								
	298	15	287	0								
TOTL	58	271	60	274	65	319						
	330	59	283	9	319	0						
HPAC	51	264	52	270	50	240	60	215				
	218	-46	218	-52	215	-25	215	0				
CLIM	51	264	52	270	50	240	60	215	60	287		
	291	27	288	18	262	22	287	72	287	0		
XTRP	69	279	71	279	56	329	60	215	60	287	84	304
	300	21	278	-1	275	-54	247	32	247	-40	304	0

JTWC - OFFICIAL JTWC FORECAST
OTCM - ONE-WAY TROPICAL CYCLONE MODEL
TOTL - TOTAL ANALOG (TYAN 78)
HPAC - HALF CLIMATOLOGY AND PERSISTENCE BLEND
CLIM - CLIMATOLOGY
XTRP - 12-HR EXTRAPOLATION

72-HOUR MEAN FORECAST ERROR (NM)

	OTCM		TOTL		HPAC		CLIM		XTRP	
OTCM	49	490								
	490	0								
TOTL	36	478	41	359						
	373	-105	359	0						
HPAC	26	446	31	336	35	282				
	299	-147	287	-49	282	0				
CLIM	26	446	31	336	35	282	35	386		
	391	-55	385	49	386	104	386	0		
XTRP	38	459	32	335	35	282	35	386	51	508
	460	1	359	24	370	88	370	-16	508	0

CHAPTER VI - TROPICAL CYCLONE SUPPORT SUMMARY

1. NAVAL ENVIRONMENTAL PREDICTION RESEARCH FACILITY

The Pocket Tropical Cyclone Model (PTCM)

(Evans, J.L., Monash University, Australia and
J.H. Chu, NAVENVPREDRSCHFAC)

PTCM is a linear tropical cyclone motion prediction scheme incorporating the effects of a large-scale environmental flow and the beta-effect. The model is based on the equations developed by Holland (1983) and has been operational in a modified form in the Australian region for a number of years. The current version of the model has been developed by Evans and Holland to be a purely objective forecasting tool, and is presently undergoing operational testing in the Australian region.

PTCM is being incorporated in the NEPRF ATCF system and a series of case studies are planned to test its effectiveness in the Northwest Pacific region. In addition, the model will be expanded to include additional terms for diagnosis of tropical cyclone motions.

THE ADVANCED TROPICAL CYCLONE MODEL (ATCM)

(Hodur, R.M., NAVENVPREDRSCHFAC)

The Advanced Tropical Cyclone Model (ATCM) was installed at the Fleet Numerical Oceanography Center in 1987 for evaluation by JTWC forecasters. Although testing in 1986 indicated that the ATCM could perform better than the OTCM, these results were not obtained during real-time runs during the 1987 season. In particular, the ATCM demonstrated a large right bias and nearly always weakened the storms with time. These effects were particularly noticeable in the ATCM forecasts of Typhoon Lynn in October, 1987.

Experiments are being performed to isolate the reason(s) for these ATCM forecast errors. A new version of the ATCM has been developed which incorporates some of the features of NOGAPS 3.0. These include a 15-

level optimum interpolation analysis and an increase in the number of model levels from 12 to 21 in order to include a high resolution planetary boundary layer. In addition, the cumulus parameterization has been modified so that the ATCM can maintain the tropical storm circulation during the forecast. Also, sensitivity experiments are being conducted to find the best structure of the initial bogus and to study the effect of increasing the horizontal resolution.

Navy Tactical Applications Guide (NTAG), Vol. 6

(Fett, R.W., NAVENVPREDRSCHFAC)

An effort is now underway to develop a series of examples demonstrating the use of high quality satellite data for analysis and forecasting in the tropics. Both polar orbital and geostationary satellite data are used to study the evolution of certain weather effects or of a particular weather phenomenon at a given time. These examples are intended for publishing in the NTAG Volume 6, Part I, Tropical Weather Analysis and Forecast Applications, and Volume 6, Part II, Tropical Cyclone Weather Analysis and Forecast Applications. NTAG Volume 6, Part I was distributed in June 1986. Part II is still in the research process. Publication is anticipated in 1988/89.

Tropical Cyclone Condition Setting Aid for Sasebo and Iwakuni, Japan

(Jarrell, J.D., Sci. Appl. International
Corporation)

A forecast aid has been developed for predicting tropical cyclone associated winds at Sasebo and Iwakuni, Japan. The aid consists of two parts. The first part is a collection of charts which relate winds observed at the two stations to the maximum sustained winds at the center of a tropical cyclone as a function of cyclone locations. The second part of the aid is a collection of diagrams which estimate the worst case arrival time of 50-kt winds.

Improvements to Combined Confidence Rating System

Harry Hamilton (ST Systems, Monterey, CA)

The Combined Confidence Rating System (CCRS) has been improved via a redesign of its weighting function. The new weighting function is derived from the following: the inverse of a covariance matrix which is a combination of the historical cross-track and along-track covariance matrices, and the objective aid forecasts. The weights are generated as follows:

a. Let Q_x and Q_y be the cross-track and along-track covariance matrices, respectively. The desired combination of these two, Q , is equal to $Q_x + aQ_y$, where a has been determined empirically to be 0.25.

b. The weight for each available objective forecast technique is the sum of all terms of the relevant technique divided by the sum of all terms of Q^{-1} . The sum of the weights for all available objective techniques must equal 1.0.

The Combined Confidence Weighted Forecast (CCWF) is generated for JTWC by summing the selected objective forecasts used in the calculations.

Automated Tropical Cyclone Forecasting System

(Tsui, T.L., Miller, R.J., and A.J. Schrader,
NAVENVPREDRSCHFAC)

The Automated Tropical Cyclone Forecasting (ATCF) system is an IBM PC compatible software package currently being developed for the Joint Typhoon Warning Center (JTWC). ATCF is designed to allow JTWC forecasters to display graphically tropical cyclone forecast information, merge and analyze synoptic wind fields, provide objective fix guidance, select optimum objective forecast

aid, and expedite the issuance of tropical cyclone warnings. One great advantage of using ATCF is the standardization of the tropical cyclone forecasting procedure, so that during the course of the tropical cyclone warning preparation, forecasters will not neglect consideration of any decisional steps or available options. ATCF automatically saves all tropical cyclone data, computes the real-time and post-storm statistics, and allows forecasters to randomly access any past storm data. A communication package included in ATCF simplifies the data transfer procedure between JTWC and Fleet Numerical Oceanography Center in Monterey, CA.

The ATCF will be installed at JTWC in January 1988 for test and evaluation. Modifications on the system will be followed to make the system be compatible with the design of the JTWC Automation Project.

North Pacific Tropical Cyclone Climatology

(Miller, R.J. and T.L. Tsui,
NAVENVPREDRSCHFAC)

A tropical cyclone climatology for the North Pacific has been developed and now is being reviewed by EGPACOM. Data used for the western basin were taken from the JTWC Tropical Cyclone Data Base and covered a period of 40 years, 1945-84. Eastern basin data spanned the 34-year period from 1949 to 1982 and were obtained from the consolidated worldwide tropical cyclone data base at National Climatic Data Center, Asheville, N.C. Storms for both basins were sorted according to month/day of the year into twenty four 31-day overlapping periods. For each period, four charts are supplied: 1) actual storm paths; 2) mean storm paths; 3) average storm speed; and 4) storm constancy and frequency.

JTWC has evaluated and offered suggestions for modifications of the climatology. The final version of the compilation should be completed in March 1988.

EOF Post-Processing Forecast Technique

(Tsui, T.L. and J.H. Chu,
NAVENVPREDRSCHFAC)

NEPRF is adapting the Empirical Orthogonal Function (EOF) post-processing tropical cyclone forecast scheme developed by Naval Postgraduate School (NPS) on the Fleet Numerical Oceanography Center computer system. The NPS EOF technique objectively

recognizes the salient patterns of large-scale horizontal wind fields with respect to the center of a tropical cyclone. This information, in terms of the EOF coefficients, will be used to modify the tropical cyclone track forecasts produced by the numerical models. The skill of this method is derived from the regression equations between the EOF coefficients and the forecast tracks of the One-way Tropical Cyclone Model (OTCM) in the western North Pacific during the period from 1979 to 1983.

2. JOINT TYPHOON WARNING CENTER

Joint Typhoon Warning Center Automation Project (JTWC-AP)

LT Brian J. Williams, USN, Typhoon Duty
Officer, JTWC Automation Officer.

A comprehensive effort is currently underway to provide JTWC with state-of-the-art, automated tools to aid the Typhoon Duty Officer (TDO) in the collection, presentation, and analysis of data. These tools will also streamline the production of the warning messages and provide decision-making aids for the TDO. Automation of JTWC will take place in two phases. The first phase is the implementation in January 1988 of the Automated Tropical Cyclone Forecasting system (ATCF). The ATCF consists of a "suite" of program modules designed to run on IBM-AT compatible microcomputers. The concept and design of the ATCF (described above by Dr. Tsui and Mr. Miller) is a cooperative effort between NEPRF and JTWC. The second phase of automation will be the implementation of the more comprehensive JTWC-AP in FY 89. The JTWC-AP will integrate features of the ATCF with a more complete advanced data base archival and retrieval system, satellite imagery looping, overlay, and increased emphasis on expert systems that make the TDO's watch routine more efficient and effective.

The hardware suite that will run the ATCF programs (described above by Dr. Tsui and Mr. Ron Miller) has five workstations connected by a file server network to share common data files (see Figure 6-1). A dedicated

terminal will provide the send/receive interface with the Automated Weather Network (AWN). Numerical forecast aids, FNOC analyses and prognostic fields, as well as near-real time synoptic data (as a back-up to the AWN) will be received via remote requests over the TYMNET public data network. The TYMNET connects the JTWC microcomputers to FNOC mainframes. Outgoing messages to customers without access to AWN are inserted into the AUTODIN system via paper tape sent to the local Navy Telecommunications Command Center (NTCC). The ATCF software and hardware implementation represents the first step toward automation of JTWC.

A major feature of the future JTWC-AP will be the reference roster data base. This data base will contain critical data about customers in JTWC's AOR. It will include storm haven information, telephone points-of-contact, notification criteria for threatened customers, geographical information, local area forecasting rules of thumb, weather reporting station locations, etc. Whenever a customer is threatened, the reference roster will automatically prompt the TDO with customer-specific information. JTWC is currently working to compile the data reference roster for the JTWC-AP project manager. The reference roster will be easily edited to add or delete information as conditions change. This feature should significantly improve the level of support to JTWC's customers.

Another important feature of the JTWC-AP is a training or playback mode which will call up archived data to realistically recreate

previous forecast scenarios. This will be possible due to the integration of satellite imagery, numerical analyses, prognostic fields, and "raw" data into one data base "tagged" by time, geography, or event (e.g., a tropical cyclone). This feature will provide the ability to display, analyze and recreate the timing of receipt of all data that was available for a past storm. This will allow a controlled training environment, especially in the off-season, as well as an outstanding tool for forecast "bust" reviews. In addition, this function will provide a complete and rich data base for post-analysis, case studies, and other research.

Future plans for the JTWC-AP include the implementation of decision-making aids (such as decision trees developed at the Naval Postgraduate School) and expert systems to aid in forecasting genesis, motion, intensity and dissipation. The JTWC-AP will provide a comprehensive real-time and archived tropical cyclone data base as well as the tools to manipulate data. This system is expected to significantly improve JTWC's operational support, while providing an excellent means for studying, improving, and "fine tuning" tropical cyclone forecasting methods and operational procedures.

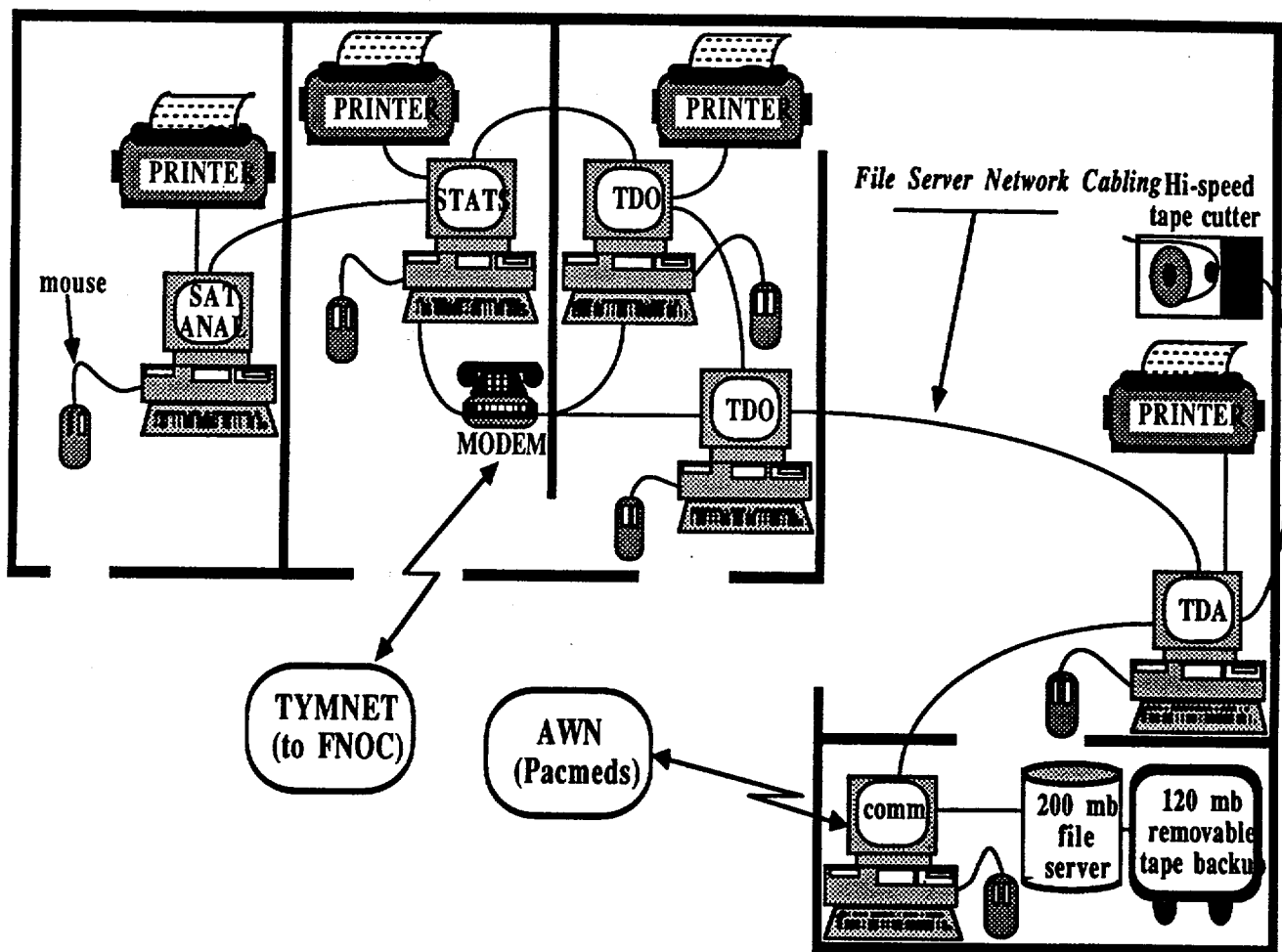


Figure 6-1. Physical layout of the ATCF in JTWC's working spaces.

ANNEX A

1. GENERAL

Due to the rapid growth of the use of microcomputers in the meteorological community and to save publishing costs, tropical cyclone track data (with best track, initial warning, 24-, 48- and 72-hour JTWC forecasts) and fix data (satellite, aircraft, radar and synoptic) are now available separately upon request. The data will be available in ASCII format on 5.25 inch "floppy" diskettes. The data sets are available on four diskettes, which include the western North Pacific and North Indian Ocean (1 January - 31 December 1987)

on two and the South Pacific and South Indian Oceans (1 July 1986 - 30 June 1987) on the other two. Agencies or individuals desiring these data sets should send the appropriate number of "floppy" diskettes (four if both data sets are desired, two if only one desired) to NAVOCEANCOMCEN/JTWC Guam with their request. When the request is received, the data will be copied onto your diskettes and returned with an explanation of the data formats. The use of floppy diskettes should facilitate the transfer of these rather large data files into your computer.

2. WARNING VERIFICATION STATISTICS

a. WESTERN NORTH PACIFIC

This section includes verification statistics for each warning in the western North

Pacific Ocean during 1987. Pre- and post-warning best track positions are not printed, but are available on floppy diskettes by request.

JTWC FORECAST TRACK AND INTENSITY ERRORS BY WARNING

Typhoon Orchid (01W)			00h	24h	48h	72h						
		Average	17	91	158	234						
		# Cases	23	19	15	11						
DTG	W#	BT LAT	BT LON	POS ER	24 ER	48 ER	72 ER	BT WN	WW ER	24 WE	48 WE	72 WE
87010812	1	7.2N	150.6E	37.7	37.6	126.7	204.5	35	-10	-5	-25	-20
87010818	2	7.2N	150.0E	65.7	53.6	130.7	168.2	35	-5	-10	-35	-10
87010900	3	7.3N	149.2E	6	152.2	252.5	242.1	40	-5	-10	-40	5
87010906	4	7.5N	148.0E	18.8	191.9	266.9	206.2	40	-5	-20	-35	5
87010912	5	7.9N	146.5E	13.4	119.5	139.2	144	45	-5	-25	-20	5
87010918	6	8.4N	144.9E	29.8	101.6	89	106.7	50	-10	-35	-10	10
87011000	7	8.8N	143.4E	13.3	49.4	60.9	147.2	55	-5	-25	20	40
87011006	8	9.2N	141.9E	29.7	26.5	47.4	207	65	-5	-10	25	40
87011012	9	9.7N	140.4E	5.9	50.4	151.1	330.5	75	-10	5	20	25
87011018	10	10.0N	139.1E	13.4	75.6	187	430	85	-15	20	25	25
87011100	11	10.2N	137.9E	5.9	11.8	93.5	390.8	95	-5	45	40	40
87011106	12	10.5N	136.8E	8.4	12	79.9	N/A	90	10	50	55	N/A
87011112	13	10.8N	135.8E	6	35.8	159.7	N/A	80	20	35	45	N/A
87011118	14	10.9N	134.9E	5.9	70.7	260.1	N/A	70	25	20	35	N/A
87011200	15	11.1N	134.0E	6	34.5	331.8	N/A	60	10	0	5	N/A
87011206	16	11.4N	133.3E	6	91.1	N/A	N/A	60	10	5	N/A	N/A
87011212	17	11.7N	132.7E	0	165.8	N/A	N/A	65	0	5	N/A	N/A
87011218	18	11.7N	132.2E	21.3	267.5	N/A	N/A	60	0	5	N/A	N/A
87011300	19	11.3N	131.6E	0	192.8	N/A	N/A	50	5	5	N/A	N/A
87011306	20	10.8N	131.1E	13.4	N/A	N/A	N/A	45	5	N/A	N/A	N/A
87011312	21	10.1N	130.7E	12	N/A	N/A	N/A	40	5	N/A	N/A	N/A
87011318	22	8.7N	130.4E	78.9	N/A	N/A	N/A	35	5	N/A	N/A	N/A
87011400	23	6.8N	129.9E	13.4	N/A	N/A	N/A	30	0	N/A	N/A	N/A

Tropical Storm Percy (02W)		<u>00h</u>	<u>24h</u>	<u>48h</u>	<u>72h</u>
Average		19	69	116	206
# Cases		9	8	4	4

DTG	W#	BT LAT	BT LON	POS ER	24 ER	48 ER	72 ER	BT WN	WW ER	24 WE	48 WE	72 WE
87041100	1	9.3N	142.9E	8.4	43	92.5	163	40	0	20	25	30
87041106	2	9.8N	142.4E	24	81.5	30.6	100.6	40	0	20	25	30
87041112	3	10.3N	140.7E	59.3	85.8	152.1	279.8	35	5	15	15	5
87041118	4	10.6N	141.0E	18.9	70.6	191.8	280.2	30	10	10	10	5
87041200	5	10.8N	140.2E	18	51.2	N/A	N/A	30	0	0	N/A	N/A
87041206	6	11.0N	139.3E	13.4	50.2	N/A	N/A	25	5	0	N/A	N/A
87041212	7	11.2N	138.4E	11.8	67	N/A	N/A	25	5	5	N/A	N/A
87041218	8	11.4N	137.7E	6	102.6	N/A	N/A	25	5	0	N/A	N/A
87041300	9	11.8N	137.3E	16.8	N/A	N/A	N/A	25	5	N/A	N/A	N/A

Tropical Storm Ruth (03W)		<u>00h</u>	<u>24h</u>	<u>48h</u>	<u>72h</u>
Average		13	141	N/A	N/A
# Cases		6	3	0	0

DTG	W#	BT LAT	BT LON	POS ER	24 ER	48 ER	72 ER	BT WN	WW ER	24 WE	48 WE	72 WE
87061800	1	19.2N	114.6E	33	168.4	N/A	N/A	30	0	5	N/A	N/A
87061806	2	19.7N	114.2E	0	120.9	N/A	N/A	30	0	15	N/A	N/A
87061812	3	20.3N	113.7E	8.2	133.7	N/A	N/A	30	0	5	N/A	N/A
87061818	4	20.8N	112.8E	11.2	N/A	N/A	N/A	35	0	N/A	N/A	N/A
87061900	5	21.3N	111.8E	12.7	N/A	N/A	N/A	30	0	N/A	N/A	N/A
87061906	6	21.9N	110.8E	13.2	N/A	N/A	N/A	25	0	N/A	N/A	N/A

Typhoon Sperry (04W)		<u>00h</u>	<u>24h</u>	<u>48h</u>	<u>72h</u>
Average		16	119	242	421
# Cases		18	15	12	9

DTG	W#	BT LAT	BT LON	POS ER	24 ER	48 ER	72 ER	BT WN	WW ER	24 WE	48 WE	72 WE
87062700	1	12.5N	137.4E	0	18.4	68.2	282.2	35	0	-10	0	35
87062706	2	13.0N	136.7E	16.8	53.3	59	270.3	45	-5	-5	10	45
87062712	3	13.3N	136.2E	42.4	71	57.9	269.7	45	0	-5	20	45
87062718	4	13.8N	135.8E	55.4	45.7	108.2	320.8	55	-5	-5	25	55
87062800	5	14.3N	135.3E	6	75.6	270.1	480.1	65	0	15	55	90
87062806	6	14.9N	135.0E	0	101	306.7	517	65	5	25	60	95
87062812	7	15.6N	134.6E	13	117.8	293.1	505.9	70	0	25	60	95
87062818	8	16.4N	134.2E	12	117.5	276.4	562.5	75	0	30	75	100
87062900	9	17.3N	133.9E	8.3	165	309.5	583.5	75	0	5	20	25
87062906	10	18.3N	133.4E	29.1	191.6	336	N/A	70	0	5	20	N/A
87062912	11	19.4N	132.8E	20.8	137.4	349.4	N/A	65	0	0	15	N/A
87062918	12	20.7N	132.0E	32.9	128.9	472	N/A	65	0	10	20	N/A
87063000	13	22.0N	131.5E	11.1	203.8	N/A	N/A	60	0	10	N/A	N/A
87063006	14	23.3N	131.3E	20.4	154.5	N/A	N/A	55	0	10	N/A	N/A
87063012	15	24.9N	131.4E	5.4	212.1	N/A	N/A	55	-5	5	N/A	N/A
87063018	16	26.7N	131.7E	6	N/A	N/A	N/A	45	-5	N/A	N/A	N/A
87070100	17	28.3N	132.6E	8	N/A	N/A	N/A	40	0	N/A	N/A	N/A
87070106	18	29.8N	134.6E	16.7	N/A	N/A	N/A	35	0	N/A	N/A	N/A

Super Typhoon Thelma (05W)

	00h	24h	48h	72h
Average	18	146	311	479
# Cases	34	31	28	24

DTG	W#	BT LAT	BT LON	POS ER	24 ER	48 ER	72 ER	BT WN	WW ER	24 WE	48 WE	72 WE
87070718	1	13.0N	149.5E	84.8	238.2	352.7	402.6	30	0	0	-30	-25
87070800	2	13.9N	148.9E	43.6	263.3	401	491.1	30	0	-5	-30	-45
87070806	3	14.5N	147.4E	58.4	280.1	510	995.5	30	0	0	-30	-70
87070812	4	14.6N	145.5E	37.6	202.8	462.2	864.3	35	-5	-20	-40	-80
87070818	5	15.0N	143.8E	34.1	8.3	128.1	350.8	40	-10	-25	-45	-60
87070900	6	15.6N	142.3E	18.9	139.9	318.5	636.9	45	5	-20	-45	-55
87070906	7	16.2N	141.0E	8.3	162.4	357.8	615.1	50	0	-25	-55	-60
87070912	8	16.5N	139.7E	13.3	109.6	336.4	529.5	60	-5	-25	-55	-45
87070918	9	16.7N	138.3E	11.5	127.8	250.1	187.5	70	-15	-35	-55	-25
87071000	10	17.0N	136.9E	6	116.8	271.7	234.3	80	0	-10	-5	30
87071006	11	17.3N	135.4E	18.9	165.2	292.1	258.2	85	0	-15	-5	35
87071012	12	17.7N	134.0E	8.3	181.4	324	288.5	90	0	-25	0	35
87071018	13	17.8N	132.5E	6	158.6	269.6	195.4	100	-5	-5	30	40
87071100	14	17.9N	131.2E	0	192.1	276.8	147.6	110	-5	10	30	25
87071106	15	17.9N	129.9E	18	122.7	168.2	108.5	120	-10	10	35	30
87071112	16	17.8N	128.8E	8.3	123.3	189	212.4	130	-10	25	45	25
87071118	17	17.6N	128.0E	16.6	104.9	188.2	307	125	-5	15	20	10
87071200	18	17.6N	127.3E	6	163.5	421.1	675.7	120	0	15	15	20
87071206	19	17.9N	126.8E	18.9	222.7	485.7	820.2	120	-5	15	10	15
87071212	20	18.5N	126.6E	8.3	141.3	382.1	762.7	115	-10	5	-5	5
87071218	21	19.2N	126.4E	29.4	190	418.3	857.9	105	-5	0	-5	20
87071300	22	19.9N	126.2E	8.2	92.3	192.6	540.2	95	-5	-10	-10	20
87071306	23	20.9N	126.0E	18.9	67.1	196.9	497.6	90	-5	-15	-15	15
87071312	24	22.1N	125.6E	12.6	47.1	217.8	524.5	90	-15	-25	-15	10
87071318	25	23.4N	125.3E	17.6	74	308	N/A	90	-15	-25	-5	N/A
87071400	26	24.7N	125.2E	6	62.7	354.2	N/A	90	-5	-10	15	N/A
87071406	27	25.9N	124.9E	0	54.9	312	N/A	90	-5	-10	20	N/A
87071412	28	27.4N	124.8E	8	102.1	346.4	N/A	90	-5	-5	20	N/A
87071418	29	28.6N	125.0E	8	186.1	N/A	N/A	85	-5	5	N/A	N/A
87071500	30	29.9N	125.5E	12	228.2	N/A	N/A	80	0	30	N/A	N/A
87071506	31	31.9N	126.3E	13	219.7	N/A	N/A	80	-5	20	N/A	N/A
87071512	32	34.4N	127.2E	24	N/A	N/A	N/A	70	0	N/A	N/A	N/A
87071518	33	36.8N	128.2E	30	N/A	N/A	N/A	55	5	N/A	N/A	N/A
87071600	34	39.0N	129.4E	101.3	N/A	N/A	N/A	40	-5	N/A	N/A	N/A

Typhoon Vernon (06W)

	00h	24h	48h	72h
Average	33	119	180	224
# Cases	21	18	14	10

DTG	W#	BT LAT	BT LON	POS ER	24 ER	48 ER	72 ER	BT WN	WW ER	24 WE	48 WE	72 WE
87071618	1	12.1N	137.5E	11.7	82.2	125.9	282.5	30	0	10	10	-15
87071700	2	12.2N	135.3E	54.1	42.9	151	209.5	30	0	10	5	-15
87071706	3	12.2N	133.1E	18.6	66.6	160.9	207.6	35	-5	5	0	-10
87071712	4	12.3N	131.0E	42.6	153.1	188.8	152.8	35	-5	5	-5	10
87071718	5	12.7N	129.7E	16.8	181.1	216.2	162.6	35	-5	0	-5	10
87071800	6	13.1N	128.9E	94.2	279.7	280.9	196.1	35	-5	-10	-10	15
87071806	7	13.6N	128.5E	112.3	212	207.6	219.4	40	-10	-20	-15	5
87071812	8	14.1N	128.1E	34.2	139.2	151.2	112.7	45	-5	-10	10	25
87071818	9	15.0N	127.5E	58	140.9	159.8	260.9	50	-10	-10	10	30
87071900	10	15.9N	126.7E	23.9	125	234.8	442.9	55	0	0	25	60
87071906	11	16.9N	125.9E	42	103.4	214.5	N/A	60	0	10	35	N/A
87071912	12	18.0N	125.3E	12	84.7	81.4	N/A	65	0	20	50	N/A

87071918	13	18.7N	124.7E	24.8	75.7	128.8	N/A	65	0	20	55	N/A
87072000	14	19.3N	124.2E	5.7	73.9	217.1	N/A	65	0	15	35	N/A
87072006	15	20.1N	123.5E	12.8	101.5	N/A	N/A	60	5	15	N/A	N/A
87072012	16	21.1N	123.0E	16.4	116.1	N/A	N/A	55	0	20	N/A	N/A
87072018	17	22.0N	122.5E	20.6	110.1	N/A	N/A	55	0	25	N/A	N/A
87072100	18	23.1N	122.2E	8.2	66.8	N/A	N/A	50	5	30	N/A	N/A
87072106	19	24.6N	121.8E	32.4	N/A	N/A	N/A	45	5	N/A	N/A	N/A
87072112	20	26.0N	121.6E	36.9	N/A	N/A	N/A	35	5	N/A	N/A	N/A
87072118	21	27.3N	121.6E	22.1	N/A	N/A	N/A	30	0	N/A	N/A	N/A

Typhoon Wynne (07W)

	<u>00h</u>	<u>24h</u>	<u>48h</u>	<u>72h</u>
Average	16	107	218	332
# Cases	40	36	30	30

<u>DTG</u>	<u>W#</u>	<u>BT LAT</u>	<u>BT LON</u>	<u>POS ER</u>	<u>24 ER</u>	<u>48 ER</u>	<u>72 ER</u>	<u>BT WN</u>	<u>WW ER</u>	<u>24 WE</u>	<u>48 WE</u>	<u>72 WE</u>
87072206	1	10.1N	168.8E	72	43	115.7	272.6	45	-5	0	-10	-30
87072212	2	10.7N	167.5E	38	90.8	83.7	246.9	45	-5	-5	-15	-35
87072218	3	10.9N	165.8E	30.6	60.8	176.4	366.8	45	0	-5	-20	-35
87072300	4	10.8N	164.2E	30.1	25.2	195.1	362.8	50	0	-5	-25	-40
87072306	5	10.8N	162.4E	18.9	120.7	277.8	475.5	50	0	-10	-40	-60
87072312	6	11.2N	160.7E	30.6	144.4	289.9	435.2	55	-5	-5	-35	-45
87072318	7	11.6N	159.2E	18.9	129.7	287.4	410.4	60	-5	-15	-40	-35
87072400	8	12.1N	157.6E	8.4	96	216	294.1	65	-5	-25	-30	-5
87072406	9	12.8N	156.2E	0	126	234.3	318.8	70	-5	-30	-30	0
87072412	10	13.6N	154.7E	18	115.3	225.6	367.1	75	-5	-20	-10	5
87072418	11	14.2N	153.1E	37.7	132.1	254.3	402.2	85	0	-10	0	15
87072500	12	15.0N	151.5E	13.1	144.1	255.1	284.5	95	0	-10	5	10
87072506	13	15.7N	150.0E	26	151	163.6	192.9	105	0	-5	5	5
87072512	14	16.4N	148.4E	13	85.2	142.8	218.4	110	-5	-5	0	10
87072518	15	17.1N	146.8E	18.9	79.6	172.5	249.2	115	-5	0	0	5
87072600	16	17.8N	145.3E	17.1	83.1	210.7	402.7	120	0	5	-5	-5
87072606	17	18.4N	143.7E	11.4	68.8	154.4	248.8	125	0	5	-5	5
87072612	18	18.9N	142.0E	6	81.7	200	261.4	125	0	0	-5	10
87072618	19	19.4N	140.7E	11.3	86.6	198.5	229.3	120	0	0	0	15
87072700	20	20.0N	139.3E	5.6	27.6	109.9	161.4	115	0	-15	-20	15
87072706	21	20.6N	138.1E	5.6	52.6	126.5	115.8	115	-5	-20	-10	5
87072712	22	21.3N	136.8E	5.6	64.6	142.9	105.9	120	-10	-10	5	5
87072718	23	22.1N	135.7E	0	44.9	123.3	172.4	115	-5	-5	15	5
87072800	24	23.0N	134.7E	12	76.1	237.3	483.2	110	5	15	50	35
87072806	25	23.9N	133.9E	16.3	99.6	285.8	557.3	110	5	25	45	40
87072812	26	24.8N	133.2E	13.2	97.3	312.1	575.6	105	10	35	35	35
87072818	27	25.7N	132.6E	5.4	86.4	314.3	545.7	100	15	35	25	25
87072900	28	26.8N	132.3E	5.4	56.5	248	364.1	95	15	40	15	5
87072906	29	27.9N	132.1E	6	144.5	397.1	461.5	85	20	30	15	5
87072912	30	29.4N	132.4E	26.2	186.8	417.4	406.4	75	15	10	10	10
87072918	31	30.7N	133.1E	12	206.7	N/A	N/A	65	10	-15	N/A	N/A
87073000	32	31.7N	134.3E	7.9	238.5	N/A	N/A	50	10	-15	N/A	N/A
87073006	33	32.2N	135.9E	16.4	265.1	N/A	N/A	55	5	-15	N/A	N/A
87073012	34	32.2N	136.3E	6	100.3	N/A	N/A	60	0	-5	N/A	N/A
87073018	35	32.3N	140.8E	7.9	117.9	N/A	N/A	60	0	-5	N/A	N/A
87073100	36	32.3N	143.1E	7.9	132.8	N/A	N/A	55	0	-10	N/A	N/A
87073106	37	32.5N	145.5E	16.3	N/A	N/A	N/A	50	0	N/A	N/A	N/A
87073112	38	32.6N	147.8E	7.8	N/A	N/A	N/A	45	-5	N/A	N/A	N/A
87073118	39	32.7N	150.2E	20.2	N/A	N/A	N/A	45	-10	N/A	N/A	N/A
87080100	40	33.6N	152.2E	24	N/A	N/A	N/A	45	-15	N/A	N/A	N/A

Typhoon Alex (08W)

	<u>00h</u>	<u>24h</u>	<u>48h</u>	<u>72h</u>
Average	15	111	204	330
# Cases	22	20	16	12

<u>DTG</u>	<u>W#</u>	<u>BT LAT</u>	<u>BT LON</u>	<u>POS ER</u>	<u>24 ER</u>	<u>48 ER</u>	<u>72 ER</u>	<u>BT WN</u>	<u>WW ER</u>	<u>24 WE</u>	<u>48 WE</u>	<u>72 WE</u>
87072300	1	10.3N	134.4E	6	102.5	261.5	418	30	0	-5	-5	5
87072306	2	10.6N	132.9E	6	130.9	271.6	461.6	35	0	0	5	0
87072312	3	10.9N	131.3E	18.9	251.1	373.1	517.9	35	0	-5	-20	-10
87072318	4	11.7N	130.1E	13.4	196.4	345.6	553.6	40	0	-10	-20	-10
87072400	5	12.7N	129.3E	48.4	175.9	342	552.6	45	-5	-10	-25	-10
87072406	6	13.9N	128.9E	13.3	61.1	191.1	229.1	50	-10	-10	-25	-10
87072412	7	14.9N	128.1E	8.3	67.2	160.1	206.7	55	0	-5	-10	0
87072418	8	15.7N	127.1E	13	99	154.8	144.4	60	0	-5	-10	5
87072500	9	16.5N	126.0E	34.6	158.6	282.1	305.6	60	5	-5	5	15
87072506	10	17.5N	125.1E	47.3	162.2	177.6	N/A	60	0	-25	-30	N/A
87072512	11	18.4N	124.4E	8.3	32.6	42	N/A	65	0	0	-10	N/A
87072518	12	19.4N	123.7E	5.7	49.4	102.9	N/A	65	0	-5	-5	N/A
87072600	13	20.3N	123.0E	11.3	72.9	146.3	N/A	65	0	-5	0	N/A
87072606	14	21.4N	122.6E	8.2	63.8	126.8	174.5	65	0	-5	15	10
87072612	15	22.6N	122.3E	12	78.6	155.1	191.6	65	0	0	20	15
87072618	16	23.8N	122.1E	6	67.4	134.1	213	65	0	0	15	10
87072700	17	25.2N	121.7E	0	136.6	N/A	N/A	60	0	5	N/A	N/A
87072706	18	26.5N	121.0E	26.3	185.5	N/A	N/A	60	0	10	N/A	N/A
87072712	19	27.8N	120.7E	16	67.5	N/A	N/A	55	0	10	N/A	N/A
87072718	20	29.2N	120.7E	16.8	63.9	N/A	N/A	50	0	10	N/A	N/A
87072800	21	30.7N	120.8E	12	N/A	N/A	N/A	40	5	N/A	N/A	N/A
87072806	22	32.2N	121.1E	19.4	N/A	N/A	N/A	30	0	N/A	N/A	N/A

Super Typhoon Betty (09W)

	<u>00h</u>	<u>24h</u>	<u>48h</u>	<u>72h</u>
Average	7	91	197	257
# Cases	32	30	26	17

<u>DTG</u>	<u>W#</u>	<u>BT LAT</u>	<u>BT LON</u>	<u>POS ER</u>	<u>24 ER</u>	<u>48 ER</u>	<u>72 ER</u>	<u>BT WN</u>	<u>WW ER</u>	<u>24 WE</u>	<u>48 WE</u>	<u>72 WE</u>
87080900	1	10.2N	132.2E	6	31.8	8.4	113.8	35	0	-10	-45	-45
87080906	2	10.4N	132.1E	13.2	79.1	74.1	130.7	40	5	0	-35	-15
87080912	3	10.7N	131.9E	5.9	8.4	121.8	235.9	45	5	-15	-55	-20
87080918	4	10.9N	131.8E	13.4	37.2	178.9	315.7	45	5	-25	-55	-15
87081000	5	11.3N	131.7E	5.9	94	235.8	362.7	55	0	-45	-55	-15
87081006	6	11.6N	131.6E	8.4	141.8	302.8	437.3	65	0	-50	-35	10
87081012	7	11.9N	131.1E	5.9	83.8	184.4	290.5	85	-5	-40	-10	-5
87081018	8	12.1N	130.4E	0	93.3	186.8	293.4	95	-5	-30	-5	-25
87081100	9	12.2N	129.6E	5.9	67.8	112.9	185.9	110	0	-5	10	-25
87081106	10	12.2N	128.6E	8.4	50.7	124.4	147.3	125	0	10	25	-30
87081112	11	12.2N	127.6E	8.4	42.5	97.6	156	140	0	20	-15	-25
87081118	12	12.3N	126.5E	0	55.6	123.2	310.1	140	0	15	-20	-25
87081200	13	12.4N	125.5E	0	66.6	133.7	184.5	135	0	0	-15	-20
87081206	14	12.7N	124.2E	16.8	59.4	144.4	181.1	125	0	-15	-25	-5
87081212	15	12.9N	122.9E	11.7	54.6	160.8	315.5	120	-5	10	0	10
87081218	16	13.3N	121.7E	8.4	75.8	208.3	342.1	115	-10	-10	-25	-20
87081300	17	13.7N	120.5E	5.8	96.1	231.8	370.5	110	-15	5	-5	-10
87081306	18	14.1N	119.0E	13.3	123.2	289.2	N/A	95	10	5	-15	N/A
87081312	19	14.4N	117.6E	16.7	90.7	303.4	N/A	100	5	-25	-45	N/A
87081318	20	14.8N	116.2E	12	175.5	344.9	N/A	105	0	-25	-30	N/A
87081400	21	15.3N	115.1E	6	151	339.5	N/A	105	0	-25	-25	N/A
87081406	22	15.7N	114.0E	8.3	103.4	287.1	N/A	115	-10	-25	-15	N/A
87081412	23	15.8N	112.7E	0	78.2	241.8	N/A	115	0	-10	5	N/A
87081418	24	15.8N	111.6E	0	54.6	70.2	N/A	115	-5	-10	15	N/A

87081500	25	16.3N	110.8E	13	64	281.9	N/A	115	-5	5	40	N/A
87081506	26	16.7N	110.1E	0	74.5	343.9	N/A	105	-5	10	30	N/A
87081512	27	17.0N	109.2E	5.7	104.3	N/A	N/A	95	-5	15	N/A	N/A
87081518	28	17.3N	108.3E	0	116	N/A	N/A	90	-10	20	N/A	N/A
87081600	29	17.5N	107.5E	0	189.3	N/A	N/A	80	-10	15	N/A	N/A
87081606	30	17.7N	106.8E	0	278.3	N/A	N/A	65	-5	15	N/A	N/A
87081612	31	18.0N	105.6E	23.6	N/A	N/A	N/A	45	0	N/A	N/A	N/A
87081618	32	18.1N	104.3E	62.4	N/A	N/A	N/A	30	0	N/A	N/A	N/A

Typhoon Cary (10W)

	<u>00h</u>	<u>24h</u>	<u>48h</u>	<u>72h</u>
Average	15	89	159	247
# Cases	39	36	33	29

DTG	W#	BT LAT	BT LON	POS ER	24 ER	48 ER	72 ER	BT WN	WW ER	24 WE	48 WE	72 WE
87081300	1	13.6N	134.0E	6	39.9	79.9	159.4	40	10	20	35	55
87081306	2	14.3N	133.1E	18.4	58.2	120.3	210	45	10	25	40	55
87081312	3	14.9N	132.2E	5.8	78	125.1	208	50	-5	5	15	25
87081318	4	15.3N	131.3E	28.9	125	209.3	317.9	55	0	20	25	35
87081400	5	15.5N	130.4E	23.1	132.5	258.8	410.2	55	10	25	40	40
87081406	6	15.8N	129.6E	31.3	121.8	234.6	426	55	10	20	30	20
87081412	7	16.0N	128.8E	17.3	101.6	243.9	454.5	60	5	10	15	15
87081418	8	16.1N	128.3E	46.5	100.9	236.1	458.8	60	5	5	10	15
87081500	9	16.2N	127.8E	24.7	24	72.2	255.1	65	0	10	5	5
87081506	10	16.3N	127.2E	12	18.2	133.1	284.2	65	0	10	-5	10
87081512	11	16.5N	126.6E	13	78.7	235.9	403.8	65	0	0	0	25
87081518	12	16.7N	126.1E	34.6	67.5	167.7	307.3	70	-5	-20	-30	0
87081600	13	16.9N	125.7E	0	91.6	168.4	302.2	65	0	-10	-10	10
87081606	14	17.0N	125.2E	18.2	96.7	198.3	287	65	5	-10	5	20
87081612	15	16.9N	124.7E	18.2	172.2	249.2	243.8	70	5	-10	20	25
87081618	16	16.8N	124.2E	21	167.7	270	274.2	75	0	-5	20	30
87081700	17	16.5N	123.8E	23.8	94	192.1	259.7	80	-5	0	20	25
87081706	18	16.4N	123.5E	5.8	71.6	174.5	266.9	85	-5	15	15	15
87081712	19	16.2N	123.0E	0	73	168.8	261.2	80	0	10	10	20
87081718	20	16.1N	122.5E	11.5	130.2	210	248.4	75	0	0	15	15
87081800	21	16.0N	121.8E	18.3	122.4	203.2	253.8	70	0	15	20	15
87081806	22	15.7N	120.9E	23.1	87.8	185.7	194.4	60	0	10	10	5
87081812	23	15.4N	120.1E	8.3	59	83.1	46.7	50	0	15	15	-5
87081818	24	15.2N	118.8E	11.6	69.5	153.4	131.1	55	0	15	0	-5
87081900	25	15.2N	117.8E	6	6	93.7	12.9	55	5	20	10	0
87081906	26	15.4N	117.0E	6	26	77.7	29.1	55	5	15	5	0
87081912	27	15.7N	116.2E	13	70.6	43.9	167.3	55	0	0	-5	-5
87081918	28	15.8N	115.1E	25	90.2	78.8	193.3	55	5	5	-10	-5
87082000	29	15.8N	114.2E	18.9	101.7	45.4	106.9	55	0	-15	-25	-10
87082006	30	15.8N	113.4E	11.5	52.1	61.8	N/A	60	-5	-20	-25	N/A
87082012	31	15.9N	112.8E	5.8	56.7	143	N/A	60	5	-20	-20	N/A
87082018	32	16.2N	112.3E	18.9	96.7	134.2	N/A	65	-5	-15	-10	N/A
87082100	33	16.4N	111.7E	6	111	212.1	N/A	65	-10	-20	-5	N/A
87082106	34	16.8N	111.1E	0	108.8	N/A	N/A	70	-15	-20	N/A	N/A
87082112	35	17.4N	110.3E	6	133.9	N/A	N/A	70	-15	-20	N/A	N/A
87082118	36	18.1N	109.1E	12.9	168.7	N/A	N/A	65	-20	-15	N/A	N/A
87082200	37	18.4N	107.8E	24.7	N/A	N/A	N/A	65	-25	N/A	N/A	N/A
87082206	38	18.5N	106.6E	13.3	N/A	N/A	N/A	65	-25	N/A	N/A	N/A
87082212	39	18.7N	105.6E	6	N/A	N/A	N/A	60	-30	N/A	N/A	N/A

Super Typhoon Dinah (11W)

	<u>00h</u>	<u>24h</u>	<u>48h</u>	<u>72h</u>
Average	17	96	172	222
# Cases	42	38	34	30

<u>DTG</u>	<u>W#</u>	<u>BT LAT</u>	<u>BT LON</u>	<u>POS ER</u>	<u>24 ER</u>	<u>48 ER</u>	<u>72 ER</u>	<u>BT WN</u>	<u>WW ER</u>	<u>24 WE</u>	<u>48 WE</u>	<u>72 WE</u>
87082100	1	12.2N	149.9E	95.1	219.7	357.7	326	25	0	-5	0	-5
87082106	2	12.2N	149.0E	70.4	201.5	193.2	54.6	30	-5	0	10	5
87082112	3	11.8N	148.0E	60	174.9	213.7	213.4	30	0	5	15	10
87082118	4	11.3N	147.0E	40.1	76.2	95	152	35	-5	0	10	15
87082200	5	11.1N	145.7E	30	42.4	85.3	143.4	40	0	20	25	25
87082206	6	11.1N	144.2E	24.7	87.1	105.2	159.6	40	5	25	25	15
87082212	7	11.1N	142.6E	18.7	94.7	139.2	215.5	40	5	25	30	15
87082218	8	11.3N	141.2E	5.9	181.9	188.3	270.7	45	5	25	30	5
87082300	9	11.4N	140.3E	11.8	155.2	208.1	260.5	45	5	-5	5	-15
87082306	10	11.6N	139.7E	23.5	88	151.7	245.5	45	10	5	-5	-5
87082312	11	11.8N	139.0E	17.6	84.3	129.3	165.6	50	5	-5	-25	-15
87082318	12	12.2N	138.2E	18.9	97.3	108.2	136	55	5	5	-25	0
87082400	13	12.8N	137.1E	36.5	75.7	105	124.1	60	0	-5	-30	5
87082406	14	13.5N	135.9E	8.4	55	175.4	254.5	65	0	-20	-25	5
87082412	15	14.0N	134.8E	8.4	71.2	187.3	249.3	70	0	-25	-20	5
87082418	16	14.6N	133.7E	5.8	81	192.1	235.5	75	0	-30	-10	5
87082500	17	15.2N	132.8E	0	51.7	150.6	224.2	85	5	-15	15	15
87082506	18	15.9N	131.8E	8.3	107.8	176.7	255.8	100	0	5	15	15
87082512	19	16.7N	131.1E	8.3	66	114.9	205.2	110	0	15	15	20
87082518	20	17.3N	130.6E	6	46.8	74	144.4	120	5	20	15	30
87082600	21	17.9N	130.2E	16.6	29.4	41.3	81.6	130	0	25	25	35
87082606	22	18.5N	130.0E	5.7	39.8	98.1	108.1	125	-5	-15	-20	-10
87082612	23	19.0N	129.8E	0	55.6	134.8	140.7	120	5	0	-10	-5
87082618	24	19.5N	129.5E	5.7	84.8	148.9	160.7	115	5	-5	-5	-10
87082700	25	19.9N	129.0E	11.3	85.9	149.8	165.3	115	5	5	5	-5
87082706	26	20.1N	128.6E	22.5	65.9	108.1	193.8	115	0	0	0	-10
87082712	27	20.4N	128.2E	5.6	36.8	81.1	282.6	115	0	0	5	-10
87082718	28	20.6N	127.8E	17.9	35.4	110.9	366	115	-5	0	0	-5
87082800	29	21.0N	127.4E	8.2	17.6	144.5	503.3	110	0	10	5	15
87082806	30	21.3N	127.0E	8.2	24.6	180	628	110	-5	5	0	15
87082812	31	21.6N	126.8E	11.2	138	401.9	N/A	105	-5	5	-5	N/A
87082818	32	22.2N	126.5E	6	84.1	266.2	N/A	95	0	-5	-10	N/A
87082900	33	23.0N	126.3E	17.6	129.6	396	N/A	90	5	-5	0	N/A
87082906	34	24.1N	126.2E	12	122.7	456.4	N/A	90	5	-10	10	N/A
87082912	35	25.2N	126.0E	18.8	173	N/A	N/A	85	5	-10	N/A	N/A
87082918	36	26.6N	126.0E	12	158.3	N/A	N/A	85	0	-10	N/A	N/A
87083000	37	28.1N	126.2E	8	166.6	N/A	N/A	85	0	0	N/A	N/A
87083006	38	30.0N	126.6E	12	169.4	N/A	N/A	85	0	-5	N/A	N/A
87083012	39	31.8N	127.0E	15.3	N/A	N/A	N/A	85	-10	N/A	N/A	N/A
87083018	40	34.0N	128.7E	23.2	N/A	N/A	N/A	75	-5	N/A	N/A	N/A
87083100	41	36.8N	130.9E	41.5	N/A	N/A	N/A	65	0	N/A	N/A	N/A
87083106	42	39.6N	133.0E	N/A	N/A	N/A	N/A	55	N/A	N/A	N/A	N/A

Tropical Storm Ed (12W)

	<u>00h</u>	<u>24h</u>	<u>48h</u>	<u>72h</u>
Average	33	120	219	278
# Cases	12	10	6	5

<u>DTG</u>	<u>W#</u>	<u>BT LAT</u>	<u>BT LON</u>	<u>POS ER</u>	<u>24 ER</u>	<u>48 ER</u>	<u>72 ER</u>	<u>BT WN</u>	<u>WW ER</u>	<u>24 WE</u>	<u>48 WE</u>	<u>72 WE</u>
87082200	1	9.8N	160.8E	36	60.8	192.8	218	25	5	5	25	30
87082206	2	10.3N	159.7E	13.2	41.9	191.2	211.9	25	5	10	20	30
87082212	3	10.8N	158.7E	16.8	90.9	232.7	249	30	0	15	35	55
87082218	4	11.3N	157.7E	13.2	169.6	281.8	302.1	30	0	20	35	55

87082300	5	12.2N	157.1E	35.2	215.7	282.2	411.5	30	-5	15	20	30
87082306	6	12.9N	156.7E	50.7	N/A	N/A	N/A	25	N/A	N/A	N/A	N/A
87082618	7	16.1N	149.1E	37.8	178.6	138.5	N/A	35	-5	15	35	N/A
87082700	8	16.4N	148.4E	54.3	165.6	N/A	N/A	35	0	25	N/A	N/A
87082706	9	17.2N	147.7E	61.1	152.9	N/A	N/A	30	5	20	N/A	N/A
87082712	10	17.8N	146.8E	26.6	36.2	N/A	N/A	30	0	15	N/A	N/A
87082718	11	18.2N	145.9E	18.9	92.4	N/A	N/A	30	0	20	N/A	N/A
87082800	12	18.4N	145.2E	50.7	N/A	N/A	N/A	25	0	N/A	N/A	N/A

Typhoon Freda (13W)

	00h	24h	48h	72h
Average	16	81	181	327
# Cases	50	47	42	34

DTG	W#	BT_LAT	BT_LON	POS_ER	24_ER	48_ER	72_ER	BT_WN	WW_ER	24_WE	48_WE	72_WE
87090418	1	12.3N	145.0E	164.1	293.3	579.7	731.2	25	0	-10	-20	-20
87090500	2	13.0N	144.0E	24.7	29.6	286.3	432.4	30	0	-5	0	10
87090506	3	13.6N	142.8E	33.5	70.5	283.8	457.4	35	0	0	5	15
87090512	4	14.3N	141.8E	23.3	317.5	578	798.5	40	0	-5	10	10
87090518	5	14.9N	141.0E	31.4	304.2	552.2	782.6	45	-5	-15	0	-5
87090600	6	14.7N	140.7E	16.7	177.9	307.1	378.3	50	0	5	5	0
87090606	7	14.5N	140.9E	42.3	139.4	234.2	273.7	55	0	5	5	-5
87090612	8	14.6N	141.3E	18.4	110.1	189.3	233.3	60	0	10	15	0
87090618	9	15.0N	141.4E	11.6	23.9	60.3	111.4	65	0	15	15	0
87090700	10	15.2N	141.4E	16.7	23.9	18	85.5	65	0	0	-5	-15
87090706	11	15.3N	141.3E	17.4	33.3	24.9	51.9	70	-5	-10	-25	-25
87090712	12	15.5N	141.2E	18.3	29.2	21.4	69.7	70	0	-10	-25	-20
87090718	13	15.6N	141.0E	16.7	6	18.2	80.4	75	0	0	-15	-5
87090800	14	15.7N	140.8E	0	58.8	29.3	109.3	80	0	-10	-20	10
87090806	15	15.8N	140.7E	6	75	34.4	126.3	85	0	-15	-20	15
87090812	16	16.1N	140.3E	5.8	70	29.5	153.9	90	0	-15	-10	20
87090818	17	16.4N	139.7E	11.5	30	98.2	274.2	95	-5	-20	-5	25
87090900	18	16.4N	139.0E	6	89.3	264.8	510.5	100	0	-15	10	35
87090906	19	16.5N	138.5E	0	92.4	285.3	540.4	110	5	5	30	45
87090912	20	16.7N	138.1E	13	50	200.7	391.2	115	0	10	30	45
87090918	21	16.9N	137.8E	5.7	94.6	258	467.3	120	0	5	15	25
87091000	22	17.0N	137.5E	13	103.1	273.1	488.1	125	0	10	20	30
87091006	23	17.2N	137.2E	0	74.2	251.2	444.6	125	0	10	20	25
87091012	24	17.3N	137.1E	12.9	97.1	273.8	431.8	120	0	15	25	25
87091018	25	17.5N	137.0E	11.4	121.9	291.9	445.9	115	5	5	15	20
87091100	26	17.7N	137.0E	12.9	105.4	238.4	382.3	110	5	10	20	20
87091106	27	17.9N	137.1E	13.3	94.9	158.8	233.1	105	-5	5	15	20
87091112	28	18.3N	137.3E	8.3	63.3	128.3	188.1	100	-5	5	10	10
87091118	29	18.6N	137.6E	16.5	74	139.2	208	95	-10	0	10	10
87091200	30	19.0N	137.9E	13.3	62.1	122	252.9	90	-10	5	10	15
87091206	31	19.4N	138.3E	12	37.7	101.5	217.5	85	-10	0	5	5
87091212	32	19.8N	138.6E	13.3	58.4	137.4	285.5	80	-10	-5	0	0
87091218	33	20.2N	138.9E	13.3	58.4	142	280.1	75	-10	-5	-5	-5
87091300	34	20.8N	139.2E	8.2	52.8	124.4	225.8	70	-5	-5	0	-5
87091306	35	21.3N	139.4E	6	13.2	96.6	N/A	65	0	0	-5	N/A
87091312	36	22.0N	139.6E	6	24.6	91.5	N/A	65	0	-5	-10	N/A
87091318	37	22.6N	139.8E	12	40.3	129.7	N/A	60	5	-5	-10	N/A
87091400	38	23.3N	139.9E	6	56.9	192.6	N/A	60	-5	-5	-10	N/A
87091406	39	24.0N	140.1E	0	68.8	154.3	N/A	55	0	-5	-10	N/A
87091412	40	24.8N	140.2E	6	94.6	141.4	N/A	55	0	0	-5	N/A
87091418	41	25.6N	140.2E	13.2	84.3	59.7	N/A	55	-5	-5	0	N/A
87091500	42	26.6N	140.2E	18	57.9	43.9	N/A	50	0	0	10	N/A
87091506	43	27.6N	140.1E	8	90.1	N/A	N/A	50	0	-5	N/A	N/A

87091512	44	28.6N	139.9E	12.1	46.6	N/A	N/A	50	0	-5	N/A	N/A
87091518	45	29.6N	140.0E	8	43.2	N/A	N/A	50	0	-5	N/A	N/A
87091600	46	30.4N	140.3E	5.2	26	N/A	N/A	45	0	0	N/A	N/A
87091606	47	31.1N	140.7E	16.5	75.1	N/A	N/A	45	0	10	N/A	N/A
87091612	48	31.9N	141.4E	6	N/A	N/A	N/A	45	0	N/A	N/A	N/A
87091618	49	32.6N	142.3E	30	N/A	N/A	N/A	40	0	N/A	N/A	N/A
87091700	50	33.4N	143.0E	18.7	N/A	N/A	N/A	30	0	N/A	N/A	N/A

Typhoon Gerald (14W)

	<u>00h</u>	<u>24h</u>	<u>48h</u>	<u>72h</u>
Average	20	97	163	193
# Cases	24	20	18	14

<u>DTG</u>	<u>W#</u>	<u>BT LAT</u>	<u>BT LON</u>	<u>POS ER</u>	<u>24 ER</u>	<u>48 ER</u>	<u>72 ER</u>	<u>BT WN</u>	<u>WW ER</u>	<u>24 WE</u>	<u>48 WE</u>	<u>72 WE</u>
87090418	1	16.3N	126.3E	21.4	167.8	263.2	294.2	35	-10	-10	-30	-45
87090500	2	16.6N	126.6E	71.3	184.2	262.6	265	35	-5	-15	-30	-45
87090506	3	16.9N	126.5E	53.2	143.9	230.9	240.7	40	-5	0	-10	-25
87090512	4	17.1N	126.5E	51.8	122.3	155.9	94.1	45	-5	-10	-15	-30
87090518	5	17.3N	126.5E	17.2	70.7	63.9	82.9	45	-5	-10	-20	-35
87090600	6	17.4N	126.5E	30.5	79.8	54.3	138.1	50	-5	-5	-15	-25
87090606	7	17.5N	126.5E	24.7	48.3	66.7	156.8	55	-5	-5	-15	-15
87090612	8	17.6N	126.4E	13.3	12	102.7	170	60	-5	-10	-30	-10
87090618	9	17.8N	126.4E	6	66.4	105.1	134.2	60	-5	-15	-35	-5
87090700	10	18.0N	126.3E	12.9	115.7	198.6	206.8	65	-5	-15	-25	20
87090706	11	18.4N	126.0E	11.4	105.3	200.6	245.5	70	-5	-10	-15	40
87090712	12	19.0N	125.6E	12.8	100.3	186.7	232.6	75	-5	-20	-5	70
87090718	13	19.5N	125.1E	8.2	87.5	138.7	208	80	5	0	35	70
87090800	14	20.0N	124.7E	13.3	78.7	155	241.8	85	5	0	45	65
87090806	15	20.2N	124.0E	13.3	106.4	178.7	N/A	90	0	5	40	N/A
87090812	16	20.4N	123.2E	12.7	74.7	212.7	N/A	100	0	20	70	N/A
87090818	17	20.6N	122.4E	0	78.2	156.3	N/A	105	-5	0	30	N/A
87090900	18	20.9N	121.9E	16.8	98	199.3	N/A	105	0	10	20	N/A
87090906	19	21.3N	121.2E	8.2	100.2	N/A	N/A	100	0	20	N/A	N/A
87090912	20	21.7N	120.5E	8.2	111	N/A	N/A	90	0	40	N/A	N/A
87090918	21	22.5N	120.0E	16.6	N/A	N/A	N/A	80	0	N/A	N/A	N/A
87091000	22	23.2N	119.5E	12.6	N/A	N/A	N/A	70	-5	N/A	N/A	N/A
87091006	23	24.1N	119.0E	12.5	N/A	N/A	N/A	55	0	N/A	N/A	N/A
87091012	24	25.0N	118.5E	12.4	N/A	N/A	N/A	30	0	N/A	N/A	N/A

Super Typhoon Holly (15W)

	<u>00h</u>	<u>24h</u>	<u>48h</u>	<u>72h</u>
Average	23	122	275	455
# Cases	43	34	33	31

<u>DTG</u>	<u>W#</u>	<u>BT LAT</u>	<u>BT LON</u>	<u>POS ER</u>	<u>24 ER</u>	<u>48 ER</u>	<u>72 ER</u>	<u>BT WN</u>	<u>WW ER</u>	<u>24 WE</u>	<u>48 WE</u>	<u>72 WE</u>
87090506	1	12.2N	168.3E	11.7	60.6	65.1	78.9	30	0	-20	-45	-55
87090512	2	12.2N	167.8E	34.8	113.3	95.8	106.1	35	-5	-25	-50	-55
87090518	3	12.3N	167.1E	56.2	130.7	108.3	131.9	45	-10	-25	-50	-55
87090600	4	12.4N	166.2E	12	72.2	183.6	306.1	45	0	-15	-30	-25
87090606	5	12.6N	165.5E	37.1	120.2	258.9	421	55	-5	-20	-30	-30
87090612	6	12.9N	164.6E	6	49.4	150.1	333.4	65	-5	-30	-35	-50
87090618	7	13.3N	163.7E	26.3	110.5	221.6	428.9	70	-5	-20	-25	-35
87090700	8	13.8N	163.0E	26.7	106.6	211.9	423.2	80	-10	-25	-25	-20
87090706	9	14.3N	162.2E	21.4	112.1	225.6	466.1	90	-5	-10	-15	0
87090712	10	14.8N	161.4E	32.2	122.4	269.6	569.3	100	-5	0	-10	10
87090718	11	15.3N	160.7E	25	124.7	313.9	643.6	105	0	0	-5	15
87090800	12	15.8N	159.9E	8.3	67.6	310.9	675.3	110	-5	0	0	10
87090806	13	16.3N	159.2E	13	72.5	344.4	737.5	115	-5	-5	5	15

87090812	14	16.8N	158.4E	5.7	109.6	413.6	810.4	115	0	-10	10	20
87090818	15	17.3N	157.6E	5.7	173.2	439.5	755.5	120	-5	-10	10	30
87090900	16	17.8N	156.8E	13.3	191.8	490.7	757	125	0	0	15	40
87090906	17	18.3N	156.2E	23.6	192.3	505.2	743.1	135	-5	10	20	45
87090912	18	18.6N	155.9E	21.3	135.6	392.1	568.8	140	-5	20	30	65
87090918	19	18.9N	155.8E	26.6	144	350	506.4	140	-5	15	35	65
87091000	20	19.4N	155.6E	18	132.9	292.1	395.5	135	5	15	35	35
87091006	21	19.9N	155.5E	12.8	134.8	242.3	376.7	130	5	10	30	25
87091012	22	20.5N	155.5E	12	121.9	233.6	378.7	125	5	15	45	45
87091018	23	21.2N	155.6E	8.2	118.7	146.4	288.6	125	5	15	40	45
87091100	24	22.0N	155.8E	8.2	76	168.1	340.3	120	10	10	10	15
87091106	25	23.1N	156.0E	6	113.8	442.1	445.8	115	10	15	5	10
87091112	26	24.0N	156.0E	12	161.6	334.8	495.1	110	5	20	10	15
87091118	27	24.8N	155.7E	13.2	159.6	314.9	482	100	5	15	15	20
87091200	28	25.6N	155.3E	18	170.4	334.3	448.3	90	5	10	20	20
87091206	29	26.0N	155.2E	10.8	117.4	264.7	330.9	80	10	5	15	20
87091212	30	26.4N	155.2E	12.3	131.5	263.2	334.1	70	15	15	20	15
87091218	31	26.7N	155.4E	24.1	138.7	234.3	349.8	65	10	15	20	15
87091300	32	26.9N	155.6E	16.1	102.1	157.1	N/A	65	0	10	15	N/A
87091306	33	27.2N	156.0E	144	135.5	297.9	N/A	65	0	5	10	N/A
87091312	34	27.4N	156.5E	55.7	125.4	N/A	N/A	55	0	5	N/A	N/A
87091318	35	27.7N	157.1E	27.2	N/A	N/A	N/A	50	0	N/A	N/A	N/A
87091400	36	28.0N	157.5E	49.1	N/A	N/A	N/A	45	0	N/A	N/A	N/A
87091406	37	28.3N	157.9E	51.7	N/A	N/A	N/A	45	0	N/A	N/A	N/A
87091412	38	28.6N	158.2E	31.9	N/A	N/A	N/A	35	10	N/A	N/A	N/A
87091418	39	28.9N	158.3E	12.1	N/A	N/A	N/A	30	10	N/A	N/A	N/A
87091500	40	29.2N	158.5E	16.8	N/A	N/A	N/A	30	5	N/A	N/A	N/A
87091506	41	29.5N	158.5E	20.8	N/A	N/A	N/A	30	0	N/A	N/A	N/A
87091512	42	29.8N	158.6E	5.2	N/A	N/A	N/A	30	0	N/A	N/A	N/A
87091518	43	30.0N	158.7E	15.9	N/A	N/A	N/A	25	0	N/A	N/A	N/A

Typhoon Ian (16W)

	00h	24h	48h	72h
Average	14	82	201	344
# Cases	33	27	23	21

DTG	W#	BT LAT	BT LON	POS ER	24 ER	48 ER	72 ER	BT WN	WW ER	24 WE	48 WE	72 WE
87092306	1	16.2N	146.8E	53.2	100.5	155.5	241.8	25	0	-15	-35	-50
87092312	2	16.3N	146.4E	21	58.7	116.3	213.7	30	0	-15	-40	-40
87092318	3	16.2N	146.0E	8.3	91.6	180.8	288.1	35	0	-15	-45	-30
87092400	4	16.3N	145.5E	29.4	117	203.7	278	45	-5	-20	-50	-20
87092406	5	16.7N	144.9E	25.9	117.3	221.9	270.1	50	-5	-25	-40	-15
87092412	6	17.4N	144.4E	8.3	68.2	186.1	257	55	-5	-35	-30	0
87092418	7	17.8N	143.8E	18.9	83	222.2	304.4	60	-10	-35	-15	10
87092500	8	18.3N	143.3E	5.7	70.3	212.4	297.8	70	-5	-25	5	30
87092506	9	18.7N	142.7E	6	66.2	175.3	264.2	80	-10	-15	10	35
87092512	10	19.3N	142.1E	12	79.8	123	223.3	90	0	20	45	50
87092518	11	20.0N	141.4E	13.3	53.6	154.9	327.7	100	5	30	35	40
87092600	12	20.6N	140.8E	5.6	50.8	240.5	483.7	110	0	0	-5	0
87092606	13	21.3N	140.3E	8.2	112.9	335.3	593.2	105	0	0	-5	-5
87092612	14	22.0N	139.7E	6	152.5	366.7	626.1	100	0	-5	-5	-10
87092618	15	22.6N	139.0E	6	150	358.9	625.6	95	0	-10	0	-5
87092700	16	23.1N	138.6E	12	157.5	373.1	646.6	90	0	-5	0	-10
87092706	17	23.2N	138.3E	6	111	246.5	425.3	90	0	0	-5	-10
87092712	18	23.2N	138.1E	8.1	81.2	159.4	285.9	85	-5	0	-5	-5
87092718	19	23.3N	138.0E	25.1	109.3	177	248.8	85	-10	0	0	-5
87092800	20	23.4N	138.0E	17.6	77	154.7	197.9	80	-5	-5	-5	-10
87092806	21	23.5N	138.0E	22.8	60.7	101.4	128.2	75	-5	-5	-5	-10

87092812	22	23.6N	138.0E	5.5	30.5	88.3	N/A	70	-5	-10	-5	N/A
87092818	23	23.7N	138.0E	12	24.6	72.7	N/A	65	-5	-10	-10	N/A
87092900	24	23.8N	137.8E	21.1	8.1	N/A	N/A	65	-5	-15	N/A	N/A
87092906	25	23.9N	137.5E	11	31.9	N/A	N/A	65	-10	-20	N/A	N/A
87092912	26	23.9N	137.3E	8.1	24.9	N/A	N/A	65	-10	-15	N/A	N/A
87092918	27	24.0N	137.1E	17.5	N/A	N/A	N/A	60	-10	N/A	N/A	N/A
87093000	28	24.2N	136.9E	8.1	149.4	N/A	N/A	60	-15	-20	N/A	N/A
87093006	29	24.5N	136.8E	12	N/A	N/A	N/A	60	-20	N/A	N/A	N/A
87093012	30	24.8N	136.7E	6	N/A	N/A	N/A	55	-15	N/A	N/A	N/A
87093018	31	25.3N	137.1E	12.4	N/A	N/A	N/A	55	-20	N/A	N/A	N/A
87100100	32	26.1N	137.9E	12	N/A	N/A	N/A	55	-20	N/A	N/A	N/A
87100106	33	26.9N	138.3E	18.8	N/A	N/A	N/A	55	-25	N/A	N/A	N/A

Tropical Depression 17W				00h	24h	48h	72h
Average				21	81	N/A	N/A
# Cases				7	3	0	0

DTG	W#	BT LAT	BT LON	POS ER	24 ER	48 ER	72 ER	BT WN	WW ER	24 WE	48 WE	72 WE
87092418	1	17.0N	161.3E	68.9	155.5	N/A	N/A	30	0	15	N/A	N/A
87092500	2	17.0N	160.7E	17.2	45.7	N/A	N/A	30	0	5	N/A	N/A
87092506	3	16.9N	160.1E	8.3	43.5	N/A	N/A	30	-5	15	N/A	N/A
87092512	4	16.8N	159.4E	13	N/A	N/A	N/A	30	0	N/A	N/A	N/A
87092518	5	16.8N	158.7E	8.3	N/A	N/A	N/A	30	0	N/A	N/A	N/A
87092600	6	16.7N	157.9E	23.8	N/A	N/A	N/A	30	0	N/A	N/A	N/A
87092606	7	16.4N	157.3E	8.3	N/A	N/A	N/A	25	0	N/A	N/A	N/A

Tropical Storm June (18W)				00h	24h	48h	72h
Average				33	165	66	N/A
# Cases				9	2	2	0

DTG	W#	BT LAT	BT LON	POS ER	24 ER	48 ER	72 ER	BT WN	WW ER	24 WE	48 WE	72 WE
87092900	1	23.7N	155.8E	18.8	169.8	84.7	N/A	35	0	5	0	N/A
87092906	2	25.2N	155.0E	54	161.4	47.6	N/A	40	-5	5	5	N/A
87092912	3	26.8N	154.1E	49.2	N/A	N/A	N/A	35	-5	N/A	N/A	N/A
87092918	4	28.0N	152.3E	40.1	N/A	N/A	N/A	35	-5	N/A	N/A	N/A
87093000	5	28.2N	149.7E	29.1	N/A	N/A	N/A	35	-5	N/A	N/A	N/A
87093006	6	28.1N	148.7E	63.5	N/A	N/A	N/A	35	-5	N/A	N/A	N/A
87093012	7	28.4N	148.6E	5.3	N/A	N/A	N/A	35	0	N/A	N/A	N/A
87093018	8	29.2N	148.7E	31.8	N/A	N/A	N/A	30	0	N/A	N/A	N/A
87100100	9	29.9N	149.1E	7.9	N/A	N/A	N/A	30	0	N/A	N/A	N/A

Typhoon Kelly (19W)				00h	24h	48h	72h
Average				16	110	183	289
# Cases				28	25	21	17

DTG	W#	BT LAT	BT LON	POS ER	24 ER	48 ER	72 ER	BT WN	WW ER	24 WE	48 WE	72 WE
87101000	1	12.8N	137.4E	34.8	213.1	305.3	459.2	30	0	-5	-5	0
87101006	2	13.3N	137.6E	68.7	243.1	396.9	587.8	35	-5	-10	-5	0
87101012	3	14.0N	137.7E	26.2	152.5	283	440.8	40	-5	0	5	15
87101018	4	14.7N	137.8E	16.7	54.9	190.2	323.7	45	0	5	20	25
87101100	5	15.3N	137.9E	25	145.2	286.7	413.8	50	0	5	15	25
87101106	6	15.7N	137.7E	18.9	141.1	265.9	410.8	55	0	10	20	30
87101112	7	16.0N	137.6E	5.8	45.6	81.1	138.7	55	5	0	15	25
87101118	8	16.2N	137.3E	26	120.5	174.6	216.1	60	5	10	15	25
87101200	9	16.4N	137.2E	18.3	92.9	157.5	207	65	0	10	20	25

87101206	10	16.8N	137.2E	23	41.5	94.6	92.2	65	0	10	20	25
87101212	11	17.3N	137.2E	8.3	24.7	117.3	148.2	70	0	20	20	20
87101218	12	17.8N	137.1E	6	47.7	147.8	169.1	70	5	20	25	25
87101300	13	18.3N	136.8E	8.3	76.8	174	182.7	75	5	10	20	0
87101306	14	18.9N	136.4E	8.3	44.9	92.1	177.9	75	0	-15	-35	-45
87101312	15	19.5N	136.1E	8.2	88.5	103.3	276.8	75	0	-20	-40	-35
87101318	16	20.2N	135.7E	12	102.8	92.5	335.6	80	-5	-20	-40	-25
87101400	17	21.3N	135.2E	8.2	97.9	88	336.9	80	-5	-20	-30	0
87101406	18	22.1N	134.5E	16.4	80.1	88.2	N/A	80	-5	-20	-30	N/A
87101412	19	23.0N	133.7E	13.2	90.7	193.1	N/A	85	-10	-25	-25	N/A
87101418	20	24.0N	133.0E	12.5	53.1	216.7	N/A	85	-10	-30	-20	N/A
87101500	21	25.0N	132.2E	5.4	38.7	294.4	N/A	90	-5	-15	10	N/A
87101506	22	25.8N	131.9E	6	151.6	N/A	N/A	90	-5	-15	N/A	N/A
87101512	23	26.7N	131.8E	6	126.1	N/A	N/A	95	-15	-10	N/A	N/A
87101518	24	27.7N	131.9E	10.6	211.5	N/A	N/A	95	-15	-5	N/A	N/A
87101600	25	29.0N	132.4E	28.8	279.7	N/A	N/A	90	-20	5	N/A	N/A
87101606	26	30.4N	133.0E	16.6	N/A	N/A	N/A	90	-30	N/A	N/A	N/A
87101612	27	32.2N	133.4E	19.4	N/A	N/A	N/A	80	-25	N/A	N/A	N/A
87101618	28	34.2N	134.4E	N/A	N/A	N/A	N/A	70	N/A	N/A	N/A	N/A

Super Typhoon Lynn (20W)

	00h	24h	48h	72h
Average	17	89	184	298
# Cases	44	41	39	31

DTG	W#	BT LAT	BT LON	POS ER	24 ER	48 ER	72 ER	BT WN	WW ER	24 WE	48 WE	72 WE
87101606	1	13.0N	155.3E	35.1	238.8	341.6	412.8	35	0	-10	-15	-30
87101612	2	13.2N	153.9E	24.1	147.2	170.7	248.3	35	0	-5	-5	-20
87101618	3	13.3N	153.2E	13.1	72.6	68.1	164.5	40	0	-5	-5	-25
87101700	4	13.3N	152.3E	16.7	36.5	114.1	126.1	45	0	0	-5	-30
87101706	5	13.3N	151.3E	8.4	76.7	144.5	133.1	55	-10	-5	-15	-30
87101712	6	13.2N	150.1E	23.4	100.9	157	145.8	55	-5	-10	-30	-30
87101718	7	13.3N	148.9E	8.4	99	166.6	190.9	60	-5	-10	-35	-25
87101800	8	13.6N	147.6E	12	146.8	223.4	251.2	65	-5	-10	-45	-25
87101806	9	14.0N	146.6E	5.8	26	12.9	53.7	70	-5	-15	-40	-5
87101812	10	14.6N	145.7E	13.1	34.5	37.3	89	75	-5	-20	-35	-15
87101818	11	15.1N	145.0E	11.6	6	13.3	131.3	80	-10	-35	-40	-10
87101900	12	15.7N	144.3E	16.7	40.1	98	245.8	90	-5	-40	-30	20
87101906	13	16.2N	143.5E	8.3	26.6	149.4	353.7	100	-10	-35	-10	25
87101912	14	16.6N	142.7E	6	39.9	145.7	256.6	115	-20	-25	-5	20
87101918	15	16.9N	141.8E	8.3	49.6	173.1	280.2	125	-10	-5	20	25
87102000	16	17.3N	141.1E	13.3	107.5	290.9	472.6	140	0	5	40	40
87102006	17	17.6N	140.2E	18.9	148.7	332.3	530.4	140	0	15	25	25
87102012	18	17.8N	139.2E	11.4	146.5	378.9	559	140	0	15	25	20
87102018	19	18.0N	138.0E	17.1	168.1	392.4	558.7	140	-5	10	20	10
87102100	20	18.0N	136.7E	30.9	145.9	342.6	466.6	140	-10	20	20	5
87102106	21	18.0N	135.3E	24.8	140.4	308.5	395.7	125	0	15	15	5
87102112	22	18.0N	134.0E	11.4	81.8	117.9	118.9	125	-5	10	5	5
87102118	23	18.0N	132.5E	26.6	74.4	34.5	146.7	115	0	10	0	5
87102200	24	18.0N	130.9E	8.3	36.4	99.6	270.2	100	5	5	-15	-5
87102206	25	18.0N	129.3E	5.7	62.4	162.2	347.7	100	0	-10	-25	-20
87102212	26	18.1N	127.8E	6	45.9	198	393.6	100	-5	-20	-15	-15
87102218	27	18.1N	126.3E	12.9	97.8	297.3	530.8	95	-5	-25	-10	-10
87102300	28	18.3N	124.9E	12.9	113.6	315.8	514	90	0	-25	-10	-10
87102306	29	18.5N	123.6E	6	107.5	260	391	90	0	-20	-5	5
87102312	30	18.8N	122.5E	11.4	118.5	235.5	N/A	90	-5	-10	-5	N/A
87102318	31	19.1N	121.6E	17	118.2	257.5	N/A	90	-5	0	5	N/A
87102400	32	19.4N	120.9E	12.8	75.3	174.2	229.4	90	-5	0	10	5

87102406	33	19.7N	120.3E	16.5	98.4	178.9	230.8	85	-5	0	15	5
87102412	34	20.0N	119.9E	0	78.6	149.1	N/A	75	0	5	15	N/A
87102418	35	20.3N	119.6E	30.6	126.4	196.6	N/A	65	5	10	0	N/A
87102500	36	20.6N	119.3E	28.7	95.6	147.4	N/A	65	0	5	0	N/A
87102506	37	20.9N	119.1E	24.6	17.8	68.1	N/A	60	5	10	5	N/A
87102512	38	21.1N	119.0E	12.7	69.7	179.4	N/A	55	5	10	5	N/A
87102518	39	21.3N	118.9E	12.7	91	N/A	N/A	45	10	5	N/A	N/A
87102600	40	21.5N	118.7E	12.7	68.7	49.3	N/A	45	0	-5	-5	N/A
87102606	41	21.7N	118.2E	23.1	73.4	N/A	N/A	40	-5	-10	N/A	N/A
87102612	42	21.6N	117.8E	66.9	N/A	N/A	N/A	35	-5	N/A	N/A	N/A
87102618	43	21.5N	117.6E	73.5	N/A	N/A	N/A	35	-5	N/A	N/A	N/A
87102700	44	21.3N	117.3E	11.2	N/A	N/A	N/A	35	-10	N/A	N/A	N/A

Tropical Storm Maury (21W)

	00h	24h	48h	72h
Average	27	107	162	183
# Cases	29	19	13	12

DTG	W#	BT LAT	BT LON	POS ER	24 ER	48 ER	72 ER	BT WN	WW ER	24 WE	48 WE	72 WE
87111106	1	14.7N	133.5E	8.3	133.4	217.2	339.6	30	0	25	35	30
87111112	2	15.0N	132.9E	23.2	141.9	223.6	279.7	30	0	30	35	45
87111118	3	15.0N	132.4E	13.3	159.7	288.9	324.9	25	5	15	20	35
87111200	4	14.5N	132.3E	42	N/A	N/A	N/A	20	5	N/A	N/A	N/A
87111306	5	13.7N	127.6E	18.9	92.6	151.9	171.5	30	0	15	15	20
87111312	6	13.6N	126.9E	66.7	221.7	349.7	395.1	30	0	10	20	15
87111318	7	13.5N	126.2E	88.4	221.8	304.3	317.1	30	0	0	10	5
87111400	8	13.5N	125.6E	5.8	25.1	88.5	141.8	30	0	5	0	0
87111406	9	13.5N	125.0E	16.7	83.7	N/A	N/A	25	0	0	N/A	N/A
87111412	10	13.5N	124.3E	8.4	N/A	N/A	N/A	25	0	N/A	N/A	N/A
87111418	11	13.4N	123.6E	26.2	N/A	N/A	N/A	25	0	N/A	N/A	N/A
87111500	12	13.2N	122.7E	13.1	N/A	N/A	N/A	25	0	N/A	N/A	N/A
87111506	13	13.0N	122.0E	21.3	46.8	111.6	50.1	25	5	10	0	20
87111512	14	12.8N	121.0E	13.1	76.9	102.2	50.7	25	5	5	10	25
87111518	15	12.8N	119.9E	12	76.8	47.4	42.4	25	5	0	10	30
87111600	16	12.8N	118.6E	21.3	87.1	52.9	40	30	0	0	10	20
87111606	17	12.9N	117.3E	12	72.6	62.9	47.3	30	0	-5	15	10
87111612	18	13.3N	116.1E	30.6	42.5	113.8	N/A	35	0	5	0	N/A
87111618	19	13.5N	115.1E	12	78.8	N/A	N/A	40	-5	0	N/A	N/A
87111700	20	13.5N	114.2E	29.5	144.3	N/A	N/A	40	-5	5	N/A	N/A
87111706	21	13.4N	113.3E	72.5	200.5	N/A	N/A	45	-10	-5	N/A	N/A
87111712	22	13.0N	112.8E	110.5	N/A	N/A	N/A	40	-5	N/A	N/A	N/A
87111718	23	13.0N	112.3E	30.6	N/A	N/A	N/A	40	-10	N/A	N/A	N/A
87111800	24	13.0N	111.9E	39.4	N/A	N/A	N/A	35	-5	N/A	N/A	N/A
87111806	25	13.0N	111.5E	8.4	42.6	N/A	N/A	35	5	5	N/A	N/A
87111812	26	12.9N	110.9E	5.8	88.7	N/A	N/A	35	5	10	N/A	N/A
87111818	27	12.8N	110.3E	8.4	N/A	N/A	N/A	30	5	N/A	N/A	N/A
87111900	28	12.7N	109.6E	21.3	N/A	N/A	N/A	30	0	N/A	N/A	N/A
87111906	29	12.3N	108.8E	18.9	N/A	N/A	N/A	25	0	N/A	N/A	N/A

Super Typhoon Nina (22W)

	00h	24h	48h	72h
Average	17	138	235	279
# Cases	40	36	32	30

DTG	W#	BT LAT	BT LON	POS ER	24 ER	48 ER	72 ER	BT WN	WW ER	24 WE	48 WE	72 WE
87111912	1	4.6N	159.0E	37.8	289	544.1	725.9	30	0	0	10	25
87111918	2	4.8N	157.7E	48.2	279.4	492.6	592	35	0	-5	15	25
87112000	3	5.2N	156.2E	49.3	217	391.8	520.3	40	5	5	25	25

87112006	4	5.8N	154.6E	8.5	182.6	353	466.7	45	0	5	25	25
87112012	5	6.5N	152.9E	13.3	114	224.7	281.4	50	-5	0	15	25
87112018	6	7.2N	151.3E	6	148.8	222.5	236.7	60	-15	0	10	20
87112100	7	8.0N	149.6E	18.8	148.6	257.9	240.5	60	-5	5	5	25
87112106	8	8.7N	147.8E	30.3	129.7	206.1	155.3	60	-5	0	0	15
87112112	9	9.5N	146.0E	13.4	81	180.3	194.8	65	-10	-5	-5	0
87112118	10	10.0N	144.3E	29.5	34.8	78.9	156.1	65	-5	0	0	-5
87112200	11	10.3N	142.7E	8.4	64.5	114.2	162.1	65	0	-5	5	-15
87112206	12	10.7N	141.0E	0	84.2	148.2	206.3	70	0	-5	0	-20
87112212	13	11.0N	139.3E	12	69.5	150.5	235.1	75	0	5	5	-30
87112218	14	11.1N	137.8E	24.7	56.8	146.9	213.7	80	5	10	0	-15
87112300	15	11.2N	136.1E	6	100.5	165	115.3	85	5	20	-10	5
87112306	16	11.5N	134.6E	13.4	137	180.2	77.6	90	0	0	-35	-15
87112312	17	11.8N	133.4E	13.2	76.9	63	110.9	90	0	-20	-70	-30
87112318	18	11.9N	132.5E	6	42	97.4	179.6	95	-5	-30	-55	-35
87112400	19	11.9N	131.6E	5.9	36.5	122.2	219.5	90	0	-30	-30	-35
87112406	20	12.0N	130.6E	6	46.4	187	276.7	100	-10	-55	-30	-35
87112412	21	12.1N	129.6E	8.4	63.2	205	304.7	105	-20	-70	-30	-30
87112418	22	12.3N	128.5E	5.9	111.7	241.6	290.7	115	-20	-30	-20	-10
87112500	23	12.6N	127.4E	18.6	181.3	329.1	309.1	125	-30	-10	-15	0
87112506	24	12.8N	126.1E	5.9	188	333.5	264.5	135	-20	10	5	10
87112512	25	13.0N	124.5E	13.1	108.8	199.4	281.2	145	-10	5	15	30
87112518	26	13.2N	122.8E	13.1	92.8	228.5	356.1	130	0	5	10	30
87112600	27	13.5N	121.0E	8.4	106.9	162.6	205.1	110	0	-5	5	45
87112606	28	14.0N	119.3E	13.1	99.8	156.9	240.9	95	0	0	-10	45
87112612	29	14.6N	117.8E	6	72.2	137.3	361.9	95	-10	-5	-15	10
87112618	30	15.2N	116.4E	5.8	96.7	215.9	400	100	0	5	10	10
87112700	31	15.9N	115.1E	6	195.8	539.8	N/A	100	0	-5	5	N/A
87112706	32	16.7N	113.8E	8.3	249.3	N/A	N/A	95	5	-15	N/A	N/A
87112712	33	17.5N	113.0E	0	311.1	N/A	N/A	95	-5	-20	N/A	N/A
87112718	34	18.6N	112.7E	5.7	238.9	N/A	N/A	95	0	10	N/A	N/A
87112800	35	19.3N	112.8E	5.7	226.2	448.2	N/A	95	5	30	20	N/A
87112806	36	19.8N	113.1E	8.2	301.8	N/A	N/A	100	0	35	N/A	N/A
87112812	37	20.3N	114.0E	11.3	N/A	N/A	N/A	80	-5	N/A	N/A	N/A
87112818	38	20.0N	115.0E	37	N/A	N/A	N/A	60	10	N/A	N/A	N/A
87112900	39	19.1N	115.4E	169.8	N/A	N/A	N/A	50	10	N/A	N/A	N/A
87112906	40	18.2N	115.4E	N/A	N/A	N/A	N/A	40	N/A	N/A	N/A	N/A

Tropical Storm Ogden (23W)				00h	24h	48h	72h
Average				26	99	N/A	N/A
# Cases				4	2	0	0

DTG	W#	BT_LAT	BT_LON	POS_ER	24_ER	48_ER	72_ER	BT_WN	WW_ER	24_WE	48_WE	72_WE
87112406	1	12.0N	111.3E	13.2	94	N/A	N/A	35	-5	5	N/A	N/A
87112412	2	12.3N	110.4E	18.6	104.1	N/A	N/A	40	-10	10	N/A	N/A
87112418	3	12.7N	109.4E	47.5	N/A	N/A	N/A	45	-10	N/A	N/A	N/A
87112500	4	13.5N	108.5E	26.7	N/A	N/A	N/A	35	-10	N/A	N/A	N/A

Typhoon Phyllis (24W)				00h	24h	48h	72h
Average				16	129	171	196
# Cases				34	25	13	13

DTG	W#	BT_LAT	BT_LON	POS_ER	24_ER	48_ER	72_ER	BT_WN	WW_ER	24_WE	48_WE	72_WE
87121018	1	7.3N	146.1E	21.6	122.3	169.3	232.9	25	5	10	25	50
87121100	2	8.1N	144.6E	8.4	131.6	246.1	300.4	30	0	5	25	35
87121106	3	8.9N	143.5E	13.3	152.9	N/A	N/A	30	0	5	N/A	N/A
87121112	4	10.0N	142.9E	8.4	172.2	N/A	N/A	30	0	5	N/A	N/A

87121118	5	10.9N	142.2E	18.7	182.3	N/A	N/A	35	0	10	N/A	N/A
87121200	6	11.6N	141.3E	6	226.9	N/A	N/A	35	0	10	N/A	N/A
87121206	7	12.2N	140.7E	0	163	N/A	N/A	35	0	10	N/A	N/A
87121212	8	12.5N	140.6E	32.2	198.1	N/A	N/A	35	0	0	N/A	N/A
87121218	9	12.7N	140.5E	55.2	261.7	N/A	N/A	35	0	0	N/A	N/A
87121300	10	12.9N	140.4E	66	N/A	N/A	N/A	30	0	N/A	N/A	N/A
87121306	11	13.2N	140.2E	54.3	N/A	N/A	N/A	30	0	N/A	N/A	N/A
87121312	12	13.3N	139.4E	18.5	N/A	N/A	N/A	30	0	N/A	N/A	N/A
87121318	13	13.1N	138.6E	11.7	N/A	N/A	N/A	30	-5	N/A	N/A	N/A
87121400	14	12.9N	137.5E	5.8	N/A	N/A	N/A	30	-5	N/A	N/A	N/A
87121418	15	11.7N	132.3E	0	67	146.9	184.1	45	0	-25	-40	5
87121500	16	11.3N	130.6E	5.9	54.3	132.6	130.2	55	0	-40	-35	15
87121506	17	11.4N	128.9E	6	80.5	169.3	171.2	65	-5	-35	-25	15
87121512	18	11.5N	127.3E	6	119.6	234.2	218.2	75	0	-25	5	45
87121518	19	11.7N	125.7E	26.4	203.6	310.6	270.3	90	-15	-20	30	40
87121600	20	11.8N	124.8E	16.8	75.7	8.4	35.6	100	0	5	45	40
87121606	21	12.2N	124.1E	8.4	75.6	168.6	132.4	90	-5	-5	35	20
87121612	22	12.6N	123.4E	5.9	79.7	132.5	128.7	85	-5	5	25	15
87121618	23	12.8N	122.8E	8.4	64.4	150.7	200.8	80	0	35	25	15
87121700	24	12.9N	122.2E	8.4	105.8	168.3	251.2	75	0	35	20	20
87121706	25	12.9N	121.6E	11.7	163.6	188.8	294.9	70	5	35	25	20
87121712	26	12.9N	121.0E	11.7	63.8	N/A	N/A	60	0	10	N/A	N/A
87121718	27	12.7N	120.3E	13.4	N/A	N/A	N/A	40	0	N/A	N/A	N/A
87121800	28	12.2N	119.3E	37.9	N/A	N/A	N/A	30	0	N/A	N/A	N/A
87121806	29	11.7N	118.1E	5.9	N/A	N/A	N/A	30	0	N/A	N/A	N/A
87121812	30	12.2N	117.1E	6	71.1	N/A	N/A	30	0	5	N/A	N/A
87121818	31	12.6N	116.3E	0	60.6	N/A	N/A	35	0	5	N/A	N/A
87121900	32	12.9N	115.6E	13.1	144.4	N/A	N/A	35	0	10	N/A	N/A
87121906	33	12.9N	114.8E	26.7	203.3	N/A	N/A	30	0	10	N/A	N/A
87121912	34	12.7N	114.1E	13.4	N/A	N/A	N/A	25	5	N/A	N/A	N/A

Typhoon Peko (02C)

	00h	24h	48h	72h
Average	19	145	310	247
# Cases	23	18	11	5

DTG	W#	BT LAT	BT LON	POS ER	24 ER	48 ER	72 ER	BT WN	WW ER	24 WE	48 WE	72 WE
87092800	1	23.5N	180.3E	12.5	39.5	215.5	300.9	75	5	-30	-40	-40
87092806	2	23.9N	180.0E	6	105.2	294	295.1	75	0	-30	-35	-25
87092812	3	24.4N	179.4E	12	105.2	273.3	192	75	0	-30	-35	-20
87092818	4	24.7N	178.4E	6	117.3	228.1	N/A	90	-20	-40	-45	N/A
87092900	5	25.2N	177.2E	10.9	146.1	205.7	232	100	-20	-25	-25	-10
87092906	6	25.7N	176.0E	12	168.7	162.3	219.4	100	-20	-25	-15	-5
87092912	7	26.4N	174.7E	17.2	115.9	157.9	N/A	100	-20	-30	-15	N/A
87092918	8	27.2N	173.2E	12.2	78.4	N/A	N/A	100	-25	-40	N/A	N/A
87093000	9	28.4N	171.9E	48	83.7	254	N/A	100	-25	-35	-20	N/A
87093006	10	29.4N	170.7E	5.2	163.4	503.8	N/A	100	-25	-25	-20	N/A
87093012	11	30.2N	169.9E	20.7	223.5	560.8	N/A	100	-25	-15	-15	N/A
87093018	12	30.9N	169.2E	13.1	195.1	558.1	N/A	95	-25	-10	-15	N/A
87100100	13	31.4N	169.0E	18	253.3	N/A	N/A	90	-25	-20	N/A	N/A
87100106	14	31.8N	169.1E	13	238.4	N/A	N/A	80	-15	-15	N/A	N/A
87100112	15	31.9N	169.5E	6	210.1	N/A	N/A	75	-10	-10	N/A	N/A
87100118	16	31.7N	170.0E	7.9	149.8	N/A	N/A	65	-10	-15	N/A	N/A
87100200	17	31.0N	170.4E	27.3	122.2	N/A	N/A	65	-10	-10	N/A	N/A
87100206	18	30.4N	170.8E	33.8	111	N/A	N/A	60	-10	-5	N/A	N/A
87100212	19	29.8N	171.5E	15.9	N/A	N/A	N/A	55	-15	N/A	N/A	N/A
87100218	20	29.4N	172.1E	24.6	N/A	N/A	N/A	50	-15	N/A	N/A	N/A
87100300	21	28.9N	172.6E	42	N/A	N/A	N/A	45	-10	N/A	N/A	N/A
87100306	22	28.0N	173.4E	67.9	N/A	N/A	N/A	35	-5	N/A	N/A	N/A
87100312	23	27.9N	174.6E	16	N/A	N/A	N/A	35	-5	N/A	N/A	N/A

b. NORTH INDIAN OCEAN

This section includes verification statistics for each warning in the North Indian

Ocean during 1987. Pre- and post- warning best track positions are not printed, but are available on floppy diskettes by request.

JTWC FORECAST TRACK AND INTENSITY ERRORS BY WARNING

TROPICAL CYCLONE 01B

	00h	24h	48h	72h
Average	23	77	90	254
# Cases	11	10	6	2

DTG	W#	BT LAT	BT LON	POS ER	24 ER	48 ER	72 ER	BT WN	WW ER	24 ER	48 ER	72 ER
87020100	1	8.7N	85.2E	34.7	181.6	254.1	311.1	75	0	0	20	40
87020106	2	9.6N	85.4E	38.1	133.1	129.5	197.1	35	0	-5	20	30
87020112	3	10.6N	85.8E	26.5	73.3	74.5	N/A	40	0	0	30	N/A
87020118	4	11.6N	86.3E	18.6	17.4	29.1	N/A	45	-5	5	30	N/A
87020200	5	12.5N	86.8E	17.6	28.8	21.3	N/A	50	0	20	40	N/A
87020206	6	13.5N	87.4E	17.5	74.9	34.4	N/A	55	0	15	20	N/A
87020212	7	14.4N	87.8E	21.2	66.3	N/A	N/A	50	5	15	N/A	N/A
87020218	8	15.3N	88.1E	25	54.3	N/A	N/A	45	5	15	N/A	N/A
87020300	9	16.1N	88.4E	34	34.4	N/A	N/A	40	10	20	N/A	N/A
87020306	10	16.9N	89.1E	11.5	111.7	N/A	N/A	35	10	20	N/A	N/A
87020312	11	17.7N	89.7E	12.9	N/A	N/A	N/A	30	0	N/A	N/A	N/A

TROPICAL CYCLONE 02B

	00h	24h	48h	72h
Average	33	166	N/A	N/A
# Cases	12	7	0	0

DTG	W#	BT LAT	BT LON	POS ER	24 ER	48 ER	72 ER	BT WN	WW ER	24 ER	48 ER	72 ER
87060206	1	17.0N	89.3E	34.9	95.7	N/A	N/A	35	-5	15	N/A	N/A
87060212	2	17.2N	88.7E	34.4	159.9	N/A	N/A	35	0	15	N/A	N/A
87060218	3	17.5N	88.5E	28.6	203.9	N/A	N/A	35	0	10	N/A	N/A
87060300	4	18.0N	88.5E	54.5	247.9	N/A	N/A	35	5	-5	N/A	N/A
87060306	5	18.5N	88.6E	37.7	261.7	N/A	N/A	40	0	-25	N/A	N/A
87060312	6	19.1N	89.1E	46.4	147.4	N/A	N/A	40	-5	-20	N/A	N/A
87060318	7	19.7N	89.6E	34.4	49	N/A	N/A	45	-5	-5	N/A	N/A
87060400	8	20.3N	90.1E	12	N/A	N/A	N/A	50	-5	N/A	N/A	N/A
87060406	9	21.1N	90.6E	8.2	N/A	N/A	N/A	55	0	N/A	N/A	N/A
87060412	10	21.9N	90.8E	33.2	N/A	N/A	N/A	50	5	N/A	N/A	N/A
87060418	11	22.8N	90.8E	40.8	N/A	N/A	N/A	40	5	N/A	N/A	N/A
87060500	12	23.7N	90.9E	32	N/A	N/A	N/A	30	0	N/A	N/A	N/A

TROPICAL CYCLONE 03A

	00h	24h	48h	72h
Average	62	165	183	208
# Cases	18	12	12	12

DTG	W#	BT LAT	BT LON	POS ER	24 ER	48 ER	72 ER	BT WN	WW ER	24 ER	48 ER	72 ER
87060506	1	16.1N	62.2E	28.8	42.1	107.2	150	45	0	10	20	35
87060512	2	16.1N	62.6E	13	98.9	134.8	123.3	45	0	5	15	35
87060518	3	16.1N	63.0E	62.4	126	90.6	337.1	45	5	10	20	45

87060600	4	16.1N	63.5E	44.2	40.6	169.6	291.5	50	0	10	20	45
87060606	5	16.1N	64.2E	51.9	127.3	209.6	139	50	5	20	25	25
87060612	6	16.1N	64.9E	80.9	175.6	198	95.4	50	5	15	25	25
87060618	7	16.1N	65.7E	126.8	223.5	234.9	109.3	50	5	10	20	20
87060700	8	17.0N	66.2E	116.8	234	206.3	99.7	50	0	0	15	20
87060706	9	17.9N	66.1E	90.7	247.1	245.1	220.5	50	0	5	15	25
87060712	10	18.9N	66.0E	102.2	217.9	208.8	255.4	50	0	15	30	45
87060718	11	19.8N	65.9E	92.8	211.1	204	313.2	50	0	20	25	25
87060800	12	20.6N	65.5E	132.6	236.3	195.4	363.7	50	0	15	25	20
87060806	13	21.0N	64.9E	45	N/A	N/A	N/A	45	0	N/A	N/A	N/A
87060812	14	21.0N	64.3E	32	N/A	N/A	N/A	40	0	N/A	N/A	N/A
87060818	15	20.9N	63.7E	28.7	N/A	N/A	N/A	35	0	N/A	N/A	N/A
87060900	16	20.4N	63.4E	32	N/A	N/A	N/A	35	0	N/A	N/A	N/A
87060906	17	19.9N	63.7E	37.5	N/A	N/A	N/A	35	0	N/A	N/A	N/A
87060912	18	19.9N	64.3E	13.3	N/A	N/A	N/A	30	0	N/A	N/A	N/A

TROPICAL CYCLONE 04B

	<u>00h</u>	<u>24h</u>	<u>48h</u>	<u>72h</u>
Average	12	N/A	N/A	N/A
# Cases	3	0	0	0

<u>DTG</u>	<u>W#</u>	<u>BT LAT</u>	<u>BT LON</u>	<u>POS ER</u>	<u>24 ER</u>	<u>48 ER</u>	<u>72 ER</u>	<u>BT WN</u>	<u>WW ER</u>	<u>24 ER</u>	<u>48 ER</u>	<u>72 ER</u>
87101500	1	14.5N	83.7E	13.1	N/A	N/A	N/A	35	0	N/A	N/A	N/A
87101518	2	16.0N	81.5E	17.3	N/A	N/A	N/A	45	0	N/A	N/A	N/A
87101600	3	16.6N	80.5E	8.3	N/A	N/A	N/A	35	0	N/A	N/A	N/A

TROPICAL CYCLONE 05B

	<u>00h</u>	<u>24h</u>	<u>48h</u>	<u>72h</u>
Average	31	193	541	872
# Cases	14	9	1	1

<u>DTG</u>	<u>W#</u>	<u>BT LAT</u>	<u>BT LON</u>	<u>POS ER</u>	<u>24 ER</u>	<u>48 ER</u>	<u>72 ER</u>	<u>BT WN</u>	<u>WW ER</u>	<u>24 ER</u>	<u>48 ER</u>	<u>72 ER</u>
87103100	1	10.7N	88.0E	5.9	251.3	540.7	872	30	5	5	10	0
87103106	2	11.9N	87.6E	59.1	408.7	N/A	N/A	30	5	0	N/A	N/A
87103112	3	13.0N	86.7E	6	358.2	N/A	N/A	35	5	-5	N/A	N/A
87103118	4	13.6N	85.7E	13.1	271.9	N/A	N/A	40	0	-15	N/A	N/A
87110100	5	13.9N	84.9E	13.1	90.2	N/A	N/A	45	-5	-15	N/A	N/A
87110106	6	13.9N	84.2E	37.8	104.2	N/A	N/A	50	-10	-20	N/A	N/A
87110112	7	13.9N	83.6E	13.3	25.1	N/A	N/A	55	-5	-10	N/A	N/A
87110118	8	13.9N	82.8E	24.1	96.6	N/A	N/A	55	-5	-25	N/A	N/A
87110200	9	13.9N	82.1E	35.5	N/A	N/A	N/A	55	-10	N/A	N/A	N/A
87110206	10	14.1N	81.5E	44.6	132.4	N/A	N/A	55	-10	10	N/A	N/A
87110212	11	14.3N	81.0E	71.1	N/A	N/A	N/A	55	-10	N/A	N/A	N/A
87110218	12	14.5N	80.6E	50.1	N/A	N/A	N/A	55	-10	N/A	N/A	N/A
87110300	13	14.8N	80.0E	21.4	N/A	N/A	N/A	40	0	N/A	N/A	N/A
87110306	14	15.3N	79.1E	N/A	N/A	N/A	N/A	25	N/A	N/A	N/A	N/A

TROPICAL CYCLONE 06B

	<u>00h</u>	<u>24h</u>	<u>48h</u>	<u>72h</u>
Average	16	113	N/A	N/A
# Cases	6	2	0	0

<u>DTG</u>	<u>W#</u>	<u>BT LAT</u>	<u>BT LON</u>	<u>POS_ER</u>	<u>24_ER</u>	<u>48_ER</u>	<u>72_ER</u>	<u>BT_WN</u>	<u>WW_ER</u>	<u>24_ER</u>	<u>48_ER</u>	<u>72_ER</u>
87111118	1	14.7N	87.3E	8.3	185.3	N/A	N/A	35	-5	0	N/A	N/A
87111200	2	14.6N	85.5E	13.3	42	N/A	N/A	35	0	-10	N/A	N/A
87111206	3	14.2N	84.0E	13.3	N/A	N/A	N/A	40	-5	N/A	N/A	N/A
87111212	4	14.4N	82.5E	12	N/A	N/A	N/A	45	0	N/A	N/A	N/A
87111218	5	15.3N	81.2E	24.7	N/A	N/A	N/A	50	0	N/A	N/A	N/A
87111300	6	16.3N	80.0E	29.4	N/A	N/A	N/A	40	0	N/A	N/A	N/A

TROPICAL CYCLONE 07A

	<u>00h</u>	<u>24h</u>	<u>48h</u>	<u>72h</u>
Average	38	119	307	421
# Cases	14	11	6	6

<u>DTG</u>	<u>W#</u>	<u>BT LAT</u>	<u>BT LON</u>	<u>POS_ER</u>	<u>24_ER</u>	<u>48_ER</u>	<u>72_ER</u>	<u>BT_WN</u>	<u>WW_ER</u>	<u>24_ER</u>	<u>48_ER</u>	<u>72_ER</u>
87120812	1	10.9N	70.7E	0	129.1	326	483.2	35	0	15	0	5
87120818	2	11.2N	70.3E	16.8	176.3	356.3	485.1	35	0	10	0	10
87120900	3	11.6N	70.0E	37.3	220.7	402.2	517.3	35	0	10	5	10
87120906	4	12.0N	69.9E	23.5	160.8	286.3	381.2	35	0	5	10	20
87120912	5	12.6N	70.0E	84.3	254.8	336.3	407.9	35	0	0	10	20
87120918	6	13.3N	70.1E	60.3	96	139.7	256.5	40	-5	0	15	25
87121000	7	13.9N	70.3E	84.8	109.3	N/A	N/A	40	-5	-10	N/A	N/A
87121006	8	14.3N	70.6E	8.4	5.8	N/A	N/A	45	-10	-5	N/A	N/A
87121012	9	14.7N	71.0E	21.4	37.5	N/A	N/A	45	-10	-5	N/A	N/A
87121018	10	15.0N	71.3E	24	54.3	N/A	N/A	45	0	5	N/A	N/A
87121100	11	15.4N	71.6E	36.5	74	N/A	N/A	40	0	-5	N/A	N/A
87121106	12	15.9N	71.9E	37.8	N/A	N/A	N/A	35	0	N/A	N/A	N/A
87121112	13	16.4N	72.3E	45.4	N/A	N/A	N/A	35	-5	N/A	N/A	N/A
87121118	14	16.9N	72.7E	54.3	N/A	N/A	N/A	30	-5	N/A	N/A	N/A

TROPICAL CYCLONE 08B

	<u>00h</u>	<u>24h</u>	<u>48h</u>	<u>72h</u>
Average	123	192	N/A	N/A
# Cases	5	3	0	0

<u>DTG</u>	<u>W#</u>	<u>BT LAT</u>	<u>BT LON</u>	<u>POS_ER</u>	<u>24_ER</u>	<u>48_ER</u>	<u>72_ER</u>	<u>BT_WN</u>	<u>WW_ER</u>	<u>24_ER</u>	<u>48_ER</u>	<u>72_ER</u>
87121800	1	10.7N	82.6E	24.7	159	N/A	N/A	30	0	10	N/A	N/A
87121806	2	10.5N	82.2E	76	N/A	N/A	N/A	30	0	N/A	N/A	N/A
87121812	3	10.4N	81.8E	128.2	176.1	N/A	N/A	30	0	0	N/A	N/A
87121818	4	10.3N	81.4E	181.9	240.6	N/A	N/A	30	0	0	N/A	N/A
87121900	5	10.5N	81.1E	206.6	N/A	N/A	N/A	25	0	N/A	N/A	N/A

c. SOUTHERN HEMISPHERE

This section includes verification statistics for each warning in the South Indian and western South Pacific Oceans from 1 July

1986 to 30 June 1987. Pre- and post-warning best track positions are not printed, but are available on floppy diskettes by request.

JTWC FORECAST TRACK AND INTENSITY ERRORS BY WARNING

Tropical Cyclone 01S

	<u>00h</u>	<u>24h</u>	<u>48h</u>
Average	25	90	196
# Cases	4	3	1

<u>DTG</u>	<u>W#</u>	<u>BT LAT</u>	<u>BT LON</u>	<u>POS ER</u>	<u>24 ER</u>	<u>48 ER</u>	<u>BT WN</u>	<u>WW ER</u>	<u>24 WE</u>	<u>48 WE</u>
86080112	1	7.6N	78.3E	24.5	91	196.4	40	0	30	40
86080200	2	7.6N	76.9E	8.4	81.5	N/A	35	5	5	N/A
86080212	3	7.4N	75.5E	32.3	99.2	N/A	30	5	0	N/A
86080300	4	6.9N	74.0E	36.5	N/A	N/A	30	-5	N/A	N/A

Tropical Cyclone 02P

	<u>00h</u>	<u>24h</u>	<u>48h</u>
Average	33	141	292
# Cases	6	4	2

<u>DTG</u>	<u>W#</u>	<u>BT LAT</u>	<u>BT LON</u>	<u>POS ER</u>	<u>24 ER</u>	<u>48 ER</u>	<u>BT WN</u>	<u>WW ER</u>	<u>24 WE</u>	<u>48 WE</u>
86112218	1	12.7N	168.8E	21.5	29	196.9	35	-5	-15	-10
86112306	2	13.6N	168.7E	8.4	75.3	388.2	45	-10	-5	5
86112318	3	14.7N	169.2E	31.4	212.7	N/A	50	0	20	N/A
86112406	4	15.7N	170.1E	40.9	250.3	N/A	55	5	25	N/A
86112418	5	16.7N	172.3E	53.1	N/A	N/A	55	5	N/A	N/A
86112506	6	17.4N	175.3E	43.9	N/A	N/A	55	-5	N/A	N/A

Tropical Cyclone 03P

	<u>00h</u>	<u>24h</u>	<u>48h</u>
Average	42	160	340
# Cases	6	4	2

<u>DTG</u>	<u>W#</u>	<u>BT LAT</u>	<u>BT LON</u>	<u>POS ER</u>	<u>24 ER</u>	<u>48 ER</u>	<u>BT WN</u>	<u>WW ER</u>	<u>24 WE</u>	<u>48 WE</u>
86121418	1	13.0N	168.0E	59.7	169.5	343.3	35	0	0	30
86121506	2	14.2N	167.4E	38	232.2	338	50	5	25	50
86121518	3	16.0N	166.3E	55	148.7	N/A	55	10	40	N/A
86121606	4	18.1N	166.0E	39.9	91.6	N/A	50	25	55	N/A
86121618	5	19.7N	166.4E	34.5	N/A	N/A	45	15	N/A	N/A
86121706	6	22.0N	167.5E	28.4	N/A	N/A	35	10	N/A	N/A

Tropical Cyclone 04P

	<u>00h</u>	<u>24h</u>	<u>48h</u>
Average	35	171	333
# Cases	18	16	14

<u>DTG</u>	<u>W#</u>	<u>BT LAT</u>	<u>BT LON</u>	<u>POS ER</u>	<u>24 ER</u>	<u>48 ER</u>	<u>BT WN</u>	<u>WW ER</u>	<u>24 WE</u>	<u>48 WE</u>
86122318	1	12.1N	176.3E	8.4	274.1	606.8	35	0	5	5
86122406	2	12.7N	176.1E	66.8	366	640.1	35	5	-5	5
86122418	3	13.6N	177.6E	17.5	66.7	204.7	45	0	0	5
86122506	4	14.4N	179.0E	46.9	117.2	312	55	0	5	-5
86122518	5	14.9N	180.6E	41	51	216.6	55	0	10	5
86122606	6	14.9N	182.2E	21.4	134.7	353.3	55	5	0	-10
86122618	7	14.9N	182.6E	12	268.2	552.1	55	10	5	-20

86122706	8	14.9N	182.3E	18.4	159.6	404.6	65	5	0	-15
86122718	9	15.0N	181.6E	11.6	78.2	82.8	65	10	0	-10
86122806	10	15.0N	180.8E	35.3	151.9	292.1	75	0	0	-20
86122818	11	15.2N	180.2E	8.3	158.8	362.5	80	0	-5	-15
86122906	12	16.1N	180.1E	5.8	75.3	196.1	80	5	-15	0
86122918	13	17.4N	180.4E	0	102.5	256.1	90	0	-5	35
86123006	14	19.0N	181.2E	8.3	127.1	186	90	-5	5	20
86123918	15	21.2N	182.0E	22.4	175.3	N/A	90	-5	20	N/A
86123106	16	23.6N	183.1E	36	434.2	N/A	65	0	10	N/A
86123118	17	25.0N	183.4E	44.3	N/A	N/A	45	0	N/A	N/A
87010106	18	25.0N	182.0E	238	N/A	N/A	30	5	N/A	N/A

Tropical Cyclone 05P

	<u>00h</u>	<u>24h</u>	<u>48h</u>
Average	41	139	281
# Cases	16	14	11

<u>DTG</u>	<u>W#</u>	<u>BT LAT</u>	<u>BT LON</u>	<u>POS ER</u>	<u>24 ER</u>	<u>48 ER</u>	<u>BT WN</u>	<u>WW ER</u>	<u>24 WE</u>	<u>48 WE</u>
86122800	1	14.7N	196.8E	41.8	98.3	161	30	10	15	15
86122812	2	15.3N	196.8E	17.4	168.3	418.5	35	15	20	10
86122900	3	15.9N	196.8E	26.6	170.8	432.7	45	20	15	-5
86122912	4	16.6N	196.9E	13.3	82.4	203.2	50	15	15	0
86123000	5	17.0N	197.4E	40.2	157.2	193.3	55	25	10	5
86123012	6	17.1N	198.2E	46.7	151	154.8	60	20	15	10
86123100	7	17.0N	199.0E	18.9	144.5	311.9	65	10	0	-5
86123112	8	16.4N	198.8E	11.5	72	111.3	60	15	25	20
87010100	9	17.2N	198.5E	45.4	42	92.3	60	15	15	15
87010112	10	17.8N	198.5E	39.9	118.3	376.1	55	15	20	10
87010200	11	18.8N	198.8E	45.4	272.2	638.3	55	10	5	0
87010212	12	19.8N	199.7E	43.5	225	N/A	50	20	5	N/A
87010300	13	20.7N	201.3E	65.6	117.9	N/A	50	15	5	N/A
87010312	14	21.8N	203.6E	83.4	129.1	N/A	50	15	15	N/A
87010400	15	23.2N	205.7E	97.8	N/A	N/A	45	5	N/A	N/A
87010412	16	24.8N	207.8E	29	N/A	N/A	40	0	N/A	N/A

Tropical Cyclone 06S

	<u>00h</u>	<u>24h</u>	<u>48h</u>
Average	38	203	365
# Cases	5	4	4

<u>DTG</u>	<u>W#</u>	<u>BT LAT</u>	<u>BT LON</u>	<u>POS ER</u>	<u>24 ER</u>	<u>48 ER</u>	<u>BT WN</u>	<u>WW ER</u>	<u>24 WE</u>	<u>48 WE</u>
87010712	1	7.1N	76.6E	21.6	172.7	312.1	35	-5	10	-5
87010800	2	8.0N	76.5E	24.5	287.2	460	35	0	15	25
87010812	3	9.4N	77.9E	37.5	162.8	313.5	35	0	10	10
87010900	4	10.9N	79.1E	29.7	189.4	376.3	35	10	10	-5
87010912	5	11.2N	79.7E	78.9	N/A	N/A	35	0	N/A	N/A

Tropical Cyclone 07S

	<u>00h</u>	<u>24h</u>	<u>48h</u>
Average	24	119	194
# Cases	5	3	2

<u>DTG</u>	<u>W#</u>	<u>BT LAT</u>	<u>BT LON</u>	<u>POS ER</u>	<u>24 ER</u>	<u>48 ER</u>	<u>BT WN</u>	<u>WW ER</u>	<u>24 WE</u>	<u>48 WE</u>
87011012	1	9.1N	97.5E	11.8	64.5	63.2	50	0	25	35
87011100	2	10.7N	98.2E	43	189.6	325.9	50	-5	-5	0
87011112	3	11.7N	99.0E	8.4	103.5	N/A	45	-5	-10	N/A
87011200	4	12.5N	99.3E	21.5	N/A	N/A	45	-10	N/A	N/A
87011212	5	12.6N	99.4E	36.5	N/A	N/A	45	-15	N/A	N/A

Tropical Cyclone 08P

	<u>00h</u>	<u>24h</u>	<u>48h</u>
Average	25	119	194
# Cases	9	7	5

<u>DTG</u>	<u>W#</u>	<u>BT LAT</u>	<u>BT LON</u>	<u>POS ER</u>	<u>24 ER</u>	<u>48 ER</u>	<u>BT WN</u>	<u>WW ER</u>	<u>24 WE</u>	<u>48 WE</u>
87011600	1	10.7N	189.0E	26.7	163	229.6	35	5	10	-25
87011612	2	10.9N	189.7E	41.7	42.6	91.4	45	0	-10	-35
87011700	3	10.7N	189.7E	21.4	115.6	291.3	55	0	-20	-15
87011712	4	11.8N	190.0E	24.3	120.4	265.5	70	-5	-20	15
87011800	5	13.6N	190.4E	13.1	202.1	392.2	90	-10	5	50
87011812	6	15.3N	191.4E	47.8	5.7	N/A	100	-10	15	N/A
87011900	7	17.4N	192.9E	8.3	79.8	N/A	90	-5	25	N/A
87011912	8	19.5N	194.1E	18.9	N/A	N/A	70	-5	N/A	N/A
87012000	9	21.5N	196.4E	28.7	N/A	N/A	40	5	N/A	N/A

Tropical Cyclone 09S

	<u>00h</u>	<u>24h</u>	<u>48h</u>
Average	37	188	422
# Cases	12	8	5

<u>DTG</u>	<u>W#</u>	<u>BT LAT</u>	<u>BT LON</u>	<u>POS ER</u>	<u>24 ER</u>	<u>48 ER</u>	<u>BT WN</u>	<u>WW ER</u>	<u>24 WE</u>	<u>48 WE</u>
87011618	1	13.9N	66.9E	35.5	303.9	630.7	45	-10	-10	5
87011706	2	14.8N	67.3E	13.1	249.5	619.7	55	-15	-15	15
87011718	3	15.6N	68.2E	64.7	265.7	514.3	65	-15	5	40
87011806	4	17.2N	68.9E	12	103.3	208.8	75	-15	25	35
87011818	5	19.1N	69.9E	46.4	128.3	138.8	65	0	40	20
87011906	6	20.4N	70.7E	39.8	140.5	N/A	55	-5	0	N/A
87011918	7	21.7N	71.1E	17.8	N/A	N/A	40	0	N/A	N/A
87012006	8	23.3N	71.2E	84.3	N/A	N/A	35	0	N/A	N/A
87012206	9	26.5N	63.2E	21	103.3	N/A	65	-15	15	N/A
87012218	10	29.2N	63.5E	5.2	217.4	N/A	55	5	-10	N/A
87012306	11	33.0N	66.5E	70.5	N/A	N/A	55	-5	N/A	N/A
87012318	12	36.8N	72.0E	36	N/A	N/A	55	-15	N/A	N/A

Tropical Cyclone 10S

	<u>00h</u>	<u>24h</u>	<u>48h</u>
Average	15	92	201
# Cases	6	5	4

<u>DTG</u>	<u>W#</u>	<u>BT LAT</u>	<u>BT LON</u>	<u>POS ER</u>	<u>24 ER</u>	<u>48 ER</u>	<u>BT WN</u>	<u>WW ER</u>	<u>24 WE</u>	<u>48 WE</u>
87011712	1	17.2N	120.9E	23.7	54.3	106.2	30	5	0	15
87011800	2	17.8N	120.5E	8.3	43.5	102.6	45	-5	0	0
87011812	3	18.7N	119.7E	5.7	47.6	196.8	55	-5	15	15
87011900	4	19.6N	118.7E	13.3	100.9	397.6	55	-15	0	20
87011912	5	20.7N	117.9E	30.5	215.8	N/A	50	15	15	N/A
87012000	6	22.1N	117.6E	11.1	N/A	N/A	50	-10	N/A	N/A

Tropical Cyclone 11P

	<u>00h</u>	<u>24h</u>	<u>48h</u>
Average	13	17	N/A
# Cases	3	1	0

<u>DTG</u>	<u>W#</u>	<u>BT LAT</u>	<u>BT LON</u>	<u>POS ER</u>	<u>24 ER</u>	<u>48 ER</u>	<u>BT WN</u>	<u>WW ER</u>	<u>24 WE</u>	<u>48 WE</u>
87011918	1	13.0N	137.7E	13.3	17.4	N/A	30	5	10	N/A
87012006	2	13.4N	136.5E	8.4	N/A	N/A	30	10	N/A	N/A
87012018	3	14.2N	134.8E	18.5	N/A	N/A	30	10	N/A	N/A

Tropical Cyclone 12S

	<u>00h</u>	<u>24h</u>	<u>48h</u>
Average	35	138	135
# Cases	9	7	5

<u>DTG</u>	<u>W#</u>	<u>BT LAT</u>	<u>BT LON</u>	<u>POS ER</u>	<u>24 ER</u>	<u>48 ER</u>	<u>BT WN</u>	<u>WW ER</u>	<u>24 WE</u>	<u>48 WE</u>
87020100	1	15.6N	123.4E	121.5	236.3	298.6	35	0	15	20
87020112	2	16.0N	122.7E	18.3	121.3	97.1	40	5	20	35
87020200	3	16.3N	122.8E	34	77.3	42.7	40	0	0	0
87020212	4	16.5N	122.5E	13.3	69.1	46.1	40	0	0	10
87020300	5	17.5N	121.1E	5.7	66.2	193.6	45	0	0	50
87020312	6	17.8N	119.9E	72.3	275.9	N/A	45	5	5	N/A
87020400	7	17.9N	118.9E	45.7	125.4	N/A	50	0	15	N/A
87020412	8	18.0N	118.0E	0	N/A	N/A	40	5	N/A	N/A
87020500	9	18.2N	117.3E	6	N/A	N/A	30	10	N/A	N/A

Tropical Cyclone 13P

	<u>00h</u>	<u>24h</u>	<u>48h</u>
Average	36	139	N/A
# Cases	3	2	0

<u>DTG</u>	<u>W#</u>	<u>BT LAT</u>	<u>BT LON</u>	<u>POS ER</u>	<u>24 ER</u>	<u>48 ER</u>	<u>BT WN</u>	<u>WW ER</u>	<u>24 WE</u>	<u>48 WE</u>
87020400	1	16.0N	189.7E	46.1	91.6	N/A	40	0	15	N/A
87020412	2	16.0N	191.1E	18.3	186.9	N/A	40	0	20	N/A
87020500	3	15.8N	192.7E	45.4	N/A	N/A	35	0	N/A	N/A

Tropical Cyclone 14P

	<u>00h</u>	<u>24h</u>	<u>48h</u>
Average	347	101	256
# Cases	8	6	4

<u>DTG</u>	<u>W#</u>	<u>BT LAT</u>	<u>BT LON</u>	<u>POS ER</u>	<u>24 ER</u>	<u>48 ER</u>	<u>BT WN</u>	<u>WW ER</u>	<u>24 WE</u>	<u>48 WE</u>
87020500	1	13.2N	163.3E	24.1	102	190.9	35	5	-10	-10
87020512	2	13.7N	164.3E	12	96.2	180.8	45	0	-5	35
87020600	3	14.7N	165.2E	24	92.9	243.8	65	0	0	40
87020612	4	15.9N	166.1E	18.3	64.5	409.9	70	0	25	45
87020700	5	17.0N	167.0E	13.3	68.7	N/A	75	5	45	N/A
87020712	6	18.3N	168.2E	23.6	182.3	N/A	55	25	45	N/A
87020800	7	20.2N	170.4E	43.4	N/A	N/A	35	25	N/A	N/A
87020812	8	22.0N	175.0E	101.8	N/A	N/A	25	25	N/A	N/A

Tropical Cyclone 15P

	<u>00h</u>	<u>24h</u>	<u>48h</u>
Average	27	120	369
# Cases	12	8	2

<u>DTG</u>	<u>W#</u>	<u>BT LAT</u>	<u>BT LON</u>	<u>POS ER</u>	<u>24 ER</u>	<u>48 ER</u>	<u>BT WN</u>	<u>WW ER</u>	<u>24 WE</u>	<u>48 WE</u>
87020706	1	13.2N	140.3E	51.2	102.6	223.2	30	5	15	-30
87020718	2	13.2N	139.5E	41.9	146.6	N/A	35	5	-10	N/A
87020806	3	13.2N	138.6E	52.6	18.9	N/A	40	10	-15	N/A
87020818	4	13.2N	137.5E	37.8	N/A	N/A	50	-10	N/A	N/A
87020906	5	13.1N	136.8E	5.8	78.9	N/A	55	-10	-30	N/A
87020918	6	12.9N	136.3E	25.1	17.6	N/A	55	-15	-35	N/A
87021006	7	12.6N	136.0E	11.7	N/A	N/A	60	-20	N/A	N/A
87021018	8	12.3N	135.5E	5.9	205.9	514.8	60	-20	-15	5
87021106	9	13.0N	135.4E	18	282.8	N/A	65	-25	-5	N/A
87021118	10	13.9N	137.0E	24.1	106.8	N/A	60	-20	-5	N/A
87021206	11	14.9N	138.4E	18.4	N/A	N/A	50	15	N/A	N/A
87021218	12	15.7N	140.0E	34	N/A	N/A	40	30	N/A	N/A

Tropical Cyclone 16P

	<u>00h</u>	<u>24h</u>	<u>48h</u>
Average	67	424	N/A
# Cases	3	1	0

<u>DTG</u>	<u>W#</u>	<u>BT LAT</u>	<u>BT LON</u>	<u>POS ER</u>	<u>24 ER</u>	<u>48 ER</u>	<u>BT WN</u>	<u>WW ER</u>	<u>24 WE</u>	<u>48 WE</u>
87020818	1	18.5N	173.6E	45.5	424.1	N/A	25	20	30	N/A
87020906	2	21.9N	177.7E	13.2	N/A	N/A	25	5	N/A	N/A
87020918	3	26.1N	180.8E	144.3	N/A	N/A	25	5	N/A	N/A

Tropical Cyclone 17S

	<u>00h</u>	<u>24h</u>	<u>48h</u>
Average	51	109	227
# Cases	10	7	6

<u>DTG</u>	<u>W#</u>	<u>BT LAT</u>	<u>BT LON</u>	<u>POS ER</u>	<u>24 ER</u>	<u>48 ER</u>	<u>BT WN</u>	<u>WW ER</u>	<u>24 WE</u>	<u>48 WE</u>
87021106	1	21.1N	53.8E	84.2	79.7	81.1	30	5	10	5
87021118	2	21.0N	54.0E	83.8	125.1	147.9	35	0	0	5
87021206	3	20.9N	54.3E	21.2	45	131.7	35	5	5	15
87021218	4	20.8N	54.8E	18.9	95.1	285	45	10	20	15
87021306	5	20.9N	55.6E	28.7	16.4	229.5	45	10	25	25
87021318	6	20.9N	56.4E	12.7	171.4	486.9	45	5	15	15
87021406	7	20.7N	56.4E	55.1	233.7	N/A	40	10	5	N/A
87021418	8	21.1N	55.7E	119.3	N/A	N/A	35	0	N/A	N/A
87021506	9	22.1N	54.6E	23	N/A	N/A	30	5	N/A	N/A
87021518	10	23.0N	53.0E	68.7	N/A	N/A	30	5	N/A	N/A

Tropical Cyclone 18S

	<u>00h</u>	<u>24h</u>	<u>48h</u>
Average	11	147	369
# Cases	7	6	4

<u>DTG</u>	<u>W#</u>	<u>BT LAT</u>	<u>BT LON</u>	<u>POS ER</u>	<u>24 ER</u>	<u>48 ER</u>	<u>BT WN</u>	<u>WW ER</u>	<u>24 WE</u>	<u>48 WE</u>
87022212	1	15.6N	123.0E	6	106.6	389.7	30	0	10	15
87022300	2	15.8N	121.4E	0	175.2	6812.6	35	0	5	5
87022312	3	15.8N	120.7E	8.3	178.9	317.4	40	0	5	5
87022400	4	16.2N	121.2E	29.3	198.9	427.8	45	0	0	20
87022412	5	17.2N	121.6E	16.6	29.4	N/A	45	0	-15	N/A
87022500	6	18.6N	121.2E	5.7	193.3	N/A	55	0	0	N/A
87022512	7	19.9N	121.0E	12.8	N/A	N/A	55	0	N/A	N/A

Tropical Cyclone 19P

	<u>00h</u>	<u>24h</u>	<u>48h</u>
Average	5	332	N/A
# Cases	3	1	0

<u>DTG</u>	<u>W#</u>	<u>BT LAT</u>	<u>BT LON</u>	<u>POS ER</u>	<u>24 ER</u>	<u>48 ER</u>	<u>BT WN</u>	<u>WW ER</u>	<u>24 WE</u>	<u>48 WE</u>
87022818	1	14.9N	197.9E	0	332.1	N/A	35	0	5	N/A
87030106	2	18.5N	200.0E	0	N/A	N/A	35	0	N/A	N/A
87030118	3		202.8E	16.3	N/A	N/A	40	-5	N/A	N/A

Tropical Cyclone 20P

	<u>00h</u>	<u>24h</u>	<u>48h</u>
Average	47	146	286
# Cases	9	6	4

<u>DTG</u>	<u>W#</u>	<u>BT LAT</u>	<u>BT LON</u>	<u>POS ER</u>	<u>24 ER</u>	<u>48 ER</u>	<u>BT WN</u>	<u>WW ER</u>	<u>24 WE</u>	<u>48 WE</u>
87030112	1	13.5N	187.4E	55.5	183.9	244.3	35	0	-10	-15
87030200	2	13.9N	190.5E	83.3	170.8	261.5	40	0	-5	-15

87030212	3	15.3N	193.3E	34.7	157	306.3	45	-5	-20	-25
87030312	4	20.5N	194.5E	89.6	185.4	333.6	60	-5	-15	-20
87030400	5	22.2N	195.3E	51.5	108	N/A	65	-10	-15	N/A
87030412	6	23.5N	196.5E	24.6	76.3	N/A	65	0	-20	N/A
87030500	7	24.9N	198.2E	16.2	N/A	N/A	55	0	N/A	N/A
87030512	8	26.2N	200.3E	36	N/A	N/A	65	0	N/A	N/A
87030600	9	28.1N	203.6E	36.5	N/A	N/A	65	0	N/A	N/A

Tropical Cyclone 21S

	00h	24h	48h
Average	47	188	307
# Cases	25	20	18

<u>DTG</u>	<u>W#</u>	<u>BT LAT</u>	<u>BT LON</u>	<u>POS ER</u>	<u>24 ER</u>	<u>48 ER</u>	<u>BT WN</u>	<u>WW ER</u>	<u>24 WE</u>	<u>48 WE</u>
87030300	1	13.7N	71.5E	34.7	242.5	449.6	30	5	15	25
87030312	2	13.2N	71.4E	8.4	108.9	277.2	35	10	25	25
87030400	3	12.5N	71.5E	44.8	307.4	566.7	40	10	20	25
87030412	4	13.0N	72.1E	72.6	273.2	468.5	40	15	25	30
87030500	5	13.0N	72.7E	123.4	327.6	449	40	25	30	40
87030512	6	13.5N	74.3E	62.7	282.9	493	40	20	10	0
87030600	7	13.7N	75.5E	42	288.4	431.8	40	10	10	-5
87030612	8	13.0N	75.6E	104.3	247.1	286.8	35	15	5	-20
87030700	9	12.1N	76.7E	21.5	136.6	157	35	0	-5	-40
87030712	10	12.0N	76.6E	119	358.7	N/A	35	0	-25	N/A
87030800	11	12.1N	75.9E	59.2	242.1	345.7	40	-5	-35	-35
87030812	12	12.7N	75.1E	12	24.7	54.9	55	-10	-10	0
87030900	13	13.4N	74.0E	16.7	94.1	197.1	70	-10	10	0
87030912	14	14.5N	73.1E	13.3	13	136.3	70	0	0	-5
87031000	15	15.3N	72.4E	5.8	62.9	232.9	65	0	-10	-20
87031012	16	16.4N	71.9E	23.8	154.2	332.5	65	-5	-15	-15
87031100	17	17.0N	71.7E	18	115.6	279.7	65	-10	-20	-10
87039112	18	17.7N	72.0E	41.8	191.6	189.7	65	-10	-15	-15
87031200	19	18.8N	72.9E	61.7	202.9	188.2	65	-15	-20	-15
87031212	20	20.1N	74.4E	51.1	84.7	N/A	55	-5	-20	N/A
87031300	21	22.1N	75.3E	45.7	N/A	N/A	50	-5	N/A	N/A
87031312	22	23.6N	74.9E	89.8	N/A	N/A	50	-10	N/A	N/A
87031400	23	24.6N	73.9E	18	N/A	N/A	45	-5	N/A	N/A
87031412	24	25.5N	73.4E	63.8	N/A	N/A	40	-5	N/A	N/A
87031500	25	27.2N	73.5E	42.3	N/A	N/A	40	-10	N/A	N/A

Tropical Cyclone 22P

	00h	24h	48h
Average	50	96	212
# Cases	7	5	3

<u>DTG</u>	<u>W#</u>	<u>BT LAT</u>	<u>BT LON</u>	<u>POS ER</u>	<u>24 ER</u>	<u>48 ER</u>	<u>BT WN</u>	<u>WW ER</u>	<u>24 WE</u>	<u>48 WE</u>
87030818	1	16.6N	163.9E	29.2	109.6	243.7	40	-5	-20	0
87030906	2	17.3N	163.7E	18.9	74	138	65	-10	5	35
87030918	3	17.9N	163.6E	39.9	132.5	256.1	65	0	-5	5
87031006	4	18.2N	163.7E	11.4	41.3	N/A	65	-10	0	N/A
87031018	5	18.8N	164.3E	13.3	124	N/A	55	0	10	N/A
87031106	6	19.5N	165.0E	22.6	N/A	N/A	40	5	N/A	N/A
87031118	7	20.2N	167.2E	216.2	N/A	N/A	35	0	N/A	N/A

Tropical Cyclone 23P

	<u>00h</u>	<u>24h</u>	<u>48h</u>
Average	25	90	166
# Cases	17	12	12

<u>DTG</u>	<u>W#</u>	<u>BT LAT</u>	<u>BT LON</u>	<u>POS ER</u>	<u>24 ER</u>	<u>48 ER</u>	<u>BT WN</u>	<u>WW ER</u>	<u>24 WE</u>	<u>48 WE</u>
87040812	1	8.6N	138.0E	5.9	109.5	120.9	35	0	10	10
87040900	2	9.3N	136.3E	16.9	67.7	111.8	40	10	15	72
87040912	3	10.3N	134.4E	21.4	59.6	158	45	10	15	10
87041000	4	11.1N	132.6E	18.9	96	123.1	45	10	15	5
87041012	5	11.2N	130.9E	38.1	110.4	125.6	45	10	10	5
87041100	6	11.7N	128.5E	18.6	66	115.2	45	10	-5	15
87041112	7	12.4N	126.2E	25.2	77.6	180.6	45	15	5	20
87041200	8	13.4N	124.2E	5.8	159.1	334.7	50	10	5	25
87041212	9	14.0N	122.8E	71.2	117.6	220.8	55	5	5	25
87041300	10	14.6N	121.4E	8.3	75.8	170.4	65	-5	20	30
87041312	11	14.9N	120.6E	5.8	69.3	177.7	55	5	5	N/A
87041400	12	14.8N	119.3E	21.4	71.5	157.9	55	-5	0	N/A
87041412	13	14.8N	117.9E	23.2	N/A	N/A	45	-10	N/A	N/A
87041500	14	15.1N	115.9E	8.3	N/A	N/A	45	0	N/A	N/A
87041512	15	15.8N	113.6E	39	N/A	N/A	45	0	N/A	N/A
87041600	16	16.6N	111.6E	54.4	N/A	N/A	35	5	N/A	N/A
87041612	17	18.4N	109.9E	43.7	N/A	N/A	35	0	N/A	N/A

Tropical Cyclone 24S

	<u>00h</u>	<u>24h</u>	<u>48h</u>
Average	35	209	509
# Cases	8	6	4

<u>DTG</u>	<u>W#</u>	<u>BT LAT</u>	<u>BT LON</u>	<u>POS ER</u>	<u>24 ER</u>	<u>48 ER</u>	<u>BT WN</u>	<u>WW ER</u>	<u>24 WE</u>	<u>48 WE</u>
87042300	1	27.1N	42.2E	8	122.8	486.4	45	-15	-40	-30
87042312	2	27.6N	41.6E	32	208.7	494.1	55	-20	-25	-20
87042400	3	28.5N	42.4E	51.8	339.5	633.8	70	-25	-15	-5
87042412	4	29.8N	44.1E	39.3	243.5	461.5	70	-5	-15	-10
87042500	5	30.8N	47.5E	16.6	105.1	N/A	65	0	-5	N/A
87042512	6	31.3N	50.6E	31.3	238.4	N/A	60	0	0	N/A
87042600	7	31.3N	53.7E	73.9	N/A	N/A	50	0	N/A	N/A
87042612	8	31.0N	56.1E	31.7	N/A	N/A	40	0	N/A	N/A

Tropical Cyclone 25P

	<u>00h</u>	<u>24h</u>	<u>48h</u>
Average	49	136	273
# Cases	7	5	4

<u>DTG</u>	<u>W#</u>	<u>BT LAT</u>	<u>BT LON</u>	<u>POS ER</u>	<u>24 ER</u>	<u>48 ER</u>	<u>BT WN</u>	<u>WW ER</u>	<u>24 WE</u>	<u>48 WE</u>
87042300	1	11.9N	189.6E	65.7	143.5	310.4	35	10	5	20
87042312	2	13.6N	190.5E	6	64.2	150.9	45	-10	-20	-10
87042400	3	15.3N	191.3E	40	107.6	322.1	55	-10	5	15
87042412	4	17.0N	192.1E	30.5	135.3	311.8	50	-5	5	10
87042500	5	19.0N	193.1E	95.5	229.6	N/A	45	5	10	N/A
87042600	6	24.0N	198.6E	30.5	N/A	N/A	30	15	N/A	N/A
87042612	7	26.2N	202.2E	80.3	N/A	N/A	25	-5	N/A	N/A

Tropical Cyclone 26S

	00h	24h	48h
Average	47	161	344
# Cases	5	3	1

DTG	W#	BT LAT	BT LON	POS_ER	24_ER	48_ER	BT_WN	WW_ER	24_WE	48_WE
87042412	1	15.0N	74.2E	11.6	144.9	344.2	40	-5	5	35
87042500	2	14.6N	74.9E	62.6	156.1	N/A	40	-5	0	N/A
87042512	3	13.9N	74.8E	54	182.9	N/A	45	-5	25	N/A
87042600	4	13.3N	74.4E	101.3	N/A	N/A	35	10	N/A	N/A
87042612	5	12.9N	73.9E	5.8	N/A	N/A	25	5	N/A	N/A

Tropical Cyclone 27P

	00h	24h	48h
Average	22	93	138
# Cases	7	5	5

DTG	W#	BT LAT	BT LON	POS_ER	24_ER	48_ER	BT_WN	WW_ER	24_WE	48_WE
87052218	1	12.3N	159.4E	13.4	87.7	67.7	35	-5	10	20
87052306	2	13.7N	158.6E	13.1	45.8	155.7	40	-5	0	10
87052318	3	15.0N	158.1E	23.9	99.6	255.6	45	0	5	10
87052406	4	15.9N	157.5E	8.3	102.6	108.6	45	0	10	15
87052418	5	16.6N	157.1E	37.8	132.1	101.7	45	10	25	20
87052506	6	16.6N	156.8E	24.7	N/A	N/A	35	5	N/A	N/A
87052518	7	17.5N	156.3E	33.2	N/A	N/A	30	0	N/A	N/A

Tropical Cyclone 28S

	00h	24h	48h
Average	56	194	450
# Cases	5	3	1

DTG	W#	BT LAT	BT LON	POS_ER	24_ER	48_ER	BT_WN	WW_ER	24_WE	48_WE
87062500	1	8.0N	87.4E	165.7	321.3	449.6	30	5	30	N/A
87062512	2	7.4N	87.3E	16.9	55.1	N/A	30	5	15	N/A
87062600	3	7.6N	86.7E	45.4	206.9	N/A	25	10	0	N/A
87062612	4	8.5N	85.8E	18.8	N/A	N/A	30	5	N/A	N/A
87062700	5	9.9N	86.6E	36.5	N/A	N/A	30	0	N/A	N/A

APPENDIX I

DEFINITIONS

BEST TRACK - A subjectively smoothed path, versus a precise and very erratic fix-to-fix path, used to represent tropical cyclone movement.

CENTER - The vertical axis or cone of a tropical cyclone. Usually determined by wind, temperature, and/or pressure distribution.

CYCLONE - A closed atmospheric circulation rotating about an area of low pressure (counterclockwise in the northern hemisphere).

EPIHEMERIS - Position of a body (satellite) in space as a function of time; used for gridding satellite imagery. Since ephemeris gridding is based solely on the predicted position of the satellite, it is susceptible to errors from vehicle wobble, orbital eccentricity and the oblateness of the earth.

EXPLOSIVE DEEPENING - A decrease in the minimum sea-level pressure of a tropical cyclone of 2.5 mb/hr for 12 hours or 5.0 mb/hr for six hours (Holliday and Thompson, 1979).

EXTRATROPICAL - A term used in warnings and tropical summaries to indicate that a cyclone has lost its "tropical" characteristics. The term implies both poleward displacement from the tropics and the conversion of the cyclone's primary energy sources from release of latent heat of condensation to baroclinic processes. The term carries no implications as to strength, size or intensity.

EYE - A term used to describe the central area of a tropical cyclone when it is more than half surrounded by wall cloud.

FUJIWHARA EFFECT - An interaction in which tropical cyclones within 700 nm (1296 km) of each other begin to rotate about one another. When intense tropical cyclones are within about 400 nm (741 km) of each other, they may also begin to be drawn closer to each other (Brand, 1970) (Dong and Neumann, 1983).

INTENSITY - The maximum wind speed, typically within one degree of the center of the tropical cyclone.

MAXIMUM SUSTAINED WIND - Highest surface wind speed averaged over a one-minute period of time. Peak gusts over water average 20 to 25 percent higher than sustained winds.

RAPID DEEPENING - A decrease in the minimum sea-level pressure of a tropical cyclone of 1.25 mb/hr for 24 hours (Holliday and Thompson, 1979).

RECURVATURE - The turning of a tropical cyclone from an initial path toward the west or northwest to a path toward the northeast.

SIGNIFICANT TROPICAL CYCLONE - A tropical cyclone becomes "significant" with the issuance of the first numbered warning by the responsible warning agency.

SIZE - The areal extent of the tropical cyclone measured radially outward from the center (e.g., radius of the outer closed isobar).

STRENGTH - The average wind speed of the inner low-level circulation, usually measured within one to three degrees of the center of the tropical cyclone.

SUPER TYPHOON (HURRICANE) - A typhoon or hurricane in which the maximum sustained surface wind (one-minute mean) is 130 kt (67 m/sec) or greater.

TROPICAL CYCLONE - A non-frontal, migratory low-pressure system of usually synoptic scale developing over tropical or subtropical waters and having a definite organized circulation.

TROPICAL DEPRESSION - A tropical cyclone in which the maximum sustained surface wind (one-minute mean) is 33 kt (17 m/sec) or less.

TROPICAL DISTURBANCE - A discrete system of apparently organized convection - generally 100 to 300 nm (185 to 556 km) in diameter - originating in the tropics or subtropics, having a non-frontal migratory character and having maintained its identity for 12- to 24-hours. It may or may not be associated with a detectable perturbation of the wind field. As such, it is the basic generic designation which, in successive stages of identification, may be classified as a tropical depression, tropical storm or typhoon (hurricane).

TROPICAL STORM - A tropical cyclone with maximum sustained surface winds (one-minute mean) in the range of 34 to 63 kt (17 to 32 m/sec) inclusive.

TROPICAL UPPER-TROPOSPHERIC TROUGH (TUTT) - A dominant climatological system (upper-level trough) and a daily synoptic feature, of the summer season, over the tropical North Atlantic, North Pacific and South Pacific Oceans (Sadler, 1979).

TYPHOON / HURRICANE - A tropical cyclone in which the maximum sustained surface wind (one-minute mean) is 64 kt (33 m/sec) or greater. West of 180 longitude degrees they are called typhoons and east of 180 degrees longitude they are called hurricanes. Foreign governments use these and other terms for tropical cyclones and may apply different intensity criteria.

WALL CLOUD - An organized band of cumuliform clouds immediately surrounding the central area of a tropical cyclone. The wall cloud may entirely enclose or partially surround the center.

APPENDIX II

NAMES FOR TROPICAL CYCLONES

Column 1	Column 2	Column 3	Column 4
ANDY	ABBY	ALEX	AGNES
BRENDA	BEN	BETTY	BILL
CECIL	CARMEN	CARY	CLARA
DOT	DOM	DINAH	DOYLE
ELLIS	ELLEN	ED	ELSIE
FAYE	FORREST	FREDA	FABIAN
GORDON	GEORGIA	GERALD	GAY
HOPE	HERBERT	HOLLY	HAL
IRVING	IDA	IAN	IRMA
JUDY	JOE	JUNE	JEFF
KEN	KIM	KELLY	KIT
LOLA	LEX	LYNN	LEE
MAC	MARGE	MAURY	MAMIE
NANCY	NORRIS	NINA	NELSON
OWEN	ORCHID	OGDEN	ODESSA
PEGGY	PERCY	PHYLLIS	PAT
ROGER	RUTH	ROY	RUBY
SARAH	SPERRY	SUSAN	SKIP
TIP	THELMA	THAD	TESS
VERA	VERNON	VANESSA	VAL
WAYNE	WYNNE	WARREN	WINONA

NOTE:

Names are assigned in rotation, alphabetically. When the last name (WINONA) has been used, the sequence will begin again with "ANDY".

SOURCE: CINCPACINST 3140.1 (series)

APPENDIX III

REFERENCES

- Allen, R. L., 1984: COSMOS: CYCLOPS Objective Steering Model Output Statistics. Postprints, 15th Conference on Hurricanes and Tropical Meteorology. Miami, Fl, Jan 9-13, 1984, pp. 14-20.
- Atkinson, G. D., and C. R. Holliday, 1977: Tropical Cyclone Minimum Sea-Level Pressure and Maximum Sustained Wind Relationship for the Western North Pacific. Monthly Weather Review, Vol. 105, No. 4, pp. 421-427 (also FLEWEACEN TECH NOTE: JTWC 75-1).
- Brand, S., 1970: Interaction of Binary Tropical Cyclones of the Western North Pacific Ocean. Journal of Applied Meteorology, Vol. 9, pp. 433-441.
- Chen, L., and W. M. Gray, 1985: Global View of the Upper-Level Outflow Patterns Associated with Tropical Cyclone Intensity Change During FGGE. Atmospheric Science Paper 392, NASA NAG 5-299, Department of Atmospheric Science, Colorado State University, Fort Collins, Colorado, 106 pp.
- Diercks, J. M., R. C. Wier and M. K. Kopper, 1982: Forecast Verification and Reconnaissance Data for Southern Hemisphere Tropical Cyclones (July 1980 through June 1982). NAVOCEAN-COMCEN/JTWC TECH NOTE 82-1, 77 pp.
- Dong, K., and C. J. Neumann, 1983: On the Relative Motion of Binary Tropical Cyclones. Monthly Weather Review, Vol. 111, pp. 945-953.
- Dunnavan, G. M., 1981: Forecasting Intense Tropical Cyclones Using 700 mb Equivalent Potential Temperature and Central Sea-Level Pressure. NAVOCEANCOMCEN/JTWC TECH NOTE 81-1, 12 pp.
- Dvorak, V. F., 1984: Tropical Cyclone Intensity Analysis Using Satellite Data. NOAA Technical Report NESDIS 11, U.S. Department of Commerce, National Oceanic and Atmospheric Administration, National Earth Satellite Service, Washington, D.C., 20233, 46 pp.
- Gray, W. M., 1979: Tropical Cyclone Origin, Movement and Intensity Characteristics Based on Data Compositing Techniques. NAVENVPREDRSCHFAC Contractor Report CR 79-06, 124 pp.
- Hebert, P. H., and Poteat, K. O., 1975: A Satellite Classification Technique for Subtropical Cyclones. NOAA Technical Memo-randum NWS SR-83, 25 pp.
- Hodur, R. M., and S. D. Burk, 1978: The Fleet Numerical Weather Central Tropical Cyclone Model: Comparison of Cyclonic and One-Way Interactive Boundary Conditions. Monthly Weather Review, Vol. 106, pp. 1665-1671.
- Holland, G. R., 1980: An Analytical Model of Wind and Pressure Profiles in Hurricanes. Monthly Weather Review, Vol 108, No. 8, pp. 1212 - 1218.
- Holliday, C. R. and A. H. Thompson, 1979: Climatological Characteristics of Rapidly Intensifying Typhoons. Monthly Weather Review, Vol. 107, pp. 1022-1034.
- Jarrell, J. D. and Somerville, 1970: A Computer Technique for using Typhoon Analogs as a Forecast Aid. Technical Paper No. 6-70. U.S. Weather Research Facility, Norfolk, VA, 39 pp.
- Matsumoto, C. R., 1984: A Statistical Method for One- to Three-Day Tropical Cyclone Track Prediction. Atmospheric Science Paper 379, NEPRF N00014-83-K-002, NSF ATM-8214041, Department of Atmospheric Science, Colorado State University, Fort Collins, Colorado, 201 pp.

- Renard, R. J., 1968: Forecasting the Motion of Tropical Cyclones using a Numerically Derived Steering Current and its Bias. Monthly Weather Review, Vol. 96, No. 7, pp. 453-469.
- Renard, R. J., S. G. Calgon, M. J. Daley, and S. K. Rinard, 1973: Forecasting the Motion of North Atlantic Tropical Cyclones by the MOHATT Scheme. Monthly Weather Review, Vol. 101, No. 3, pp. 206-214.
- Sadler, J. C., 1979: Tropical Cyclone Initiation by the Upper-Tropospheric Trough. NAVENVPREDRSCHFAC Technical Paper No. 2-76, 103 pp.
- Sadler, J. C., M. A. Lander, A. M. Hori, and L. K. Oda, 1987: Tropical Marine Climatic Atlas, Volume II Pacific Ocean. University of Hawaii Report No. UHMET 87-02, 27 pp.
- Sikora, C. R., 1976: A Reevaluation of the Changes in Speed and Intensity of Tropical Cyclones Crossing the Philippines, FLEWEACEN TECH NOTE: JTWC 76-2, 11 pp.
- Weir, R. C., 1982: Predicting the Acceleration of Northward-moving Tropical Cyclones using Upper-Tropospheric Winds. NAVOCEANCOMCEN/JTWC TECH NOTE 82-2, 40 pp.
- Wirfel, W. P., and S. A. Sandgathe, 1986: Forecast Verification and Reconnaissance Data for Southern Hemisphere Tropical Cyclones (July 1982 through June 1984). NAVOCEANCOMCEN /JTWC TECH NOTE 86-1, 102 pp.

APPENDIX IV

PAST ANNUAL TROPICAL CYCLONE REPORTS

Copies of the past
Annual Tropical Cyclone
Reports
can be obtained through:

National Technical Information Service
5285 Port Royal Road
Springfield, Virginia 22161

Refer to the following acquisition numbers when ordering:

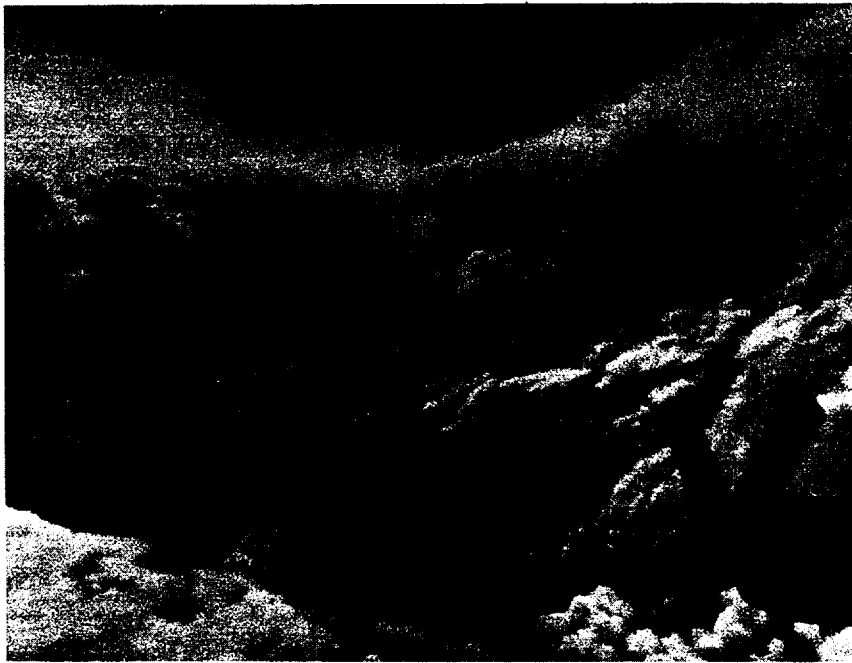
<u>YEAR</u>	<u>ACQUISITION NUMBER</u>
1959	AD 786147
1960	AD 786148
1961	AD 786149
1962	AD 786128
1963	AD 786208
1964	AD 786209
1965	AD 786210
1966	AD 785891
1967	AD 785344
1968	AD 785251
1969	AD 785178
1970	AD 785252
1971	AD 768333
1972	AD 768334
1973	AD 777093
1974	AD 010271
1975	AD A023601
1976	AD A038484
1977	AD A055512
1978	AD A070904
1979	AD A082071
1980	AD A094668
1981	AD A112002
1982	AD A124860
1983	AD A137836
1984	AD A153395
1985	AD A168284
1986	AD A184082

REPORT DOCUMENTATION PAGE

1. REPORT SECURITY CLASSIFICATION UNCLASSIFIED		1d. RESTRICTIVE MARKINGS	
2. SECURITY CLASSIFICATION AUTHORITY		3. DISTRIBUTION/AVAILABILITY OF REPORT AS IT APPEARS IN THE REPORT/ DISTRIBUTION UNLIMITED	
4. DECLASSIFICATION/DOWNGRADING SCHEDULE		5. MONITORING ORGANIZATION REPORT NUMBER(S)	
6. PERFORMING ORGANIZATION REPORT NUMBER(S)		7a. NAME OF MONITORING ORGANIZATION NAVOCEANCOMCEN/JTWC	
7. NAME OF PERFORMING ORGANIZATION NAVOCEANCOMCEN/JTWC	8b. OFFICE SYMBOL <i>(If applicable)</i>	7b. ADDRESS (City, State and ZIP Code) COMNAVMAR BOX 17 F.P.O. SAN FRANCISCO, CA 96630	
8. ADDRESS (City, State and ZIP Code) COMNAVMAR BOX 17 F.P.O. SAN FRANCISCO, CA 96630		9. PROCUREMENT INSTRUMENT IDENTIFICATION NUMBER	
9. NAME OF FUNDING/SPONSORING ORGANIZATION NAVOCEANCOMCEN/JTWC	8b. OFFICE SYMBOL <i>(If applicable)</i>	10. SOURCE OF FUNDING NOS.	
10. ADDRESS (City, State and ZIP Code) COMNAVMAR BOX 17 F.P.O. SAN FRANCISCO, CA 96630		PROGRAM ELEMENT NO.	PROJECT NO.
11. TITLE (Include Security Classification) 1987 ANNUAL TROPICAL CYCLONE REPORT		TASK NO.	WORK UNIT NO.
12. PERSONAL AUTHOR(S)			
13a. TYPE OF REPORT ANNUAL	13b. TIME COVERED FROM JAN 87 TO DEC 87	14. DATE OF REPORT (Yr., Mo., Day) 1987	15. PAGE COUNT 213 PLUS i-xii
16. SUPPLEMENTARY NOTATION			
17. COSATI CODES		18. SUBJECT TERMS (Continue on reverse if necessary and identify by block number)	
FIELD	GROUP	TROPICAL CYCLONES	
		TROPICAL STORMS	
04	02	TROPICAL DEPRESSIONS	
		TYPHOONS/SUPER TYPHOONS	
		TROPICAL CYCLONE RESEARCH	
		METEOROLOGICAL SATELLITE	
19. ABSTRACT (Continue on reverse if necessary and identify by block number) ANNUAL PUBLICATION SUMMARIZING TROPICAL CYCLONE ACTIVITY IN THE WESTERN NORTH PACIFIC, BAY OF BENGAL AND THE ARABIAN SEA, AND SOUTH PACIFIC AND SOUTH INDIAN OCEANS. A BEST TRACK IS PROVIDED FOR EACH SIGNIFICANT TROPICAL CYCLONE. A BRIEF NARRATIVE IS GIVEN FOR ALL TYPHOONS AND SELECTED TROPICAL CYCLONES IN THE WESTERN NORTH PACIFIC AND NORTH INDIAN OCEAN. ALL RECONNAISSANCE DATA USED TO CONSTRUCT THE BEST TRACKS ARE PROVIDED. FORECAST VERIFICATION DATA AND STATISTICS FOR THE JOINT TYPHOON WARNING CENTER (JTWC) ARE SUBMITTED.			
20. DISTRIBUTION/AVAILABILITY OF ABSTRACT UNCLASSIFIED/UNLIMITED <input checked="" type="checkbox"/> SAME AS RPT. <input checked="" type="checkbox"/> DTIC USERS <input type="checkbox"/>		21. ABSTRACT SECURITY CLASSIFICATION UNCLASSIFIED	
22a. NAME OF RESPONSIBLE INDIVIDUAL FRANK H. WELLS		22b. TELEPHONE NUMBER <i>(Include Area Code)</i> 671-344-5240	22c. OFFICE SYMBOL NOCC/JTWC

BLOCK 18 (CONTINUED)
TROPICAL CYCLONE BEST TRACK DATA
TROPICAL CYCLONE FORECASTING
AIRCRAFT RECONNAISSANCE
DYNAMIC TROPICAL CYCLONE MODELS
TYPHOON ANALOG MODEL
TROPICAL CYCLONE STEERING MODEL
CLIMATOLOGY/PERSISTENCE TECHNIQUES
TROPICAL CYCLONE FIX DATA

The Black Swan insignia of the 54 WRS Typhoon Chasers is included in dedication to the squadron's forty-three year's of support to the tropical cyclone forecast and warning mission. The nature and extent of their involvement with the USPACOM tropical cyclone warning system is best described by their last Commander, Lt. Col. Don H. Owen, during his 1987 Tropical Cyclone Conference briefing, "As we deactivate on 1 October, we will not be flying with you, literally, but our hearts and wishes for successful typhoon forecasting remain with you in the future."



Looking across the starboard wing and outboard engine of the 54th Weather Reconnaissance Squadron (54 WRS) WC-130 aircraft, the camera captures a section of the spectacular inner wall of Typhoon Wynne's (07W) eye. The tight curvature of the eye wall cloud shows across the top of the image. (The pentagons near the center of the photograph are due to sunlight glare off the lens diaphragm of the camera.) At the time the picture was taken, 260010Z July 1987, the aircraft reconnaissance mission (AF8610507 WYNNE) was fixing the eye over the Philippine Sea, 250 nm (463 km) north of Guam and 48 nm (89 km) west of the island of Pagan in the northern Marianas. The circular eye diameter was 16 nm (30 km) and the minimum sea-level pressure at that time was 922 mb (Photo courtesy of Detachment 3, 1st Weather Wing and Kenneth W. Reese, Captain, USAF).



The Air Force Air Weather Service celebrated its 50th anniversary on 1 July 1987. The insignia that was designed for the occasion is displayed here in recognition of Detachment 1, 1st Weather Wing's enormous contribution to the NAVOCEANCOMCEN/JTWC tropical cyclone forecast and warning support to the U. S. Pacific Command. Twenty-eight years of cooperation between Navy and Air Force personnel working at NAVOCEANCOMCEN/JTWC have resulted in one of the finest tropical cyclone forecasting centers in the world.